STRUCTURAL AND FUNCTIONAL DIFFERENTIATION OF TELEOST SKELETAL MUSCLE

Stuart Eggington

A Thesis Submitted for the Degree of PhD
at the
University of St Andrews

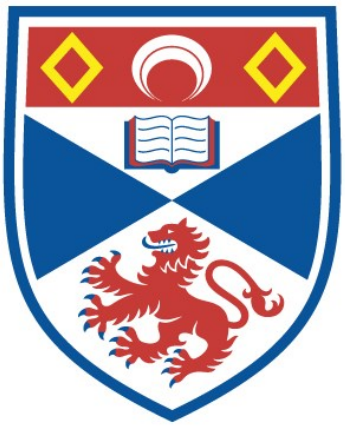

1983

ProQuest LLC.
789 East Eisenhower Parkway
P.O. Box 1346
Ann Arbor, MI 48106 – 1346

Abstract: Structural and Functional Differentiation of Fish Skeletal Muscle

by S. Eggington, B.Sc.

The lateral musculature of elvers is differentiated into two fibre types on the basis of alkaline-labile (pH 10.2) myofibrillar ATPase activity. Slow muscle forms a relatively homogeneous fibre population, whereas fast muscle shows a heterogeneity with respect to both fibre size, and position in the myotome. The low aerobic capacity of slow fibres reflects the energetic requirement of anguilliform locomotion. A morphological continuum of myogenic cells occurs within mature, differentiated myotomal muscle similar to that described for embryonic myogenesis. No evidence could be found for regional growth nodes. Small fast fibres ($<100\mu m^2$) represent immature, but differentiated fibres undergoing hypertrophy. There is considerable variation in the capillary supply to both fast and slow muscle, and between homologous muscles of different species. Methods are described to determine the minimum sample size required for a stable, reproducible parameter estimate, and to assess the orientation of the capillary network. This is shown to be highly anisotropic. Capillary volume and surface densities are thought to be the most appropriate indices to use with fish muscle. The spring migration of elvers is shown to be a mixed population, of similar annual composition. The main migratory wave are true post-metamorphic, juvenile eels. There is a partial (Precht type 3) compensation in Vo_2 on acclimation to 10° and $29^{\circ}C$. The extent of the physiological acclimation reflects the environmental constraints of the migration. Differences in structure and

complexity of multiple and focal innervation were investigated using fast muscle from representative teleosts. Endplate structure is similar in both types. Cod ventral spinal nerves have fewer motor, but more sensory axons than homologous nerves in eel. A novel way of visualising the extent of inter- and intra-segmental branching of nerves, intracellular marking of nerve routes with cobalt, reveals extensive branching in cod myotomes and cross-innervation between at least 3 segments. In eel, branching is restricted to a single myotome. These results reflect the mechanical and nervous control over the locomotory waveform.

In submitting this thesis to the University of St. Andrews I understand that I am giving permission for it to be made available for use in accordance with the regulations of the University Library for the time being in force, subject to any copyright vested in the work not being affected thereby. I also understand that the title and abstract will be published, and that a copy of the work may be made and supplied to any bona fide library or research workers. 166 pages.

I was admitted as a research student under Ordinance No. 12 on and as a candidate for the degree of Ph.D. on ; the higher study for which this is a record was carried out in the University of St. Andrews between 1979 and 1982.

I STUART EGGINTON hereby certify that this thesis which is approximately 40 000 words in length has been written by me, that it is the record of work carried out by me, and that it has not been submitted in any previous application for a higher degree.

date: 6.12.82

I hereby certify that the candidate has fulfilled the conditions of the Resolution and Regulations appropriate to the degree of Ph.D. of the University of St. Andrews and that he is qualified to submit this thesis in application for that degree.

Date:

STRUCTURAL AND FUNCTIONAL DIFFERENTIATION OF TELEOST SKELETAL MUSCLE

A thesis submitted to the University of St. Andrews for the degree of Doctor of Philosophy

by

Stuart Egginton

Department of Physiology
University of St. Andrews

December 1982

DECLARATION

I hereby declare that the research reported in this thesis was carried out by me, and that the thesis is my own composition. No part of this work has been previously submitted for a higher degree. The research was conducted in the Department of Physiology, United College of St. Salvator and St. Leonard, University of St. Andrews, under the direction of Dr. I.A. Johnston.

CERTIFICATE

I hereby certify that Stuart Egginton has spent eleven terms engaged in research under my direction, and that he has fulfilled the conditions of General Ordinance No. 12 (Resolution of the University Courts No. 1, 1967), and that he is qualified to submit the accompanying thesis for the degree of Doctor of Philosophy.

Acknowledgements

I wish to express deep gratitude to my supervisor, Dr. Ian Johnston, for unfailing support and tolerance of an Anguillophile. Sincere thanks are also due to members of the "Fish Lab.", past and present, who have helped to make my stay in St. Andrews both profitable and enjoyable. Similarly, the friendship of many others in the Physiology Department will be greatly missed. Special thanks to: Murray Coutts for excellent assistance with photography and the EM; Hugh Forbes for bullying local fishermen into landing conger eels; Keith Sillar for the use of, and help in operating, his electrophysiological "rig"; Jim Milne for invaluable help with catching elvers; Dr. Bob Pitman for advice on silver intensification and other methods; Dr. Hans Hoppeler, Institute of Anatomy, Bern, for use of pre-publication manuscripts and advice; Dr. Antti Soivio, Department Zoophysiology, Helsinki, for hospitality and re-kindling my interest in research; Mrs. Christina Lamb for deciphering my hieroglyphics and typing the manuscript; family and friends for support and encouragement throughout.

Finally, I wish to thank the N.E.R.C. for generously supporting the first two years of this study, and the Department of Physiology for the provision of a Maitland-Ramsay Scholarship for the third year.

To my wife, Enid

For understanding, and seemingly endless patience;
it can't have been easy taking second place to an eel!!

"The first million years were the worst..."

Marvin, the Paranoid Android
The restaurant at the end of the Universe
Douglas Adams

CONTENTS

SUMMARY

Chapter 1

A brief introduction is given to relevant aspects of the structure, biochemistry, electrophysiology and mechanical properties of fish locomotory muscle.

Chapter 2

The lateral musculature of elvers is differentiated into two fibres types on the basis of alkaline-labile (pH 10.2) myofibrillar ATPase activity. Slow muscle comprises ~7% body cross-section and forms a 2-fibre deep layer around the trunk, with invaginations along the horizontal septum and fin insertions. There is a high glycogen content, but weak staining for lipid and aerobic marker enzymes. Mean fibre cross-sectional area is 167μm^2, with few fibres > 800μm^2. A large proportion of the trunk (66% body cross-section) consists of fast fibres (mean area, 328μm^2), with a large size range (5% > 1400μm^2). These have an alkaline-stable ATPase, and "en plaque" innervation. Superficial fibres stain for both glycogen and aerobic enzymes. Deep fibres > 200μm^2 show no staining for lipid, glycogen, SDH, or COX; those fibres < 120μm^2 (~ 5% of fast muscle) stain heavily for glycogen. Extracellular lipid constitutes 12% of body cross-sectional area, but rarely appears as intracellular deposits. The number of capillaries/fibre are among the lowest values known for teleosts, being 0.98, 0.33 and 0.12 for slow, superficial fast and deep fast fibres, respectively. The low aerobic capacity of slow muscle reflects the energetic requirements of anguilliform locomotion.

Chapter 3

Regional variation in muscle fibre types was examined by morphometric analysis of electronmicrographs, along a transect from skin to vertebral column (fibres 1-14, respectively). Small (204μm^2) slow fibres form a

relatively homogeneous population: mitochondria, myofibril, SR and T-system volume densities are 0.214, 0.610, 0.021 and 0.003, respectively; however, some difference is found between peripheral and lateral line triangle fibres. Fast fibres show a marked heterogeneity in fine structure, dependent on both position and size; superficial fibres ($333\mu m^2$, 3-4 deep) are smaller than deep fibres ($775\mu m^2$, 6-12 deep) and have a significantly higher V_V(mit,f), 0.076 vs 0.012. Volume densities of myofibrils, SR and T-system are 0.804, 0.060 and 0.004, respectively, for deep fibres; those $< 100\mu m^2$ constitute up to 5% of fast muscle and have a higher V_V(mit,f), 0.043, more glycogen, and slightly lower V_V(SR,f), 0.056. This is the first quantitative study of regional differences in fine structure of fish skeletal muscle. The metabolic subpopulations of fast fibres may correspond to different growth stages. The relatively poor development of fast muscle SR is correlated with the low frequency, high amplitude of the propagated waveform characteristic of eel swimming.

Chapter 4

The growth pattern of fish skeletal muscle presents a useful model for analysis of cellular differentiation. A morphological continuum of myogenic cells occurs within mature, differentiated myotomal muscle similar to that described for embryonic myogenesis. Differentiating cells are closely associated with large fast fibres, located near large interstitial spaces. Differentiation appears to precede innervation, with sarcomeregenesis apparent in myoblasts. The small fibres considered to be growth stages in many species, including elvers, are immature, but differentiated fast fibres undergoing hypertrophy. The retention of a relatively high aerobic capacity may be associated with the aerobic catabolism of lactate, but they are unlikely to form a differentially-recruited population during swimming. The unusually large V_V(sp,f) of fibres adjacent to the myosepta appears to be a longitudinal extension of the fibre insertion ("tendon") where contractile

efficiency is compromised, and not a result of delayed sarcomere formation, as found in amphibian myotomes.

Chapter 5

There is considerable variation in the capillary supply to both fast and slow muscle, and between homologous muscles of different species. Capillary density appears to be positively correlated with mitochondrial content in aerobic muscle: $V_V(mit,f)$ and $N_A(c,f)$ in Conger slow and fast muscle are 0.227, 615mm^{-2} and 0.027, 21.3mm^{-2}, respectively. Sample size directly affects the accuracy of an index, and a method is described to determine the minimum sample number required for a reproducible, stable estimate. For both Conger slow and fast muscle this is around 500 fibres, but is substantially reduced in species with a higher capillary density. Of the common indices in use to describe the capillary supply, $N_N(c,f)$ and $\bar{N}(c,f)$ are most useful for fish muscle, and indicate the required minimum sample size for accurate determination of $N_A(c,f)$. Experimental protocol needs to reflect the anatomical heterogeneity, particularly with regard to variable fibre and capillary sizes, and the circulatory physiology of fish. This is the first study to assess the orientation of the capillary network in fish muscle, which is shown to be highly anisotropic. Capillary density, therefore, is a good estimate of the length density from which $V_V(c,f)$ and $S_V(c,f)$ can be derived. These more fully describe the functional limitations of the capillary bed, and are considered to be the most appropriate for fish muscle with its sparse, heteregeneous capillary supply. For Conger slow muscle these are 0.016 and 135cm^{-1}, and for fast muscle, 0.0007 and 4.7cm^{-1}, respectively. This underlines the highly anaerobic nature of fast muscle.

Chapter 6

Juvenile eels (elvers) were sampled during their spring migration up the River Severn, Avon; this is a mixed population, with a similar annual composition. The main migratory wave is considered to be the developmental

inflexion point, i.e. where the influence of metamorphosis is complete and growth commences. Weight and length are 0.25 ± 0.05g and 7.1 ± 0.4cm; $\dot{V}o_2$ = 0.16mg.g.hr^{-1} and critical (residual) oxygen concentration 1.04mg.l^{-1}. The experimental animals are shown to be true post-metamorphic, juvenile eels. There is a partial (Precht type 3) compensation in $\dot{V}o_2$ on acclimation to 10° and 29°C, 0.22 ± 0.05 and 0.42 ± 0.09mg.g.l^{-1}, respectively. Older (yellow and silver) eels show a reduced compensation over a similar range of temperatures. Little evidence can be found for a large structural reorganisation, as found in other teleosts, although V_V(mit,f) is higher in 10°C (0.26) than 29°C-elvers (0.19). Slow muscle N_A(c,f) is similar for both groups, 2473 and 2347mm^{-2}, with the difference countered by a small adjustment in capillary size, such that S_V(c,f) is the same for both groups, 314 and 310cm^{-1}, respectively.

Alternate mechanisms for maintaining metabolic and locomotory efficiency may include the adjustment of circulatory haemodynamics. The extent of the physiological acclimation reflects the environmental constraints of a spring migration, and is complimented by changes in behaviour.

Chapter 7

Differences in structure and complexity of multiple- and focal innervation were investigated using fast muscle from representative teleosts; cod and eel. Endplate structure is similar in both species, with a model category of 22-25nm for synaptic vesicle diameter. Similar membrane resting potentials are also found, -62.2 and -58.3mV. However, the composition of the ventral ramus is markedly different; cod motor axons are larger than those of eel, 133 vs 53μm^2, and fewer in number, 90 vs 134. There is a larger population of sensory (1-3μm^2) axons in cod VR, 1181 vs 90. The classification of a spinal nerve, as mixed or consisting of two separate rami, depends on the anatomical location of the sample. A novel way of visualising the extent of

inter- and intra-segmental branching of the spinal nerve, intracellular marking of the nerve route with cobalt, reveals a diffuse pattern of branching within cod myotomes, and a significant amount of cross-innervation between at least 3 myotomes. In eel, branching is restricted to a single myotome. The results may be explained by the mode of swimming: cod utilises a high frequency, low amplitude waveform (the wavelength apparently determined by simultaneous contraction of around 4 myotomes) that is dependant on peripheral modulation; swimming in eel is almost independant of peripheral (sensory) feedback, relying extensively on a spinal cord pattern generator.

Chapter 8

General conclusions arising from the work are discussed, with some potentially profitable directions for future work.

FISH SKELETAL MUSCLE

Design of the trunk

Swimming in a high density medium requires a large amount of power as inertial forces produce a significant pressure drag, relative to air, and propulsion against a yielding medium is energetically wasteful (Webb 1978; Videler 1981). Power requirements of terrestrial locomotion usually increase linearly with speed (V), whereas aquatic locomotion requires a power increment $\propto V^3$. Buoyancy partially offsets these limitations, removing the need for weight economy and enabling fish to carry the large muscle mass necessary to generate power for rapid swimming. This constitutes 40-75% of the body mass, depending on body form and mode of swimming (Greer-Walker and Pull 1975; Lindsey 1978; Bone 1978), up to 90% of which is fast contracting fibres. Physical limitations are also reflected in the arrangement of segmental musculature; the unequal V-shape of primitive fish myotomes is thought to prevent dorso-ventral flexion during swimming (Willemse 1966; Bone 1978) and overlapping W-shapes in higher forms (Nursall 1956; Kryvi and Totland 1978) may prevent "slippage" of non-extensible myosepta (Videler 1981). Superficial red fibres are usually oriented parallel to the body surface, whereas the minimal ($\sim$3%) shortening of all fast fibres during swimming, irrespective of position, requires large angles to the fish axes (Alexander 1969; Raamsdonk et al 1977).

Fibre types

Segregation of trunk musculature into 2 main fibre types, first recognised in Torpedo on the basis of colour (Lorenzini in 1678, see Bone 1978), is thought to reflect the differential power requirements for burst and cruise swimming. Many workers rely on this classification (Boddeke et al 1959; Greer-Walker and Pull 1975) in the absence of a universally applicable alternative (Bone 1978; Johnston 1981a). Red (slow) muscle usually forms a

thin layer around the trunk (Bone 1966) or a discrete wedge, the "lateral line triangle" (Johnston et al 1974). It constitutes 0.5 to 29% of the myotome (Greer-Walker and Pull 1975), being highest in pelagic and lowest in dermersal species. Apparent similarity between mammalian slow oxidative (SO), fast oxidative glycolytic (FOG) and fast glycolytic (FG) fibre types and those found in fish (Goldspink 1977) may be only superficial (Raamsdonk et al 1980).

Slow muscle

Histochemically, this usually contains large lipid and glycogen reserves (Love 1980), high activities for TCA cycle marker enzymes such as succinic dehydrogenase (SDH), a low alkaline-stable myofibrillar ATPase (m.ATPase) activity (Johnston et al 1972, 1974; Patterson et al 1975; Korneliussen et al 1978), high myoglobin concentrations (Love 1980) and many capillaries (Mosse 1978, 1979). The distribution and activity of aerobic enzyme systems is related to muscle fatigue resistance (Burke et al 1973), and the biochemical measurements of m.ATPase activity with contraction velocity (Bárány 1967). Most workers consider this muscle relatively homogeneous, although the dogfish Scyliorhinus canicula is a good example of regional variability. The outermost layer of large fibres shows little staining for SDH or m.ATPase activity, but an intense stain for glucose-phosphate-isomerase; the next layer of small diameter fibres have a high SDH activity; the deeper 2 or 3 layers have a slightly greater m.ATPase activity and less SDH activity (Bone and Chubb 1978; Bone 1978). The high aerobic capacity of fish slow fibres is reflected in the large volume density of mitochondria, among the highest known for striated muscle, which approach that of endotherm ventricles (Bossen et al 1978; see Johnston 1981a, 82c for fish). The extent of the sarcoplasmic reticulum (SR) is varied, although higher than in amphibians and may resemble some twitch fibres (Johnston 1980a).

In vitro determination of key enzyme maximal activities has been used to describe the relative importance of different pathways of energy metabolism (Crabtree and Newsholme 1972); those from oxidative pathways usually have high activities in slow muscle (Johnston and Moon 1980a). Lipids are a major source of energy during swimming (Bilinski 1974; Driedzic and Hochachka 1978), with ketonebodies most important in elasmobranchs and fatty acids in teleosts (Zammit and Newsholme 1979). It has been thought that red muscle both provides glucose for white muscle activity, and oxidises lactate (Wittenberger et al 1975), although the low activity of key glyconeogenic enzymes makes this unlikely (Johnston and Moon 1979).

Some pelagic fish have an internalised slow muscle e.g. skipjack tuna *Katsuwonus pelamis* where an efficient heat exchanger (rete) maintains an elevated muscle temperature (Carey and Teal 1966). This muscle has a 10-fold increase in mitochondria, and a more highly developed capillary bed, than superficial muscle (Bone 1978b). Similar results are found in *Euthynnus pelamis* (Guppy et al 1979) and *Thunnus thunnus*, where m.ATPase activity of the deep red muscle is much higher than in more sedentary species (Johnston and Tota 1974).

Intermediate muscle

This "pink" muscle lies between red and white zones, having an aerobic capacity and m.ATPase activity between that of the other types (Johnston et al 1974; Patterson et al 1975; Kryvi 1977; Flood 1979; Kryvi et al 1980), although with a myosin light chain composition similar to fast muscle (Johnston et al 1977). This may constitute a larger bulk than slow fibres, around 10% in carp *Carassius carrasias* (Mosse and Hudson 1977). The only study of their involvement in swimming found recruitment between slow- and fast muscle thresholds (Johnston et al 1977).

Fast muscle

Fast fibres have a low aerobic capacity, sparse capillary network, high m.ATPase activity and large myofibril volume density (Love 1980; Bone 1978; Johnston 1981a). Mitochondrial content is quite variable, around 0.5 to 1.0% in primitive species such as sharks (Kryvi 1978; Totland et al 1981) but especially high in multiply-innervated teleosts e.g. brook trout Salvelinus fontinalis, 8.9% (Johnston and Moon 1981) and tench Tinca tinca, 4.5% (Johnston and Bernard 1982). The sarcotubular system is more extensive, relative to slow (Nag 1972; Kryvi 1978), and resembles the situation in amphibians (Peachey 1965; Flitney 1971; Totland 1976; see also Johnston 1980a). Glycolytic enzyme activities, e.g. phosphorylase and phosphofructokinase, are usually 2-3 times higher in fast than slow muscle (Crabtree and Newsholme 1972; Johnston 1977; Newsholme et al 1978; Walesby and Johnston 1979; Johnston and Moon 1979). In Salmo gairdneri, the redistribution of blood during activity increases from around 9% at rest to over 40% of the cardiac output diverted to the slow muscle, at the expense of the fast muscle system (Daxboeck et al 1982). Although the energy cost of locomotion is lower for fish than mammals, the scope for activity appears to be 10-100 times less (Brett 1972), suggesting a high dependance on anaerobic activity metabolism. From measurements of swimming efficiency and oxygen consumption ($\dot{V}o_2$), Smit et al (1971) calculated that goldfish Carassius auratus produce 80% of their energy requirements in this way. However, anaerobic capacities can be modified by a number of external factors (Hazel and Prosser 1974; Boström and Johansson 1972; Johnston and Moon 1980; Johnston 1981a). Glycogen is used by both fibre types during swimming although in carp, swimming at 3 $L.sec^{-1}$, 80-85% is utilised by the fast muscle (Johnston and Goldspink 1973a). There is considerable inter-specific variability in the importance of aerobic glycolysis (Johnston 1977; Newsholme et al 1978; Johnston and Moon 1980a; Walesby and Johnston 1980), with the relatively high capacity in trout fast muscle

assumed to be sufficient to support sustained activity (Johnston and Moon 1980b).

In many fish, notably salmonids (Greene 1913; Johnston et al 1975; Patterson et al 1975), but also cod (Greer-Walker 1970; Korneliussen et al 1978) and angler fish (Bone and Chubb 1978), a 'mosaic' arrangement of small diameter SDH +ve fibres are found among the large fast fibres. In rainbow trout Salmo gairdneri they possess a lower m.ATPase activity (Johnston et al 1975). Some workers consider them to be a distinct fibre type (Boddeke et al 1959; Hulbert and Moon 1978), and others to represent growth stages of fast fibres (Johnston et al 1975; Korneliussen et al 1978; Johnston and Moon 1980b). Whether or not these represent a differentially recruited fibre population is uncertain (Hudson 1973; Altringham and Johnston 1981).

In all vertebrate fast muscle free cytoplasmic Ca^{2+}-binding proteins (parvalbumins) are found, with very low concentrations in slow and cardiac muscle; an interesting exception is the shrew heart which contracts at > 1000 beats/minute and has a high titre (19μM, Le Peuch et al 1978). They reach very high concentrations in fish fast muscle, reaching 15% of the soluble proteins, and display a high Ca^{2+}-affinity, being structurally related to other muscle Ca^{2+}-binding proteins (TnC, calmodulin; Perry 1979). It is thought that they are able to induce rapid relaxation by sequestering Ca^{2+} before the SR Ca^{2+}-pump. Subsequent transfer of Ca^{2+} from parvalbumins to SR regulates intracellular free $[Ca^{2+}]$ (Pechere et al 1977). It is not known the extent to which parvalbumin concentration is correlated with SR content, although the efficacy of parvalbumin-regulation must ultimately depend on the activity and distribution of the SR Ca^{2+}-pump.

Growth

The precise origin of vertebrate muscles is varied, tetrapod limb muscles develop in situ from mesenchymal differentiation of lateral plate-

derived cells, fin muscles from somitic (myotomic) mesoderm (see Fischman 1972 for refs.). Mechanisms controlling myogenic stem cell number (≙ number of muscle fibres) are unknown, but assumed to be genetically-derived. In most muscles of higher vertebrates fibre number does not increase after post-embryonic differentiation, although in some neonates post-natal proliferation continues, in relation to the developmental stage reached at birth (Bridge and Allbrook 1970; Goldspink 1972); growth is characterised by increased fibre diameter and length. In contrast, many fish increase fibre number throughout life (Greer-Walker 1970) resulting in a wide range of fibre size, irrespective of innervation pattern (Weatherley et al 1979; Willemse and van den Berg 1978). Rapid embryonic growth, associated with high protein turnover rates, is followed by a slower post-embryonic hypertrophy. In most mammals, skeletal muscle is 20-25% of body weight at birth, increasing during post-natal growth to 45-50% (w/w and protein content) at adult (Goldspink 1980). Growth is therefore limited by the (aerobic) anabolic activity. Presumptive myoblasts (myosatellite cells, MSC) are mononucleate, mitotically active cells which accumulate at pre-determined sites of muscle origin (Mauro 1961; Fischman 1972). Myoblasts are formed from elongation of MSC into spindle-shaped cells containing myofilaments, but no mitotic activity. Myotubes are a multinucleate syncitia, showing post mitotic characteristics, formed by cytoplasmic fusion of myoblasts (Fischman 1972; Moss and Leblond 1971). This fusion appears to stimulate myofibrillar protein synthesis and proliferation of mitochondria. The serial addition of sarcomeres parallels any post-natal increase in muscle length (Goldspink 1972). Increase in myofibril number during fibre hypertrophy results from longitudinal splitting of existing (peripheral) fibrils after reaching a mechanically-limited size; the Z-disc lattice ruptures, possibly due to lateral tension development caused by a mis-match of actin and myosin lattices (Patterson and Goldspink 1976).

Nervous system and locomotion

The nervous system co-ordinates proprioceptive and exteroceptive impulses; in vertebrates it can be considered in 3 distinct regions - brain, spinal cord, and peripheral nerve net. Undulatory movement (swimming) appears to be controlled largely by the spinal cord, the brain merely modifying the basic rhythmn (Grillner 1975; Roberts 1981). Fish spinal cord occupies the entire vertebral canal, giving risé to the segmental dorsal (sensory) and ventral (motor) roots. The primitive condition (Amphioxus) appears to be where the sensory root lies adjacent to the myoseptum and the motor root emerges mid-myotome, in an alternating pattern down the cord (Kappers et al 1967). Spinal cords resembling that of higher vertebrates first appear in the Chondrichthyes (elasmobranchs) with the formation of spinal ganglia. Further development occurs in the Osteichthyes (bony fishes) such that teleost and mammalian spinal cords are broadly similar (Kappers et al 1967). Large motor cell bodies are located in the ventrolateral grey matter, giving rise to trunk muscle efferents (Bernstein 1970). In all fishes but the Petromyzonts spinal roots are thought to join, forming the mixed spinal nerves (Kappers et al 1967), although this is disputed (Roberts 1969). Little comparative work has been done; most detailed studies are restricted to cranial nerves (e.g. Young 1933) although some data is available for elasmobranch (Roberts 1969), agnathan (Teräväinen and Roväinen 1971) and teleost spinal nerves (Barets 1961).

The basic element of swimming is an alternate contraction of contralateral segments, passing an undulatory wave down the body. The phase lag between rostral and caudal myotomes remains constant, since swimming speed increases linearly with the frequency of the propagated wave (Grillner 1975). Fins may be used as stabilisers (e.g. thunniform locomotion), or have an active role in swimming (labiform locomotion), although in most species they are pressed close to the body to reduce drag (Lindsey 1978; Webb 1978).

Both central oscillator and peripheral reflex mechanisms have been described for co-ordination of the propagated wave (Grillner and Kashin 1976; Grillner and Wallen 1977; Roberts 1981). In eel, swimming is determined largely by intrinsic activity of the spinal cord: the integrity of the peripheral nervous system (associated with skin, muscle and connective tissue) is not essential to conduct a locomotory rhythm (Gray 1936). Similarly, severing over 50% of sensory roots does not abolish the phase-coupling of locomotory movements in dogfish trunk (Grillner 1975); i.e. both eel and dogfish can maintain intersegmental co-ordination without spinal cord afferents. Interestingly, some primitive species can show co-ordinated swimming after spinal cord transection. This is not so with most higher teleosts, which require a large degree of facilitation from the brain stem, in addition to the spinal cord generator (Grillner 1975). Exteroceptive stimuli generated by movement modify the locomotory co-ordination, since the firing of sensory afferents determines the rhythmn and is correlated with increased swimming speed, in elasmobranchs (Grillner 1975; Roberts 1981): some spinal motoneurons cannot sustain intrinsic activity at the correct frequency, in the absence of proprioceptor feedback. Terrestrial vertebrates possess a range of complex proprioceptors; however, neuromuscular spindles have not been observed in fish (Roberts 1969; Bone 1978) and other sensory organs may provide feedback during locomotion. Two specialised nerve terminations are known in elasmobranchs: coiled Wunderer corpusles in the dermis, and elongate Poloumordwinoff endings in fin muscles of skates and rays (see Roberts 1969). In addition fine, free nerve endings are found in (or adjacent to) the myosepta of Petromyzon (Johnston 1908). Myxine (Bone 1963), Scyliorhinus (Roberts 1969) and Pleuronectes (Kappers et al 1967). Their receptive field (sensory dermatome) overlaps half a myotome in teleosts (Roberts 1981) or ~ 6 myotomes at the most hypaxial portion in dogfish (Roberts 1969).

Innervation and Recruitment

In all groups of fish the superficial slow fibres are innervated by small diameters (myelinated) axons, forming a number of en grappe terminations; junction potentials are elicited in response to depolarising stimuli, closely resembling the true slow (tonic) fibres of amphibians (Barets 1961; Anderson et al 1963; Hagiwara and Takahashi 1967; Stanfield 1972). From measurements of membrane space constants, endplate separation is thought to be 150-200μm (dogfish, Stanfield 1972). Where more than one slow fibre type exists, a similar innervation pattern is present (Bone 1978). Hagfish slow fibres are innervated by two axons, originating at each myoseptal end (Jansen et al 1963); other species may have more extensive multiple innervation (Barets 1961; Bone 1966). Slow fibres do not propagate action potentials, although Stanfield (1972) considered some recorded inward Na^+ currents large enough to suggest the mechanism may exist; this remains largely unsupported and requires further investigation. However, junction potentials may be large: Myxine slow fibres produce a depolarisation up to 30mV, elevating the membrane potential near zero (Andersen et al 1963). It has been suggested that the fundamental differences between slow and fast fibres resides in E-C coupling, with fast twitch characteristics depending on inactivation of Ca^{2+}-releasing mechanisms by membrane depolarisation (Yamamoto 1972).

One of the most important factors determining contractile properties, metabolism and division of labour of fish muscle during swimming is thought to be the type of fast muscle innervation (Bone 1978; Johnston 1981a). Elasmobranchs, Agnathans, Chondrosteans, Holosteans and Dipnoans all possess fast muscle with focal (terminal) innervation (Bone 1964; Johnston 1981a). This resembles the situation in amphibia, reptiles, birds and mammals,

although in fish the en plaque endplates are situated at the fibre end(s). Typical overshooting, propagated action potentials (similar to other vertebrate fast twitch fibres) are produced by membrane depolarisation in elasmobranchs (Hagiwara and Takahashi 1967). The fast fibres appear to be entirely dependant on anaerobic glycolysis for energy production during activity (Kryvi 1977; Bone 1978; Johnston 1981a; Chapter 5). Little information about the electrophysiology or mechanical properties of fast muscle in focally-innervated teleosts is available.

Fast muscle in taxonomically advanced teleosts, including the Perciformes and Cypriniformes which together account for nearly $^{4}/_{5}$ of the Superorder, have a multiple (distributed) innervation (Takeuchi 1959; Barets 1961; Bone 1964; Johnston 1981a). This pattern, unique among the vertebrates, consists of a diffuse network of axons across the myotome, with each fibre receiving up to 23 motor terminations. It is not clear if each endplate is derived from a single axon (Hudson 1969), or whether pre-terminal branching results in a number of different endings on individual and adjacent fibres (Altringham and Johnston 1981), as found in slow muscle (Barets 1961). In sculpin, Myoxocephalus scorpius, each fibre receives 2-5 axons from each of 3-5 spinal nerves, giving rise to a number of morphologically varied endplates, around 700μm apart (Hudson 1969). The density of neuromuscular junctions is similar in cod, Gadus morhua, with 9-23 endplates/fibre, irrespective of fibre diameter (Altringham and Johnston 1981). However, superficial fast fibres have a larger number of endplates than deep fast fibres. Multiply-innervated fast fibres either fail to overshoot, or do so close to zero potential (Takeuchi 1959; Barets 1961; Hidaka and Toida 1969; Hudson 1969) with rare spike potentials (Yamamoto 1972). Stimulation of spinal nerves in Myoxocephalus produces junction potentials associated with local, graded contractions or, on manipulation of the Ringer ion

composition, a propagated action potential (up to a 20mV overshoot) giving a fast twitch (Hudson 1969). The physiological relevance of the latter response is unclear, as no information is available concerning in vivo ion concentrations or flux. The presence of summated junction potentials is good evidence for polyneuronal innervation (Hudson 1969). Selective activation of different size fibres could only occur if the membrane properties are different e.g. a small fibre with a lower threshold for action potential generation may be activated at a stimulus frequency producing only junction potentials in large fibres. The greater density of endplates in cod superficial fast muscle therefore requires a lower stimulus (from a larger number of axons) to elicit contraction, and may be recruited before the deep muscle. This extension of the range of swimming speeds over which fast muscle can be recruited is reflected in the emg records and metabolite analysis; skipjack tuna Katsuwonus pelamis (Brill and Dizon 1979), rainbow trout (Hudson 1973), carp (Johnston et al 1977; Bone et al 1978), striped bass Morone saxatilis and bluefish Pomatomus sultatnix (Freadman 1979), brook trout Salvelinus fontinalis and saithe Pollachius virens (Johnston and Moon 1980a,b). At low speeds the slow fibres alone are active, but as velocity increases a threshold is reached for (sustainable) fast fibre recruitment. This varies, being 0.5 $L.s^{-1}$ for carp, 0.8 - 0.9 $L.s^{-1}$ for saithe, 1.4 $L.s^{-1}$ for rainbow trout and 4.5 $L.s^{-1}$ for bluefish. In general, the glycolytic potential is augmented by a large aerobic capacity, 15 to 20% of slow muscle (Johnston and Moon 1981). Interestingly, emg recordings from fast muscle active at low speeds is similar to those of slow muscle (Johnston et al 1977; Johnston and Moon 1980a), suggesting that junction potentials may be responsible for fast muscle activity at low speeds.

Mechanical properties

The complex arrangement of myotomal fibres makes preparation for mechanical experiments extremely difficult, most studies using the more discrete fin, jaw or opercular muscles (Hidaka and Toida 1969; Yamamoto 1972; Flitney and Johnston 1979). Isolated fast fibre bundles from dogfish trunk muscle produce twitches on supramaximal stimulation (half time to maximum tension, $t_{\frac{1}{2}}$ = 20 msec), slow fibres giving a prolonged contraction ($t_{\frac{1}{2}}$ = 100msec, Johnston and Bone, unpublished); fused tetani are found > 8Hz in both types. Similarly, cuckoo ray Raja naevus fast pectoral fin muscle produces tetani around 5Hz, $t_{\frac{1}{2}}$ = 25.6msec (Johnston 1980). In both species maximum tension is developed at 20Hz. Maximum (unloaded) shortening velocity (V_{max}) for isolated dogfish fast and slow fibres is 1.64 and 0.75 sec^{-1}, respectively (Altringham and Johnston 1981), giving a fast:slow ratio of 2.2. Amphibian slow fibres have a V_{max} 10-20% that of twitch fibres (Lannergren 1978). The innervation pattern is similar in amphibian and fish slow muscle, but used either for maintaining posture or locomotion, respectively. The large number of endplates/fibre is multiply-innervated fast muscle is reflected in a different range of tetanic fusion frequencies. Adductor operculi muscle in the cichlid Tilapia mossambica produce graded, fused tetani in both fast and slow fibre bundles, with maximum tension developed up to 500 and 400 Hz, respectively. V_{max} for fast and slow fibres are 2.6 $L.sec^{-1}$ and 1.5 $L.sec^{-1}$ (Flitney and Johnston 1979), giving a slightly reduced ratio of 1.7. Fast muscle responds to single stimuli, whereas slow muscle requires 5Hz. In cod tetanic fusion frequencies are around 40Hz, with maximum tension developed around 200-300Hz; $t_{\frac{1}{2}}$ = 15.4msec (Johnston 1980d), V_{max} = 1.01 and 0.53 $L sec^{-1}$, respectively (Altringham and Johnston 1982). The rate of tension development is dependant on stimulation frequency in cod and Tilapia, where $t_{\frac{1}{2}}$ is 6.5 fold greater in fast than slow fibres, activated at 200Hz. The production of a locomotory wave is therefore likely to be determined by both intrinsic (maximum)

contraction velocity, and fibre membrane properties.

Neuromuscular transmission

The structure of vertebrate neuromuscular junctions (nmj) is well documented (Birks et al 1960; Heuser and Reese 1977). Nerve junctions are usually embedded in the sarcolemma. The presynaptic (nerve cell) membrane to post synaptic (muscle fibre) membrane gap is around 20nm, with an apparent reduction in the complexity of the sub-junctional apparatus from mammals > amphibians > fishes (Best and Bone 1973; Heuser and Reese 1977; Kordylewski 1979). Low molecular weight (100-300) molecules are involved in synaptic transmission, with a single nerve cell thought to possess the synthetic machinery for only one - Dale's Principle. Although the same transmitter may have different actions on different post-synaptic cells (e.g. acetylcholine on vertebrate skeletal and heart muscle), the existence of 2 transmitters in mature cells is controversial (Heuser and Reese 1977). Acetylcholinesterase (AChe), is the only esterase to be demonstrated in fish muscle (Andersen et al 1963), although monoaminergic transmission has been suggested for slow fibres (Korneliussen 1973). Glutamate and γ-amino-butyric acid (GABA) mediate excitation and inhibition of crustacean skeletal muscle, respectively (Atwood 1972), with glycine and GABA found in inhibitory synapses of mammalian and fish spinal cord (Grillner and Wallen 1980).

Temperature acclimation

The geographical distribution of many freshwater ectotherms is determined by their physiological tolerance to temperature fluctuations, which may be up to 20°C (diurnal) or 30°C (seasonal). Temperature directly affects enzyme kinetics, with most enzymes (under saturating conditions) doubling the catalytic rate (V_{max}) over a 10°C rise ($Q_{10} = 2$). Many fish exhibit metabolic rate compensation to reduce these changes to tolerable proportions; there may also be a reduced osmoregulatory ability and

impaired CNS function on cold-acclimation (Prosser 1973). The acclimatory response has been classified as Type 1-5 by Precht: over-, perfect-, partial-. zero-, or inverse-compensation (Prosser 1973). Whole body metabolism ($\dot{V}o_2$) shows compensation in rainbow trout (Evans et al 1962), European eel (Jankowsky 1966), Japanese eel (Chan and Woo 1978), ide (Jankowsky and Korn 1965) and goldfish (Smit et al 1974); similar results have been reported for tissue homogenates of brain (Evans et al 1962), liver (Kanungo and Prosser 1959) and skeletal muscle (Evans et al 1962). The mudminnow Umbra limi which inhabits shallow, freshwater habitats show a virtually perfect temperature compensation in $\dot{V}o_2$ between 5° and 20°C (Hanson and Stanley 1969). Likewise, the mummichog Funchulus heteroclitus maintains a relative thermal independance over the range of temperatures found in its salt water marsh habitat during the growth and breeding seasons, 13° to 29°C (Targett 1978). The compensation in locomotory activity is reflected in a positive correlation between maximum swimming speed and acclimation temperature (Griffiths and Alderdice 1972; Smit et al 1974; Brett 1979).

Some metabolic pathways show almost perfect thermal compensation, with the response of others reflecting their relative importance at different temperatures; "metabolic reorganisation" has been thoroughly reviewed (Hazel and Prosser 1974). The pentose phosphate cycle may increase (Kanungo and Prosser 1959; Hochachka and Hayes 1962; Hazel and Prosser 1970) or, more unusually, to remain unaltered (Moerland and Sidell 1981) on cold acclimation. There is a general increase in the enzymes of aerobic (TCA cycle) metabolism (Jankowsky and Korn 1965; Malessa 1969; Wodtke 1974; Sidell 1977, 1980), but the specific activity of carp liver succinate oxidase is unaltered at different temperatures (Wodtke 1976). The enzymes of glycolysis are more variable (Hochachka and Somero 1968; Hazel and Prosser 1974); although a positive

compensation has been reported for muscle LDH a lack of, or inverse, compensation is noted in many species (Wilson 1977; Shaklee et al 1977; Sidell 1980; Jones and Sidell 1981). Similarly, increased activity of muscle PFK is found in cold acclimated winter flounder (Longerich and Feltham 1978), goldfish (Freed 1971) and killifish (Moerland and Sidell 1981).

The length of acclimation required reflects the half-life of protein turnover, usually 4 to 8 weeks for aquatic ectotherms, but this (and the type of response) is dependant on many factors including photoperiod (Prosser 1973; Smit et al 1974; Hazel and Prosser 1974; Johnston and Maitland 1980). Three primary enzyme characteristics are thought to be preserved during acclimation: regulatory sensitivity (response to modulator types and concentrations, and substrate concentrations), catalytic capacity (support of metabolic demands), and structural stability (conformational integrity and reduced lability at cell temperature) (Somero 1975b). Observed metabolic responses are thought to represent a compromise between maximisation of these individual properties (Hazel and Prosser 1970, 1974; Somero 1975, 1978). Maximal enzyme-substrate affinity is maintained at normal (habitat) temperatures, by a parallel reduction in Michaelis constant (K_m) with temperature. At physiological substrate concentrations K_m may be more important than catalytic activity per se (Somero and Hochachka 1971), although in some species it is not affected by temperature acclimation (Wodtke 1976). Cold acclimation is thought to require an increased incorporation of unsaturated fatty acids into phospholipids to maintain membrane fluidity ("homeoviscous" response, Simensky 1974). Function of membrane-bound enzymes is impaired below the transition temperature; therefore, ectotherms must adjust the temperature-sensitive membranes accordingly (Johnston and Roots 1964; Hochachka and Somero 1973; Cossins 1977). The degree of modulation of purified enzyme acitivity by crude lipid extracts has been shown to depend on the prior thermal history

of the membrane, not enzyme (Hazel 1972). However, the correlation between membrane viscosity and unsaturated lipid content may not be present in fish (Knipparth and Mead 1968) and, although a downward shift occurs in the Arrhenius plots of (muscle) mitochondrial enzymes from cold-acclimated goldfish, no correlation could be found with membrane composition (Thillart and Modderkolk 1978). The variability of results may be explained (in part) by the annulus model (Metcalfe 1975) whereby membrane proteins select the specific lipids required for activation, within the membrane; the thermotropic behaviour of this enzyme-lipid complex may be different from the whole membrane.

Wilson (1977) showed that goldfish M4-LDH isozyme was more temperature-sensitive when pH varies with the physiological temperature coefficient, than under constant pH. In contrast to endotherms, that regulate arterial blood to slightly alkaline pH, ectotherm blood pH varies inversely with temperature, maintaining a constant relative alkalinity with respect to the neutral point of water (Howell et al 1970). A similar condition is found for intracellular pH in skeletal and cardiac muscle of dogfish (Heisler et al 1976). An alternative strategy is to regulate a constant protein net charge, rather than a constant OH^- : H^+ ratio, by means of dissociation in peptide-linked histidine residues; in rainbow trout, the effect of temperature on pH optima is consistent with this "imidazole alphastat hypothesis" (Hazel et al 1978).

The mechanisms underlying adjustment in metabolic rate with seasonal changes in temperature are thought to involve a change in gene expression, protein synthesis/degredation, and the microenvironment of key enzyme systems (Sidell 1977; Shaklee et al 1977; Thillart and Modderkolk 1978; Sidell 1980). Synthesis of temperature-specific isozymes may increase enzyme activity in these species with duplicated gene loci (polyploid fish, Somero 1975a), such

adjustments are absent, or very rare, in diploid species (Somero 1975a; Shaklee et al 1977). Many skeletal muscle enzymes have variation at an individual gene locus, giving different alleles (allozymes, Johnston 1982d), which may provide some selective advantage (Johnson 1977; Place and Powers 1979). The most common allozyme of killifish B-LDH in northern latitudes is the most efficient catalyst at low temperatures (Place and Powers 1979). However, there is insufficient data to determine the individual advantage of such polymorphism (Johnston 1982a).

Morphometric analysis

Stereology is a body of mathematical methods relating n-dimensional parameters defining a structure, to n-1 dimensional measurements obtained from probes (sections) of the structure, using geometric probability theory (Weibel 1980). Hence, the 3-D volume of a mitochondrion is visible as a 2-D profile; a membrane, approximating a 2-D sheet, appears as a line; and a 1-D myosin filament as a point. Accurate information is only possible if methodology is carefully controlled at each analytical stage, to give statistically representative samples. Sampling regimes are available for different levels of organisation: animal (samples), organ (blocks), cell (sections), and organelle/structure (micrographs) (Gundersen 1977; Cruz 1976). Similarly, sample, site and size are very important, though rarely reported, leading to variation between authors e.g. with respect to muscle S.R. content. In theory, sections should be random with respect to both organ and cellular structure - isotropic uniform random (IUR). Modelling isotropic (randomly orientated) structures is relatively easy since the orientation distribution readily allows statistically random samples (probes) to be obtained. Anisotropic structures (those showing a preferred orientation) are correspondingly more difficult to analyse accurately, especially biological material which is often partially anisotropic e.g. SR, mitochondria. This requires some compromise, such as using oblique sections or a non-optimal (though defined) method (Weibel 1979; Cruz-Orive 1982).

Analysis is broadly based on the Principle of Delesse, formulated in 1847: the volume density of a component equals the areal density of its profile on a section. Profile dimensions are quantified using a test system of points and lines overlaid on the image, and counting the coincidence of points and profile image, and of lines and profile boundary. Therefore, n-1 dimensional measurements are made with s-dimensional probes, where s=0, 1 or 2 (i.e. point, line or circle). The terms "section" and "probe" have precise mathematical meaning (see Weibel 1980), biological interpretation of these terms is part of the optimisation process mentioned (above). The basic (quantitiative) descriptor is the density of components within a containing space or structure (phase), i.e. the quantity per unit volume, area or length. Different indices, symbols and notations are in use (see Underwood 1970; James 1977; and Weibel 1979); for clarity the double symbol form of Weibel is adopted. The first letter defines the component parameter and the second (subscript) the reference phase e.g. the (numerical) capillary density is given by $N_A(c,f)$: the number (N) of capillaries (c) per unit area (A) of muscle fibre (f). A systematic 2-D point count (using a non-random lattice test system) is the most efficient method of volume density analysis (Mathieu et al 1981); for maximum efficiency the number of occupied points should be $\triangleq$ the number of features analysed (James 1977).

CHAPTER 2

INTRODUCTION

The most common classification scheme for muscle types separates fibres on the basis of their contraction velocity (Close 1972). It is widely accepted that the speed of contraction is correlated with the activity and pH stability of the Ca^{2+}-activated myofibrillar ATPase (Bárány 1967; Bone 1978; Flitney & Johnston 1979). This scheme may be extended to include reference to the enzyme and metabolite profile (Nemeth et al 1979), in order to distinguish between muscles of a similar speed of contraction, but differing patterns of enzyme activity (Close 1972; Bone et al 1978; Akster and Osse 1978).

Heterogeneity in the histological appearance of teleost skeletal muscle has been known for some time (Greene, 1913), but there has been no attempt to analyse the variation in fibre structure or distribution of fibre types, with respect to position in the myotome. Previous studies on fish muscle histochemistry and fine structure have usually involved random, or semi-random, sampling of different muscle regions. Many workers extrapolate the data from small sample sizes to imply a homogeneity of fibre type throughout the myotome. In eels, the elongate body and anguilliform mode of swimming is reflected in a relatively stable red:white muscle ratio along the length of the trunk, in contrast to the sub-carangiform locomotion shown by cod, which demands a dramatic increase in the proportion of red muscle towards the caudal peduncle (see also Mosse and Hudson 1977). This is of considerable advantage for reproducible sampling of the muscle.

The small size of the elver introduces difficulties in studying the differentiation of muscle fibre types using biochemical criteria alone. Qualitative histochemistry, on the other hand, allows the identification of enzyme systems without microdissection and gives directly comparable results for different anatomical regions of the intact specimen. With such a small animal a more detailed examination of regional differences in fine structure,

fibre types, and vascularisation within the myotome is possible, than can be made with larger fish. Such detailed description is essential to an understanding of the developmental processes (fibre proliferation and differentiation) underlying metamorphosis and post-embryonic muscle growth in this type of fish.

There have been few histological studies concerning primitive teleosts, although some qualitative and semi-quantitative data is available for sub-adult eels (Boström and Johansson 1972; Willemse and de Ruiter 1979; Hulbert and Moon 1978a). Similarly, there is little information available about the capillary supply and blood flow to fish muscle (Stevens, 1968; Boddeke et al 1959). The results indicate a correlation between muscle activity, as a function of aerobic capacity, and the development of the capillary network (Bone 1978; Mosse 1978). This study provides the first qualitative description of muscle fibre type heterogeneity within the myotome and the first quantitative description of capillarisation, in a teleost with focally innervated fast fibres.

MATERIALS AND METHODS

Fish

Elvers were trapped on their upstream migration in the lower reaches of the River Severn, Avon, U.K., during February and March 1979; transported on ice and maintained in recirculated, filtered tapwater at 20 $\pm$ 1°C for six months prior to sampling. Freshwater life was therefore 10-11 months and age around $2\frac{1}{2}$ - $3\frac{1}{2}$ years (Boëtius 1976), and corresponded to Stage IVA of Strubberg's (1913) morphological classification.

Weight and length were, respectively, 0.14 $\pm$ 0.10g; 7.3 $\pm$ 0.35cm (mean $\pm$ S.D., n=16). Lyophilised tubifex was fed to satiation 2-3 times per week and feeding was stopped two days before sampling. Photoperiod was maintained at approximately 12L : 12D.

Qualitative changes were investigated in samples caught throughout the migratory period (early February - mid April; see also Chapter 6), and in laboratory-maintained animals up to a period of 12 months.

Histochemistry

Fish were pithed and the sample region located (Fig. 2.1a), this includes the point of maximum flexure and a relatively constant ratio of red:white muscle. The right side was carefully excised before severing the backbone and, in routine examination, dorsal and ventral fin masses removed to assist sectioning. Tissue blocks ($<5mm^3$) were mounted on chilled cryostat chucks, with a thick filter paper interface, in an inert embedding medium (OCT Compound) and immediately immersed in semi-solid iso-pentane (2-methylbutane), cooled in liquid mitrogen, (-159°C) for 30 secs. The degree of freezing damage was assessed by Normosky interference microscopy, and conditions adjusted for optimal tissue preservation. Use of talcum powder (Willemse and de Ruiter, 1979) gave only minimal improvement

in section quality. Blocks were allowed to equilibrate to the cutting temperature of -22 to -18°C for 30 mins., and serial sections cut at 8-10μm on a Slee cyrostat microtome. Sections were supported on dry coverslips and incubation began within a few minutes of cutting. Up to 3 sets of coverslips were incubated simultaneously, under differing conditions (see below), in order to determine the staining characteristics of individual fibres. All incubations were performed on unfixed sections at room temperature (20°C): fixation (10% formalin, neutral Ca^{2+}-formol) or lower temperatures (4°C) gave no improvement in section quality. Sections were mounted (without dehydration) in glycerol jelly on glass slides, and photographed using FP4 (ASA 125) with monochromatic green light or Ektachrome 64 tungsten-balanced film, printed on Cibachrome.

(i) Myofibrillar ATPase (mATPase):

Sections were stained using a modification of the method of Guth and Samaha (1969). Preincubation was carried out in 18mM $CaCl_2$, 100mM 2-amino-2-methyl-1-propanol (221 buffer) at pH 10.0 - 10.6. Optimal differentiation of fibre types was obtained at 7 mins., pH 10.2. Control incubations lacked ATP, or included sodium azide (50mM) to inhibit mitochondrial ATPase activity. Acid pre-incubation (0.1N sodium acetate/acetic acid buffer, pH 4.0 - 5.0, 30 sec. - 2 mins.) failed to give a staining reversal.

(ii) Succinic dehydrogenase (SDH):

Incubation was carried out using 80mM sodium succinate, 50mM potassium phosphate buffer, pH 7.4, and 1mg ml^{-1} nitroblue tetrazolium (NBT) as the electron acceptor (Nachlas et al 1956).

Long incubation times, 2 to 3 hours, were required to give a significant staining reaction. Controls either included sodium azide (50mM), or replaced succinate with malonate, in the incubation medium.

The presence of phenazine methosulphate (PMS), which demonstrates coenzyme-linked, extramitochondrial dehydrogenase activity (Pearse, 1972) failed to improve the degree of staining (cf. Mellgren and Mathisen 1966).

(iii) Cytochrome oxidase (COX):

Sections were incubated in freshly-prepared incubation medium (10ml) containing: cytochrome-c (10mg), catalase (30µg), sucrose (100mg), and 3'3'-diaminobenzidine (15mg) in 0.15M phosphate buffer, pH 7.4, for 15-30 minutes. Control incubations lacked cytochrome-c.

(iv) Lipid:

Staining was carried out using Sudan Black B (saturated solution in propylene glycol) for 30-60 minutes. Control sections were rinsed in acetone prior to staining.

(v) Glycogen:

Sections were incubated for 30-90 mins. in 1% periodic acid, washed thoroughly with tap water and stained with Schiff reagent for up to 60 mins. (PAS reaction; McManus 1946, see Bancroft and Stevens, 1977). Control sections were incubated with 1% amylase in 100mM phosphate buffer, pH 6.3, for 60 mins. prior to incubation, or had the periodic acid incubation omitted.

(vi) Acetylcholinesterase:

Preterminal axons and endplates were stained using the method of Naik (1963). Strips of muscle were pinned on cork strips and fixed using 10% neutral formalin in 0.1N sodium acetate-acetic acid buffer, pH 5.2, for 3 hours at 4°C. Incubation (12 hours, 20°C) was in a freshly-prepared solution containing: 2.5% $CuSO_4.5H_2O$ (0.2ml); 3.7% glycine (0.2ml); 0.1N buffer (8.8ml); and the supernatant from 15mg acetylthiocholine iodide, 0.3ml copper sulphate (added dropwise) and 0.7ml water. Control incubations included eserine sulphate (0.05mM) to inhibit non-specific esterases (Pearse 1972). Muscle was cleared, and small fibre bundles mounted, in glycerol.

Semi-thin sections

Araldite-embedded tissue (see Chapter 3) was sectioned at 0.5 - 1.0μm, flattened on warm slides, dried overnight and stained with 0.5% toluidine blue in 0.5% sodium tetraborate at 60-70°C, or p-phenylenediamine (PPDA; Korneliussen 1972) in 1:1 isopropanol:methanol at room temperature. After washing, sections were dried and mounted in DPX.

Anatomical parameters

Fibre areas were determined from photomicrographs (X50) of PAS-stained cyostat sections projected (X17.5) onto paper and quantified by planimetry: Summagraphics digitiser, interfaced with an Olivetti P6060 minicomputer, using an incremental stream rate of >10 co-ordinate pairs/sec. from a sensitised bit pad of c.0.1mm resolution. With set magnifications, all muscle fibres around the lateral line triangle were sampled within a standard area; this differs from the usual count of a standard number of fibres, and was thought to give a more representative sample to account for regional variation. The percentage of extracellular lipid, red and white muscle was determined in a similar manner from projections of whole-body cryostat or semi-thin sections.

Capillarisation

Tissue was prepared as for the ultra-structure study (Chapter 3). Myotomal regions suitable for analysis were chosen after a preliminary study, using semi-thin sections in conjunction with histochemistry. Tracings of low power electron micrographs (X3300 - X4800 final magnification), were used to quantify mean fibre area, $\bar{a}(f)$, mean fibre circumference, $\bar{b}(f)$, mean number of capillaries per fibre, $\bar{N}(c,f)$, mean capillary area, $\bar{a}(c)$, mean capillary circumference, $\bar{b}(c)$, and mean capillary contact length per fibre, $\bar{l}(c,f)$. Other indices were derived by simple manipulation of measured data (see Table 2.2).

Scanning electron microscopy (SEM)

Gross organisation of the trunk was studied using a Cambridge SEM. Elvers were fixed at resting length as for transmission electron microscopy (TEM) and steaks dehydrated in either alcohol or acetone, to preserve and remove the lipid stores, respectively. Some samples were subjected to cryo-fracture (snapping in absolute ethanol cooled in liquid nitrogen) in order to look more closely at the myosepta and adipocyte structure. Tissue was stabilised with amylacetate, critical-point dried using CO_2, and splutter coated with gold. Specimens were viewed on a Cambridge Stereoscan 600, EHT 15-25kV and spot size 0.3mm, and photographs recorded on FP4.

Chemicals

Glycerol Jelly, 221 buffer, NBT, cytochrome c and catalase were obtained from Sigma, Poole; OCT embedding compound from Raymond Lamb Ltd., London; all other reagents, analar grade where appropriate, were obtained from BDH Chemicals, Poole.

RESULTS

Macroscopic appearance

The distinct difference in colour usually found between fast and slow fibres in teleosts is absent. Slow fibres in the juvenile eel have a pale yellow appearance; this has led some workers to sample elver muscle as a whole, having failed to recognise the existence of different muscle types (Boström and Johansson, 1972). Slow fibres occur all the way around the trunk circumference as a two-fibre deep layer, invaginating along the hosizontal septum and fin insertions (Fig. 2.1b), and represents around 10% of the muscle mass; slow and fast muscle comprising $7.5 \pm 0.950\%$ and $66.3 \pm 0.509\%$ of body cross-sectional area ($\bar{x} \pm$ S.D., n=8), respectively. The myosepta are clearly defined (Figs. 2.22, 2.28, 2.29), as is the lateral line nerve located c.1/3 along the horizontal septum from the skin (Fig. 2.27). The distinct separation of the "red" and white muscle masses is evidenced by a small space appearing between the two layers, especially in araldite sections (Figs. 2.22-23), and is clearly evident under the SEM. Such a connective tissue fascia is more distinct in the adult (Willemse and de Ruiter 1979). Both muscle types stained only weakly with PPDA, in contrast to the adult (Willemse and de Ruiter, 1979) and muscle from other species (trout) stained at the same time.

There are extensive lipid deposits, $12.9 \pm 0.398\%$ of body cross-sectional area ($\bar{x} \pm$ S.D., n=8), with the extensive subcutaneous deposits (Fig. 2.22 and 2.31) often seen close to the myoseptal insertions with the skin (Fig. 2.29). The largest extracellular accumulations are found adjacent to the vertebral column (Fig. 2.22), chiefly along the horns of the haemal arch, at the head of the lateral line triangle, and around the apex of vertebrae (neural arch), and at the base of the fins (Fig. 2.1b). However, this pattern is not uniform along the body. For example, the

apical deposits are elongate and heart-shaped, as seen in LS, , with the broadest portion located in the inter-vertebral regions. Using these anatomical features as reference points, specific regions of the transect can be described and individual fibres located on different sections (Fig. 2.1b).

A qualitatively similar picture is seen in elvers from the earliest available specimens, and those maintained in the laboratory for up to 12 months. There is, however, a gradual proliferation of fibres within the "red" muscle, giving a three-fibre deep layer; a widespread fibre hypertrophy leads to an increase in trunk girth and body weight (see Chapter 6). This is in contrast to the reported growth by fibre hypertrophy alone, in red muscle of eels < 10cm (Willemse and van den Berg 1978).

Fibre size

Slow fibres show an even spread of size around a modal category of 240-360μm^2, with few fibres found >800μm^2 (Fig. 2.18a). Fast fibres show a bi-modal distribution of sizes (Fig. 2.18c) with those fibres <120μm^2 all being of intermediate staining intensity for the aerobic enzymes (Fig. 2.18e, Table 2.1); only three profiles of this type appeared outside this size category. The rest of the fast muscle shows an even spread across a large size range, with c.5% of fibres being >1400μm^2 (Fig. 2.18c). The contribution of fibres sectioned at angles other than TS to the distribution is unknown. However, these erroneously high values are likely only to spread the range of values, rather than substantially alter the modal values (see Chapter 3).

Histochemistry

In common with other teleosts, eel slow fibres have a poly-axonal, multi-terminal pattern of innervation (Bone 1964); whereas fast fibres are innervated by a single "en-plaque" endplate, demonstrable only at one myoseptal end (Figs. 2.25-26). This is in agreement with the situation

described for elasmobranchs (Bone 1978) but not with the scheme proposed by Barets (1961), who envisaged innervation from both ends of the fibre (see also Chapter 7). Fish muscle contraction velocity has been shown to be related to biochemical measurements of myofibrillar ATPase activity (Johnston et al 1972; Flitney and Johnston, 1979) and the histochemical staining reaction following alkaline (pH 10.4) pre-incubation (Johnston et al 1974). Elver slow fibres are alkaline labile and fast fibres are alkaline stable (pH 10.2). Both types of fibre show homogeneous staining for ATPase, irrespective of position or fibre size (Figs. 2.2 and 2.3). No true intermediate, or "pink" fibres could be detected (Johnston et al 1974).

The slow muscle layer also shows an even distribution of staining for the aerobic enzymes and metabolites studied (Figs. 2.4-9). In all cases, the intensity of staining is greater than any of the fast fibres (Table 2.1), but required considerably longer to develop a significant reaction product than other species similarly treated. The homogeneous reaction along the length of fibres (Fig. 2.19) is in apparent agreement with the quantitative results found in mammalian muscle (Pette et al 1980), but contrary to the distribution of mitochondria (see Chapter 3). This may be due to tissue damage causing inactivation of the mitochondria or, more likely, due to a lack of strict correlation between SDH activity and mitochondrial location; it is known that the NBT-formazan complex has a high affinity for protein, and tends to precipitate on lipid-water interfaces (Mellgren and Mathisen 1966).

Fast muscle fibres show a staining profile for enzymes and metabolites which is dependent on both position and size (Figs. 2.2, 4, 6, 8, 10). Large fibres show a homogeneous low reactivity with all staining procedures tested, whereas the smallest fibres in the deep regions, and the most superficial layer of fast muscle, show some SDH and COX activities and a

moderately high PAS staining reaction (Figs. 2.4-10). The occurrence of small fast fibres appears to be random within the deeper regions of the myotome (Fig. 2.28) although closely associated with a larger fibre (see also Chapter 4). The frequency progressively decreases towards the superficial regions, where no PAS +ve fibres can be seen.

Capillarisation

In common with many fish species, histochemical identification of capillaries is unsatisfactory. The clearest reaction found is the localisation of carbonic anhydrase activity (Ridderstale 1979), but this pale reaction is less suitable than morphological identification from semi-thin sections, which was adopted for subsequent analyses. Fig. 2.21 shows a camera lucida tracing of fibres and associated capillaries along a transect from the skin to the vertebral column (see Fig. 2.1b). The various indices of vascularisation show an increase in capillary supply from the fast to slow systems: deep white < superficial white < "red" muscle (Table 2.2). There are no detectable differences in the capillary supply to fibres of different sizes within any group. Deep white fibres have a very anaerobic character with 88% having no capillary contact; however, the superficial white muscle is better supplied, with some fibres having contact with two capillaries (Fig. 2.30). Interestingly, there is a large portion of the slow ("aerobic") muscle without any direct capillary contact (Fig. 2.30).

DISCUSSION

In order to locate more precisely the various metabolic sub-populations, and as an aid to parallel ultrastructure studies (Chapter 3), the characteristic morphology of each cross-section was noted, and used as a frame of reference (Fig. 2.1b). This enabled assumptions about fibre-type heterogeneity to be tested, and led to the recognition of a possible six different categories of fibre (Table 2.1).

Methodological

It is known that there are limitations to the specificity of histochemical reactions (Mellgren and Mathisen 1966). Biochemical analyses have shown that single, microdissected fibres, from histochemically-homogeneous populations, may have a heterogeneous distribution of enzyme activities; although quantitative histochemistry suggests enzymatic homogeneity within fibres of a single motor unit (Nemeth et al 1979). The (focal) innervations pattern of elver fast muscle would appear to make a morphological distinction between motor units very difficult, and it is therefore necessary to rely on gross differences in the histochemical profile to outline functional subunits.

Previously, fibre typing in the eel has been carried out mainly on adults, and has relied on the histochemical demonstration of m.ATPase activity (European eel; Willemse and de Ruiter 1979), or in conjunction with SDH and LDH activities (American eel; Hulbert and Moon 1978a). Care has to be taken in interpreting results based on m.ATPase activity alone, since classification of fibre types may be based purely on pH stability, rather than true differences in specific activity (Guth and Samaha 1972). It has been shown that classifications based on m.ATPase activity vs. m.ATPase and metabolic enzyme activities, are not equivalent (Nemeth et al 1979; Nemeth and Pette 1981); the former groups ("fast", "intermediate", "slow") can be divided into many different subgroups

(Bass et al 1969; Khan 1977). Indeed, the correlation between speed of contraction and m.ATPase activity may not be as straightforward as first thought, since this enzyme may not be rate-limiting for the in vivo velocity (Guth and Samaha 1972). Histochemically, both mammalian tonic (true slow) and fast-twitch muscle may possess a high m.ATPase activity, with the slow-twitch ("intermediate") muscle having a low activity (Guth and Samaha 1969). Muscle with high contraction velocities may have a considerable aerobic potential (Revel 1962); in addition, biochemical assays have shown that red muscle from rabbit has an m.ATPase activity 25-55% higher than white muscle (Syrový and Gutman 1971). A similar relationship between red and white muscle activity is also described for the agnathan Myxine (hagfish; Dahl and Nicolaysen 1971), and anuran tail muscles (Watanabe et al 1978). However, such comparisons take no account of specific or phylogentic, differences and such red fibres are thought not to be equivalent to the type I fibres described for mammals or birds (Andersen et al 1963; Teräväinen 1971; Dahl and Nicolaysen 1971; Watanabe et al 1978). In elasmobranchs and teleosts, however, the m.ATPase activity would appear to parallel the contraction velocity (Bone et al 1978; Flitney and Johnston 1979).

Experimental

On this basis, two fibre types have been described in the Brook trout (Johnston & Moon 1980a), three in carp (Johnston and Maitland 1980) and five in dogfish (Bone & Chubb 1978). Similarly, histochemical staining for m.ATPase activity reveals two distinct classes of fibre in the elver trunk, both having a homogeneous reaction throughout their size range and position within the myotome (Figs. 2.2, 2.3). No fibres with an intermediate m.ATPase activity or pH stability were found, as has been reported for a number of other species (Johnston et al 1974, Patterson et al 1975, Bone and

Chubb 1978). In contrast, a small population of intermediate fibres are reported within the fast muscle of the American eel (Hulbert and Moon 1978a), but are thought not to occur in adult European eel (Willemse and de Ruiter 1979); whereas "displaced" fibres are reported for both Atlantic species (Hulbert and Moon 1978a, Willemse and de Ruiter 1979). These occur as a discontinuous layer of fast fibres located among the slow muscle, and vice versa. It is possible that the superficial white muscle described in this study, for the young eel, gives rise to such populations. It should be possible to resolve the origin of such fibres by means of immunohistochemical reactivity to the different myosins (Raamsdonk et al 1980).

Elver fast muscle can be further sub-divided into 3 metabolic sub-groups on the basis of staining for aerobic enzyme activities (SDH, COX) and metabolites (glycogen, lipid) (Table 2.1) i.e. SW, (SMW + SDW), (MW + DW). Such a mixture of fibre sizes has been known in salmonid "mosaic" muscle for some time (Greene 1913; Boddeke et al 1959) and gives a similar discontinuous PAS reactivity (Johnston et al 1975). In carp (Johnston et al 1977) and flathead (Mosse and Hudson 1977), the small PAS+ve fast fibres may be further differentiated on the basis of their stability to alkaline (pH 10.4) pre-incubation prior to staining for m.ATPase activity (Patterson et al 1975). It has been suggested (Hulbert and Moon 1978a) that the small fast fibres may represent a functionally separate fibre type in eel. Since they cannot be classified as "pink" or true intermediate fibres (see also Willemse & de Ruiter 1979; Hulbert and Moon 1978a) on the basis of the m.ATPase activity, it is possible that they constitute a fast oxidative fibre group. On the other hand, the relatively high glycogen content and aerobic enzyme activities are consistent with the situation found in newly differentiated fibres in both mammals and fish (Waterman 1969; Goldspink 1972). In trout, these small PAS +ve fibres are thought to provide a site for the

aerobic catabolism of lactate, formed during fast muscle anaerobic glycogenolysis (Johnston and Moon 1980a). The small proportion of the white muscle mass formed by these fibres in elver (~5%) and the lack of a significant glyconeogenic potential in eel white muscle (Hulbert & Moon 1978b) suggests that this can only be of minor significance in elvers.

The histochemical profile of slow muscle fibres indicates a more aerobic metabolism than that of the adjacent fast fibres; however, the long incubation time required suggests a low, absolute, aerobic potential; less than usually associated with fish slow fibres (Bone 1978; Johnston 1981a). This was confirmed by parallel incubations for SDH, which gave the order of staining intensity trout >cod >elver. The pale yellow colour of the slow muscle is also indicative of a low aerobic potential, since the red appearance of fish slow muscle reflects the amount of myoglobin and extent of capillary blood present. Differentiation of the small and large fibres was difficult due to the fairly even staining of all fibres. The proliferation of slow fibres during 8-10 months of tank life, from a 2- to a 3 or 4-fibre layer, is at odds with the study of Willemse & van den Berg (1978) that suggests growth by proliferation only occurs after eels attain 10cm. Differences in the growth rate of the two animal groups may account for this discrepancy, but more experimentation is required to resolve the important question of growth pattern (see Chapter 4).

Fast fibres are focally innervated by a single "en-plaque" type endplate (Figs. 2.25, 2.26); this type of fast fibre innervation appears to be typical of primitive teleosts (Bone 1964, 1978), of which eels are a common example. The low aerobic capacity and capillary supply to deep fast fibres in the eel is compatible with a similar pattern of fibre recruitment to that found in other primitive fish (Chapter 5). Interestingly, Grillner and Kashin (1976) have reported electrical activity in the white muscle of adult

eels, even at low swimming speeds. This resembles the pattern of fibre recruitment found in higher teleosts, with multiply innervated fast fibres, where it is often possible to record electromyograms over a wide range of swimming speeds (Hudson 1973; Johnston and Moon 1980b). The superficial white muscle in the elver shows a more aerobic character than the deep white fibres, and may represent a functional sub-type of the fast fibre system. There is some evidence, in the coalfish, that the superficial fast fibres can be recruited at lower swimming speeds than deeper fast fibres (Johnston and Moon 1980b); and some differences in the innervation of these two regions has been shown in the cod (Altringham and Johnston 1981). Electromyographical studies in the carp have shown the order of recruitment of fibre types with increasing swimming speeds to be slow > fast aerobic (intermediate) > fast glycolytic (Johnston et al 1977). Further e.m.g. studies would be required to discover whether the pattern of fibre recruitment in eels differ from that reported for dogfish (Bone 1966) and herring (Bone et al 1978), as the possibility remains that electrical activity recorded in eels at low swimming speeds originates from these superficial aerobic fibres.

Comparative data for the vascularisation of fish muscle is limited to a few teleosts and elasmobranchs (Mosse 1979; Flood 1979) and for a chondrostean, Acipenser stellatus (Kryvi et al 1980), many of the indices being borrowed directly from mammalian studies. Such quantification (Totland et al 1981, Johnston 1982a, 1982b) may be correlated to the metabolism of highly aerobic, homogeneous muscle types, but seem to be inappropriate for muscle with a sparse, and heterogeneous, capillary supply (see Chapter 5). In the elver, the proportion of fibres in direct contact with the capillaries within the red, superficial white, and deep white regions are, respectively, 72.5%, 26.5%, and 12.4% (Table 2.2). The average number of capillaries per fibre for the three categories are 0.98, 0.33, 0.12

(RF, SW, DW). The white muscle appears to have only slightly fewer capillaries/fibre than that of other species: Acipenser, 0.2 (Kryvi et al 1980); Australian salmon, 0.14 - 0.27 (Mosse 1979); Myxine and the flathead having similar values, around 0.6 - 0.7 (Flood 1979; Mosse 1979). However, the slow fibres, with 0.98 capillaries/fibre, has significantly less than that found in the above species: 2.3, 1.9 - 4.2, 2.76, and 5.3 - 6.6, respectively. Regional differences in the slow muscle capillary supply may differ by a factor of 2 in some large species (Mosse 1979; see also Chapter 5), but this is difficult to investigate in elvers with such a narrow layer of red fibres. Regional differences in the fine structure of elver muscle is evident (Chapter 3), and this would indicate that a similar variability is probably present. The range of values found in fish is illustrated by comparing the elver to the pelagic Anchovy, which has 12.9 capillaries per slow fibre, resulting in over 50% of the fibre surface being vascularised (Johnston 1981b). Only 70% of elver slow fibres are in direct contact with capillaries. It would appear, therefore, that elver slow muscle has a lower aerobic capacity than found in many other fishes, using similar criteria (Bone 1978; Johnston 1981a). The superficial white fibres have a capillary density between that of red and deep white fibres, and is in agreement with the situation reported for the intermediate fibre layer in Acipenser and Myxine. This correlates well with the relative aerobic capacity, as shown by histochemistry. The poor vascularisation of the fast muscle is in agreement with the low intramuscular oxygen tension found in yellow eels, Po_2 = 1-3mm Hg (Jankowsky 1966).

The downstream, sexual, migration of the silver eel is associated with increases in activity of muscle aerobic enzymes and intracellular lipid content (Boström and Johansson 1972; Lewander et al 1974; Pankhurst 1982). The increase in red muscle volume with sexual maturity ranges from around 5%

in immature (yellow) eels up to 13.3% in adult (silver) eels (Pankhurst 1982). Other estimates give similar results, ranging from 8.8% in yellow eels (Greer-Walker & Pull 1975) to 16% in bronze eels (Hulbert & Moon 1978). This pattern of increased aerobic metabolism would appear to be a common feature of migration (Fontaine 1975). In the yellow eel, the low respiration rate (Berg and Steen 1965) and moderate gill surface area (Byczkowska-Smyck 1958) are reflected in its slow swimming and bottom-dwelling habits (Deelder 1970). The small diameter red fibres, and lack of a well-developed lateral line wedge, led Boddeke et al (1959) to classify the eel as a "sneaker" i.e. sharing neither the characteristics of a high-powered burst swimmer, nor those of a sustained swimmer. With respect to migration, then, the present study suggests that the elver reacts somewhat differently to other species. Migration involves periods of prolonged active swimming and even under laboratory conditions elvers are usually active, especially if flowing water is present (see also Deelder 1959). Although the slow muscle system is moderately well developed, the histochemical and capillary data indicates a surprisingly low aerobic capacity. This is supported by the low oxygen consumption of elvers, during both basal and active metabolism, relative to the young of other Mediterranean species (Alekseyeva 1973). Assuming that a good correlation exists between activity pattern and metabolism, as is found in other fish (Johnston & Moon 1980a,b; 1981a), then the contrast between aerobic scope and migration requires some explanation.

This apparent discrepancy would be removed if the energetic cost of the upstream migration is less than at first supposed, either as a result of behavioural and/or functional adaptation. It is known that some species of fish, e.g. cod and plaice, only swim with favourable tides and shelter on the sea bed against opposing tides (Harden-Jones 1977). Such a mechanism has been suggested for the seawater-freshwater orientation of glass eels

(Creutzberg 1958), and "selective tidal transport" has been shown in the American elver which achieves upstream migration on flood tides, seeking refuge in slack water during the ebb (McCleave and Kleckner 1982)and the time elvers move out of the tidal reaches of a river some considerable growth has taken place (Tesch1977) and, possibly, an increased anaerobic energy potential which would be needed for the more dramatic movement into streams (Tesch 1977). In addition, the propagated locomotory wave in anguilliform locomotion is characteristically of high amplitude and low velocity (Gray 1933). It would appear that this form of swimming is energetically most efficient at low speeds (Webb 1978), and the range of efficient sustained swimming speeds will therefore be restricted, relative to carangiform and sub-carangiform locomotion. This would suggest a limited and rather inflexible aerobic scope for activity, which is consistent with the observed low aerobic potential of the slow muscle.

Table 2.1 Summary of the histochemical staining profile of elver trunk muscle.

	Myotomal fibre type and position					
Enzyme or metabolite	RF 0–2	SW1 2–4	SW2 2–4	MW 6–8	DW 10–12	SDW 6–12
Myofibrillar ATPase	0	+++++	+++++	+++++	+++++	+++++
SDH	+++	++	+	0	0	+
COX	++++	++	+	0	0	+
PAS	+++++	++	+	0	0	++
Lipid	+++	+	+	0	0	0

0 = background stain only, + = light stain, +++++ = heaviest stain. The red fibre category (RF) includes all part of the slow fibre system. SW1 refers to the superficial white muscle adjacent to the lateral line triangle, and SW2 to the superficial white fibres from peripheral myotomes. MW and DW refer to the medium-and deep-white fibres, respectively. SDW indicates the small fibres of the fast fibre system, found in the MW and DW regions. The numbers at the head of each column refer to the number of fibres deep from the skin (see Fig. 2.1B).

Table 2.2. Indices of vascularisation in the elver trunk sampled at three positions. Mean ± S.D.

Fibre type	No. of fibres and capillaries sampled	mean fibre area (μm^2)	mean number of caps./fibre	mean fibre perimeter(μm)	mean capillary contact length/ fibre (μm)	vascularised fibre perimeter	mean + capillary area(μm^2)	area of muscle supplied by Unit area of capillary(μm^2)
	$N(f), N(c)$	$\bar{a}(f)$	$\bar{N}(c,f)$	$\bar{b}(f)$	$\bar{l}(c,f)$	$\frac{\bar{l}(c,f)}{\bar{b}(f)}$	$\bar{a}(c)$	$\frac{\bar{a}(f).N(f)}{\bar{a}(c).N(c)}$
Slow Fibres (RF)	131, 59	190.5±193.5 (179.3± 66.9)	0.98±0.78 (1.35±0.58)	52.6±17.0 (55.2±17.7)	4.8±3.2	0.087	13.5±7.52	33.0
Superficial white fibres (SW)	117, 17	274.4±211.1 (269.5±232.9)	0.33±0.63 (1.26±0.57)	70.3±93.0 (60.6±26.2)	4.4±3.7	0.073	12.4±7.58	199.2
Deep white* fibres (DW)	137, 9	286.7±240.7 (349.9±296.5)	0.12±0.33 (1.0)	63.4±32.0 (70.1±32.5)	3.3±2.0	0.047	10.9±3.00	400.4

Note: Figures in brackets indicate values for the vascularised portion of the muscle only i.e. includes fibres in direct contact with a capillary. *includes SDW fibres. No significant difference was detected between MW and DW fibres, for any parameter; nor could any correlation be found with fibre size. + includes only those blood vessels $<50\mu m^2$. This corresponds to the morphological classification adopted by Casley-Smith et al, 1975.

Fig. 2.1. a) Outline of an elver used in this study; samples were taken at a position between the two arrows, located posterior to the cloaca and within the anterior portion of the ventral fin.

b) Diagrammatic cross-section of an elver trunk at the point of sampling, showing the anatomical details used in mapping each section. The numbers along the transect refer to the number of fibres deep from the skin, and are used in the delineation of the muscle regions under study. Major blood vessels are found adjacent to the myospeta, with the largest occurring within the fascia dividing R and S layers, and at the base of LT (the lateral cutaneous vein). Muscle makes up $73.8 \pm 5.05\%$ ($\bar{x} \pm$ S.D; $n = 8$) of the body cross-sectional area at this point, and varies little along the body (anteriorly or posteriorly) for at least a similar distance to that used in sampling.

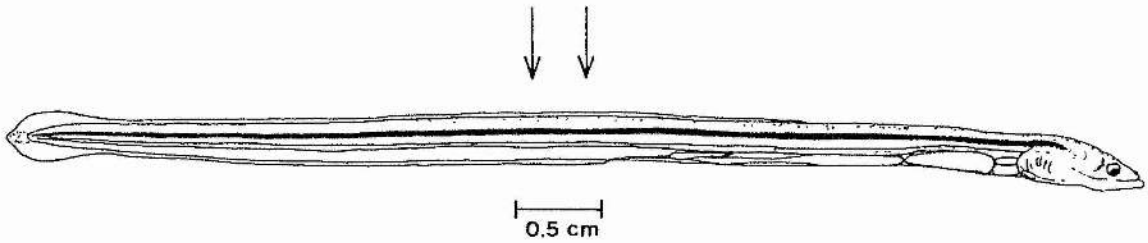

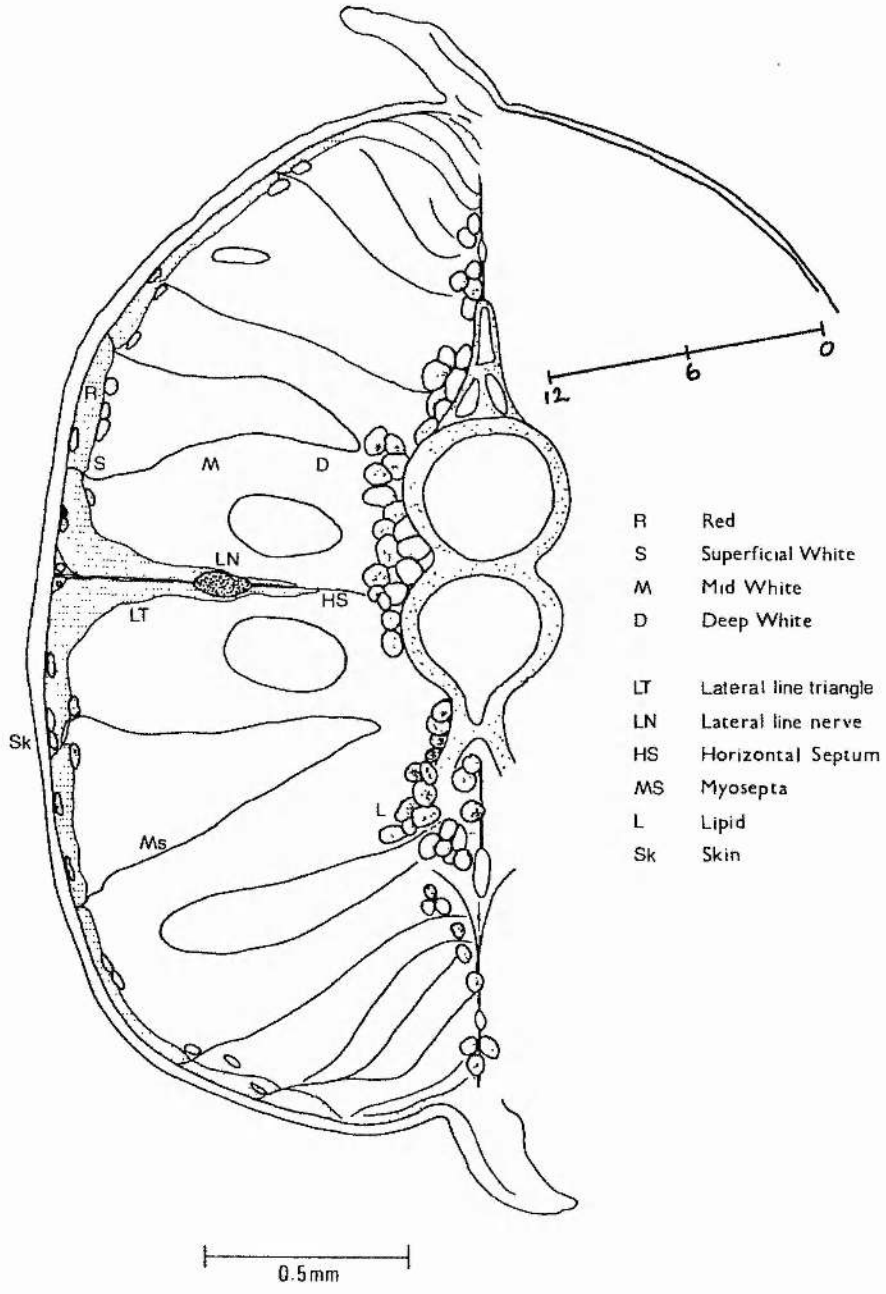

R	Red
S	Superficial White
M	Mid White
D	Deep White
LT	Lateral line triangle
LN	Lateral line nerve
HS	Horizontal Septum
MS	Myosepta
L	Lipid
Sk	Skin

Figs. 2.2. - 2.11. Histochemical staining, frozen sections:

Fig. 2.2. Myofibrillar ATPase; showing the region around the lateral line triange (LT). Homogeneous staining can be seen in both the slow (pale) and fast (dark) fibres. Skin and melanophores are visible on the left, with myospeta and the lateral line nerve (LN) towards the centre. 10μm section. Scale bar = 100μm.

Fig. 2.3. Myofibrillar ATPase; detail showing the distinct segregation of the slow and fast fibres. Adjacent, epaxial, myotome to that shown in Fig. 2.2. 8μm section. Scale bar = 20μm.

Fig. 2.4. SDH; area around LT, showing the moderate staining for slow (dark) fibres and the slight reaction found in the superficial white fibres (SW1, see Table 2.1). 10μm section. Scale bar = 100μm.

Fig. 2.5. SDH; detail of adjacent myotome showing the intermediate reactivity of the superficial white fibres (SW2, see Table 2.1) relative to the slow (dark) and fast (pale) fibres. 8μm section. Scale bar = 20μm.

Fig. 2.6. COX; area around LT showing intermediate staining of the SW1 fibres. 10μm section. Scale bar = 100μm.

Fig. 2.7. COX; peripheral myotome showing the more intense staining reaction of slow than fast fibres. Note the clearer delineation of reaction products, and reduced background staining, compared to the SDH stain. 8μm section. Scale bar = 20μm.

Fig. 2.8. PAS; area around LT showing the variability of glycogen deposits within the fast fibres, relative to the slow (dark) fibres. Skin, myosepta and lateral line nerve are also stained. Note the depth of the SW1 zone. Staining of the skin is mainly restricted to the epidermis. 10μm section. Scale bar = 100μm.

Fig. 2.9. PAS; adjacent myotome showing the progressive reduction of stain from the SW1 to SW2 regions. 8μm section. Scale bar = 20μm.

Fig. 2.10. PAS; detail of SDW showing the higher staining than the adjacent DW fibres, which are delineated by stain in the vicinity of the sarcolemma. 8μm section. Scale bar = 10μm.

Fig. 2.11. Sudan Black; detail of peripheral myotome showing the relative difference in lipid deposits between the slow (dark) and fast (pale) fibres. 8μm section. Scale bar = 20μm.

2

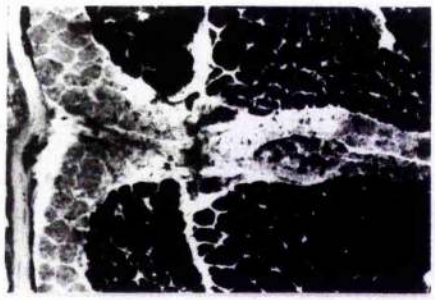

3

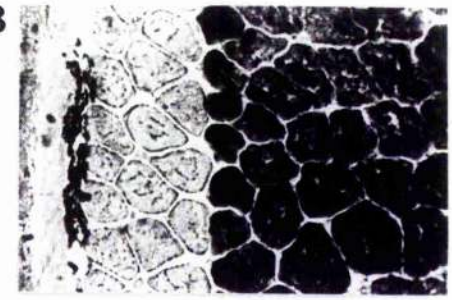

4

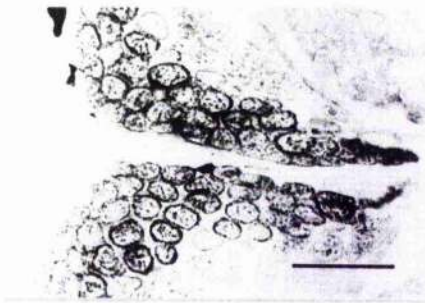

5

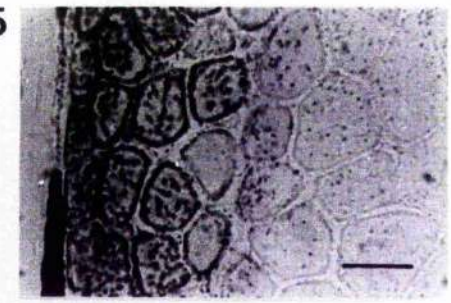

6

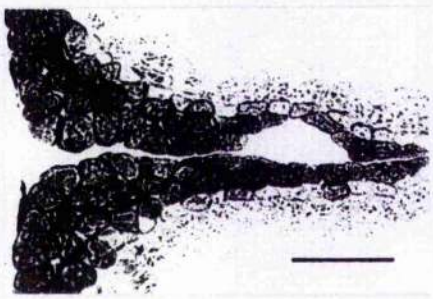

7

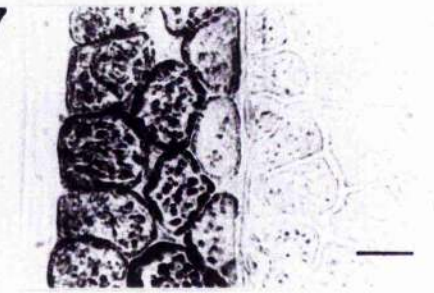

8

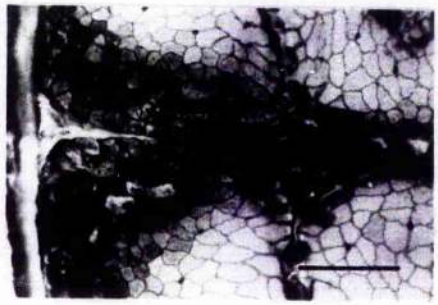

9

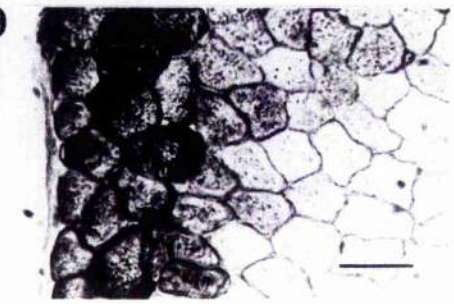

10

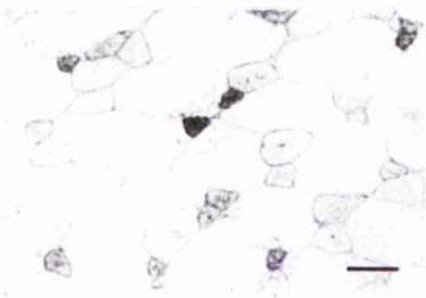

11

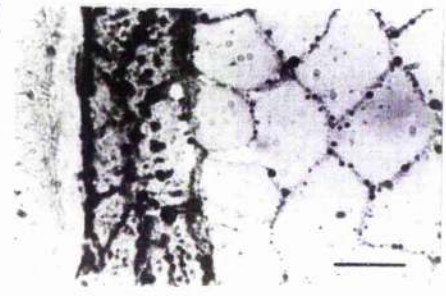

Fig. 2.18. Histograms showing the frequency distribution (%) of fibre cross-sectional area, $\bar{a}(f)$, determined by planimentry of PAS-stained frozen sections.

a) Slow muscle (RF, n=378)

b) Superficial white muscle (SW1 + SW2)

c) Deep white muscle (MW + DW + SDW)

d) Combined data for all fast fibres (n=1729)

e) Expanded view of the small fast fibre data (SDW)

Note the contribution of the SDW to the bimodal distribution of the fast fibre size, extending the large range seen within the fast system.

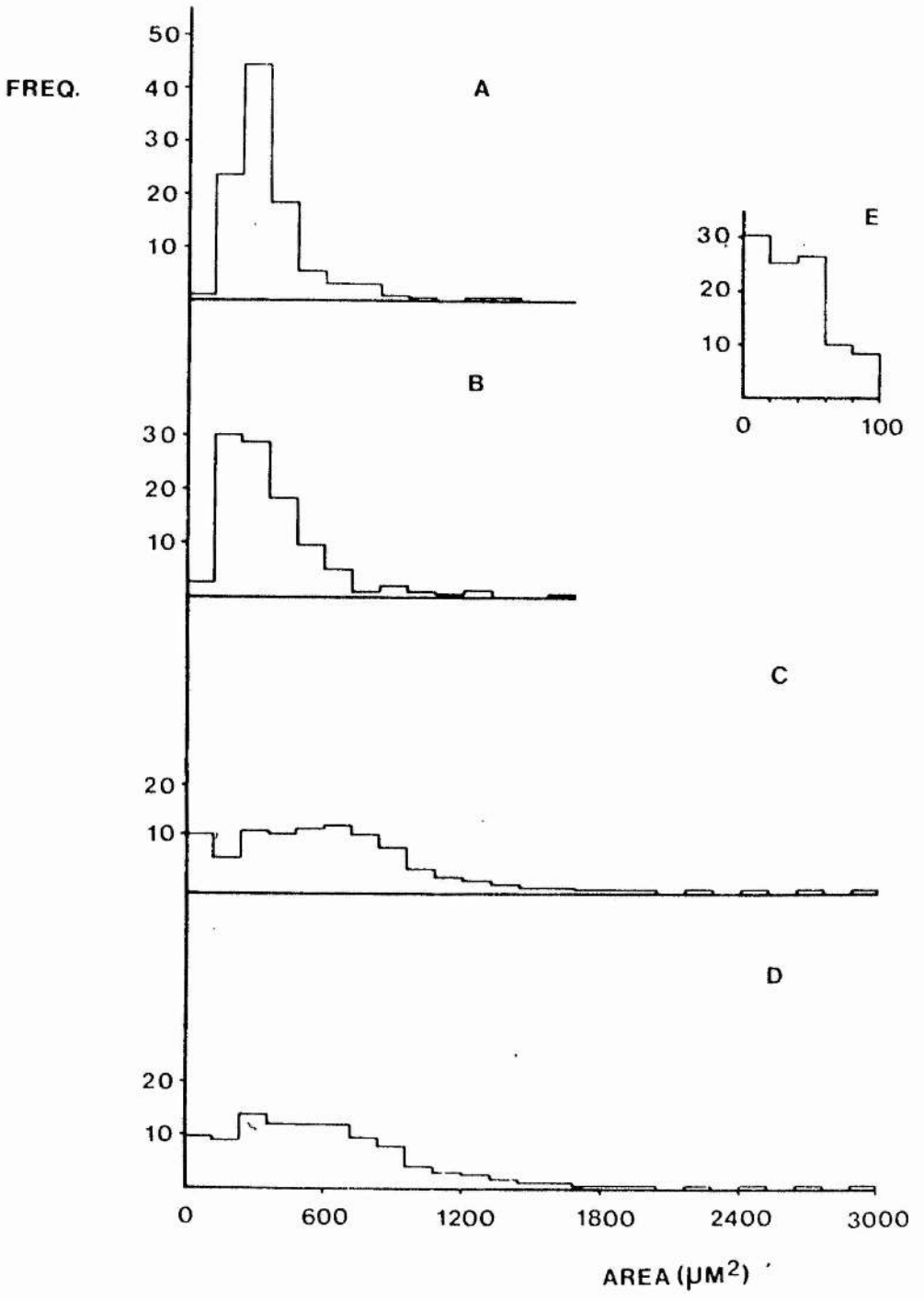
FREQ.
A
B
C
D
E
50
40
30
20
10
0
100
0
600
1200
1800
2400
3000
AREA (μM2)

Fig. 2.19. Histochemical staining for SDH activity; frozen section of slow fibres at the level of the transect (see Fig. 2.1b) showing even staining along the whole length of the fibres. L.S., 10μm section. Scale bar = 10μm.

Fig. 2.20. Semi-thin section of epaxial myotomes illustrating the thickness of the myosepta, relative to muscle fibre size. The preferential localisation of lipid and major (venous) blood vessels along the myospeta is also shown. Capillary supply to the red muscle is evident; note especially the location of a number of vessels adjacent to the RF-SW interface. Toluidine Blue stain, 0.5μm section. Scale bar = 100μm.

Fig. 2.21. Transect of elver muscle from the skin towards the vertebral column, showing the relationship of fibre size within the various regions under study and relative distribution of capillaries. Stipple = RF, hatching = SW fibres. Camera lucida tracing of semi-thin section.

Fig. 2.22. Semi-thin section (T.S.) of the LT region. Note the slow muscle layer (darker fibres) and large lipid deposits associated with the invagination. Nuclei, capillaries and lateral line nerve are also clearly visible, as is the vertebral column of the apex of the LT. Scale bar = 100μm.

Fig. 2.23. Semi-thin section (T.S.) of slow (RF) and fast (SW) muscle interface (fascia, F) showing the relative size of the lipid deposits (see also Fig. 2.31.). Skin is visible at the bottom, and the differing capillary supply is evident. Material from an older elver than used in this study, as shown by the proliferation of slow fibres into a 3 or 4 fibre deep layer. Note the presence of small fibres (growth stages) within the slow muscle, but not within the superficial fast. Scale bar = 40μm.

Fig. 2.24. Semi-thin section (L.S.) of MW muscle showing the insertion of fibres into the myoseptal sheet (MS). Note the large lipid deposits and the numerous darkly staining myonuclei, undifferentiated pericytes and connective tissue fibroblasts. This region also contains large blood vessels, afferent and efferent, and small nerve bundles running normal to the plane of section, on both sides of the myoseptum. Scale bar = 40μm.

19

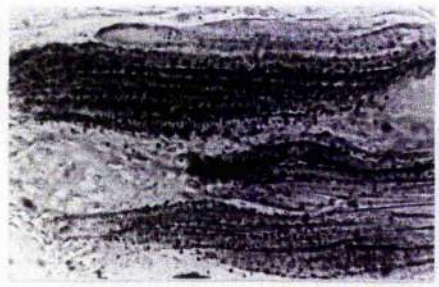

20

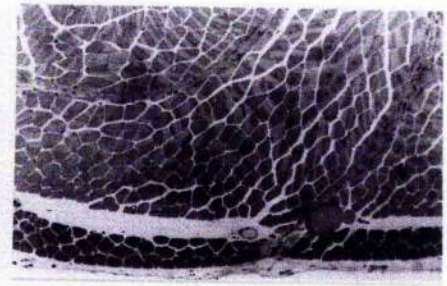

21

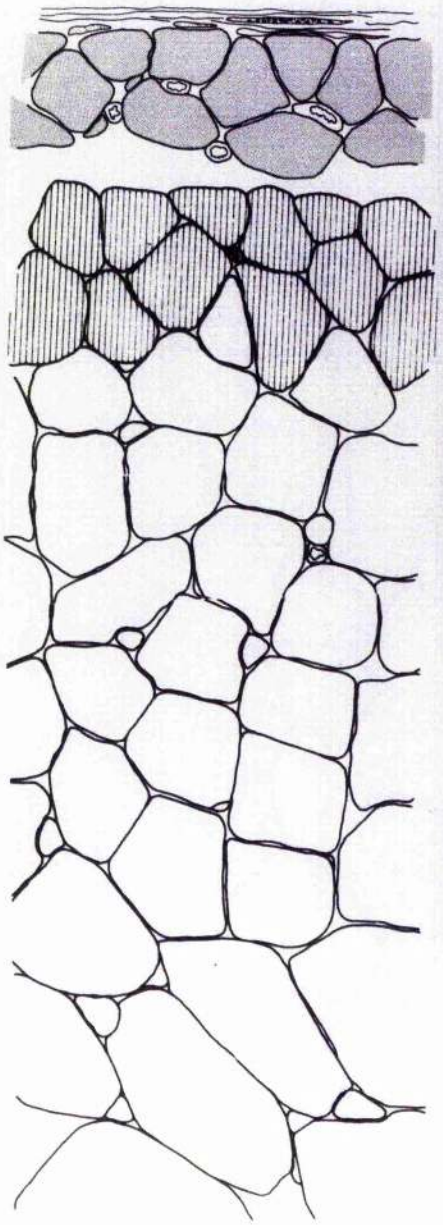

22

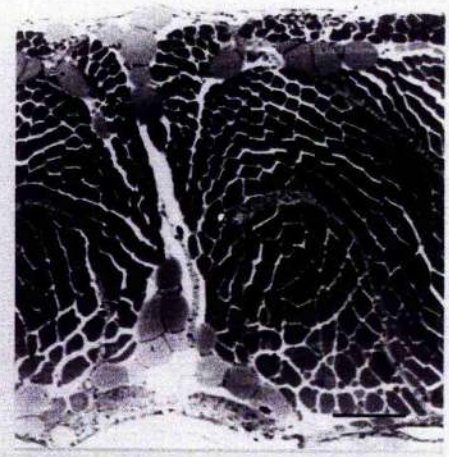

23

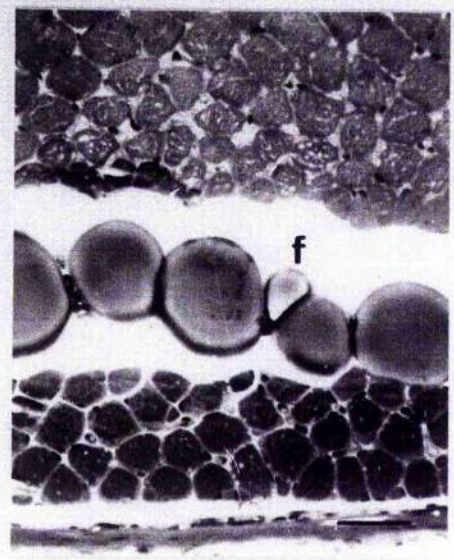

24

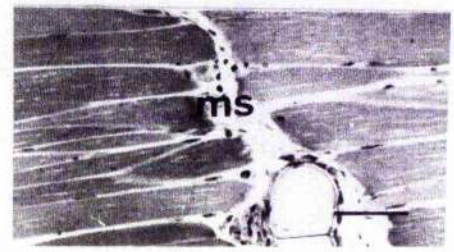

Fig. 2.25. Teased fibre bundle; histochemical staining for acetylcholinesterase activity. Glycerol-cleared sample from fast muscle showing typical striation pattern and an "en-plaque" endplate (detached and reflexed) with multiple sites of stain deposit. MW region. Scale bar = 20μm.

Fig. 2.26. Similar preparation to Fig. 2.25, but showing a prominant pre-terminal axon. Scale bar = 20μm.

Fig. 2.27. Semi-thin section (T.S.) of the LT slow muscle (dark fibres) and surrounding fast fibres. Note the large lipid deposits (L) and prominant lateral line nerve (LN). The horizontal septum (top, centre) is seen to run along one side of the central portion, unevenly dividing the lipid deposits. Capillaries are clearly visible as open circles with darkly staining endothelial pericytes. Toluidine Blue stain, 0.5μm section. Scale bar = 100μm.

Fig. 2.28. Semi-thin section (T.S.) of fast muscle, MW (bottom) and DW (top) regions. Note the close association of some fibres with the myosepta, and the presence of small fibres at the "apices" of large fibres. The sparse distribution of capillaries is also evident, and an intramuscular bone (bottom, right). Scale bar = 100μm.

Fig. 2.29. Semi-thin section (T.S.) of myotomal apex (centre) within the epaxial quadrant. LT apex is visible (top, left) and vertebral column (bottom, right). The close association of the blood supply and myosepta is seen, being exaggerated in this section of the tip of the cone-shaped myotome. Scale bar = 50μm.

Fig. 2.30. Frequency distribution of the capillary contact made by fibres of the three main muscle types, RF, SW and DW. Note the spread of values for both RF and SW fibres, and especially the large percentage of slow fibres without any capillary contact.

25

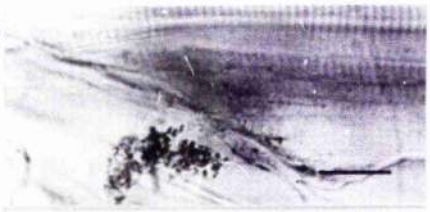

26

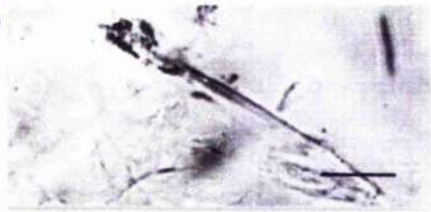

27

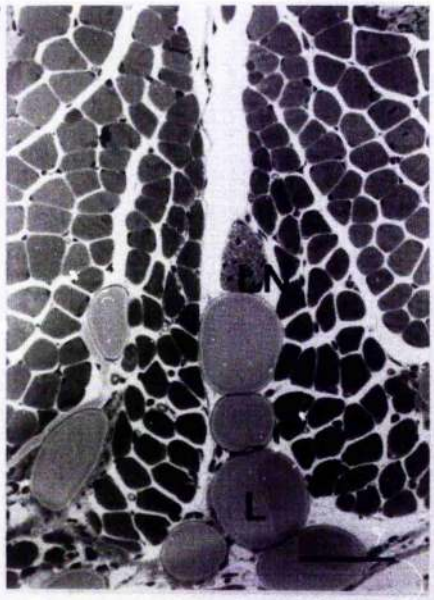

28

29

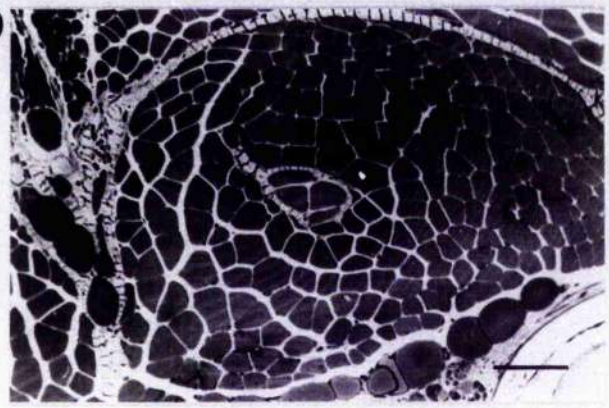

30

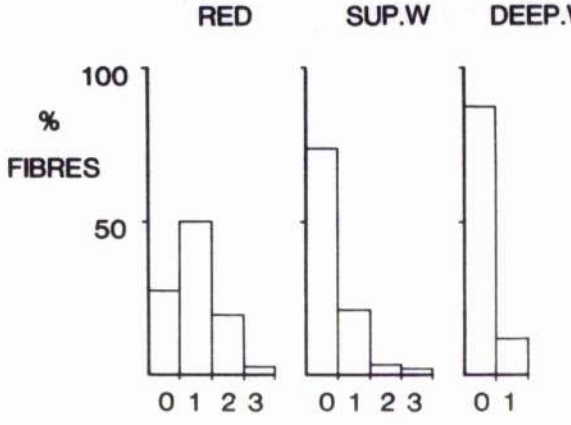

Fig. 2.31. SEM, elver trunk, alcohol dehydrated. The extent of subcutaneous lipid deposits is obvious; note the relative size of slow muscle fibres (right). Adipocytes and abundant connective tissue are also shown. Intra-fibre lipid can be seen (right), as well as small inter-fibre deposits. Sample taken epaxial to myo-septal insertion to the skin (bottom, left); sectioned material Scale bar = 5μm.

Fig. 2.32. SEM, elver fast muscle. The more even sectioning is evident, and the range of fibre sizes apparent. Capillary profiles were difficult to identify, and resolution of satellite cells was not possible. Alochol-dehydrated material. Scale bar = 10μm.

31

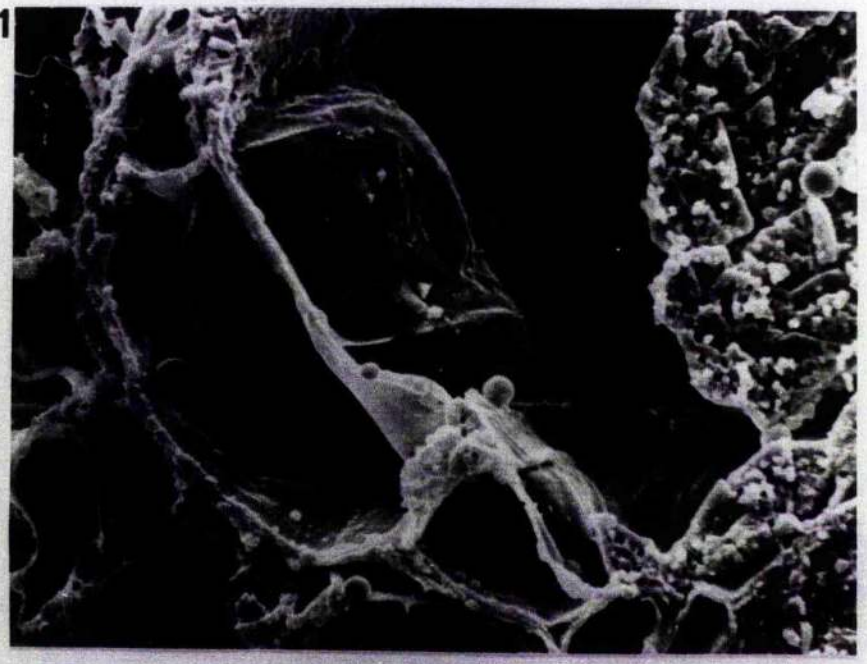

32

Fig. 2.33. SEM, elver fast muscle, MW region. Acetone-dehydrated material. Removal of the inter-fibre lipid reveals the extent of the connectives linking individual fibres. Relief-patterns of fibre striations can be seen. Satellite cell profiles were visible along the length of some fibres, but detailed resolution was not possible. Sectioned material, with the splaying of muscle fibres being due to fixation shrinkage. Scale bar = 10μm.

Fig. 2.34. SEM, conger slow muscle, alcohol dehydration, cryo-fractured specimen. The adipocyte network covering the lipid deposits is clear; qualitatively very similar to homologous cells in elver muscle. The absolute size of the lipid globules is greater than in the elver, giving a similar size difference between the lipid deposits and slow muscle fibres in both species. Scale bar = 10μm.

Fig. 2.35. SEM, conger slow muscle. Cryo-fracture of alcohol-dehydrated material showing the uneven fracture planes within the fibres, reflecting the heterogeneous composition. Scale bar = 10μm.

Fig. 2.36. SEM, conger fast muscle. Similar preparation to Fig. 2.35, but displaying a much more homogeneous fracture pattern. The close-packing of the fibres is clearly seen, as are the different sizes of fibre. Scale bar = 10μm.

33

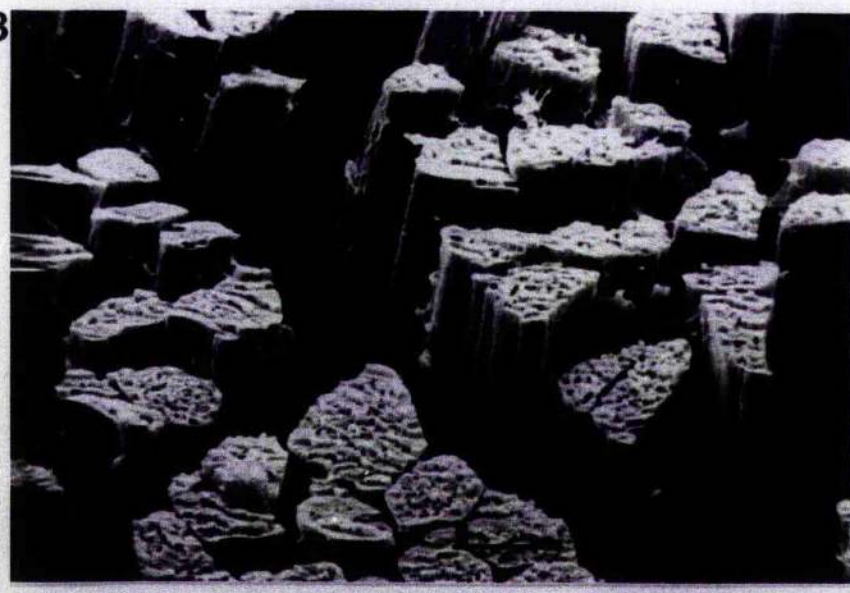

34

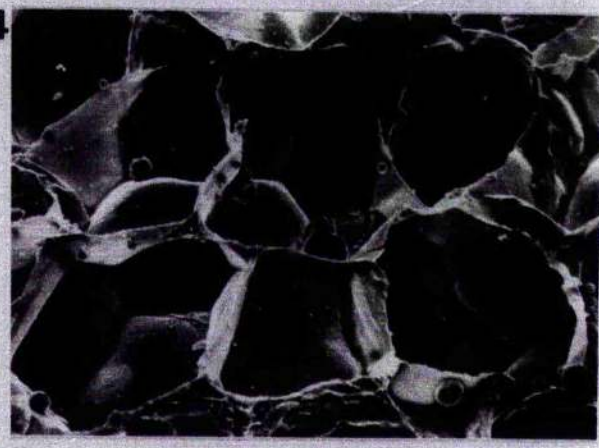

35

36

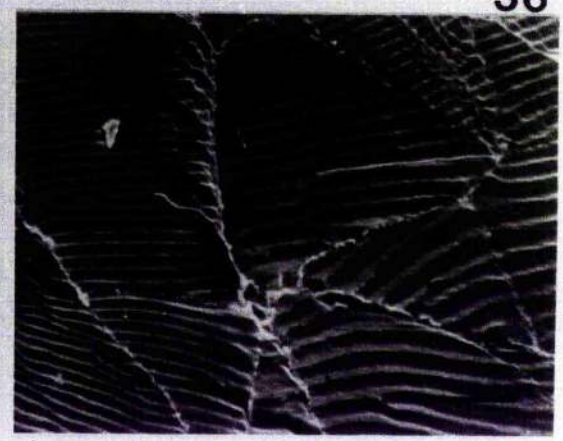

CHAPTER 3

INTRODUCTION

Two distinct fibre populations can be distinguished in the parietal (trunk) muscle of elvers on the basis of histochemical staining for m.ATPase activity (Chapter 2). Although fast fibres show a uniform staining reaction for m.ATPase, the apparent aerobic potential is highest in the most superficial fibres, and the smallest of the deep fibres. Mammalian twitch muscle fine structure is known to correlate with the histochemical and contractile properties (Close 1972) i.e. fine structure reflects the physiological function of the muscle. Little information is available, however, concerning the correlation of such parameters in fish and, in view of the range of gross structure and function (Bone 1978), this may be a significant omission. In the context of the present study, such an examination is necessary before any attempt can be made to utilise this (apparently) simple system for investigating developmental differentiation, or environment-induced plasticity, of the muscle during the elvers' varied life history.

No information is available with respect to the heterogeneity of contraction velocities, or biochemistry, of muscle fibres within the myotome. Some general conclusions can, however, be derived from the degree of structural variation, since this must impose direct physical and metabolic limitations on the cells. The small number of quantitative fine structure studies have all dealt with advanced teleosts (see Bone 1978 for refs.); this is the first study of skeletal muscle from a primitive teleost.

MATERIAL AND METHODS

Fish

Specimens were taken from the same population of animals as in Chapter 2, killed a few weeks later. These were slightly larger, weight and length being 0.31 ± 0.16g and 7.6 ± 0.70cm. (mean $\pm$ S.D., N = 28), respectively.

Tissue preparation

Fish were pithed and pinned on strengthened cork strips with the body in a straight position, approximating resting length. The muscle was carefully dissected from the right side, either with or without the skin remaining on the left (untouched) side, leaving a maximum diffusion distance for the fixative of 2-3mm. Muscle was fixed <u>in situ</u> using 3% gluteraldehyde in 0.15M phosphate buffer, pH 7.4, at 20°C for either 4 (small samples) or 24hrs. (whole body samples). Difficulty was experienced in obtaining good contrast in sections of slow muscle. This was improved by thorough rinsing in buffer prior to commencing fixation, and frequent changes during fixation, possibly due to the extraction of mucus, soluble protein, and lipid from the cut surfaces of the body. Small pieces of muscle from the sample region (epaxial myotome adjacent to the lateral line triangle, posterior to the cloaca; see Fig. 2.1) were further rinsed and post-fixed in 1% OsO_4, pH 7.4, for 60-90 minutes. Samples were then rinsed, dehydrated in a series of alcohols up to absolute, cleared in propylene oxide (1,2-epoxypropane) and embedded in Araldite CY212. Various attempts were made to improve section contrast and resolution, including altering fixative concentrations by a factor of 4, and using either of the fixatives singly, for varying times. Tissue preservation was checked for temperature effects; room temperature (20-22°C) was superior to the low temperature (4°C) fixation often preferred

in ectotherm studies. This was assumed to be due to an increase in fixative penetration, relative to elevation of autolytic rate (Flitney 1965). Reduction in section quality due to autolysis was discounted in a series of experiments using Karnovsky-type fixation (4% paraformaldehyde, 3% gluteraldehyde; freshly prepared before use) as a more rapidly penetrating fixative (Karnovsky 1965). Leaching of soluble material by rinsing was confirmed. Rapid dehydration, commencing at 70% strength, increased contrast appreciably, although to a lesser extent than demonstrated in insect skeletal muscle (Colquhouin et al 1980).

Sectioning

Samples were picked at random from a pool of 36 (TS) or 20 (LS) blocks from 18 and 10 fish, respectively. Sections were cut on an ultramicrotome (OM-U2 , Reichert, Austria) and semithin (0.5µm) sections used to check orientation and position of sampling. In order to section at a similar level for that in the TS analyses, the LS blocks were paired down through the vertebral apices to the level of the nerve cord, before sections were collected. The heterogeneity of the material - extensive extracellular lipid deposits, muscle, bone - limited the thickness to which sections could be reliably cut without support, especially in view of the large block faces required to ascertain spatial relationships between individual fibres and the reference frame.

The complex orientation of muscle fibres within fish myotomes is thought to be related to the presence of near-isometric contraction, giving little sarcomere shortening (c.3%) even at maximal body flexure (Alexander 1969). This means that, in any one plane of sectioning, only a moderate percentage of fibres will be cut in true TS. The analysis of volume densities is relatively insensitive to the plane of sectioning (Weibel 1980), but perimeter and area estimates are highly dependent on the angle between fibre axis and

section plane (Table 3.1). It is possible, by estimating the fibre orientation (see also Zumstein et al 1982), to select only those fibres that are sectioned close to true TS, i.e. β $<20^{o}$ (Table 3.1). Thus, there is only a relatively low probability that a representative sample of a fibre category will be available for viewing in any one section. This probability is increased as a squared function of grid aperture and large mesh sizes, e.g. 50 or 75 apertures mm^{-1}, are necessary for the large field of view required to sample whole fibre categories in one section. Those sections showing a pale gold interference pattern (80-90nm) were picked up either on uncoated small, 200 mesh, copper grids, or on Formvar-coated hexagonal large, 75 mesh, grids (Rasmussen et al 1975); the latter giving a maximum field of view of c.0.1mm^{2}. Sections were double-stained with uranyl-acetate and lead citrate. Improvement in section contrast was possible by block staining with uranyl acetate, but not with phosphotungstic acid (Robinson 1977) which selectively stained membranes. Optimal staining was obtained using 0.4% uranyl acetate in 50% ethanol and freshly-prepared lead citrate (Reynold 1963) for 2-3 hours and 3-4 mins., respectively. Sections were viewed under a Phillips 301B electron microscope at 40kV, and electromicrographs projected at appropriate magnifications (see below).

Analyses of any one fibre type were taken from a single section, although the random orientation of sections and grid supports often required adjacent fibre types to be analysed from different sections in order to obtain sufficient number of whole fibres. In practice, <10 sections per block were required for complete analysis, giving a maximum spatial separation of <900nm between samples.

Mapping the sample area

With semithin sections viewed under low power (X 50, LM) a co-ordinate system was established using the characteristic fibre pattern, vertebral column, myosepta, lipid deposits, lateral line nerve and skin as reference points. Individual fibres viewed under the EM could then be located on this

map, and assigned to a particular category, dependant on its size and position within the myotome (see Table 3.2).

Stereological analysis

Analyses followed the theoretical models of Weibel (1973, 1979) using a simple, coherent quadratic test system (equivalent to grid A-100, Weibel 1980). Electromicrograph negatives (X1500-4500) of whole fibres were projected onto a 1cm square-lattice counting grid at varying magnifications (X 2.5-4.2) such that the grid spacing was $>1 <1.5$ X the average myofibrillar diameter:

(Eq. 1) $d > l_a$ where d = lattice spacing

l_a = average length of component axis

(Weibel 1973). The myofibrillar diameter was chosen for the value of l_a as this is the major component in any one fibre grouping. Volume densities were determined by point-counting at line intercepts, such that:

(Eq. 2) $V_V = \frac{P_i}{P_t}$ where V_V = volume density

P_i = number of points falling on a component

P_t = total number of points falling on a profile (fibre)

With components of varying sizes, a different value for d is optimal and for maximal accuracy multiple grid sizes are required (Weibel 1973). Using a single (average) value for d will cause those components for which d is > optimal to be underestimated, and those components for which d is < optimal to be overestimated. However, with components of similar size this error is small, relative to experimental error, and only in the case of the inter-myofibrillar space (the smallest component analysed) will it become significant. Although many fibres analysed were not sectioned in true TS (see above), point-counting estimates are relatively insensitive to the angle of sectioning, or the degree of anisotropy of the components (Weibel 1973, 1980).

Muscle fibres do not easily fit into the idealised categories on which these models are based, and so these assumptions were tested using a group of 10 SW fibres, linearly spread across the myotome. Analysis using 4 different size grids gave the most reproducible results when the above criterion was fulfilled (Eq. 1). Orientation of the grid to 6 different angles (over a 180° range) showed no preferential orientation, as revealed by volume density estimates of myofibrils and nuclei; variation due to grid orientation was $\sim$ 5%, whereas non-optimal grid size accounted for up to 20% variation. The results obtained agree well with those found by planimetry ($>$ 95% agreement), both methods giving similar values for reproducibility ($>$ 97%).

Counting was carried out blind, with profiles identified by plate number only, and selecting negatives at random to reduce bias. Initially, replicate counts were made, utilising a new orientation of the grid. The two sets of data were compared and those showing $>$ 5% variance rejected. As this rarely happened, the procedure was abandoned for subsequent analyses, since reproducibility was obviously $>$ experimental error or natural variance. In the case of the smallest fibres, where Pt is small, triple counts were routinely made such that Pt was around 200. This gives the method a resolution, defined as (1/Pt) of $\sim$ 0.005; i.e. all components $>$0.5% by volume may be quantified (Table 3.3.). If this value of Pt was approached, the results were always checked by planimetry (Chapter 2). The mitochondrial and sarcoplasm content of the subsarcolemmal (SS) and intermyofibrillar (IMF) zones were quantified separately. The SS zone was taken to extend from the sarcolemma to the envelope of the peripheral myofibril edges, and the IMF zone constituting the rest (centre) of the fibre. As the extent of the SS zone will clearly affect the magnitude of V_V (mit,f), the total mitochondria and sarcoplasm volume densities were calculated as well.

Using the assumption that sections represent a random sample of fibre composition, a relationship can be established between P_i and P_t to give an estimate of methodological error:

$$(\text{Eq.3}) \qquad E_{V_V} = 0.6745 \sqrt{\frac{1 - V_V}{P_t \cdot V_V}} \qquad \text{(Weibel 1973)}$$

where E_{V_V} = expected relative error in volume density estimation

It follows that as $P_t \underset{\rightarrow}{} \infty$, or $V_V \underset{\rightarrow}{} 1.0$, then $E_{V_V} \underset{\rightarrow}{} 0$ (Fig. 3.1). On this basis, rare components in a fibre require a prohibitively large number of points to be counted for an acceptable error (Fig. 3.1). If the inter-fibre variance is > intra-fibre variance, and the sample is statistically representative of the population, the error in estimation of population mean is $\propto \Sigma P_t$, and not the summed error of individual profile analyses; i.e. as $n \underset{\rightarrow}{} \infty$, then $E_{V_V} \underset{\rightarrow}{} 0$, over a given (moderate) range of values for P_t. e.g. (1) for a fibre with a mitochondrial content of 5%, and a total number of counted points of 175, then

$$\sqrt{n} = 1 \quad P_t = 175 \quad V_V = 0.057 \quad E_{V_V} = 0.22$$

but for twenty such fibres, then

$$\sqrt{n} = 20 \quad P_t = 175 \quad V_V = 0.057 \quad E_{V_V} = 0.05$$

Such an optimisation approach for biological quantification (i.e. accuracy per unit effort) is gaining widespread acceptance (Zumstein et al 1982), especially when the inter-sample variance is >>intra-sample variance (Gundersen & Østerby 1981).

Estimates of fibre cross-sectional area were calculated from point-count data:

(Eq. 4) $A = P_t.d^2$ where A = profile area
d = grid spacing

and compared to direct planimeter measurements over a range of fibre sizes (Fig. 3.2).

e.g. (2) $P_t = 323$

EM magnification = X3400

projection magnification = X3.2

lattice spacing = 1cm.

$$\bar{a}(f) = 323 \left\{ \frac{1 \times 1}{(3400 \times 3.2)^2} \right\} \times 10^8 = 272.9\mu m^2$$

planimeter estimate = $274.0\mu m^2$

The deviation was not significant in most cases, and the method was subsequently adopted for all experiments which didn't require planimetric estimate of perimeter lengths.

Formally, the estimation of fibre area is given by:

$$\bar{a}(f) = \sum_{i=1}^{i=n} a(f)i \Big/ \sum_{i=1}^{i=n} N(f)i$$

for planimetry

$$\bar{a}(f) = \left(\sum_{i=1}^{i=n} Pi \cdot d^2 \right) \Big/ \sum_{i=1}^{i=n} N(f)i$$

for point counts

Projected LS profiles (final magnification X 45000 - X 60000, 30-40 profiles per group, see Figs. 3.19 and 3.20) were quantified for the sarcotubular system using planimetry:

(Eq. 5) $V_V = \frac{\sum a_i}{A_t} = \frac{A_i}{A_t}$

where a_i = individual component area
A_i = summed component areas
A_t = projected (sample) area

At these magnifications, a group of 4-6 myofibrils were analysed in each profile, over a distance of 3-4 sarcomeres. Errors in quantification are the summed errors of individual tracings, but reproducibility remained acceptable at >95%. Profiles were selected at random within a fibre, but excluded the peripheral myofibrils and the subsarcolemmal zone (Fig. 3.30).

Chemicals

All reagents for electronmicroscopy were supplied by EMscope, Kent, England.

RESULTS

Following a previous description of the gross morphology and histochemical staining characteristics (Chapter 2), and a preliminary investigation of fine structure using light microscope (semi-thin sections) and electron microscope (low power) material, a group of nine fibre categories within the elver trunk were identified for further study (Table 3.2). Mean minimal resolutions for the categories RF, SW, MW, DW, and SDW were 0.42, 0.52, 0.37, 0.35 and 0.54%, respectively, for individual fibres; and reduced to 0.007, 0.01, 0.008, and 0.008%, for the experimental group (Table 3.3). The expected error, relative to the mean, for different component volume densities and counts is illustrated (Fig. 3.1).

A transect from the skin to vertebral column, as outlined in Fig. 2.1b, shows a dramatic decrease in mitochondrial volume density, $V_{V(mit,f)}$ correlated with a gradual increase in myofibrillar content, $V_{V(mf,f)}$ from around 60 to 80%, and a marked increase in average fibre cross-sectional area, $\bar{a}(f)$; see Fig. 3.16.

The slow fibres show a moderate mitochondrial content (21.4%) and correspondingly low myofibrillar content (61.0%). No significant difference is seen between the outer and inner layers of slow fibres in the epaxial myotomes (RFo and RFi), and the data was combined (Tables 3.4, 3.5). The

lateral line slow fibres (RF1) are similar, but show a slightly larger size (Table 3.6), and a slightly lower mitochondrial content for a given fibre size (Fig. 3.9).

No significant difference could be found between the two categories of superficial fast fibres, SW1 and SW2, despite the differences noted in apparent aerobic capacity (Chapter 2). The data is combined, Tables 3,4, 3.5, and reveals a position between slow and deep white fibres with respect to area, mitochondria and myofibrils (Fig. 3.16). The deeper regions, (MW, DW) have the characteristic appearance of fibres with a low aerobic capacity (Chapter 2) with a large area and myofibril content, but very low mitochondrial content (Tables 3.4, 3.5). Although the regions are very similar, some difference is evident (Fig. 3.17).

The small, PAS +ve fibres, $<120\mu m^2$ described in Chapter 2 are present as a morphologically distinct population. A similar arbitary limit to the size range was allocated to this fibre type, $<100\mu m^2$, and this fits well into the distribution of fibres at the apices of larger fibres. This is the expected size when fixation shrinkage is taken into account, over the frozen-section estimates given in Chapter 2 (Goldspink 1961).
In the majority of cases, the fibre was either entirely enclosed by the basal lamina of the adjacent large fibre, or had remnants associated with its periphery (Figs. 3.8, 3.10). Some difference between small fibres from MW and DW regions are evident, Fig. 3.17, but these are relatively minor. The elevated mitochondrial content, compared to other fast muscle, is surprisingly low for a presumptive growth stage, and is less than found in SW fibres (Table 3.4). The nuclear content of these fibres are around 5X that found for all other categories, which show very similar results, around 2% (Table 3.4).

The relationship between fibre area and mitochondrial volume shows a slight positive correlation within the slow fibres, but no correlation within the superficial fast fibres (Figs. 3.9a and b, respectively). The deeper fast fibres show an initial slight negative correlation up to around 600μm^2, after which no correlation exists (Fig. 3.9c). The mitochondria of slow fibres have poorly developed cristae (Figs. 3.12-15), and are more abundant at the fibre ends (Figs. 3.14 and 3.15). This accumulation of mitochondria at the fibre ends is in conflict with a qualitatively homogeneous histochemical reaction for aerobic enzyme systems (Chapter 2), and quantitative histochemical evidence for homogeneous enzyme activity along individual mammalian fibres (Pette et al 1980). Mitochondria in the fast fibres are more spherical and show a marked decrease in cristae number from superficial to deeper fibres (Figs. 3.5, 3.7) and are usually restricted to a narrow subsarcolemmal zone. The intra-fibre distribution of mitochondria shows an interesting pattern, with RF, SMW and SDW having the majority located in the SS zone; whereas SW, MW and DW have most mitochondria located within the intermyofibrillar (IMF) zone (Table 3.5). A further indication of the importance of the SS zone is found in the distribution of unstructured sarcoplasm, both RF and SW have fairly equal SS and IMF sarcoplasm content (sarcotubular system + ground substance), whereas the SS zone is more extensive in the small fast fibres, and the reverse is true for the large fast fibres (Table 3.5).

Little variation is seen in T-system volume between the groups analysed, 0.003 to 0.004 (Fig. 3.27), indicating this as a non-limiting stage in excitation-contraction coupling (E-C). The volume of SR, however, shows large differences between slow and fast muscle (Fig. 3.28), correlating well with the physiological function. The slightly higher value for SW compared to DW, V_V(SR,f) - 0.068 vs 0.060, requires further explanation.

DISCUSSION

Studies on the ultrastructure, and biochemistry, of fish muscle have often employed random sampling of different fibre tyes (e.g. "red", "intermediate", or "white"); no attempt being made to quantify regional differences in fine structure. This study shows that the structure of fast fibres varies according to both size and position within the myotome (Table 3.4). Similar qualitative conclusions have been reached in elasmobranchs (Kryvi and Totland 1977) and some teleosts (Johnston and Lucking 1978) using histochemical techniques.

The moderate V_V(mit,f), 0.214, of elver slow fibres is in contrast to the poor cristae development (Figs. 3.13-15) and low SDH activity (Chapter 2). The trend of increasing mitochondrial content with fibre area (Fig. 3.9a) indicates an elevated metabolic rate in large, relative to small fibres. Limitations in the use of SDH as a marker for aerobic activity have been mentioned, but even when a more specific, non-droplet localisation of COX is used (Seligman et al 1968), a similar low aerobic potential is indicated (Chapter 2). The specific activity of elver mitochondria would, therefore, appear low in comparison to other fish (see Johnston 1981a). A correspondingly reduced tissue oxygen demand may explain the low fibre-capillary contact (<1.0 cap./fibre, Chapter 2). The intracellular lipid content is likewise indicative of a low aerobic metabolism, V_V(lip,f) = 0.002 with a maximum recorded value of only 0.02. This is in marked contrast to the large amount of lipid found within the slow fibres of the migratory bronze and silver eels (Hulbert and Moon 1978a; Pankhurst 1982), reflecting their increased aerobic capacity (Böström and Johansson 1972). Interestingly, the conger eel has similar mode of swimming to these animals (anguilliform

locomotion) and a relatively high lipid content (V_V(lip,f) = 0.179; Chapter 5); the behaviour of the animal, on the other hand, is more like the sedentary yellow eel. It would be interesting to determine whether such a difference is due merely to the power requirements of a larger animal (allometric relationship), or to more subtle differences in the habitat environment. In elvers, the homogeneous SDH activity would appear to show an even distribution of mitochondria along the fibre length (Chapter 2), although the slow fibres show an accumulation of mitochondria at the ends (Figs. 3.14 and 3.15). This may be a direct response to the poorly developed capillary network, since the major blood vessels enter the myotome at the myosepta, and divides to form the capillary bed. A Po_2 gradient will be established from myoseptum to myotome, and this is mirrored by the longitudinal distribution of mitochondria within the fibres. The venous return in eels has a relatively high Po_2 (around 60mm Hg), this being $\sim$10X the fast muscle Po_2 (Jankowsky 1966), indicating a relatively low oxygen extraction. This distribution, of both blood vessels and mitochondria, may be found in a number of fish e.g. Conger slow and cod fast fibres.

The higher mitochondrial volume (7.6%) in superficial fast fibres (3-4 fibres deep) is in agreement with the histochemical evidence for an intermediate aerobic capacity to that found in the red, and deep white, regions of the trunk (Chapter 2). This may reflect the preferential recruitment of these fibres with increasing speed. Such "intermediate" zones have been reported for a number of species e.g. dogfish (Bone and Chubb 1978) and rainbow trout (Johnston et al 1975), although there is insufficient evidence to determine whether or not this represents a zone of preferential recruitment within the fast muscle (Grillner and Kashin 1976).

The mechanism of fibre proliferation in fish would appear to be similar to that during mammalian embryogenesis (Fischman 1972; Chapter 4), although fibre number may increase throughout life (Greer-Walker 1970; Willemse and van den Berg 1978, Chapter 1). Small fast fibres are assumed to be the aerobic growth stages (Greer-Walker 1970), and elver muscle appears to show a similar pattern. SMW and SDW fibres have a high glycogen content (Chapter 2), extensive ribosomes and endoplasmic reticulum (ER; Figs. 3.8, 10 and 11), and a large nucleus volume density in comparison with the surrounding fast muscle - 0.065 vs 0.021. The mitochondrial volume density (0.043) closely parallels the histochemical pattern, but would appear fairly low for a presumptive aerobic metabolism; indeed, it is only half that found in the superficial fast muscle (0.076; see Table 3.4). The highly polarised distribution of mitochondria between the SS and IMF zones (Table 3.5) suggests that the proliferation of inter-myofibrillar mitochondria occurs at a reduced rate, when compared to those in the SS zone (cf slow muscle distribution of mitochondria, Table 3.5). It is likely that the low V_V(mit,f) is correlated with the animals' slow growth rate, and the post-differentiation state of the fibres (see Chapter 4). The occurrence of such fibres is similar in both the mid- and deep white muscle, but appears to be relatively sparse in the superficial layers. Also, small fibres ($<75\mu m^2$; $\bar{a}(f) = 48.1$, n=16) are frequently found within the red muscle. The morphological distinction between these fibres and their neighbours is much less than found within the fast muscle, and become unclear at a smaller size ($\sim 80\mu m^2$), due to the moderate size and more aerobic nature of the fully differentiated fibres. Nucleus, cytoplasm, mitochondria and myofibril volume densities are 0.093, 0.164, 0.173 and 0.576, respectively. The discontinuous distribution of growth stages poses an interesting question as to the pattern of fibre proliferation, especially

within the fast muscle: it is likely that those fast fibres adjacent to, and in intimate contact with, the myosepta (Figs. 3.6, 3.18) make a significant contribution to growth within this zone, as they presumably must grow in step with the myosepta. This will be considered further (Chapter 4). It would seem likely, however, that the small (SMW, SDW) fibres represent different growth and maturation phases of the fast muscle, rather than a functional sub-population as suggested earlier (Hulbert and Moon 1978a; see also Chapter 2). The delineation of such stages within the proliferation of mature (differentiated) muscle has not been established for any fish species (see Chapter 4).

The mitochondrial content of deep fast fibres (1.2%) is probably only sufficient to support resting metabolism (e.g. maintenance of ion gradients, protein turnover etc.); similar results have been obtained for various sharks (Kryvi 1977). However, the mitochondrial fraction is significantly higher in many teleosts (e.g. rainbow trout and carp) which have multiply innervated fast muscle (Johnston and Moon 1981a). In this pattern of innervation a remarkable degree of control over the pattern of fibre recruitment during activity is possible (Chapter 7). Interestingly, electromyographical studies have shown that some of these species recruit fast fibres at relatively low swimming speeds. For example, the threshold speed for the recruitment of fast fibres in brook trout and carp is 1.8 and 2.1 body lengths/second, respectively (Johnston et al 1977; Johnston and Moon 1980a). Thus, in contrast to the eel, the aerobic capacity of trout fast muscle is higher, and the metabolic differentiation between fast and slow muscles less distinct. Fast fibres of both sharks and eel are focally innervated by a single basket-like endplate (Bone 1964; Fig. 2.13; Chapter 7). Electromyographical evidence from dogfish, Scyliorhinus canicula (Bone 1966), and the Pacific herring, Clupea pallensia (Bone et al 1978) show that slow fibres are alone responsible for sustained activity in these species, and

that fast fibres are only used during periods of burst swimming. The low aerobic capacity of elver (deep) fast muscle is consistent with this pattern of fibre recruitment. Direct confirmation of this would require e.m.g. recordings, which would be difficult to obtain from such small fish. However, a study of fast muscles from higher teleosts (multiply innervated) has shown a wide range of enzyme activities and mitochondrial content (Johnston and Moon 1981a) such that some species have aerobic capacities little different from that found in the eel. Until more data is available it is not possible to say whether a good correlation exists between pattern of fibre recruitment and fibre innervation, in view of the large range of possible recruitment patterns. For example, some higher teleosts only recruit fast fibres at near maximal swimming speeds (Freadman 1979) and the eel (focally innervated) has been reported to recruit the fast muscle even at the lowest swimming speeds (Grillner and Kashin 1976). The low aerobic potential of the fast muscle is in agreement with the available oxygen supply (as determined by capillary content, see Chapter 2) and the measured tissue Po_2 (Jankowsky 1966) in eel fast muscle. There is, therefore, a surprising amount of extracellular lipid deposits (Chapter 2) within the fast muscle, since this reserve is usually associated with aerobic metabolism. Unlike later stages of the life history, where lipid globules are found between most fast fibres (Chapter 7), the lipid deposits in elvers are usually restricted to discrete storage regions; this indicates that it is not a constantly utilised source of energy. The excess activity of lipogenic enzymes, over lipolytic enzymes, in yellow eel hepatocytes (Renaud and Moon 1980) suggests that these reserves are probably related to the eel's marked resistance to starvation, and its annual period of torpor (Bertin 1956), rather than routine metabolism.

The appearance of the T-system and sarcoplasmic reticulum (S.R.) is similar to other teleost striated muscle, with a well-defined triad located at the Z-line and usually an accumulation of S.R. around the distinct M-line (Figs. 3.19, 3.20). In any study of myotomal heterogeneity, the sarcotubular system must form an important part, since no quantitative information in available concerning its variability. The T-system comprises a similar volume in each of the fibre groups studied (RF, SW, MW, DW, SDW) and varies only between 0.33 and 0.44% (Fig. 3.28; Table 3.7). Elver slow muscle has a similar content to that found in elasmobranchs (0.33, 0.57%, Kryvi 1977) but higher than salmonid teleosts (0.10%; Nag 1972) and mammalian slow twitch or amphibian tonic fibres (Johnston 1981a). The fast muscle is similar to other species reported, though considerably less than found in Galeus (0.89%; Kryvi 1977). As a consequence, the differential T-system volume in fast, relative to slow, muscle that is found in most animals is much reduced (Table 3.7), and may reflect the reduced physical limitations of excitation-contraction coupling found in the relatively small fibres of the juvenile eel.

The SR content of elver slow fibres (2.10%, Table 3.67) is only half that for homologous muscle in some elasmobranchs (4.6-4.9%, Kryvi 1977) and rainbow trout (5.1%, Nag 1972), but is similar to that found in the slow muscle of the pelagic anchovy (2.7%, Johnston 1981b) which has markedly different locomotory habits. The fast muscle $V_{V(SR,f)}$, on the other hand, is similar to elasmobranch fast fibres (0.05 - 0.06 vs 0.06 - 0.07). In trout fast and slow muscle, the ratio of Ca^{2+}-activated ATPase (the Ca^{2+} pump) activity in isolated S.R. vesicles is c.2:1, with a similar ratio for total Ca^{2+}-uptake by 10μm frozen sections (McArdle and Johnston 1981), although the volume density of SR is c.3:1 (Nag 1972). In general, the % SR in fish fast muscle is much higher than that found in mammalian fast fibres,

and this correlates with the absolute rates of Ca^{2+} -uptake by frozen sections. For example, guinea pig vastus has 4.6% SR, compared with 13.7% for trout fast fibres (Eisenberg and Kuda 1975; Nag 1972). Despite lower body temperatures (10°C vs 37°C) the rate of Ca^{2+} -uptake by trout SR is c. 2.8X higher than that found in rat E.D.L. (McArdle and Johnston 1981). The higher value for $V_{V(SR,f)}$ in SW, compared to DW, fibres is anomalous (Table 3.6) since a lower value would be expected if they do indeed form a population of earlier-recruited fibres. The distribution of individual estimates (Fig. 3.27) suggests that this may be a sampling artefact, but a very large sample would be required to resolve this problem.

The rapid cycles of contraction and relaxation found in fish, especially at high swimming speeds, necessitates a very efficient Ca^{2+} -sequestering system. For example, in juvenile salmon (25-28 cm), accelerating to 10 body lengths/second, each tail beat cycle is complete within 60msec. (Wardle 1975). This requires the muscle on either side of the body to contract every 30msec. As a consequence, free Ca^{2+} needs to be sequestered extremely rapidly to facilitate full relaxation of the muscle before the next contraction is initiated. This necessity for rapid relaxation in carangiform swimming is shown in the presence of an extensive SR and high parvalbumin concentrations. Although nothing is known about the parvalbumin content of elver muscle, it is clear that there is only a moderate development of the fast muscle SR. However, not all forms of fish locomotion require such high tail beat frequencies as found in carangiform or sub-carangiform swimming where small amplitude, high frequency waves of contraction are passed down the caudal part of the body (Lindsey 1978). The anguilliform type of locomotion utilises high amplitude, low frequency waves of propagated contraction along a much larger portion of the body length, giving rise to a slower, more rhythmic, pattern of swimming (Gray 1933). Increased swimming speed is achieved by a mixture of increased amplitude and only small

increases in frequency (Gray 1933; Grillner and Kashin 1976). Hence, the range of contraction times for each body segment in this form of locomotion is less than that found for carangiform and sub-carangiform swimming. This agrees quite well with the observed $V_{V(SR,f)}$ in elver fast muscle being similar to sharks, but only half that of rainbow trout. It also correlates well with the frequency of wave propagation, and maximal swimming speed, of eel (primitive teleost) <shark (elasmobranch) <trout (higher teleost); corresponding to anguilliform, thunniform, and sub-carangiform locomotion, respectively (Lindsey 1978). Unfortunately, this study provides the only available data for a primitive teleost and the correlation of such data with the pattern of fast muscle motor innervation requires a lot more data before it can be reasonably tested (see also Chapter 7).

TABLE 3.1 Error of cross-sectional area measurement due to section angle

Angle (β)	Error
5°	0.9962
10°	0.9848
15°	0.9659
20°	0.9357
25°	0.9063
30°	0.8660
35°	0.8192
40°	0.7660

Error is calculated, using the relationship $a^1(f) = a(f).\ \cos\beta$ where $a^1(f)$ is the actual fibre area and $a(f)$ is the measured area; β is the angle formed between the fibre- and body longitudinal axes. It can be seen that fibres section $<20^\circ$ off-axis will have <6% error in the estimate of $a(f)$.

TABLE 3.2 Fibre categories examined within the trunk muscle of the elver

Symbol	Description	Position
RFo	Outer red fibres	1 fibre deep, adjacent to the skin
RFi	Inner red fibres	2 fibres deep from the skin
RFl	Lateral line fibres	1-4 "
SW1	Superficial white fibres	3-6 "
SW2	Superficial white fibres	3-4 "
MW	Mid white fibres	6-8 "
DW	Deep white fibres	10-12 "
SMW	Small mid white fibres	6-8 "
SDW	Small deep white fibres	10-12 "

Note: SW1 and SW2 refer to the superficial white fibres adjacent to the lateral line triangle, and adjacent to the peripheral myotomes, respectively (see Fig. 2.1).

TABLE 3.3 Resolution and error estimates of point-count analyses for different fibre groups.

Group	n	$\bar{P}_t$	V_{Vmin}	V_{Vmax}	R_F	$E_{V_V min}$	$E_{V_V max}$	R_G	$E_{V_V min}$	$E_{V_V max}$
RF	22	224	0.004	0.616	4.5×10^{-3}	0.711	0.036	2.0×10^{-4}	0.152	0.008
$[RF_o + RF_I]$	61	246	0.020	0.732	4.1×10^{-3}	0.301	0.026	6.7×10^{-5}	0.039	0.003
$[SW_1 + SW_2]$	43	193	0.031	0.663	5.2×10^{-3}	0.271	0.035	1.2×10^{-4}	0.041	0.005
MW	34	272	0.022	0.831	3.7×10^{-3}	0.273	0.018	1.1×10^{-4}	0.047	0.003
DW	47	282	0.011	0.748	3.5×10^{-3}	0.381	0.023	7.5×10^{-5}	0.056	0.003
[SMW + SDW]	69	185	0.014	0.736	5.4×10^{-3}	0.416	0.030	7.8×10^{-5}	0.050	0.004

Note: The group code refers to the scheme outlined in Table 2.2; n = number of fibres included in the analysis; $\bar{P}_t$ = mean number of points falling on individual fibres; V_{Vmin} and V_{Vmax} = minimum and maximum recorded volume densities; RF = resolution level per individual fibre, $\frac{1}{\bar{P}_t}$; R_G = resolution level for the experimental group, $(\frac{1}{\bar{P}_t}.n)$; E_{V_V} = expected relative error (Eq.2; Fig. 3.1).

TABLE 3.4 Morphometric analysis of fibres located within the epaxial myotome adjacent to the lateral line triangle. Mean ± S.E.M.(n).

Fibre group	N° of fibres deep from skin	$\bar{a}(f)$ (μm^2)	$V_{V(mit,f)}$	$V_{V(mf,f)}$	$V_{V(nuc,f)}$	$V_{V(SP,f)}$
Slow Fibres	1 - 2	204.4 ± 12.8 (61)	0.214 ± 0.0080 (58)	0.610 ± 0.0105 (58)	0.021 ± 004.2 (58)	0.154 ± 0.0061 (58)
Superficial White	3 - 4	332.7 ± 43.5 (43)	0.076 ± 0.0060 (42)	0.719 ± 0.0120 (42)	0.017 ± 0.0037 (42)	0.185 ± 0.0087 (42)
Mid White[1]	6 - 8	648.1 ± 51.8 (34)	0.023 ± 0.0028 (34)	0.793 ± 0.0130 (34)	0.022 ± 0.0050 (34)	0.161 ± 0.0087 (34)
Deep White[1]	10 - 12	775.0 ± 54.0 (47)	0.012 ± 0.0012 (48)	0.804 ± 0.0128 (48)	0.021 ± 0.0021 (48)	0.173 ± 0.0120 (48)
Mid White (large)	6 - 8	666.8 ± 49.8 (33)	0.023 ± 0.0028 (33)	0.800 ± 0.0112 (33)	0.020 ± 0.0039 (33)	0.158 ± 0.0085 (33)
Mid White (small)	6 - 8	29.8 ± 4.0 (24)	0.042 ± 0.0085 (23)	0.573 ± 0.0350 (23)	0.129 ± 0.0319 (23)	0.255 ± 0.0186 (23)
Deep White (large)	10 - 12	791.3 ± 53.2 (46)	0.011 ± 0.0010 (47)	0.808 ± 0.0127 (47)	0.010 ± 0.0018 (47)	0.171 ± 0.0122 (47)
Deep White (small)	10 - 12	25.1 ± 3.5 (45)	0.043 ± 0.0112 (24	0.653 ± 0.0320 (24)	0.065 ± 0.0208 (24)	0.239 ± 0.0242 (24)

1. Values corrected for the presence of small fibres ($<100\mu m^2$), in proportion (area/area), to give the regional average.

TABLE 3.5 Intra-fibre regional differences in component volume densities, and lipid stores. Mean ± S.E.M.(n).

Fibre group	Subsarcolemmal zone		Intermyofibrillar zone		
	$V_{V(mit.f)}$	$V_{V(sp,f)}$	$V_{V(mit.f)}$	$V_{V(sp,f)}$	$V_{V(lip,f)}$
RF	0.145 ± 0.0069 (48)	0.104 ± 0.0058 (48)	0.068 ± 0.0039 (48)	0.064 ± 0.0036 (48)	0.002 ± 0.0006 (58)
SW	0.023 ± 0.0043 (33)	0.109 ± 0.0076 (33)	0.041 ± 0.0031 (33)	0.091 ± 0.0044 (33)	0
MW	0.006 ± 0.0019 (26)	0.057 ± 0.0065 (26)	0.015 ± 0.0011 (26)	0.105 ± 0.0072 (26)	0
DW	0.001 ± 0.0003 (39)	0.056 ± 0.0043 (38)	0.011 ± 0.0010 (38)	0.137 ± 0.0102 (38)	0
SMW	0.039 ± 0.0080 (23)	0.206 ± 0.0196 (23)	0.003 ± 0.0013 (23)	0.049 ± 0.0075 (23)	0
SDW	0.042 ± 0.0123 (22)	0.192 ± 0.0278 (22)	0.003 ± 0.0011 (22)	0.048 ± 0.0081 (22)	0

Note in particular the virtual absence of intracellular lipid stores, even in the red fibres. Also, the inverse relationship between fibre area and extent of the subsarcolemmal space, in contrast to the intermyofibrillar space, not detectable in the average values given in Table 3.4. The marked difference between the two mitochondrial compartments is discussed in the text.

TABLE 3.6 Morphometric analysis of fibres located within the region of the lateral line triangle. Mean ± S.E.M. (n).

	RF_1	SW1
Number of fibres deep from the skin	1 - 4	3 - 7
$\bar{a}(f)$ (μm^2)	394.8 ± 34.0 (23)	534.3 ± 47.9 (10)
$V_{V(mt,f)}$	0.217 ± 0.0170 (22)	0.089 ± 0.0076 (10)
$V_{V(mf,f)}$	0.610 ± 0.0257 (20)	0.536 ± 0.0457 (10)
$V_{V(nuc,f)}$	0.027 ± 0.0052 (22)	0.010 ± 0.0036 (10)
$V_{V(sp,f)}$	0.170 ± 0.0189 (22)	0.188 ± 0.0087 (10)

TABLE 3.7 Sarcotubular system. Volume densities of different fibre regions. Mean ± S.E.M.(n).

	Sarcoplasmic Reticulum	T-System
Red Fibres	0.0210 ± 0.0093 (34)	0.0031 ± 0.0014 (34)
Superficial White	0.0681 ± 0.0155 (30)	0.0037 ± 0.0007 (30)
Mid White	0.0474 ± 0.0139 (30)	0.0030 ± 0.0014 (30)
Deep White	0.0595 ± 0.0166 (30)	0.0038 ± 0.0010 (30)
Small Deep White	0.0557 ± 0.0168 (32)	0.0044 ± 0.0016 (32)

Fig. 3.1. Double-log plot of expected error in volume density estimates vs total number of points counted during the stereological analysis. Calculated results are shown for three magnitudes of component volumes, 0.5, 5 and 50% of fibre area.

Fig. 3.2. Estimates of fibre cross-sectional area calculated from point-count analysis. $\bar{a}(f)_{calc.}$ and measured by planimetry, $\bar{a}(f)_{plan.}$ from elver slow muscle. The good agreement (correlation coefficient = 0.9940) is expected to increase with $\bar{a}(f)$, i.e. P_t, and is minimal for most categories. This time-saving routine was adopted for all preliminary studies and when perimeter readings were not required. It is less useful when $\bar{a}(f)$ is small (e.g. SMW, SDW) or with irregularly-shaped profiles, since random alignment of the fibre and counting grid may cause significant deviation from the plotted line, $r = 1.0$ (e.g. myoseptal fibres, Chapter 4).

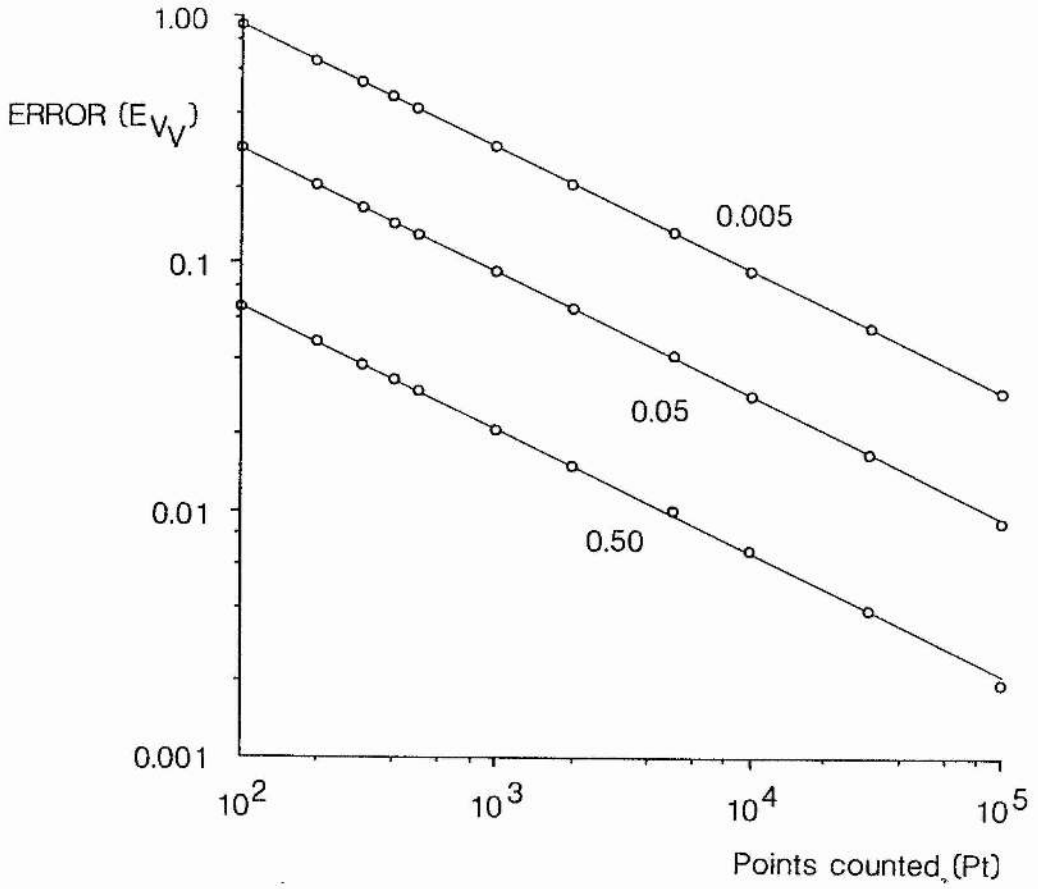
1.00
ERROR (E_{V_V})
0.1
0.01
0.001
0.005
0.05
0.50
10^2
10^3
10^4
10^5
Points counted, (Pt)

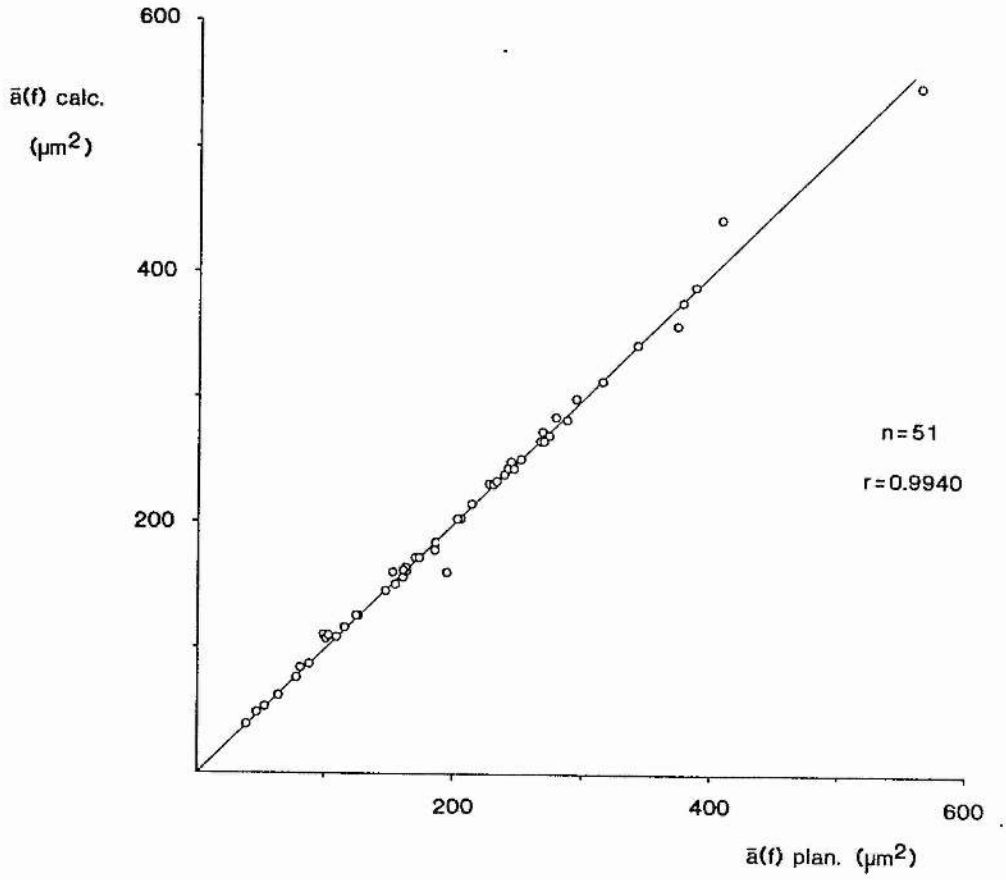
600
ā(f) calc.
(μm²)
400
200
n=51
r=0.9940
200
400
600
ā(f) plan. (μm²)

Figs. 3.3. - 3.8. Electronmicrographs of elver skeletal muscle.

Fig. 3.3. T.S., low power view of lateral red fibres, RF_o and RF_i. Note the skin (stratum compactum, upper left), prominent nuclei and mitochondria. An undifferentiated "pericyte" (upper right), capillary (bottom centre) and sparse intra-fibre lipid deposits are also visible. Scale bar = 5μm.

Fig. 3.4. T.S., low power view of deep white muscle (DW) showing the range of fibre size. Note the absence of lipid, the sparse distribution of mitochondria, and the very heterochromatic nucleus. The periodic striations, seen in all but the smallest fibres, illustrates the difficulty of obtaining "true" T.S. sections from muscle with large, variably oriented fibres. Scale bar = 10μm.

Fig. 3.5. T.S., fast fibre (DW) showing the pallisade appearance of the peripheral myofibrils and the more irregular shape of central myofibrils. Note the small mitochondrion (M) and close myofibril packing. Elements of the sarcotubular system are also visible, together with the basal lamina, sarcolemma and subsarcolemmal vesicles. Scale bar = 0.5μm.

Fig. 3.6. T.S., periphery of fast fibre (MW) in intimate contact with the myoseptum (MS). Note the increased subsarcolemmal space, the disruption of peripheral myofibrils, and the internalised aspect of some connective tissue. Scale bar = 0.5μm.

Fig. 3.7. T.S., central myofibrils of fast fibre (DW) showing the rounded appearance, and small number of cristae found in the intermyofibrillar mitochondria. Elements of the sarcotubular system (lateral cisternae) are evident. Scale bar = 0.25μm.

Fig. 3.8. T.S., small fibre (SDW) still enclosed within the basement membrane (basal lamina, BL) of the larger fibre, left. At this stage, four myofibrils are present and a prominent nucleus, but with few subsarcolemmal mitochondria. Note the abundance of subsarcolemmal vesicles. Scale bar = 1.0 μm.

3

4

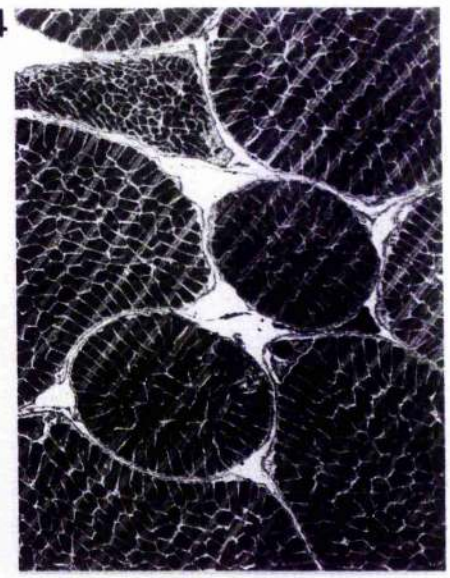

5

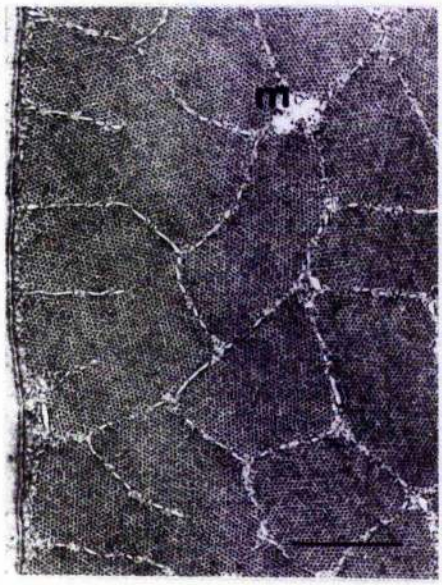

6

7

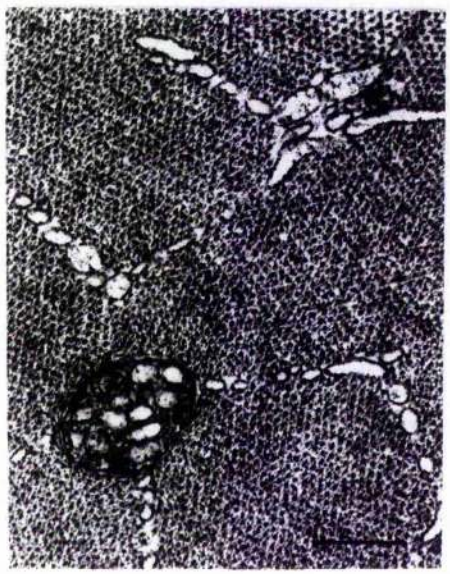

8

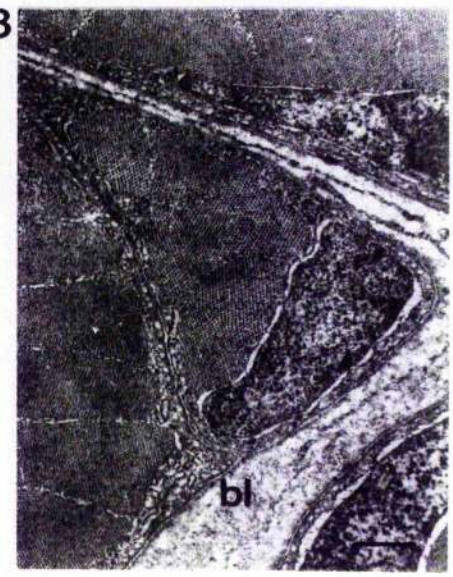

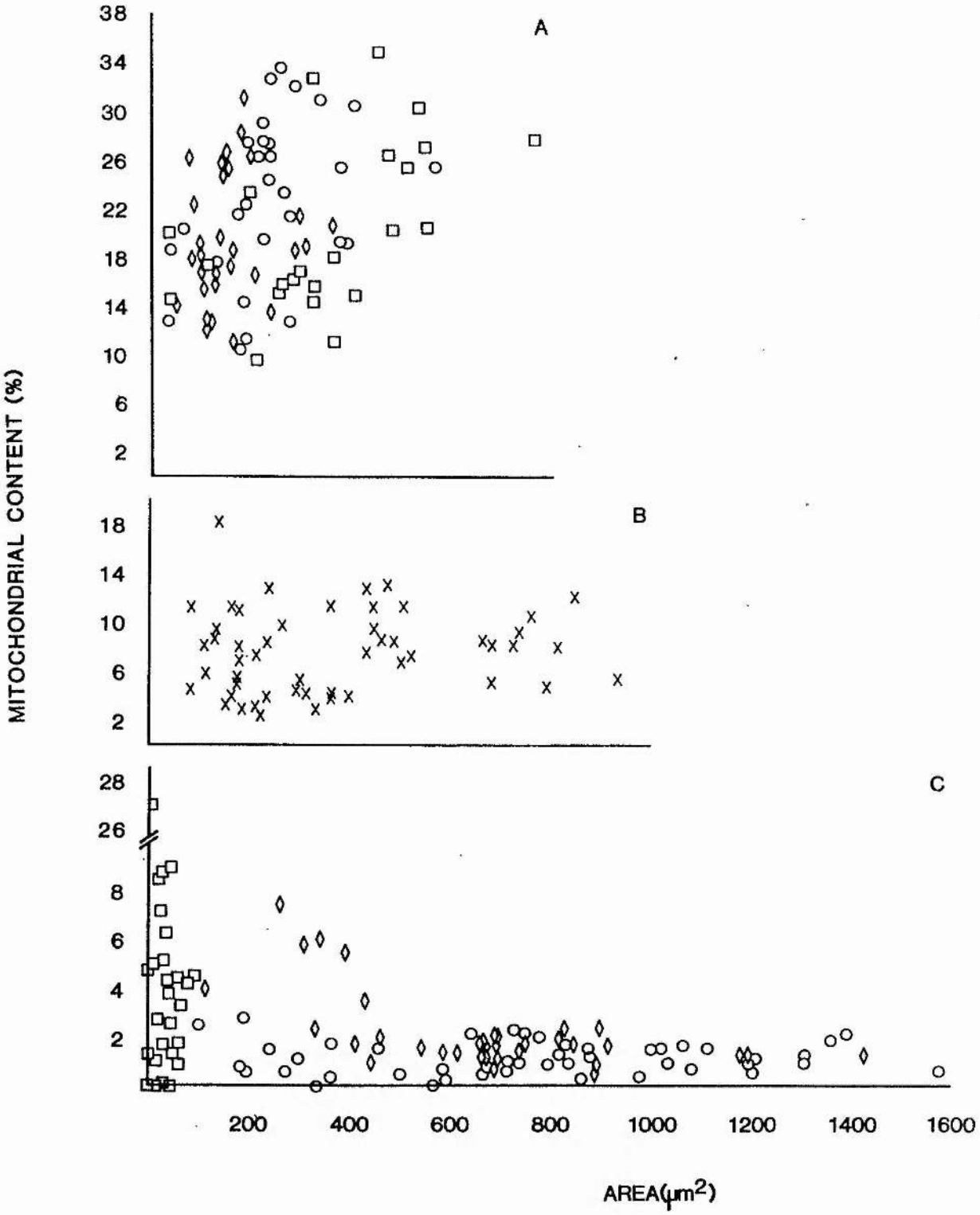

Fig. 3.9. Plots of mitochondrial content vs fibre area, for seven fibre categories.

a) Slow fibres: ◇ = RF_o 0 = RF_i □ = RF_1

b) Superficial fast fibres: X = SW1 + SW2

c) Deep fast fibres: □ = SDW ◇ = MW o = DW

Figs. 3.10. - 3.15. Electronmicrographs of elver skeletal muscle.

Fig. 3.10. T.S., young fast fibre (SDW) showing a double layer of "peripheral" myofibrils, large nucleus, and high mitochondrial volume density. Disruption of the basal lamina covering both large and small fibres has commenced. Subsarcolemmal glycogen deposits are seen as black dots. Scale bar = 0.5µm.

Fig. 3.11. T.S., later growth stage (SDW) showing the parallel development of central myofibrils and mitochondria. The striations typical of MW and DW fibres are present, and the glycogen content much reduced. Scale bar = 5µm.

Fig. 3.12. T.S., interface of RF (left) and SW (right) layers, showing the fascia (F) and some difference in section contrast between the two regions. The capillary (centre), with an erythrocyte in the lumen, is seen to be in contact with 5 different fibres, of 2 different types. Such "shared" capillaries are common along the fascia. The capillary has the usual villi projecting into the lumen, and a nucleated epidermal cell present. Large subsarcolemmal populations of mitochondria are visible in the slow fibres. Scale bar = 2µm.

Fig. 3.13. L.S., slow fibre (RF_i) subsarcolemmal mitochondria, showing cristae development. Also shown are the small triads, sparse SR vesicles and relatively poor myofibril contrast. Glycogen granules are visible in the intermyofibrillar spaces. Scale bar = 0.5µm.

Fig. 3.14. L.S., Slow fibre (RF_o) showing the accumulation of mitochondria at the end of a fibre. Edges of the staggered myofibrils are visible (MF) as is one of the nuclei (N) and small lipid droplets (L). Scale bar = 2µm.

Fig. 3.15. T.S., slow fibre (RF_1) sectioned in a similar region to Fig. 3.14. The mitochondrial content is seen to be over 90% of the cross-sectional area. Nucleate erythrocyte is seen in adjacent capillary (top right) with undifferentiated pericytes (centre right) between fibres. The latter cell type is particularly common in this region of the slow muscle. Scale bar = 2µm.

10

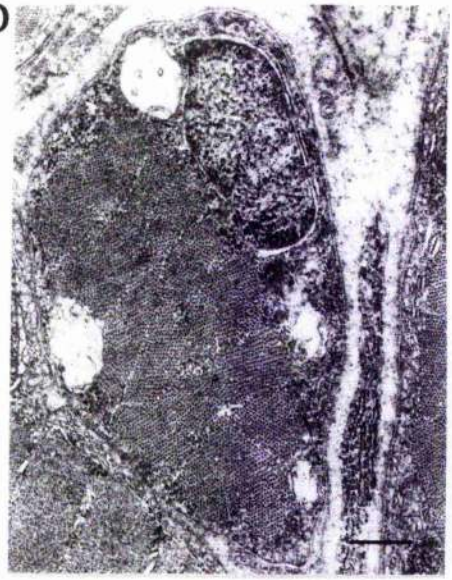

11

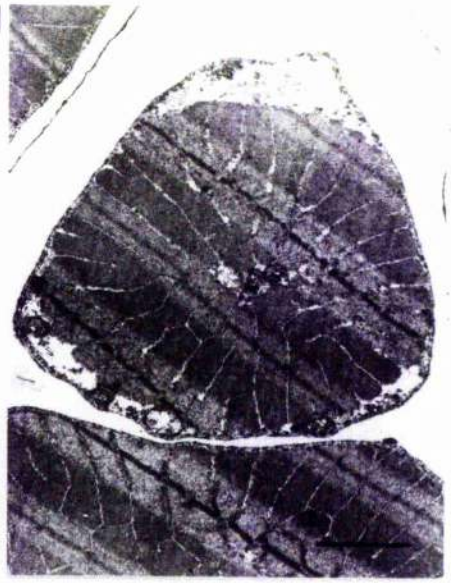

12

13

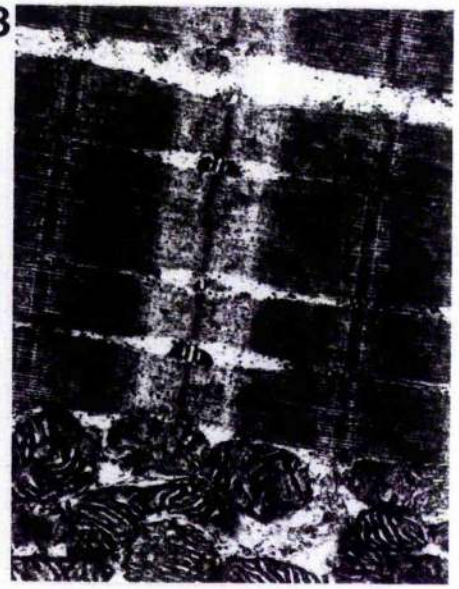

14

15

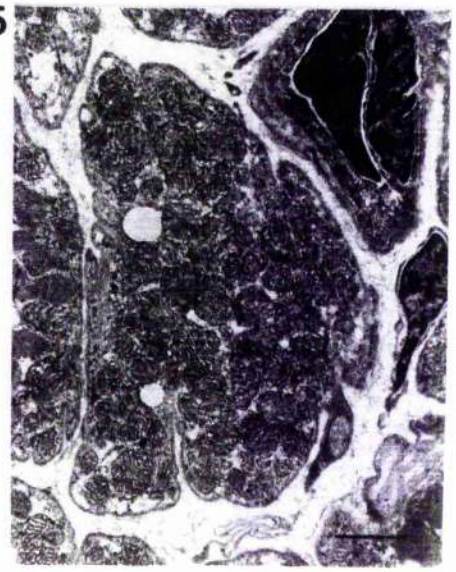

Fig. 3.16. Histograms showing the relative change in components along the transect from skin (left) to vertebral column (right). Stippled bars = slow fibres (RF); SW, MW and DW are shown from left to right. The values for MW and DW include SMW and SDW mean values, combined in proportion to their occurrence (area/area). Note the regular rise in fibre area, $\bar{a}(f)$, with a corresponding decrease in mitochondrial content, and relatively large sarcoplasm component.

Fig. 3.17. Histograms showing the difference in component values with fibre size and position within the fast muscle; SMW + MW on the left, SDW + DW on the right. Note the large variance of mitochondrial contents for both the small fibre categories.

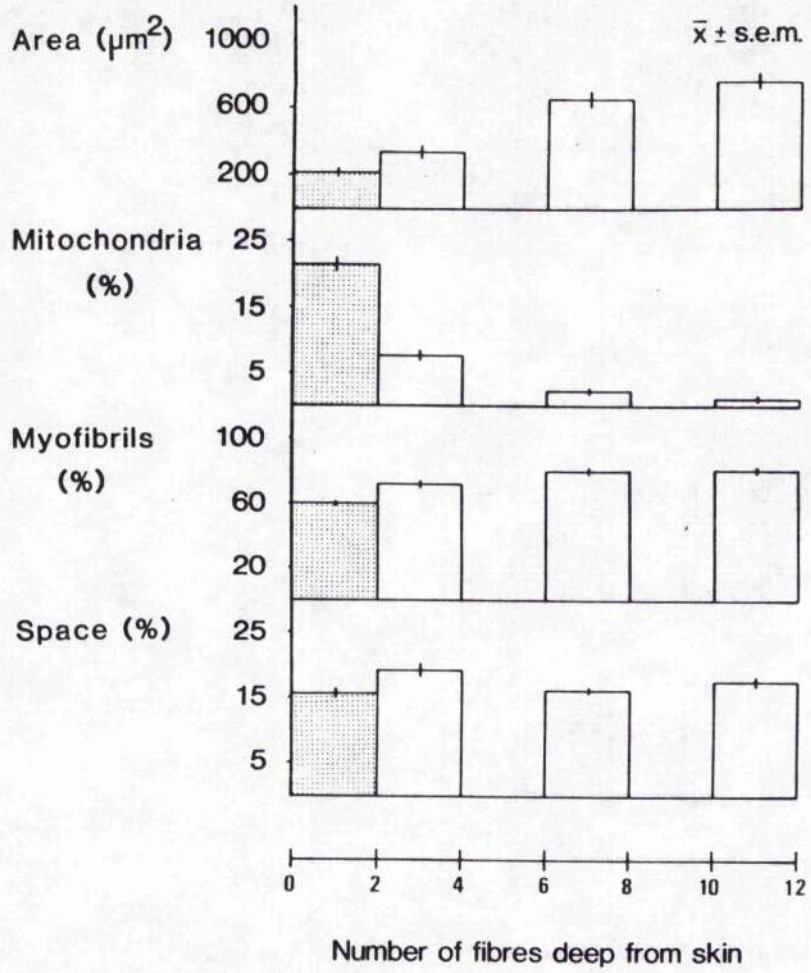
Area (μm²)
1000
600
200
x̄ ± s.e.m.
Mitochondria (%)
25
15
5
Myofibrils (%)
100
60
20
Space (%)
25
15
5
0
2
4
6
8
10
12
Number of fibres deep from skin

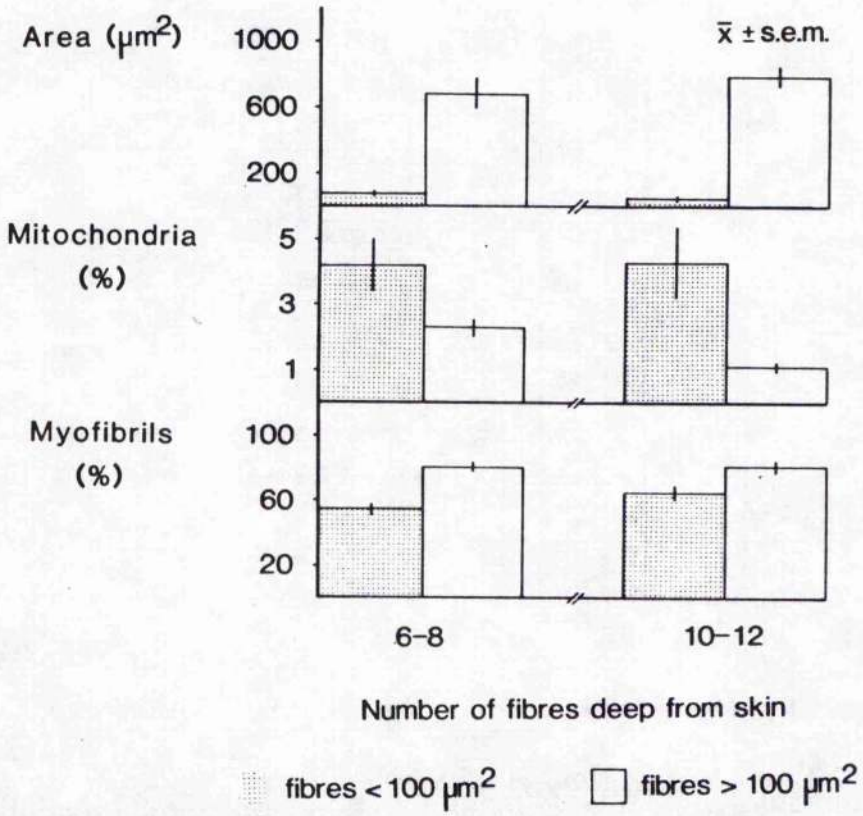
Area (μm²)
1000
600
200
x̄ ± s.e.m.
Mitochondria (%)
5
3
1
Myofibrils (%)
100
60
20
6–8
10–12
Number of fibres deep from skin
fibres < 100 μm²
fibres > 100 μm²

Figs. 3.18. - 3.22. Electronmicrographs of elver fast muscle (DW).

Fig. 3.18. L.S., tapering end of fibre showing the sarcolemmal invaginations inter-digitating with the myoseptum (MS); compare this to the T.S. profiles seen in Fig. 3.6. The sarcolemma appears to be thickened, shown darker, with a less distinct, broader, basal lamina than is usually present. The invaginations extend up to 2 sarcomeres deep into the fibre. The striation pattern (integrity) of the myofibrils is complete and usually ends at a Z-disc. Numerous subsarcolemmal vesicles and filaments are present, these filaments being seen end-on in the T.S. sections. Scale bar = 1µm.

Fig. 3.19. L.S., sarcotubular system sectioned at the level of the T-system showing the triad composition, a transverse tubule (at the level of the Z-disc) flanked by terminal cisternae (TC). The lateral cisternae (LC) are broad and extend over a large portion of the sarcomere, with some overlap of the LC originating from different TC at the M-line. Scale bar = 0.5µm.

Fig. 3.20. L.S., showing the highly organised sarcomere structure with near perfect register of I- and A-bands (I, A), well-defined triads (T) and Z-discs (Z), and a distinct M-line (M). Scale bar = 0.5µm.

Fig. 3.21. L.S., showing the tapering of a moderate-sized fibre towards the myoseptal insertion. Note the close register of sarcomeres and the gradual reduction in myofibril width at the fibre periphery. Scale bar = 2µm.

Fig. 3.22. L.S., peripheral view of SW fibre, showing a heterochromatic, elongate nucleus. Scale bar = 1µm.

18

19

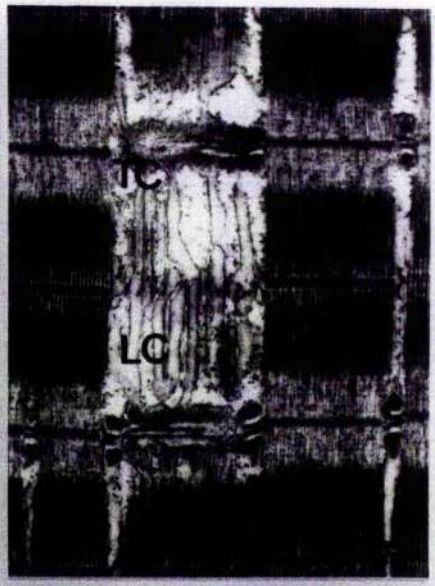

20

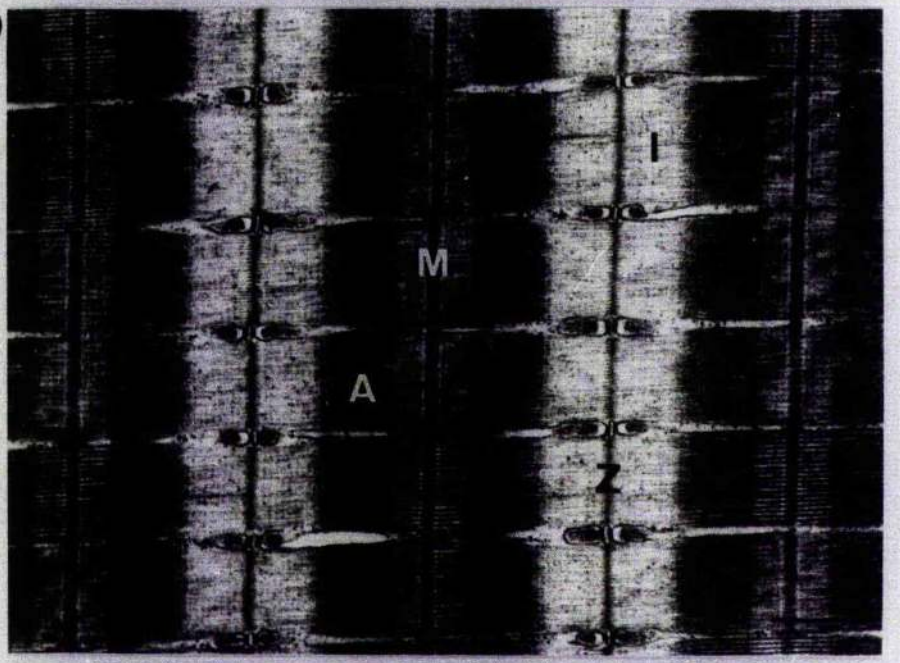

21

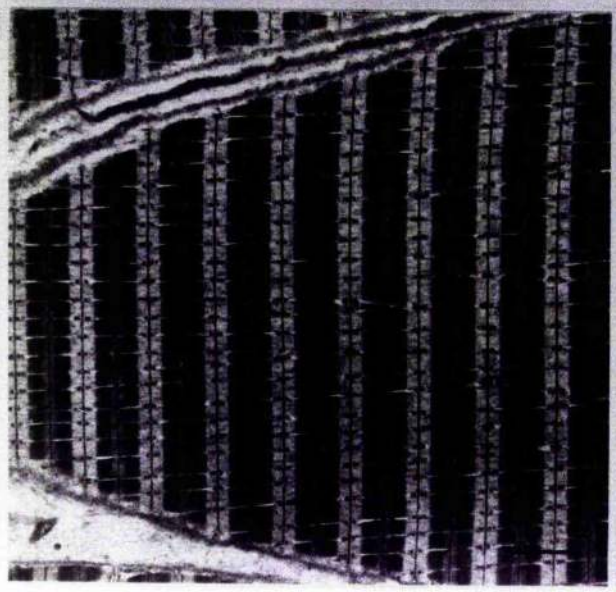

22

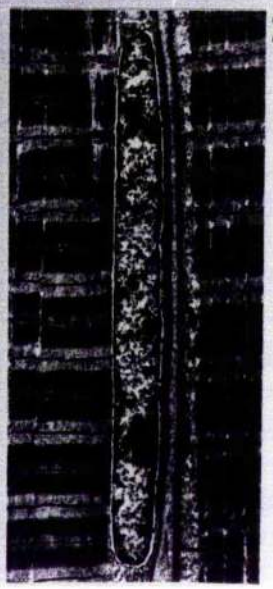

Figs. 3.23. - 3.26. High power electronmicrographs of elver fast muscle (DW).

Fig. 3.23. T.S., showing the sarcotubular and subsarcolemmal vesicles. Sarcolemma and basal lamina are clearly visible (bottom). The small change in section plane causes a striking difference in the pattern of contractile proteins, within the A-band region. Scale bar = 0.2μm.

Fig. 3.24. Oblique section, showing the invasion of T-tubules between myofibrils. The characteristic A- and I-band patterns of the myofilaments are visible, as well as the basket-weave appearance of the Z-disc (Z), in the near-T.S. profile. Scale bar = 0.25μm.

Fig. 3.25. T.S., the A-band region of a fibre, showing the structure of the fibre perimeter, including the basal lamina, sarcolemma and subsarcolemmal vesicles. These vesicles are assumed to be pinocytotic, since profiles of "open" vesicles are often seen, both in T.S. and L.S. The similarity, and close proximity, of the sarcotubular and subsarcolemmal vesicles is clearly shown. Scale bar = 0.2μm.

Fig. 3.26. T.S., central myofibril sectioned in the A-band (region of actin-myosin overlap) showing the change in the double-hexagonal pattern (upper right) on the formation of crossbridges (centre). Scale bar = 0.1μm.

23

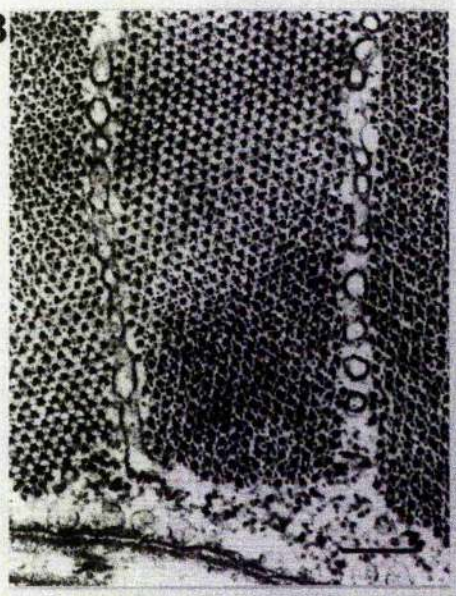

24

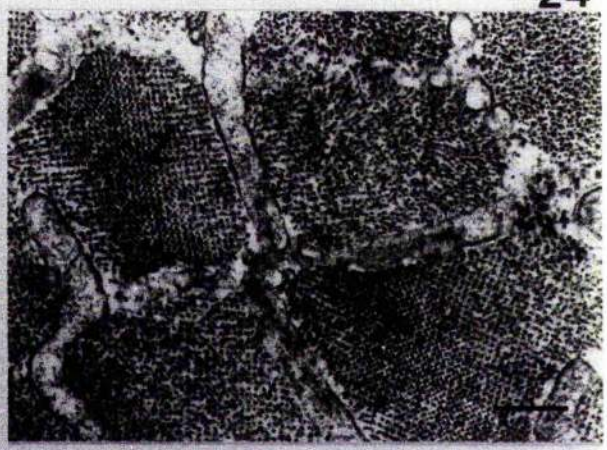

25

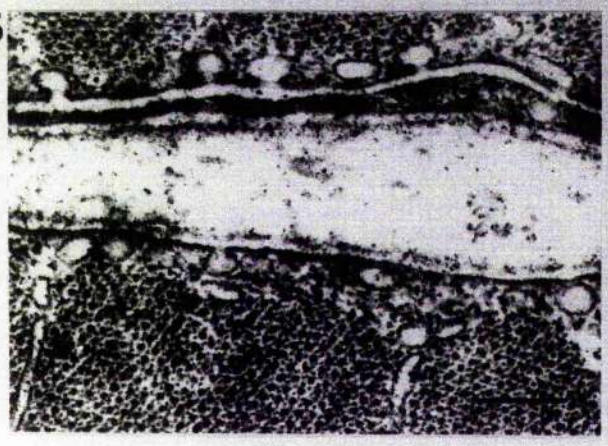

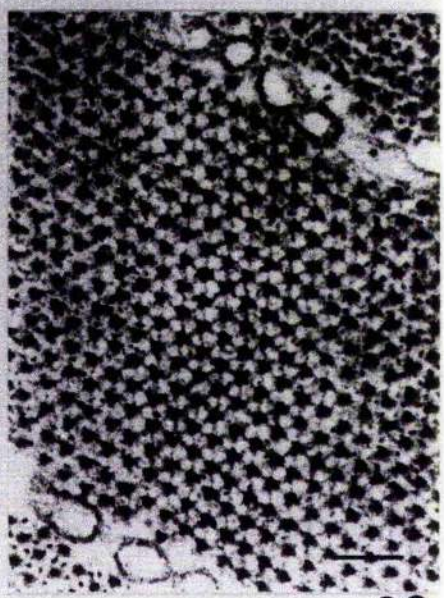

26

Fig. 3.27. Histogram showing the distribution of values for T-system content within the different fibre groups. Plot of frequency (%) vs fractional volume (% fibre area). Arrows denote mean value of each sample.

Fig. 3.28. Similar to Fig. 3.27, for the S.R.

Fig. 3.29. Plots of the total sarcotubular system (S.R. + T-system) for the different fibre groups.

Fig. 3.30. Distribution of values when calculated with reference to either whole-fibre (F) or myofibrillar (MF) area. Clearly, a transect across a fibre with a large subsarcolemmal or inter-myofibrillar space (cytoplasm) will give an erroneously low value for the sarcotubular content, relative to any analysis that relates the volume of the sarcotubular system to the myofibril area that it serves. The plotted variables were analysed in slow fibres and only small differences in the calculated means were found. However, the distribution of values represented in the analysis of the myofibrillar compartment was assumed to be a better estimate of physiological variation between the samples. Calculated means (F vs MF estimates) for T-system, S.R. and total sarcotubular system were 0.28 vs 0.31; 1.89 vs 2.10; and 2.17 vs 2.41%, respectively.

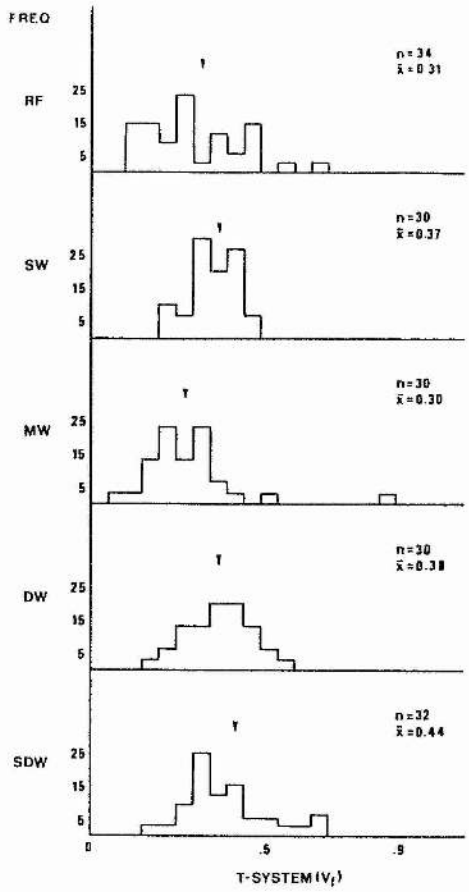
FREQ
RF
n=34
x̄=0.31
SW
n=30
x̄=0.37
MW
n=30
x̄=0.30
DW
n=30
x̄=0.38
SDW
n=32
x̄=0.44
25
15
5
0
.5
.9
T-SYSTEM (Vf)

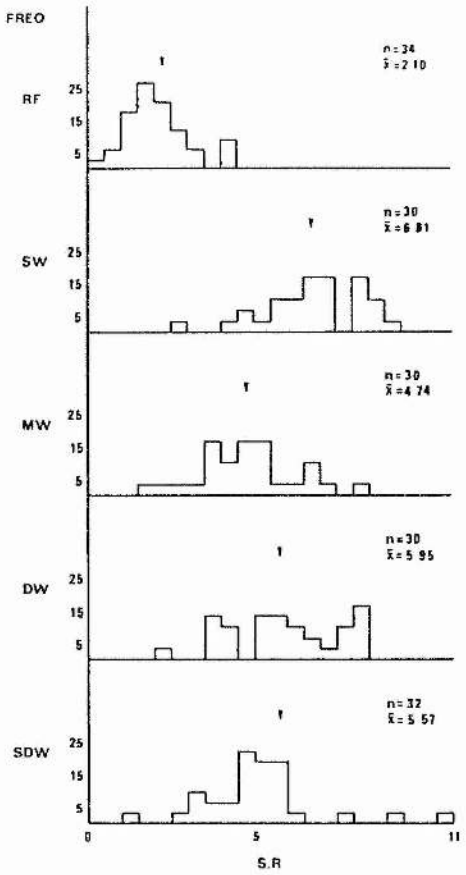
FREQ
RF
n=34
x̄=2.10
SW
n=30
x̄=6.81
MW
n=30
x̄=4.74
DW
n=30
x̄=5.95
SDW
n=32
x̄=5.57
25
15
5
0
5
11
S.R

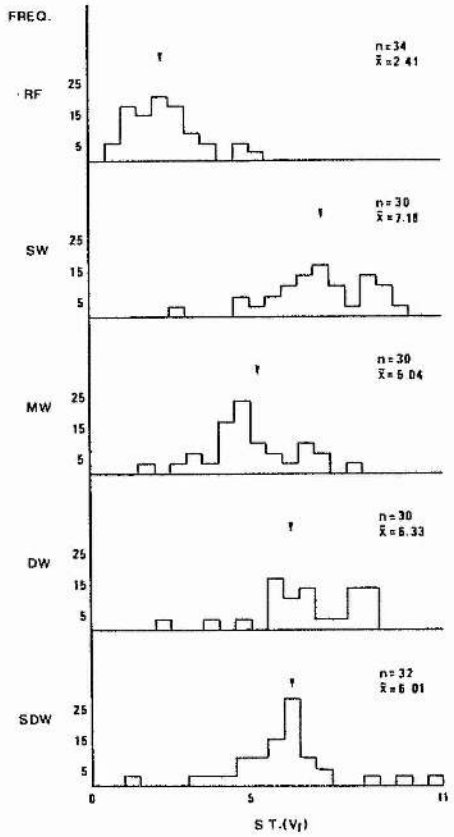
FREQ.
RF
n=34
x̄=2.41
SW
n=30
x̄=7.18
MW
n=30
x̄=6.04
DW
n=30
x̄=6.33
SDW
n=32
x̄=6.01
25
15
5
0
5
11
S T.(Vf)

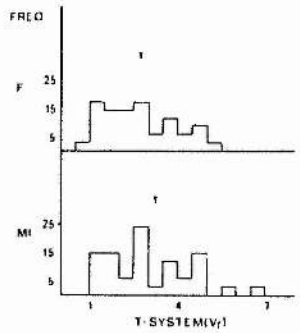
FREQ
F
M
25
15
5
1
4
7
T-SYSTEM(Vf)

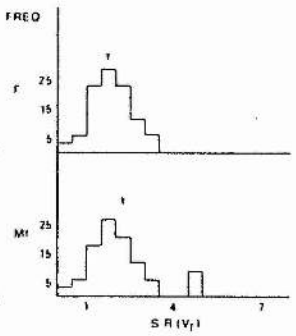
FREQ
F
M
25
15
5
1
4
7
S R (Vf)

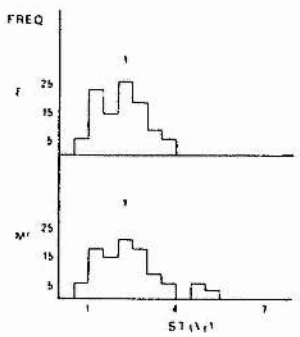
FREQ
F
M
25
15
5
1
4
7

CHAPTER 4

INTRODUCTION

The growth of fish skeletal muscle presents an interesting model for the study of fibre differentiation, since most stages of myogenesis can be found in mature myotomes. The anatomical separation of the two major fibre types, and their sequential appearance during development, has proved useful in a number of studies concerning cellular differentiation in embryonic and early post-natal fish (Nag and Nursall 1972; Raamsdonk et al 1978). Little attention has been paid to the regulation of myotomal growth within mature, fully differentiated muscle; this essentially represents an extension of the mammalian neonatal condition into adult life, with muscle growth being the result of fibre hyperplasia and hypertrophy.

It is not known whether the factors controlling the recruitment of stem cells into developing fibres, within a muscle of adult phenotype, are the same as those which initiated embryonic myogenesis. The discontinuous growth pattern in fish muscle suggests that this may not be the case. In addition, the growth of fibre-precursor cells within a mature muscle is unlikely to parallel the accelerated development of embryonic myogenesis, where fibre differentiation may be complete between 30 and 90 days post-fertilization (Nag and Nursall 1972; Raamsdonk et al 1978; Proctor et al 1980). Proliferation of fibres may be achieved by two different mechanisms. The original myogenic stem cell stock may remain dormant for a variable period of time, giving rise to an apparent hyperplasia; alternatively, there may be a continuous production/replication of stem cells, or true hyperplasia. The proximate factors controlling these processes may be quite different, and the existence of two or more populations of myogenic stem cells cannot be ruled out. There is only indirect evidence for the development of myosatellite cells (MSC) into young fibres, although the passage of MSC daughter nuclei into mature fibres has been observed, following a temporal sequence of ^{3}H-thymidine uptake in rat muscle (Moss and Leblond 1971). Such a process is supported by

morphological evidence (Anastasi et al 1979). However, the relevance of MSC to hypertrophying fibres has been questioned (James 1976; Schultz 1978), and in mature muscle their role may be that of a reserve stem cell population, used only in the regeneration of damaged tissue (Mauro 1961; Shafiq et al 1967; Schultz 1978; Snow 1978). The term "myosatellite cell" to describe both cell lines, therefore, may be a misnomer; fish muscle should provide a useful preparation to study their proposed dual function.

In restricting this study to the deeper regions of the myotome, a major limitation of embryonic studies is overcome since the final phenotype of a cell is known in advance. It has been suggested that part of the heterogeneity of myotomal muscle may be due to the occurrence of two different growth patterns (Chapters 2 and 3). The possible existence of regional growth nodes is examined at two sites within the myotome, using ultrastructural criteria to determine the developmental sequence. Small (SDW) fast fibres within the main body of the myotome are considered as either a growth stage, or a functional sub-type of fast muscle. Those fibres that show evidence of an extensive myoseptal connection are examined with regard to the pattern of hypertrophy, and the presence of active hyperplasia.

MATERIALS AND METHODS

Fish

Specimens were caught, transported and maintained under similar conditions to those described previously (Chapter 2), but represent the following year's migration. As far as could be ascertained the age, and developmental stage, were the same as the animals used in Chapter 3. Weight and length were 0.2175 $\pm$ 0.0173g and 6.8 $\pm$ 0.175cm (Mean $\pm$ S.D.), respectively (n=6).

Electron microscopy

The tissue sample site was the same as described in Chapter 2, and preparation as described in Chapter 3. Morphometric analysis was performed on fibres from deep fast (DW) muscle. Fibre cross-sectional area, a(f), and perimeter, b(f), were determined by planimetry of profiles from TS sections (Chapter 2).

The increase in surface area due to myoseptal invagination was calculated:

(Eq. 4.1.) $$I = \frac{\left[\overline{b(f)}_{tot} - b(f)_{env}\right]}{b(f)_{env}}$$

where $b(f)_{tot}$ = total perimeter length

$b(f)_{env}$ = perimeter length of the fibre envelope (see Fig. 4.14)

The proportion of fibre perimeter in contact with the myoseptum was calculated:

(Eq. 4.2.) $$\bar{I}\ (ms,f) = \frac{b(f)_{cren}}{b(f)_{env}}$$

where $b(f)_{cren}$ = length of crenulated perimeter (see Fig. 4.13).

RESULTS

Qualitatively, there was no difference in the morphology of the SMW and SDW fibres described earlier (Chapter 3) and the present group of small fast fibres ("myotomal" fibres; Table 4.1, Fig. 4.4). The histochemical profile is consistent with growth stages described for other species, having a more aerobic character than the large DW fibres and a much higher glycogen content (Chapter 3). The fine structure mirrors this situation with respect to mitochondrial content and glycogen granules (Fig. 4.4). Scattered throughout the muscle are numerous myosatellite cells (Mauro 1961) and various fibre-precursor stages that correspond quite closely to the scheme proposed for salmonid myogenesis (Nag and Nursall 1972; Kilarski and Kozlowska 1979).

In this study the term "myosatellite cell" (MSC) is restricted to the mononucleate cells located at the periphery of a mature muscle fibre, being external to the sarcolemma but internal to the basal lamina (Fig. 4.1). These spindle-shaped cells have a prominent, heterochromatic nucleus surrounded by a narrow band of vesicle-filled cytoplasm. This morphology resembles mammalian myosatellite cells (Fischman 1972) and is broadly similar to both anuran (Maruenda and Armstrong 1978) and elasmobranch MSC's (Kryvi 1975). The appearance of the myoblast is similar (Fig. 4.2), but contains a larger proportion of poorly-structured or empty cytoplasm, and an elevated mitochondrial content. The contractile filaments (actin and myosin) and sarcotubular elements (S.R. and T-system) are highly organised even in the very early stages of sarcomere formation, and are aligned in a similar manner to those in the adjacent mature muscle fibres (Fig. 4.8). When the 2-4 myofibril stage is reached, sarcomeres are structurally indistinguishable from those in mature fibres (Fig. 4.7). Insufficient evidence was available to precisely determine the time of myoblast fusion, although it is clear from LS sections that it occurs before the proliferation of central myofibrils.

Development of myotubes into immature fibres is a continuum of form, and appears to be virtually complete in all fibres $> 25\mu m^2$. The young fibre then resembles large fast fibres, having around 70% myofibrils (Fig. 4.26), although the mitochondrial content ($V_V(mit,f) \simeq 0.05$) remains elevated (Fig. 4.27). In all stages the subsarcolemmal zone predominates (Table 4.2). The basal lamina, or remnants, is visible around all young myotomal fibres $< 20\mu m^2$ and occasionally up to $40\mu m^2$ (Fig. 4.3); it is seen to reseal around the large neighbour before the growing fibre reaches $100\mu m^2$ (Figs. 4.3. and 4.4). The presence of pericytes (mononucleate, undifferentiated cells, $4\text{-}6\mu m^2$) in the interstitial space may initially cause some confusion, but there can be morphologically distinguished from true MSC's which are always located at the apex of a fibre in TS sections. (Figs. 4.1 and 4.6). Occasionally, a MSC can be found adjacent to a developing young fibre (Fig. 4.5).

The fibres that are seen to have extensive and intimate contact with the myoseptum along part, or all, of their length are referred to as "myoseptal" fibres. In TS sections $> 95\%$ of all fast fibres adjacent to a myosepta are of this type (Fig. 4.24 and 2.17), although they are histochemically indistinguishable from fibres within the rest of the myotomal bulk. In general, they are much larger than the small myotomal fibres (Fig. 4.13) and show a larger variance of component volume densities (Figs. 4.4, 11, 27; Table 4.1). The cells and fibres lying adjacent to the myosepta show a wide variety of form; numerous fibroblasts and pericytes are visible within, and around, the myoseptum. The small number of MSC; present are invariably on the myoseptal edge of a fibre, but have a similar appearance to those from deeper within the myotome. Structurally, the major difference between myoseptal and myotomal fibres becomes clear at the myotube stage, $\bar{a}(f) < 15\mu m^2$, when the extensive sarcoplasmic space first develops. This large, undifferentiated space remains a distinguishing feature until the fibres are quite large, $\bar{a}(f) \simeq 500\mu m^2$ (Fig. 4.2b). At this point the myoseptal fibres resemble the

myotomal fibres in all but the myoseptal connection. These invaginations can be seen in all myoblast-type cells, and in many cases before the appearance of myofilaments, up to fibres of quite large dimensions ($\bar{a}(f)$ = 1000-1200μm^2). In cross-section, there is a sequential reduction in myoseptal contact with increasing fibre size, resulting from the maintenance of a relatively constant length of the fibre envelope in contact with the myoseptum (Figs. 4.9 and 4.10). In line with this progression, the mitochondria and nuclear volumes decrease with increasing fibre area (Fig. 4.27). Morphometric analysis was limited to fibres $< 900\mu m^2$, although profiles lacking myoseptal contact are only seen for large fibres, $\bar{a}(f)$ = 1000 to 1200μm^2. The extent of the contact can be assessed by the increase in fibre surface area, which may almost double (Fig. 4.15; Table 4.2). The variability in the depth of invagination is reflected in the poor correlation between increase in surface area and the proportion of fibre periphery in contact with the myoseptum (Fig. 4.15). Those fibres that show only a small increase in surface area when a large portion of the perimeter is invaginated, usually have a much reduced subsarcolemmal space. Developing myoblasts are found in a position between the myoseptum and fibres $> 800\mu m^2$. A developmental sequence is found thereafter, with small fibres being found adjacent to the larger mature fibres, $> 1000\mu m^2$. Some "myoseptal fibre" profiles are likely to represent sections of the normal (myotomal) fibre-end insertion into the connective tissue sheath (Fig. 4.20). However, in TS sections it is difficult to distinguish between these fibres and those in which the myoseptal contact is extended along the fibre length (Fig. 4.21).

DISCUSSION

Myogenic cells

Myosatellite cells (MSC) are considered to be myogenic stem cells, or resting myoblasts (Mauro 1961; Shafiq et al 1967), since they are the only mitotic myonuclei. Although there is little question that the total number of myonuclei increases with age, there is conflict as to whether the number of MSC remains constant (Fischman 1972) or decreases (Schultz 1978; Schmalbruch and Hellhammer1977); however, this is probably correlated with the developmental stage of the animal. Incorporation of (mitotic) nuclei into mature muscle fibres has not been observed in fish, although the successful labelling of elasmobranch MSC (Kryvi and Eide 1977) is indicative of similar functions to the mammalian and anuran counterparts. This is supported by a number of ultrastructural similarities (Fischman 1972; Kryvi 1975; Maruenda and Armstrong 1978). Elver MSC nuclei vary from smooth to lobular (Fig. 4.1) but appear quite similar to those described for anurans (Maruenda and Armstrong 1978). The stem cells do not, however, show the marked difference in density of subsarcolemmal, pinocytotic vesicles found between the MSC and muscle fibres in elasmobranchs (Kryvi 1975; Fig. 4.8).

Axial asymmetry is found throughout the sample range, as observed using both transmission - and scanning electronmicroscopy, with respect to both cell bodies and the alignment of intracellular organelles (Figs. 4.2 and 4.8). The orientation of myoblasts in vertebrates, both <u>in vitro</u> and <u>in vivo</u>, is mediated by a cytoplasmic microtubular array (Fischman 1972) and is thought to be controlled, at least in part, by endogenous electric fields (Hinkle et al 1981). A similar microtubular system has been described in trout (Kilarski and Kozlowska 1979), and it is likely also to be present in elver myoblasts. The temporal sequence of myofilament production is similar to that in trout (actin appearing before myosin) where production is known to occur in discrete regions

of the cell (Kilarski and Kozlowska 1979). Assembly of sarcomeres begins as soon as Z-disc material is present (Fig. 4.8) and the characteristic striation pattern appears at an early stage of development, when only 1 or 2 myofibrils are present. The mono-axial, single MSC profile/fibre found in elver fast muscle contrasts sharply with the multi-axial (many cellular extensions) MSC envisaged for elasmobranch muscle (Kryvi 1975). In addition, elasmobranch muscle is assumed to possess more than one MSC/fibre (Kryvi 1975). It is not know whether this difference merely reflects the different fibre size between the animals, thereby maintaining a similar MSC density, or indicates a true difference in growth potential. Elver slow fibres, on the other hand, may have two myosatellite cells per fibre, usually on opposite sides. This parallels the more frequent occurrence of MSC in mammalian slow, relative to fast muscle (Schmalbruch and Hellhammer 1977). This gives rise to an apparent difference in growth potential, with the number of MSC/unit fibre area in slow muscle being approximately twice that in fast muscle. On the basis of fibre size distribution and number, however, it has been suggested that fast muscle grows by both hypertrophy and hyperplasia, whereas slow muscle grows by hypertrophy alone in eels $<$10cm (Willemse and van den Berg 1978). There is some evidence to suggest that this delineation may be inaccurate (Chapter 2). It is also possible that the activity of MSC's in the two muscle types is different. This is difficult to establish on ultra-structural criteria alone, although the wide variation in SDW fibre size around some large fast fibres (Fig. 2.28) suggests that continuous hyperplasia may occur in fast muscle, with a discontinuous proliferation of MSC being found within slow muscle.

The range of growth patterns described for different species of fish may also reflect inter-, as well as intraspecific differences in MSC activity. In this way it has been shown that the shark, Etmopterus spinax mainly utilises

fibre hypertrophy (Kryvi and Eide 1977) whereas cod, Gadus morhua, appears to increase fibre number throughout life (Greer-Walker 1970). Similarly the eel, Anguilla anguilla, is known to add new fibres up to 30cm (Willemse and van den Berg 1978) although small PAS +ve fibres are visible in specimens of around half the maximum length ($0.5L_{max}$, pers. obs.). The rainbow trout, Salmo gairdneri, reduces fibre proliferation at about $0.2L_{max}$ and relies on fibre hypertrophy thereafter (Weatherley et al 1979). The determining factors of the growth pattern are not known; growth rate per se seems not to be important, although the final size attained in each species does (Johnston 1982a). These patterns do, however, reflect a different emphasis being placed on the two possible roles for the MSC, and deserve further investigation.

Myotomal fibres

The use of ultrastructural criteria alone cannot determine the functional differences between cell lines, but can isolate fibre types on morphological grounds that are indicative of potential function. Early myotomes found during post-natal development have a high volume density of nuclei, mitochondria, endoplasmic reticulum (ER) and free ribosomes; this is assumed to be associated with the active synthesis of contractile proteins (Fischman 1972). A similar morphology, with the addition of an extensive cytoplasm volume and glycogen deposits, would seem to place the SDW fibres within this scheme. However, the relatively low volume density of mitochondria (0.056, Table 4.1) indicates that any phase of accelerated growth (cf embryonic development) must be restricted to those cells $<20\mu m^2$ (Figs. 4.7, 4.8); thereafter the apparent aerobic capacity declines with increasing fibre size, although it remains above that of the surrounding, large diameter fibres (Fig. 4.2b). This would agree with the reports of "red-like" myosin in fish myotubes (Raamsdonk et al 1977, 1978, 1980) indicating an initial slow-type, aerobic metabolism that is quickly replaced by the adult (fast) phenotype during the early myotube stages.

Differentiation would appear to begin before the establishment of any neuromuscular contact in elver muscle; although it is possible that such junctions could have been missed, the small size of these cells makes this unlikely with LS sections. A similar pre-innervation change in fibre type has been noted during myogenesis in fish embryos, using both ultrastructural (Kilarski and Kozlowska 1979) and immunohistochemical criteria (Raamsdonk et al 1978, 1980).

The typical fast fibre "Fibrillenstrukter" pattern (pallisade peripheral myofibrils and irregular central myofibrils) also appears early in fibre development, and suggests that the peripheral growth pattern noted for large fibres (Patterson and Goldspink 1976) originates in the early myotube (Figs. 4.4 and 4.5). In view of the low growth rate of the animal, it is to be expected that the differential between growth and mature fibres will be small. The virtual absence of capillary contact (Table 4.1) indicates that oxygen delivery is not a limiting factor in fibre proliferation, and this is supported by the presence of a high mitochondrial content in only the smallest fibres. The lack of differentiation between SDW and DW fibres on the basis of M.ATPase suggests that differentiation is complete and that the structural differences merely reflect the immaturity of a growing fast fibre. A decrease in fibre $V_V(mit,f)$ would occur in line with increasing $\bar{a}(f)$, unless there was a compensatory proliferation of mitochondria. As the basal requirements of elver fast muscle appears to be around 1-2% mitochondria (Fig. 3.13c), the elevated $V_V(mit,f)$ in SDW may provide an aerobic capacity in excess of the requirements for growth. Although these fibres only form a small percentage of the muscle (5%, Chapter 2), a similar portion is found in much larger animals (yellow eel and conger eel). This suggests that it is not merely a juvenile characteristic, but that they serve a constant, if small, role in muscle function.

In mammalian muscle, fibre differentiation has been assumed to be under extrinsic (neuronal) control with a common embryonic, slow fibre type which assumes an adult phenotype, dependent on the innervating motoneuron (Dubrowitz 1970; Perry 1979). This dependence of phenotype on motor innervation pattern is well documented for adult muscle (Buller et al 1960; Vrbova 1980; Lømo 1976), as is the development of reciprocal mechanical properties by cross-reinnervation experiments (Buller et al 1960; Bagust et al 1981). Although the activity of the innervating motorneurones has a direct effect on the muscle phenotype (Jolesz and Sréter 1981), it is known that muscle can have a reciprocal effect on the properties of the nerve (Lewis et al 1978) and muscles of different metabolic types can show a modified response to dual innervation by fast and slow nerves (Goldring et al 1981). In this way, the activity pattern of muscle per se can have a marked effect on the structure of the myotome (Raamsdonk et al 1978), the differentiation of metabolic fibre types (Govind and Kent 1982), and mechanical properties (Salmons and Vrbová 1969).

Some workers consider that "white-like" fibres are the original cell line, reflecting the spontaneous and apparently uncoordinated activity of fish embryos; this then develops into a "red-like" fibre, coinciding with the development of sustained, co-ordinated swimming movements (Nag and Nursall 1972; Proctor et al 1980). Again, this suggests direct, neuronal determination of the adult phenotype. In contrast, there is evidence that an adult, differentiated myofibril pattern is found in myotubes, preceding the development of neuromuscular contact (Sréter et al 1972; Obinata et al 1976). In fish, slow-type myosin has been demonstrated to be present in myotomes (Raamsdonk et al 1978) where morphologically-differentiated fibres are present before any endplates are formed (Kilarski and Kozlowska 1979). It would appear, then, that fibre differentiation is initially controlled by intrinsic factors,

but may subsequently be modified by its pattern of innervation. The findings of the present study supports the scheme of pre-innervation (morphological) differentiation, as this is complete within very small fibres. It would appear, therefore, that the small PAS +ve fibres have been erroneously described as "growth" fibres; in general, they do not represent myogenic cells, but rather a post-differentiation cell line that is undergoing hypertrophy. It is likely that this also applies to similar fibres described in other species. This identification of a similarly well-defined myogenic progression in mature muscle, to that found in embryos, offers an alternative model system for the study of the intrinsic factors underlying fibre differentiation. The possibility exists that the initial metabolic fibre type is not modified by their subsequent innervation.

The apparently contradictory studies regarding the initial myogenic fibre type in fish muscle may be a result of using different criteria. In brown trout, the (histochemically) embryonic form continues to be expressed after the ultrastructural differentiation of the fibre has begun (Proctor et al 1980). In this case, therefore, the histochemical profile does not seem to reflect the morphological development; the pattern of embryonic and adult myogenesis would seem to require confirmation by a number of techniques.

Myoseptal fibres

The possible existence of regional growth nodes, as found in the initiation of muscle development in both mammalian limbs (Fischman 1972) and fish embryos (Raamsdonk et al 1977 ; Kilarki and Kozlowska 1979) has not previously been considered for a mature, growing muscle. At first it was considered that myoseptal fibres form part of a static population, with growth being the result of hypertrophy in-step with the spreading of the myoseptum (Chapter 3). The progressive development of these fibres with increasing cross-sectional area, and the appearance of young fibres at their myoseptal perimeter, suggests

instead that this may represent an addition to the myotomal bulk by a sequential "budding-off" of mature fibres from the myoseptum. Such a progression is less evident within the slow muscle, where a lower frequency of myoseptal fibres occurs. Any cross-section of a fish trunk is likely to include a number of fibre ends, inserting into the myoseptal sheaths, due to their pattern of orientation within the myotomes (Figs. 4.17 and 4.19). In most species, e.g. cod, this insertion (equivalent to mammalian tendons) is very short, in the majority of elver fibres seen in LS, it lasts for only 2-3 sarcomeres and occurs evenly around the fibre end (Figs. 3.15 and 3.18). In fibres running alongside the myoseptum, however, this invagination can be seen to run down one side of the fibre for part, or all, of the length (Fig. 4.21). For most fibres, the subsarcolemmal space is very narrow at the myoseptal insertion and, in some cases, this invagination may disrupt the peripheral myofibrils (Fig. 3.6). It would appear, therefore, that in this region contractile efficiency is sacrificed for a mechanically stronger anchorage. In myoseptal fibres the SS space is significantly extended, in all but very large fibres. It is unlikely, therefore, that random TS sections would cut through all tendon-like insertions, and at such an angle to produce an erroneously high sarcoplasmic space. In eels, the myosepta are severely swept backwards (both laterally and vertically) such that many of the profiles are likely to result from an extended myoseptal contact, due to the orientation of the fibres (Figs. 4.18 and 4.21). In elvers, where the myotomes are narrow, this may result in only a small portion of a fibre being free of such connections (Fig. 4.21).

The elevated mitochondrial content, relative to similarly-sized myotomal fibres, is present up to quite large sizes, $\bar{a}(f) > 500\mu m^2$ (Fig. 4.27), although the low nuclear volume density (0.04) is not indicative of an elevated growth rate. The large amount of undifferentiated sarcoplasm ($\sim$ 42%; Table 4.2)

may be present as a physical buffer zone, in order to allow a certain amount of contraction of the myofibrils with the sarcolemma attached to a relatively static barrier. The similar ratio of SS to IMF space between myoseptal and small myotomal fibres suggests that this compensation is not complete, and the values only approach those for large myotomal fibres at $\bar{a}(f) > 800\mu m^2$. The aerobic capacity is similar to that found in SDW fibres ($V_V(mit,f) = 0.059$) and is supplied with a greater capillary contact (Table 4.1), although this is still low in comparison with fast muscle of other species (Johnston 1981a; Chapter 5) and is probably due entirely to the increased vascular density of the myoseptal region (Chapter 3).

Two forms of myogenesis have been described in amphibians, with either sarcomeres being present in the mononucleate myoblasts (during hindlimb development) or a delayed production (in the myotomal musculature) until the multinucleate myotube stage (Kielbówna and Koscielski 1979). The differential sarcoplasm content between small myotomal and myoseptal fibres may suggest an anatomical parallel with amphibian muscle, where there is an increase in cytoplasm volume density during myoblast hypertrophy, prior to myofibrillogenesis. The large $V_V(sp,f)$ found in elver myoseptal fibres, relative to myotomal fibres, may be a remnant of a similar process; however, such a different in growth pattern would have to be demonstrated by more direct means, for example by incorporation of radio-labelled amino acids. As there appears to be little or no difference in the myogenic stem cell morphology from the two regions of the muscle, the existence of separate MSC populations seems unlikely. In addition, the low frequency of MSC occurrence in the myoseptal regions would indicate an emphasis on growth by hypertrophy; there is little evidence to support the existence of a myogenic node.

TABLE 4.1. Morphometric analysis of muscle growth, from two fibre populations within the mid- and deep white regions of elver trunk. Mean ± S.E.M. (n).

Fibre Group	V_V(nuc,f)	V_V(mf,f)	V_V(mit,f)	V_V(sp.f)	$\bar{a}$(f) μm^2	$\bar{b}$(f) μm	$\bar{N}$(c,f)	$\bar{l}$(c,f)
Myotomal	0.114	0.566	0.056	0.267	29.85	15.56	0.014	0.001
	±0.0199	±0.0268	±0.0071	±0.0152	±3.177	±1.242	±0.0145	±0.0013
	(69)	(69)	(69)	(69)	(69)	(69)	(69)	(69)
Myoseptal	0.041	0.483	0.059	0.418	228.5	90.4	0.094	0.011
	±0.0077	±0.0325	±0.0048	±0.0283	±23.49	±7.658	±0.0367	±0.0043
	(64)	(64)	(64)	(64)	(64)	(63)	(64)	(46)

Note: Sample site was the same as described earlier (Fig. 2.1); symbols are as in Table 3.3. Myotomal fast fibres refers to the SMW and SDW groups in a previous study (Table 3.4); myoseptal fast fibres refers to fibres at a similar level of the myotome that are intimately associated with the connective tissue sheath (myoseptum).

TABLE 4.2. Morphometric analysis of fibre regional variation, elver fast muscle. Mean ± S.E.M.(n).

Fibre group	V_V(mit,f)		V_V(sp,f)		$\bar{I}$(ms,f)	I
	SS	IMF	SS	IMF		
myotomal	0.050 ±0.0066 (69)	0.006 ±0.0014 (69)	0.218 ±0.0173 (69)	0.048 ±0.0045 (69)	0	0
myoseptal	0.043 ±0.0051 (52)	0.017 ±0.0023 (52)	0.341 ±0.0344 (52)	0.071 ±0.0069 (52)	0.491 ±0.0194 (46)	0.256 ±0.0292 (46)

Note: Detailed analysis of samples described in Table 4.1; SS refers to the subsarcolemmal zone, defined as the region between the sarcolemma and the envelope formed by peripheral myofibril edges; IMF refers to the corresponding intermyofibrillar zone, the extent of which clearly varies with state of maturity, and hence fibre area. The estimate of fibre perimeter in contact with the myoseptum, $\bar{I}$(ms,f), and the relative increase in fibre surface area, I, were calculated from planimetry of fibre perimeter (see Fig. 4.1 for details).

Fig. 4.1. Myosatellite cell at the apex of a large DW fibre (bottom), showing the heterochromatic, lobular nucleus and the close association with the "parent" fibre. A distinct separation between the two sarcolemmas is evident, but the MSC is seen to be enclosed by the intact basal lamina. Scale bar = 0·5 µm.

Fig. 4.2. Late myoblast stage showing the presence of a fully developed myofibril and aggregations of myofilaments. The relative volume of mitochondria is evident, as are the vesicles, one of which is seen opening to the inter-sarcolemmal space. The vesicle density is seen to be similar in both the myoblast and large fibre. The prominent basal lamina, BL, is seen to enclose the cell. Scale bar = 0·5 µm.

Fig. 4.3. Late myotube showing remnants of the BL, which is resealing around the large fibre. The extension of the "pallisade" myofibrils carries them across the cell, although the sarcotubular system shows a fully functional, fast fibre morphology. The adjustment of the large fibre to accommodate the growing myotube, is seen to leave a depression at the fibre apex (left). Scale bar = 1·0 µm.

Fig. 4.4. Late myotube, still showing a high nuclear and mitochondrial content. The basal lamina has still not ruptured. The development of central myofibrils is beginning, with an invagination of the sarcotubular system into splits that have appeared at the apices of the largest myofibrils. Scale bar = 1·0 µm.

Fig. 4.5. Late myotube, showing the unusual occurrence of both the young fibre and an MSC, both enclosed within the large fibres basal lamina. Scale bar = 1·0 µm.

Fig. 4.6. Undifferentiated pericyte, showing the usual elongate pear-shape, with the thin cytoplasmic "tail" wedged between the two large DW fibres. Scale bar = 1·0 µm.

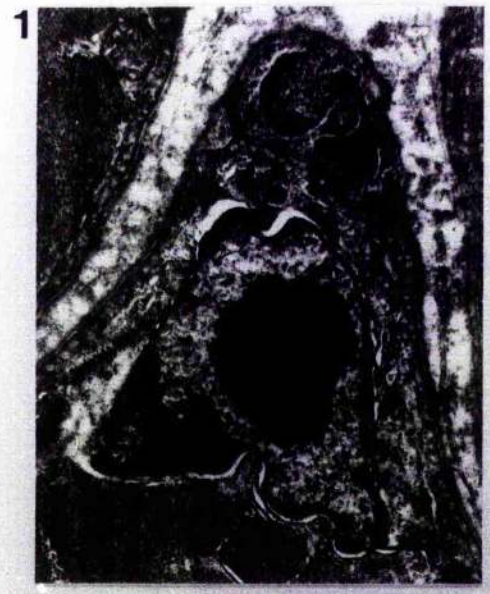
1

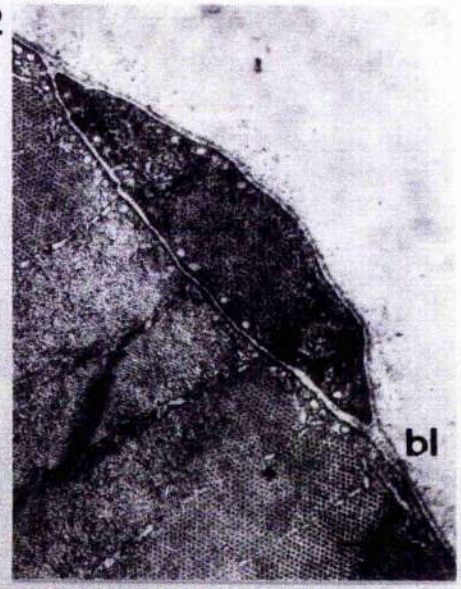

2

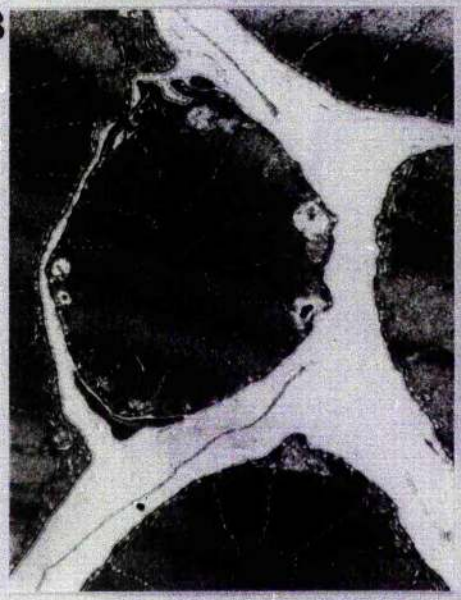
3


4


5


6

Fig. 4.7. Fast muscle myotube, showing the very large nucleus volume density, and four developed myofibrils. The basal lamina is still intact, although a projection is seen to be progressing within the inter-sarcolemmal space. In this way, the large fibre re-seals the BL around itself, before the myotube is fully separated by BL rupture. Scale bar = 1·0 µm.

Fig. 4.8. Late myoblast/early myotube. An unusually empty, somewhat expanded profile. The myofilament assembly is clearly seen to commence with actin coalescing onto Z-disc material, and proceed in a staggered manner across the cell. The sarcotubular system is seen to be assembled in advance of the sarcomeres it will serve. Extensive populations of rough endoplasmic reticulum (RER) and ribosomes are evident within the sarcoplasm.
Scale bar = 1·0 µm.

7

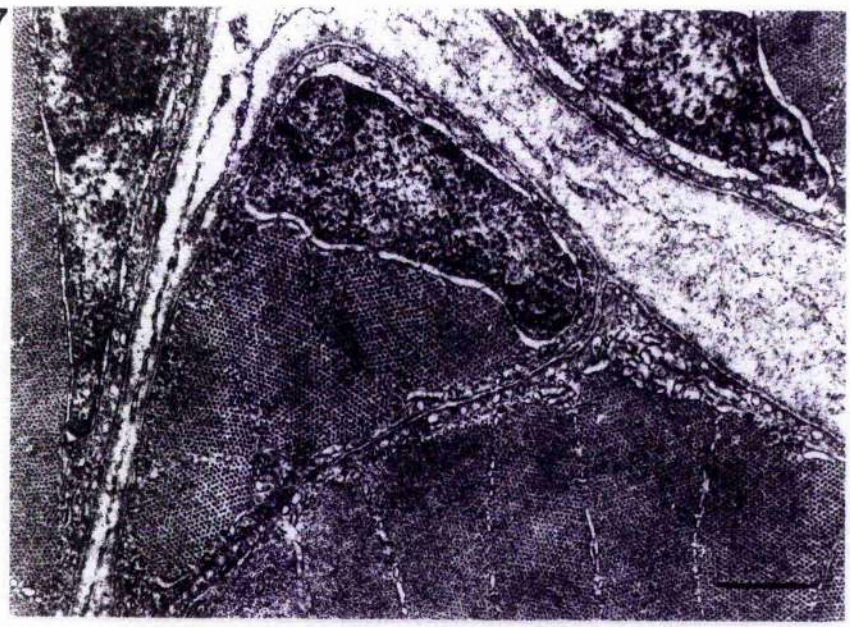

8

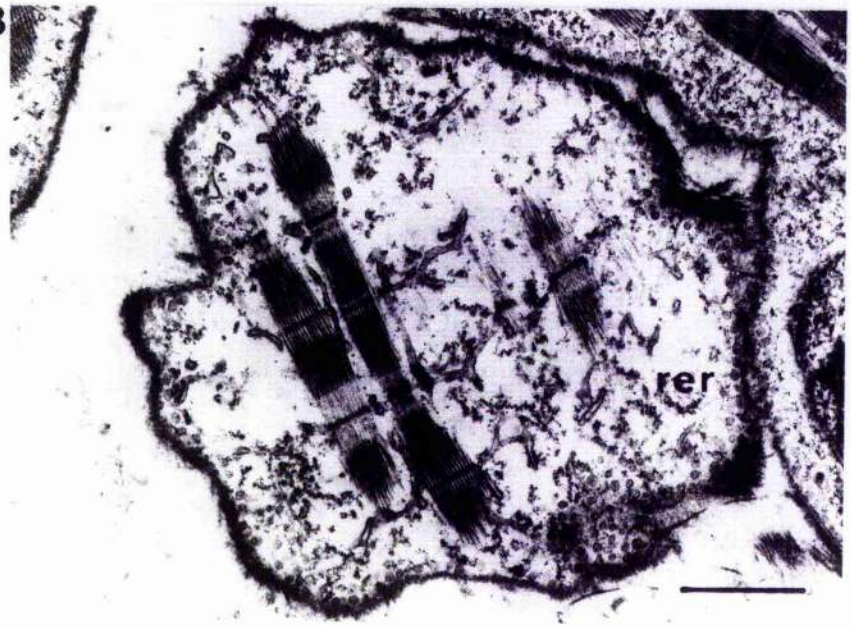

Fig. 4.9. Young myoseptal fibre showing the common, flattened appearance of many of these fibres. The crenulated fibre edge in contact with the myoseptum (MS) is seen to have relatively poorly developed interdigitations with the connective tissue sheath. Scale bar = 2 μm.

Fig. 4.10. Similar fibre to Fig. 4.9, in LS view, showing the extension of both the fibre and attachments. Note that the striations are in good register with the large, myotomal fibre (top, right) and appear to be functionally competent. Scale bar = 5 μm.

Fig. 4.11. Fibres adjacent to the myoseptum, on both sides, display extensive connections. An extreme case is seen (top, left) where a highly crenulated fibre is seen peripheral to the myoseptum. Such fibres are normally seen to be surrounded by the connective tissue. Scale bar = 2·5 μm.

Fig. 4.12. Fibre nearly surrounded by the myoseptum, showing an extensively invaginated periphery. Note the presence of a fibroblast (centre, right) and nerve axons running within the connective tissue matrix. Scale bar = 2 μm.

9

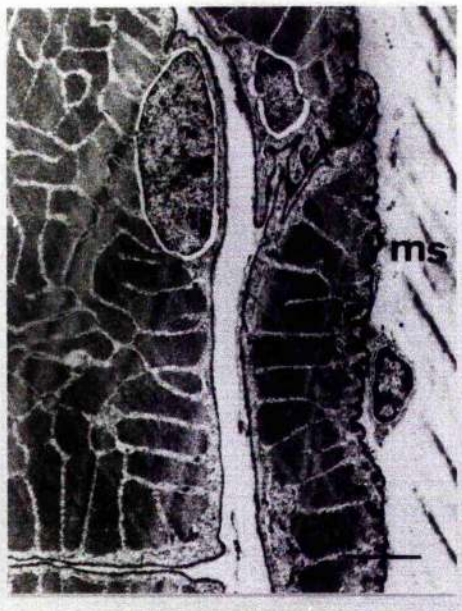

10

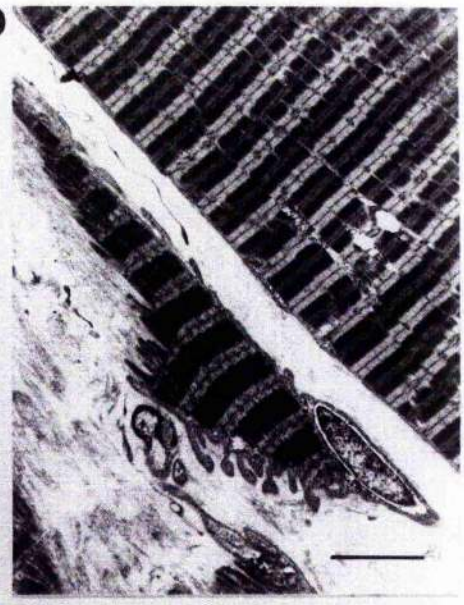

11

12

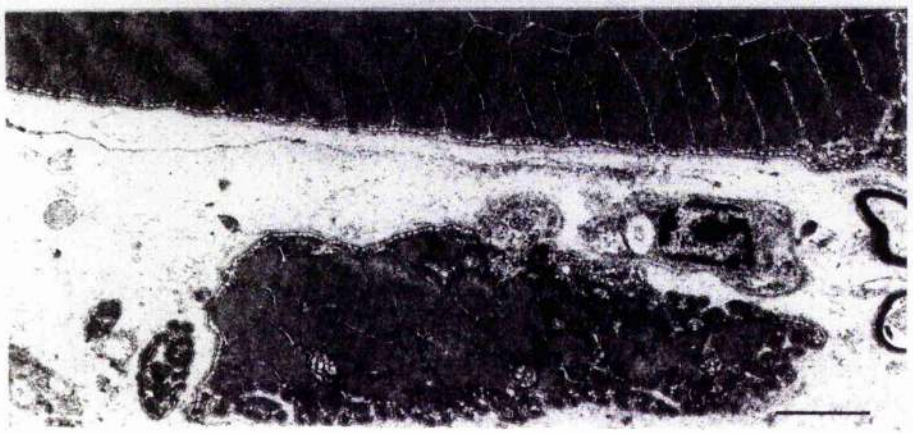

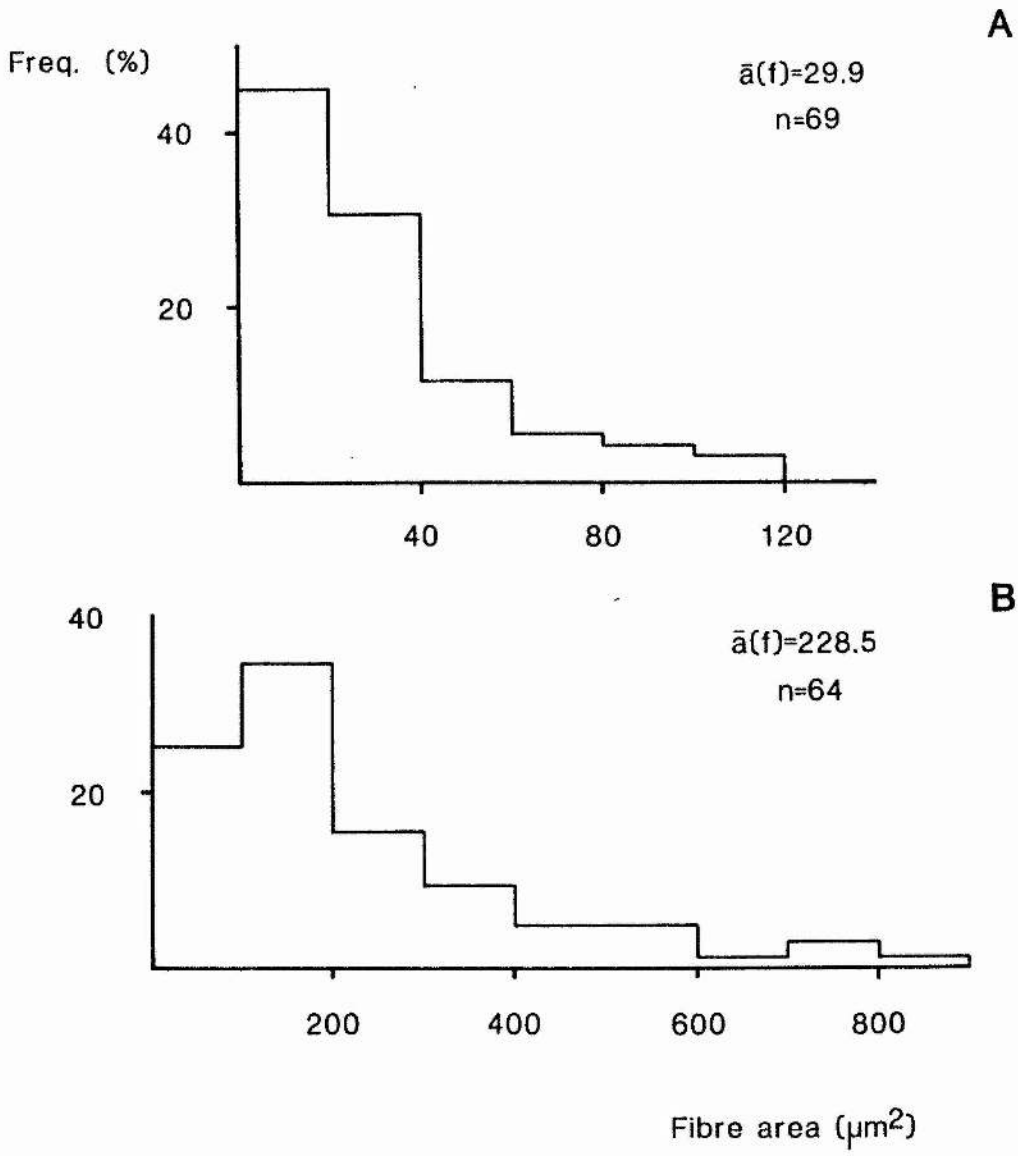

Fig. 4.13. Size distribution of myotomal (A) and myoseptal (B) fibres used in the morphometric analyses, taken at random from the sample sites described in the text. Note the larger range of fibre size seen in the myoseptal fibres. The frequencies reflect the numerical density of different size categories within the fast muscle, with the largest portion of small myotomal fibres being $< 50 \mu m^2$ (A) and a model category of $100-200 \mu m^2$ for the myoseptal fibres (B).

Fig. 4.14. Diagrammatic outline of a medium-sized myoseptal fibre showing the method used to quantify the amount of sarcolemmal invagination. The contact with the connective tissue is taken to be between the two arrows. A planimetric estimate of the total fibre perimeter is made, $b(f)_{tot}$, followed by an estimate of the fibre perimeter of an equivalent, though "smooth", fibre by tracing the envelope of the sarcolemmal projections (see enlarged portion) to give $b(f)_{env.}$ In the example, this amounts to an increase of 45% in the fibre surface area. By expressing the length of the fibre envelope between the arrows as a percentage of total fibre envelope (i.e. the fibre perimeter), an estimate of the extent of invagination is given; in this case, 48% of the fibre periphery is in contact with the myoseptum.

Fig. 4.15 Graph of the two estimates, showing the variability of the parameters and the different complexity of invaginations for a similar length of myoseptal contact. Those fibres showing a large proportion of their perimeter in contact with the myoseptum, but having only a small increase in surface area, usually had a much reduced sub-sarcolemmal space and only shallow invaginations.

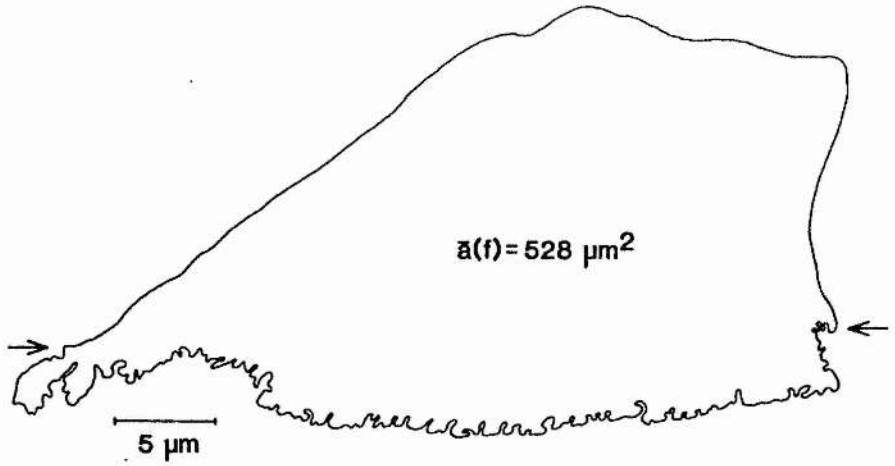

$b(f)_{tot}$ = 247 µm Rel. increase = 0.45

$b(f)_{env}$ = 111 µm Invaginated perim. = 0.48

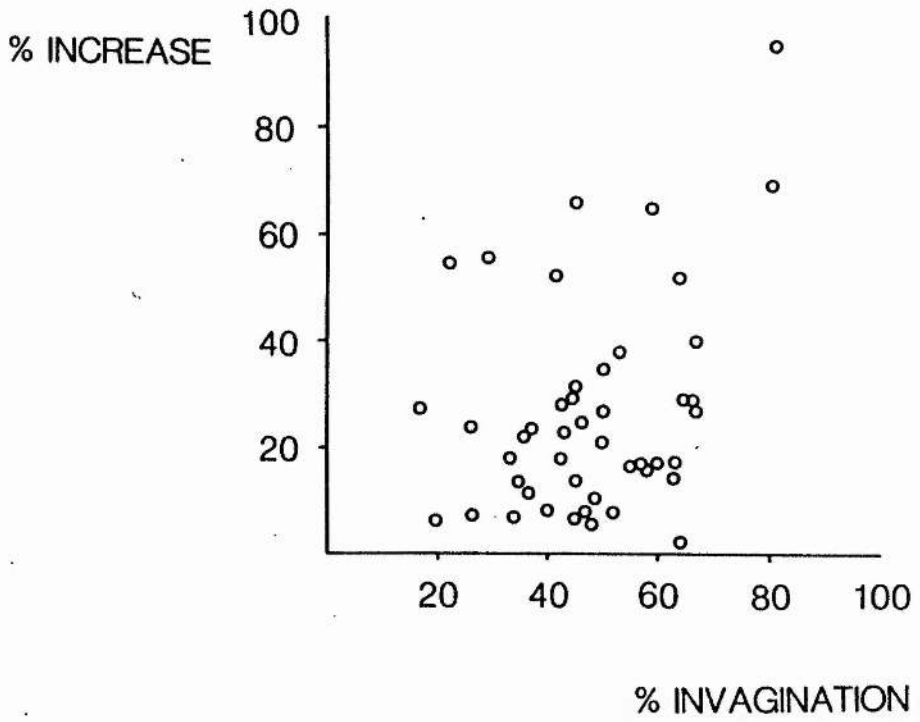

Fig. 4.16. Simplified outline of myotomes in the two main groups of fishes, elasmobranchs (top) and teleosts (bottom). The 3-dimensional myotome is shown sliced around its mid point, with the sloping projections directed rostral and caudal to the mid line.

a) dogfish anterior myotome, showing the "1½W" shape; caudal myotomes are similar, though more compressed.

b) cod anterior myotome, displaying a shallow "W" shape; the caudal myotome (c) is more steeply swept. In eel, the longitudinal processes may be more pronounced such that the anterior myotomes would resemble the pattern outlined in (c). The caudal myotomes, then, would be still more exaggerated. Note that the myotomes are fully interlocking, such that a TS section of the body will pass through a number of myotomes, some more than once. (Myotome shape after Nursall, 1956).

Fig. 4.17. Diagrammatic outline of the course taken by myotomal muscle fibres in a typical teleost, followed through successive myotomes. The helices are, therefore, composed from the orientation of many fibres inserting into myosepta in a linear sequence (from Alexander, 1969). Dorsal (top) and lateral (bottom) views are shown; se = subsidiary epaxial bundle

me= main epaxial bundle oe = obliquuus externus

oi= obliquus internus

Note that this hierarchy of fibre orientation is present within the complex myotomal shapes outline in Fig. 4.16.

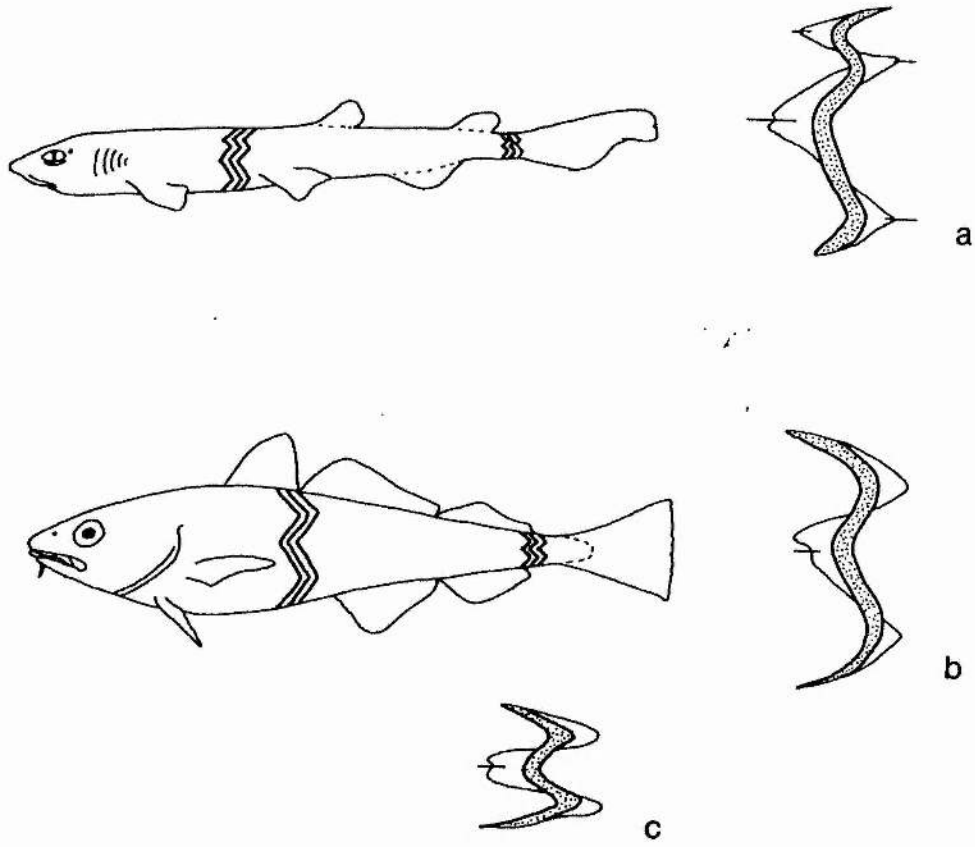
a
b
c

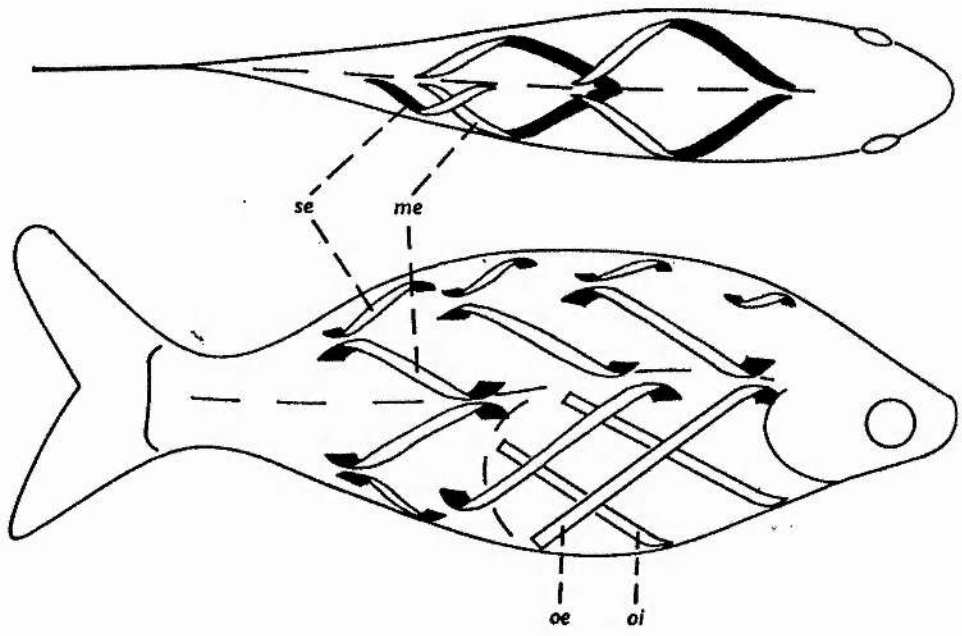
se
me
oe
oi

Fig. 4.18. In the steeply-swept myotomes of the eel, the helical arrangement of fibres will result in a different angle of myoseptal insertion, dependant on the angle the muscle fibre makes with the body axis. In this way, the extent of the myoseptal invagination will depend on the plane of sectioning, x and y. Fast muscle fibres may form large angles with the longitudinal axis of the fish (vertical line) up to 40° (Alexander 1969). This situation is further complicated, as a similar view can be obtained at 90° to this plan. R = rostral, L = lateral, ms = myoseptum.

Fig. 4.19. When one combines the convoluted myotome shape (Fig. 4.16) with the supra-myotomal organisation of fibres into helices (Fig. 4.17), and the variability of an individual fibre's angle of insertion into the myoseptum (Fig. 4.18), the complexity of trunk structure is apparent. As many myotomes are viewed in any TS section, the varied orientation of fibres results in a wide range of sectioning angles. TS sections are illustrated for elasmobranch (a) and teleost (b) trunk musculature, viewed from the caudal aspect. t = tendon, pc = posterior cone, ac = anterior cone (from Alexander 1969). Note that those fibres, in the teleost trunk, that run at large angles to the plane of sectioning run close to the myoseptal sheaths (see Fig. 4.10).

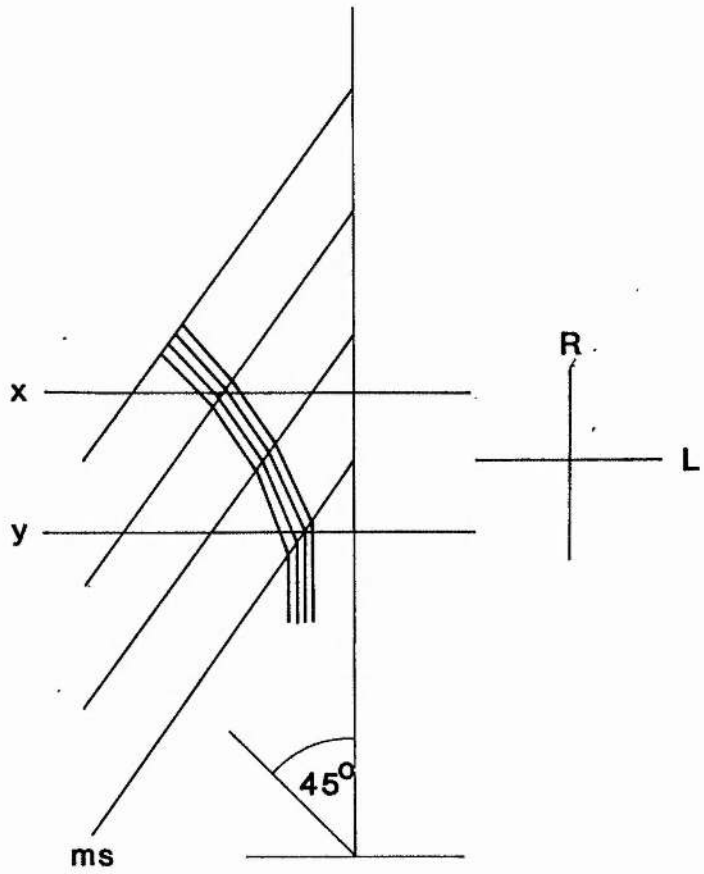
x
y
R
L
45°
ms

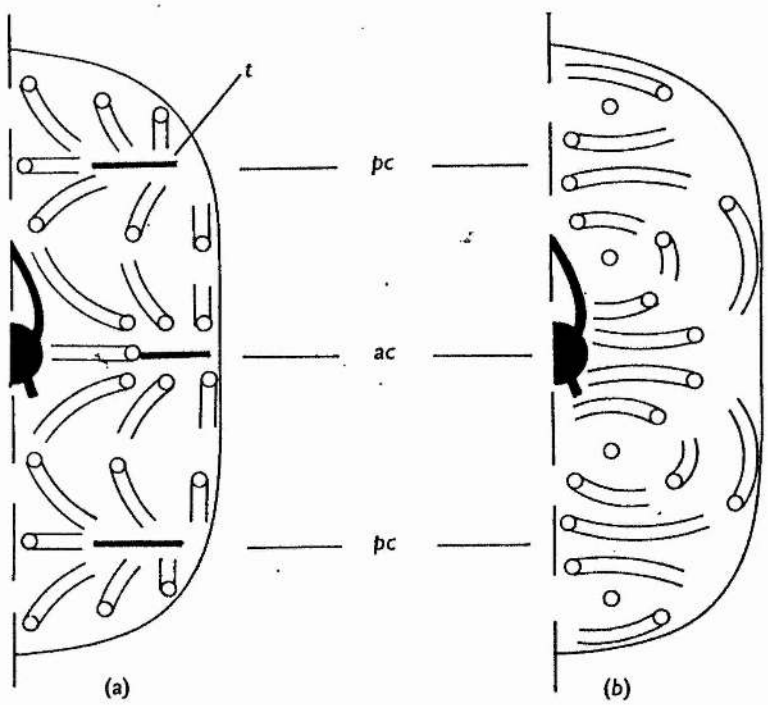
t
pc
ac
pc
(a)
(b)

Fig. 4.20. Normal, tendon-like insertion of myotomal muscle fibres into the myoseptal sheets (ms). Fibre a) represents the profile seen when the orientation is approximately normal to the myosepta; fibre b) shows the lateral extension of the profile when the fibre orientation is oblique to the myoseptum.

Fig. 4.21. Scheme to show the varying patterns of myoseptal contact, using the exaggerated situation found at a myotome apex. Fibre a) has an extended myoseptal invagination along part of its length (hatched portion) until the orientation of fibre axis and myoseptum diverge. Fibre b) represents a fibre considered to be in contact with the myoseptum along all its length; clearly, this could only occur if the fibre ran part way across a myotome. This represents the situation shown in electronmicrographs of small fibres, with one edge extensively invaginated. Fibre c) crosses the myotome at an angle to the myosepta, forming an extended myoseptal contact at both ends of the fibre. As the myotome width, d, is reduced (in caudal myotomes or young fish), the proportion of the fibre without myoseptal contact is reduced (clear area). Note that such a fibre will form an angle to both the horizontal and vertical axes.

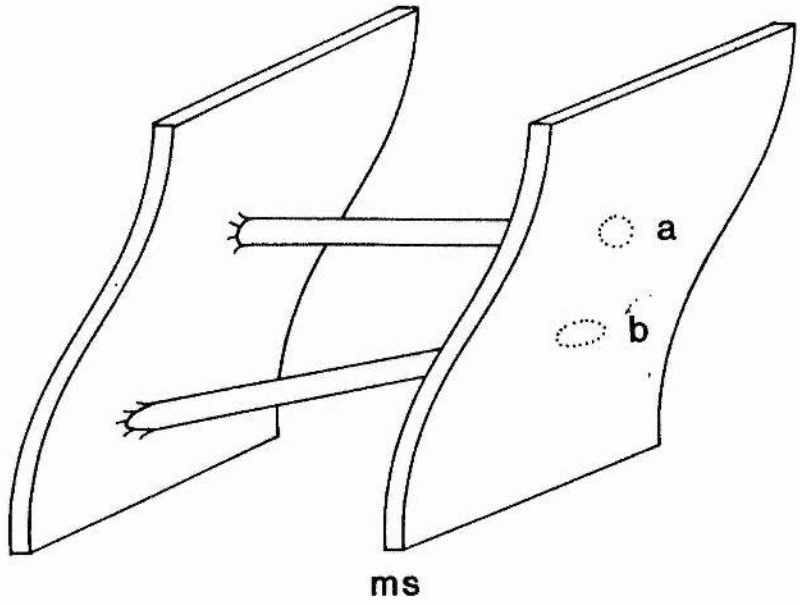
a
b
ms

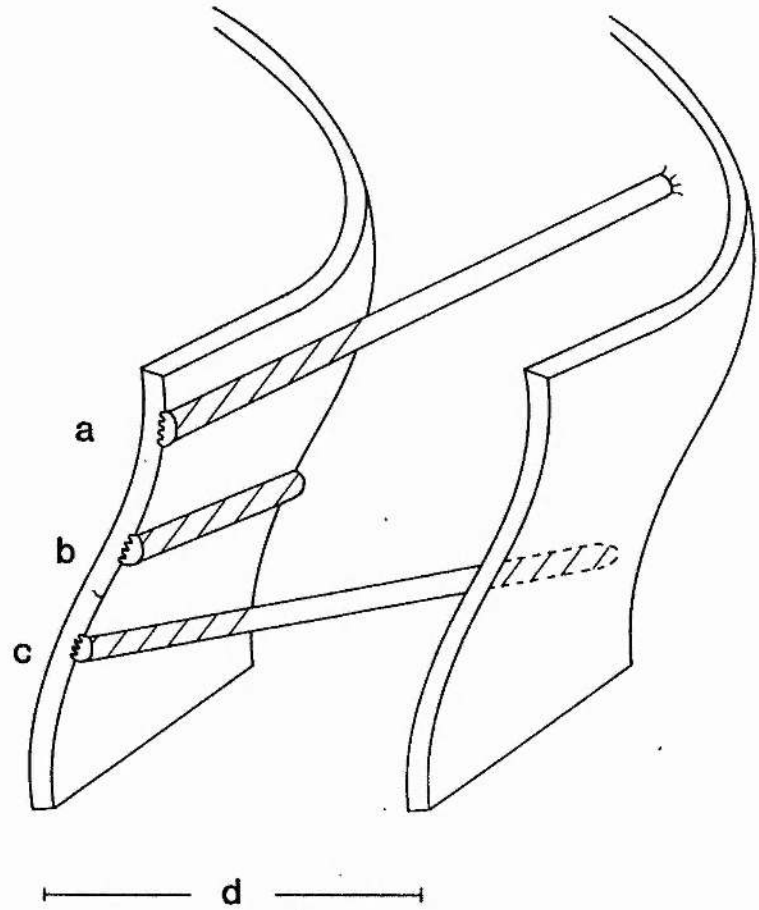
a
b
c
d

CHAPTER 5

INTRODUCTION

The vascularisation of skeletal muscle is known to co-vary with fibre mitochondrial content in a wide variety of mammals (Weibel et al 1981). It is clear that oxygen supply is dependent on many factors, including the density and surface area of capillaries, blood flow, perfusion distribution, myoglobin content and other variables affecting the oxygen-haemoglobin equilibrium and rate of mitochondrial respiration. Muscle capillarisation has been correlated with metabolic fibre type (Romanul 1965; Hudlická et al 1978), body size (Krogh 1919; Schmidt-Nielsen and Pennycuik 1961; Weibel et al 1981), whole animal $\dot{V}O_2$ (Hoppeler et al 1981b), and the effects of experimental hypertrophy (Rakusan et al 1980; James 1981). Although many different indices of capillary supply are in use, it is clear that none provide an adequate description of the physical dimensions of the capillary bed.

In mammalian limb muscles, the analysis is complicated since a mixture of fibre types are present, and a capillary may supply 3 or more metabolically distinct fibres. In contrast, the segmental trunk muscle of fishes is separated into distinct layers of different fibre types. This would seem to offer a useful model for determining the quantitative relationships between the capillary supply and metabolism of specific fibre types.

Several theoretical, and practical, limitations affect the representative sampling of the capillary supply to fish muscles. Slow muscle is composed of a mixed size range of small diameter, aerobic fibres with a relatively homogeneous capillary distribution. In all but very large fish, the sample area is restricted to a narrow, superficial layer of muscle. No such limitation on the sample area is found within the fast glycolytic fibres, which make up 90 - 95% of the myotome; however, the sparse distribution of capillaries makes quantification difficult. The sampling protocol must also take into consideration the heterogeneity of the capillary network, and any

adjustment that reflects the structural variation within a myotome. In addition, many of the indices used to described the capillary supply to fish muscle(Kryvi and Totland 1977 ; Flood 1979) were originally derived for use with the more regularly-organised mammalian limb muscles, and comparison of striated muscles from these two types of animals gives widely differing results (Mosse 1978). This demands a more thorough analysis than has so far been attempted, if anything other than a gross description is required. The mathematical modelling of anisotropic structures, such as capillaries, is complicated and requires information derived from isotropically, uniform, random sections (Weibel 1980; Mathieu et al 1982; Cruz-Orive 1982). These are technically difficult to obtain from muscle samples and a compromise methodology has been developed (Mathieu et al 1982), allowing the estimation of the performance limits in the gas exchange and blood perfusion systems.

In the present study, a suitable methodology was developed for an accurate estimate of the capillary oxygen supply to poorly vascularised muscle, such as found in primitive teleosts. The various indices are critically appraised in order to adopt those which best describe the physiological requirements of the muscle. A large species, the conger eel, was used in order to minimise the sampling errors found in small fish (Chapter 2); morphometric analysis of fibre types was also performed in order to assess the co-variance of capillary supply and muscle fine structure.

MATERIALS AND METHODS

Fish

Conger eels (Conger conger, L.) were trapped in St. Andrews bay; weight and length were 2444 $\pm$ 945.3g, and 112.6 $\pm$ 30.03cm., respectively ($\bar{x} \pm$ S.D., n = 5). Specimens were maintained for 1-3 weeks before sampling at ambient (North Sea) temperatures of 8-10°C.

Tissue preparation

Fish were stunned and decapitated; small bundles (2-3mm diameter) of fast and slow muscle fibres were rapidly excised from epaxial myotomes, immediately posterior to the cloaca, and prepared for electron microscopy as described previously (Chapter 3). No attempt was made to fix the vascular bed by perfusion. In this way, the samples were analogous to the RF and DW fibres described for the elver, from a similar region of the body (Fig. 2.1). Ten blocks of transversely-orientated, and five blocks of longitudinally-orientated fibre bundles were prepared from each sample site, in each of the five fish. Analysis utilised data from two resolution levels; semi-thin sections and electronmicrographs.

Capillary distribution

Semi-thin sections (0.5µm) were cut from 6 fast and 5 slow muscle blocks selected at random, but including at least 1 from each animal. Measurements of fibre cross-sectional area, $\bar{a}(f)$, number of capillaries, N(c), and number of fibres, N(f), were made directly from toluidine blue-stained sections (magnification x400) using a microscope drawing arm in conjunction with the planimeter system described earlier (Chapter 2). Measurements were made to all fibres in discrete bundles on each section, amounting to 250-300 slow or 200-250 fast fibres per section. Analysis was performed at regular increments of sample size, N(f) = 20 or 100, to obtain both cumulative and sub-sample means, calculated for both individual fish and grouped data. The change in estimate of the population mean was plotted against the sample size, i.e.

number of fibres included in the analysis, N(f). An optimal, minimum, sample size may then be directly read off the graph, corresponding to the point at which the population mean begins to plateau (Figs. 5.8, 18, 19).

(i) Capillary density, the number of capillaries per unit area of muscle fibre, was derived from the equation:

$$(\text{Eq. } 5.1) \qquad N_A(c,f) = \sum_{i=1}^{i=n} N(C)_i \; / \; \sum_{i=1}^{i=n} a(f)$$

(ii) Capillary to fibre ratio was determined using:

$$(\text{Eq. } 5.2) \qquad N_N(c,f) = \sum_{i=1}^{i=n} N(c)_i \; / \; \sum_{i=1}^{i=n} N(f)_i$$

(iii) Average number of capillaries in contact with a fibre was calculated:

$$(\text{Eq. } 5.3) \qquad \bar{N}(c,f) = \sum_{i=1}^{i=n} \frac{\left[N(c)_i \; / \; f_i \right]}{n}$$

where f_i = individual fibre profile

(iv) Sharing factor, the average number of fibres in contact with a capillary, has been confused with the reciprocal of $N_N(c,f)$. However, this is only true for the special case of a homogeneous capillary and fibre distribution pattern. The error caused by this erroneous assumption will increase as $N_A(c,f)$ declines, and the correct value has to be empiracally determined, using:

$$(\text{Eq. } 5.4) \qquad \bar{N}(f,c) = \sum_{i=1}^{i=n} \frac{\left[N(f)_i \; / \; C_i \right]}{n}$$

where C = individual capillary profile.

Note that this is not the same as the average number of muscle fibres per capillary, which is merely the reciprocal of $N_N(c,f)$, as used in other studies (Boddeke et al 1959; Mosse 1978).

Capillary anisotropy

The orientation of capillaries was determined in conger slow muscle, using the same TS sections as used in the calculation of $N_A(c,f)$ and 10 LS sections from blocks chosen at random, with 2 blocks from each fish. The LS sections contained profiles of 7-12 fibres. The numerical density of capillaries, with reference to muscle fibre area, was determined using the "forbidden line" rule (Gundersen 1977) in conjunction with a quadratic counting grid (A100, Weibel 1980), such that:

$$\text{(Eq. 5.5)} \qquad Q_A(c,f) = \sum_{i=1}^{i=n} N_{(c)i} \; / \; (d^2 . \sum_{i=1}^{i=n} Pi)$$

where d = lattice spacing

Pi = number of line intercepts

falling on muscle fibre profiles. (Weibel 1980; Mathieu et al 1982).

The length density of a component is related to its numerical density by:

$$J_V \propto Q_A(\Theta)$$

where $Q_A(\Theta)$ is the numerical density derived from a section whose normal (a projection at 90° to the section) forms an angle, Θ, with the axis of anisotropy. For T.S. sections, $\Theta = 0$ and for L.S. sections, $\Theta = \pi/2$

For perfect anisotropy, $J_V = Q_A(o)$

For perfect isotropy, $J_V \simeq 2.Q_A$ (Weibel 1980)

As the muscle capillary bed has a high (although unknown) degree of anisotropy, and as it is technically very difficult to determine Θ in sectioned material it is necessary to evaluate the concentration parameter (K) using:

$$J_V = C(K, \Theta).\ Q_A(\Theta)$$

using the assumption of a spherical-normal distribution of component orientation, it has been shown (Mathieu et al 1982; Cruz-Orive 1982) that:

K = 0 for an isotropic (random) distribution

K = +∞ for a component oriented parallel to the axis of anisotropy (e.g. multi-core wires)

K = -∞ for a component oriented parallel to the plane of anistropy (e.g. cartwheel spokes)

A simplified method of estimating K uses the ratio of numerical densities from TS and LS sections:

$$\frac{Q_A(0)}{Q_A(\pi/2)} = \frac{c(K,\pi/2)}{c(K,0)} \equiv K$$

from which c(K,0) can be calculated (Table 1, Mathieu et al 1982; see Fig. 5.19). Once this proportionality constant is known, the capillary length density can be calculated from any TS section; using:

$$J_V(c,f) = c(K,0).\ Q_A(0) \qquad \text{i.e.}$$

(Eq. 5.6) $$J_V(c,f) = c(K,0).\ N_A(c,f)$$

This allows the calculation of the capillary volume, and surface densities:

(Eq. 5.7) $$V_V(c,f) = \bar{a}(c).\ J_V(c,f)$$

(Eq. 5.8) $$S_V(c,f) = \bar{b}(c).\ J_V(c,f)$$

where the capillary density is an estimate of the volume of blood within the capillary network, representing the maximal oxygen delivery to the muscle; $\bar{a}(c)$ is the mean capillary cross-sectional area. The capillary surface density is an estimate of the total capillary surface area available for blood-tissue gas exchange, and represents the structural limitations to muscle oxygen flux; $\bar{b}(c)$ is the mean capillary circumference.

Morphometric analysis

Ultrathin sections were taken from the TS blocks used for analysis of capillary density; analysis of fibre composition, and capillary dimensions, were performed as described earlier (Chapter 3). The large size of the fast

fibres prevented a representative proportion of the largest fibres (7-10000μm^2) being included in the analysis, using electronmicrographs of whole profiles, since part of the fibre was usually obscured by a grid support. A group of 10 fibres, $\bar{a}(f) \doteq 2000\mu m^2$, were analysed with and without a strip of black card, equivalent in size to a grid support, laid across the image. Comparison of the two sets of data revealed $<2\%$ difference, indicating a very uniform intra-fibre distribution of components. Large fibres were subsequently included in the analysis, using data from electronmicrographs of fibres with regular profiles, transected by a grid support in the mid region (n=8, see Table 5.5).

RESULTS

The elongated body of the conger eel shows a progressive, though shallow, increase in the proportion of slow muscle, rostral to caudal and displays a similar type of locomotion to that described for the freshwater eel (Chapter 2). The structure and organisation of the trunk muscles are similar to those in the elver (Chapters 2 and 3) and other teleosts (Johnston 1981a), except that the slow muscle layer is bounded on both sides by an extensive adipocyte population (Fig. 2.34 ; 5.1a). There is a moderately well developed capillary network in these regions (Fig. 5.1c), which may contribute to the muscle oxygen supply. The majority of lateral anastomoses, seen in LS sections of the muscle, appear to be associated with inter-fibre lipid deposits.

Only those blood vessels that consisted of endothelium and pericytes were considered to be capillaries, following the approach adopted by workers on mammalian muscles (Casley-Smith et al 1975; Mathieu et al 1982; see Fig. 5.6). As the accuracy of derived parameters requires a good estimate of capillary dimensions, particular attention was paid to the errors involved in simply measuring all small blood vessels. The distribution of capillary size in slow muscle is clearly asymmetric (Fig. 5.12); only a small proportion of larger blood vessels are found within the myotome, usually being restricted to the region of the myosepta. This distribution is also seen in elver (Chapter 2) and tench (Fig. 5.9) slow muscles, and approximates a log-normal distribution pattern. Inclusion of all "capillary-like" vessels in the analysis introduces only a small error in the calculation of $\bar{a}(c)$ for slow muscle (Fig. 5.12). Fast muscle, however, contains a significant proportion of very large blood vessels (venules) and a broader distribution of smaller vessels that could, erroneously, be included in any calculation of capillary supply (see Fig. 5.12).

Slow muscle shows a highly skewed distribution of fibre cross-sectional areas, with only 12% being $>2000\mu m^2$ (Fig. 5.3). The fast muscle displays a much larger range of fibre size with 12.5% of the fibres $>9000\mu m^2$; a similar

concentration of small diameter fibres as described for the elver is present, in contrast to the even distribution found in slow muscle (Fig. 5.3). Slow fibres have a high mitochondrial and intracellular lipid content, 23 and 18%, respectively (Table 5.4, Fig 5.14), restricting the contractile apparatus to less than 50% of the fibre area. In common with Anquilla, the large intercellular lipid deposits (Figs. 2. and 5.1) may be present as a preadaptation for winter torpor, or as an additional buoyancy mechanism. The mitochondria show a moderate cristae development (Fig. 5.14) and, with the proximity of a regular capillary network, this gives the fibres an appearance usually found in muscle with a well developed aerobic metabolism (Bone 1978; Johnston 1981a). Fast fibres have very little intracellular lipid, a small mitochondrial compartment (around 3%, Table 5.5, Fig. 5.16) and a restricted capillary contact (Table 5.5). In contrast to the situation in slow muscle, the mitochondria and lipid deposits are evenly distributed between the subsarcolemmal and inter-myofibrillar zones (Tables 5.4 and 5.5). Inclusion of data from very large fast fibres in the morphometric analysis has only a small effect of component values (Table 5.5). The morphology, therefore, is indicative of a very anaerobic metabolism.

Sharing factor, $\bar{N}(f,c)$, varies little between either sub-samples or muscle types (Fig. 5.4) and is clearly of limited usefulness as a descriptor of the aerobic scope of a muscle (Table 5.2), although care must be taken to avoid ambiguous presentation of numerical density estimates (Table 5.3). The capillary density, $N_A(c,f)$, is seen to co-vary with mean fibre cross-sectional area, $\bar{a}(f)$ (Figs. 5.18 and 5.19), and the capillary to fibre ratio, $N_N(c,f)$. $N_A(c,f)$ was 615 and 21.3mm^{-2} for slow and fast muscle, respectively; these values are low, relative to homologous muscles in other teleosts (Table 5.9) and mammals (Table 5.6). This is reflected in the small proportion of fibre periphery that is in contact with capillaries, $\bar{l}(c,f)$, which is only 13 and 1.0%

in slow and fast muscle, respectively (Tables 5.4 and 5.5). In both elver and conger muscles, no correlation could be found between the apparent oxygen demand of an individual fibre, and the capillary supply. For each muscle type the number of capillaries around a fibre, N(c,f), and the vascularised perimeter, l(c,f), show no consistent relationship with either fibre cross-sectional area, surface:volume ratio, or mitochondrial content. In addition, although the intra-sub-sample variance is always large (for all indices), the inter sub-sample variance is usually quite small (especially for numerical density estimates). This would suggest that the capillary supply to an individual fibre is random, but that the apparently heterogeneous distribution of capillaries results in a fairly even tissue capillary supply.

The variability of $\bar{a}(f)$, estimated as sample mean/extrapolated population mean, falls to below 10% after N(f) = 400 for both fibre types, irrespective of the sample increment used (Figs. 5.18, 5.19). Despite the differences in magnitude of $N_A(c,f)$ a similar, surprisingly large, sample size is required for a reproducible estimate in both fibre types. Slow muscle shows a 10% variation in mean values between N(f) = 200 and 300 (Fig. 5.19). In addition to N(f), the variation in population mean is determined by individual variation of the samples (animals) used in the analyses. In the present study, it was found that N(f) = 100 is sufficient to obtain a reproducible estimate of both $\bar{a}(f)$ and $N_A(c,f)$ population means for an individual fish (Fig. 5.11), although 4-5 times this figure is necessary to obtain a representative value for the species mean (Figs. 5.18 and 5.19). For conger eel, then, a sample of 75-100 fibres from each of 5 fish is desirable for any analysis of the muscle capillary supply. It should be stressed that this minimum sample size is not an absolute figure, as there is a subjective element in the procedure since the choice of the plotted sample increment will affect the final result. However, this is not sufficient to reduce the additional accuracy such a step gives to the analysis (Figs. 5.18 and 5.19).

A remarkable degree of anisotropy is seen in the slow muscle capillary network; only around 5% of the capillary profiles seen in TS sections of muscle are cut longitudinally. In LS sections these lateral ananastomoses are seen to account for nearly 10% of the capillary profiles, and this is reflected in the high value of the concentration parameter, K = 16.80 (Table 5.7). Values for the derived parameters, capillary volume and surface density, are presented (Table 5.8) and their significance discussed.

DISCUSSION

Methodology

The most widely accepted model for oxygen supply is based on a cylinder of tissue served by a straight, unbranched capillary at the centre (Krogh 1919). This requires assumptions about the uniformity of capillary supply, blood flow, oxygen diffusion and tissue respiration rates that are rarely found in vivo (Longmuir 1978). In spite of this, most authors have used the relative densities of muscle fibres and capillaries, estimated in transversely-sectioned material, and a hexagonal model of the capillary bed has been shown to give good predictions of mammalian muscle Po_2 (Akmal et al 1978). This regular pattern was noted in a survey of different mammals, where slow muscle has capillaries in all the large interstitial spaces, and the fast muscle has capillaries in alternate spaces, giving a capillary to fibre ratio of 2:1 and 1:1 respectively.* Before any corresponding model can be derived for fish, more data is required concerning the arrangement of capillaries, since a regular array is probably only appropriate to muscle with a fairly uniform fibre size. The increase in girth of a fish myotome, by recruitment of new fibres, provides an irregular array of interstitial spaces. Capillaries may be expected to preferentially grow along pathways of least resistance, resulting in an irregular distribution pattern. Evidence for such a mechanism is found in the longitudinal orientation of new capillaries of experimentally-hypertrophied mouse EDL (extensor digitorum longus; James 1981), and the location of lateral anastomoses adjacent to inter-fibre lipid deposits in conger slow muscle.

A widely used supply index for the regular mammalian capillary network is the sharing factor, or number of muscle fibres surrounding a capillary, $\bar{N}(f,c)$. It is relatively insensitive, with a range of only 1.99 (rat soleus)

*(Schmidt-Nielsen and Pennycuik 1961).

to 3.22 (dog tongue) (Plyley and Groom 1975). The use of such an index for fish muscle (Kryvi et al 1980) is rather surprising, since it takes no account of the fibre packing; although the range of values in fish muscle is larger, 2-6, it does not reflect differences in capillary density and an average of 3 is found in all muscle types of eels (Table 5.2).

An averaged estimate of oxygen supply is the capillary to fibre ratio, $N_N(c,f)$, but this also shows little variation among mammalian muscles ($\bar{x}$ = 1.49; Plyley and Groom 1975). It does, however, reflect some adaptive changes e.g. repetitive stimulation of fast muscle motor nerves at slow muscle frequency, results in a 1.5-fold increase (to 2.18) in rabbit FHL (flexor hallucis longus; Brown et al 1976). The 100-fold range of reported values for fish muscle (Table 5.3) gives this index a large descriptive potential, although its sensitivity to change in muscle aerobic capacity remains untested.

The mean number of capillaries in contact with a fibre, $\bar{N}(c,f)$, is thought by many workers to reflect the oxygen demand of the muscle fibres. Although not synonymous with $N_N(c,f)$, both indices have been labelled "capillaries per fibre" in the literature, causing some confusion (Table 5.3). Again, the range of values found in mammalian muscles is small, 3.0 to 3.8 across a 23-fold range of fibre size, but shows a good correlation with $N_N(c,f)$ ($r = 0.746$, $n = 16$; Plyley and Groom 1975). This would suggest that the capillary supply to whole muscles and individual fibres are matched, with one giving a good estimate of the other. In fish muscle, across a similar range of fibre size, values are found <1.0 and >12.0 (Table 5.3). The lack of correlation found between $\bar{N}(c,f)$ and $\bar{a}(f)$ (Fig. 5.13) may be explained in terms of the muscle composition, since the magnitude is likely to depend on both fibre geometry, and size distribution. Interestingly, the increased oxygen uptake efficiency associated with the greater surface

area: volume ratio in the flattened slow muscle fibres of Anchovy (Johnston, 1982), is also accompanied by an elevated $\bar{N}(c,f)$ (Table 5.3). This indicates that capillary supply may be a limiting factor in muscle respiration; correspondingly, there is a 2-fold increase in carp slow muscle during acclimation to a 26°C difference in temperature (to 4.8 at 2°C; Johnston 1982b). Little improvement in descriptive power is afforded by measuring capillary-fibre contact length, $\bar{l}(c,f)$, which varies in a qualitative manner much the same as $\bar{N}(c,f)$ (Tables 5.4 and 5.5; see also Table 2.2, Kryvi et al 1980 and Johnston 1981a). The inter-capillary distance shows a log-normal distribution in some muscle (Rakusan et al 1980), and reflects the proportion of patent capillaries in response to varying Po_2 (Hamilton and Dow 1965). Unfortunately, it is difficult to interpret similar results obtained from fast muscle in fish, where the distances are very large and the capillary distribution apparently heterogeneous.

Capillary density, on the other hand, is considered to be a good index of tissue oxygen consumption in a wide range of animals (Anderson and Henriksson 1977; Mosse 1979; Wiebel et al 1981), reflecting the extent of capillary supply. The co-variance of capillary density and mitochondrial content is well documented for mammalian muscle, with respect to metabolic fibre type distribution (Brown et al 1976; Hoppeler et al 1981); their experimental modification (Cotter et al 1973), where an increase in capillary density is due to the growth of new capillaries (Myrhage and Hudlická 1978); and the change in aerobic capacity with endurance training (Anderson and Henriksson 1977; Ingjer 1979). Unfortunately, there is considerable variation in the estimates among workers, indicating the need to standardise the methodological approach. For example, the reported values for cat gastrocnemius range from 379 to 2341 capillaries mm^{-2} (Plyley and Groom 1975). The wide variety

of methods used to localise capillaries in muscle (see Plyley and Groom 1975; Mosse 1978) undoubtedly causes a degree of variability: histochemically-stained or dye-injected cryostat sections, histological wax sections, semi-thin sections, and low-power electronmicrographs have all been adopted by various authors as being the best available method. In this study, indian-ink injection consistently underestimated the capillary content of a muscle, and alkaline phosphatase incubation of cryostat sections proved unsatisfactory (see also Mosse 1978). The only consistent result obtained in this manner was that of carbonic anhydrase localisation (Ridderstale 1979), although the weak nature of the reaction proved problematical. Sampling large numbers of fibres requires a relatively low magnification which may be obtained with semi-thin sections, whilst retaining a sufficiently high resolution for the unequivocal, morphological, identification of capillaries. The heterogeneous oxygen permeability across a muscle (Longmuir 1978) is mainly due to the variable interstitial space, and analysis of capillary supply may be further standardised by using fibre area as the stereological reference phase (Chapter 1); i.e. calculate $N_A(c,f)$, the number of capillaries per unit cross-sectional area of muscle fibre (Hoppeler et al 1981).

The information available from transverse sections is limited, as it gives no indication of the 3-D geometry of the capillary bed. For example, any increase in tortuosity of the capillaries will not be detected in TS sections, although it will result in a functional increase in capillary density (Appell and Hammersen 1978). Therefore, any improvement over the methods so far discussed (above) must take account of the length of capillaries, relative to muscle fibre volume, in the quantification of capillary supply. From this, the capillary volume density, $V_V(c,f)$, and surface density, $S_V(c,f)$, may be calculated; providing an estimate of the volume of capillary blood and available surface area for gas exchange, respectively. It has been assumed

that the higher value of many capillarisation indices in fish slow, relative to mammalian red muscle, reflects the higher $V_V(mit,f)$ (Johnston 1982a). However, maximal oxygen delivery to a muscle will depend both on the number of capillaries adjacent to a fibre, and the mean fibre area. The broad range of fibre sizes in fish muscle, and shared oxygen delivery between different metabolic fibre types (Flood 1979), are additional problems. Furthermore, capillary dimensions are either ignored, or assumed to be relatively constant, whereas considerable inter-specific variation is found (Table 5.9). In the light of more recent work, then, it is clear that there is a considerable degree of overlap between mammalian and fish slow muscles, with respect to both mitochondrial content and capillary supply (Table 5.); $V_V(c,f)$ or $S_V(c,f)$ may be better descriptors, as they take account of both capillary dimensions and density. Other indices may still be useful: the magnitude of $N(f)$ required for a stable estimate of $N_A(c,f)$ varies as a function of $\bar{N}(c,f)$, and this information is required for maximal accuracy of derived estimates. It can be shown that as $N(f)$ increases, Type 1 (sampling) error tends to zero and any variation in the estimate of population mean will be due to Type 2 (methodological) error and natural variability, only. Such a value will not then change with any further increase in $N(f)$. The dependance of the optimal sample size on both anatomical and metabolic factors is illustrated by carp slow muscle, which requires a lower value of $N(f)$ than conger slow muscle, for a stable sample mean (Figs. 5.11 and 19). This reflects both a higher $N_A(c,f)$ and lower $\bar{a}(f)$. Inter-specific variation can be misleading, however, since tench slow muscle requires $N(f) > 100$, even though $N_A(c,f)$ is higher and $\bar{a}(f)$ is lower than carp slow muscle (Fig. 5.8).

Comparative Physiology

Any description of the vascular system of fishes requires a sufficient knowledge of cardiovascular and haemodynamic properties (blood flow, pressure differentials, end-capillary Po_2), before using indices based on a model mammalian system. Such information is extremely difficult to obtain from unrestrained fish; for example, an elevated blood pressure (BP) is recorded from fish inverted during experimentation, whereas anaesthesia results in an increased gill resistance but a reduced BP (Randall 1970; Farrell and Smith 1981). It is understandable, then, that most workers attempt the quantification of oxygen supply by indirect analysis. Capillary supply is likely to be affected by both gross respiration and cellular metabolism; it is therefore important to consider the major differences in functional design, and maximum capacities of the respiratory systems, between fishes and mammals. There is a 10-15 fold reduction in maximum rate of oxygen consumption ($\dot{V}o_{2\ max}$) for ectotherms, relative to homeotherms (Bennett 1978). This is mirrored by a reduction in oxygen-binding capacity of the blood and a lowered systemic blood pressure (Table 5.1), which may be as low as 10mm Hg in the venous return (Randall 1970). Blood pressure is normally determined by peripheral resistance, blood volume, and the pressure differential established by the heart. This relationship between pressure and volume is illustrated phylogenetically, with Osteichthyes (bony fish) generally having a lower blood volume and higher BP than the Chondrichthyes (elasmobranchs) (Table 5.1). Within the Osteichthyes, average blood volumes are estimated as 2.2 - 3.6, 3.1 and 3.5% body weight for teleosts, holosteans and chondrosteans, respectively (Prosser 1973). The comparative anatomy of the circulation also needs to be considered, since there is a large drop in pressure between the ventral and dorsal aortas due to the branchial resistance. This resistance, due to the fine blood vessels perfusing

the gills, may account for 20-30% of the ventral aorta BP is elasmobranchs, and 40-50% in teleosts (Prosser 1973; Randall 1970; Farrell and Smith 1981). The low dorsal aorta BP, relative to homeotherm arterial pressures, requires a decrease in the peripheral (systemic) resistance to maintain efficient perfusion and oxygen supply to the muscle. This may be achieved by an increase in $\bar{a}(c)$, since flow resistance is inversely proportional to the 4th power of blood vessel radius, and/or an increase in $N_A(c,f)$. These parameters are inter-related via the Poiseuille equations for a single cylinder:

(Eq. 5.9) $$F = \frac{N \pi r^4 \Delta P}{8 \eta l}$$

(Eq. 5.10) $$R = \frac{8 \eta l}{N \pi r^4}$$

where
- F = blood flow rate
- N = number of capillaries
- r = capillary radius
- ΔP = pressure differential (driving pressure)
- η = blood viscosity
- l = cylinder length
- R = hydrostatic resistance

It can be shown that a dramatic increase in the efficiency of oxygen supply results from the subdivision of large vessels, involving only a small increase in ΔP (Schmid-Schönbein 1981). From the limited data available, however, it seems likely that capillary dimensions in fish are similar to those found in mammals of comparable body weight e.g. rat heart = $40\mu m^2$, catfish slow muscle = $20\mu m^2$. This would suggest that the regulation of oxygen supply is derived from variability in the extent of the capillary network. Some degree of morphological adjustment may be possible, such as in the haemoglobinless fish Chaenocephalus aceratus, where $\bar{a}(c) = 54\mu m^2$ (Table 5.6). In view of the physiological response of the cardiovascular

system to counteract the lack of haemoglobin in this fish (elevated blood volume and cardiac output, see Table 5.1), the coincident adjustment of the capillary net work would emphasise this as being a limiting step in tissue respiration. The relative importance of physiological and anatomical responses to muscle plasticity remains to be determined. The species-specific response to hypoxia acclimation, where some fish show an adjustment of capillary supply (Johnston and Bernard 1982) may provide a useful approach for the elucidation of this problem.

In higher teleosts, the capillary supply mirrors the change in mitochondrial content, under a variety of experimental conditions (Johnston 1981a; Johnston and Bernard 1982). However, the correlation between these two parameters is more complex than generally realised (Weibel et al 1981), with some mammalian muscles showing an increase in $V_V(mit,f)$ with no adjustment in the capillary supply (Müller 1976). In a number of African mammals, muscles having a similar $V_V(mit,f)$ may have a 4-fold difference in $N_A(c,f)$ (Weibel et al 1981). Such variability has led a number of workers to dispute the correlation between capillary supply and muscle oxidative capacity (Schmidt-Nielsen and Pennycuik 1961; Loats et al 1978; Maxwell et al 1980), since "white" muscles may have similar capillary densities to some "red" muscles. During anaerobic metabolism, for example, a fast muscle may require an efficient blood supply for the delivery of glycolytic substriates, or the removal of metabolites such as lactate (see Gray and Renkin 1978). This is particularly important for fish, especially elasmobranchs such as dogfish, that have an absolute dependance on anaerobic glycolysis for fast muscle metabolism. The endurance is limited by the extent of glycogen stores (Bone 1978; Bone and Chubb 1978), and the prolonged recovery period following exhaustive exercise is correlated with a low capillary density (Fig. 5.20).

Although the available data is incomplete, it would appear that elasmobranchs and teleosts are represented by different slopes of the $V_V(mit,f)$ vs $N_A(c,f)$ graph (Fig. 5.20). More importantly the primitive teleosts and elasmobranchs, sharing the same innervation pattern and assumed to show a similar recruitment pattern of the muscle, occupy different areas of the graph. This may reflect a broader range of swimming speeds for these teleosts that is usually assumed (Grillner and Kashin 1976). Those species with polyneurally-innervated fast muscle, the higher teleosts, have a much higher capillary density, correlating well with both the pattern of fibre recruitment and the transient appearance of lactate during exercise (Johnston and Moon 1981; Wokomo and Johnston 1981).

Such comparisons may be valid, although the scatter of data suggests that $N_A(c,f)$ is not sufficiently flexible to adequately describe the capillary supply to fish muscle. For example, the elver has been shown to have a relatively low aerobic capacity (Chapters 2 and 3 Fig. 5.13), whereas the small fibre area results in a moderate $N_A(c,f)$ (Table 5.8). Similarly, the large capillary size in Chaenocephalus will result in a greater blood volume than indicated by the low capillary density (Table 5.6). Clearly, an index is required that describes the functional potential of muscle capillary supply. A preliminary attempt to estimate the length density, $J_V(c,f)$, for mammalian muscle used an approximation of $N_A(c,f) \times 1.12$ (Hoppeler et al 1981). Although this was subsequently reduced to $c(K,0) = 1.034$ (Mathieu et al 1982), the estimate for conger slow muscle is even lower, reflecting the highly anisotropic arrangement of the capillaries (Table 5.7). In other fishes, dye-injection has revealed a meandering pattern for individual capillaries (Barets 1961; Flood 1979); it is possible that this is an artefact of immersion fixation at less than resting length (Zummstein et al 1982), although

no comparative data is available to indicate whether or not eels are representative of other species. The derivation of a small proportionality constant, $c(K,0) = 1.016$, means that capillary density is a reasonable estimate of $J_V(c,f)$, when determined from true TS sections and a sufficiently large sample size. It is to be expected that the frequency of capillary branches would be less in fish, relative to mammalian muscle since most branching occurs at the myosepta (Chapter 3). In addition, the smaller contractile unit (limb muscles vs mytomes) is likely to be served by fewer lateral branches, that preferentially follow the longitudinal interstitial spaces (see above).

The pale yellow appearance of the slow muscle, and the large proportion of fast muscle, reflects the low blood volume of the species, This is reflected in the low $V_V(c,f)$ for slow muscle which, despite being somewhat larger than suggested by the estimate of capillary density due to a large $\bar{a}(c)$, is less than for most species (Fig. 5.2 ; Table 5.9). More significantly, the low value of $S_V(c,f)$ indicates that a limited oxygen delivery is available to the working muscle, supporting the contention that a restricted aerobic scope is a function of anquilliform locomotion (Chapter 2). The real value in such an index, however, will lie in determining the limiting step in cellular respiration for a muscle under exhaustive exercise or endurance training; such information is not available for fishes.

In mammals, $V_V(mit,f)$ and $J_V(c,f)$ are scaled to the same power of body mass ($Mb^{0.8-0.9}$) as $\dot{V}o_{2max.}$, using regression analysis (Weibel et al 1981). Such allometric relationships are unknown for fish, and is difficult to estimate from published results as some workers fail to report the size of animal for which data is presented. As fish employ accessory buoyancy mechanisms (swimbladder, lipid stores) to control their density, the effect of size <u>per se</u> is likely to be less of a limitation than for terrestrial

locomotion. There are many similarities between Anguilla and Conger, so that the effect of a large size difference (0.25g vs 2500g) on capillarisation indices is probably indicative of fish in general, showing a shallow allometric relationship (Table 5.8). The differential power requirement for fast and slow swimming (Chapter 1) will offset some of the density advantage, and this is shown by the larger difference in fast, relative to slow muscle between the two species (Table 5.8).

Conclusions

A major unresolved problem is the longitudinal variation in capillary supply within a myotome. It has been suggested that $N_A(c,f)$ will increase along the length of a muscle, in compensation for the reduced blood Po_2 at the venule end (Wolff et al 1975). This agrees with the suggestion that tissue hypoxia is a stimulus for new capillary formation (Hudlická and Schroder 1978). However, the effect of an unequal distribution of mitochondria, and hence $\dot{V}o_2$, along a fibre length on the pattern of branching within fish muscle, is unknown. In both Anguilla and Conger slow muscle fibres the volume of mitochondria in the subsarcolemmal zone is approximately twice that in the intermyofibrillar zone; in fast muscle the distribution is more even, and in the small fast fibres of the elver, more pronounced. This agrees with the assumption that the subsarcolemmal mitochondrial supply the energy for active transport of metabolites in oxidative fibres, and provide a limiting factor for endurance performance in mammals, where the capillary supply does not change (Müller 1976). In contrast to mammals, where endurance training results from repetitive isotonic exercise, fish muscle endurance is a response to isometric contractions. The limiting factors in oxygen delivery to fish muscle are, therefore, likely to be underlined by an analysis of endurance training, taking into account the distribution of mitochondria within a fibre, and the geometry of the capillary bed.

In view of the considerable heterogeneity now known to exist within the myotome, and the virtual lack of information concerning capillary size and distribution, it is clear that much of the published data on fish muscle needs to be reviewed. Both $N_N(c,f)$ and $\bar{N}(c,f)$ may give a reasonable estimate of the capillary supply, although their use as comparative indices is limited to the more rounded fibres of muscle with a high capillary density. They provide a useful baseline from which the magnitude of sample size required for an accurate estimate of $N_A(c,f)$ may be inferred. Using data from two resolution levels would appear to be optimal: the large sample size available with semi-thin sections to calculate $N_A(c,f)$, and the greater magnification of electronmicrographs for measurement of capillary dimensions. Indices that described a higher organisation level, $V_V(c,f)$ and $S_V(c,f)$, are probably the most appropriate for use with heterogeneous muscles, with respect to $\bar{a}(f)$ and $\bar{a}(c)$.

TABLE 5.1. Cardiovascular differences between fishes, birds and mammals of similar body size.

Species	Blood Vol. (% B.W.)	Blood Press. (mm Hg)	Heart Rate (beats/min)	Cardiac Output (ml/kg/min)
dog	8.3	$^{112}/_{56}$	90-100	-
rat	8.0	$^{130}/_{91}$	350	286
duck (♂)	10.2	$^{175}/_{100}$	175	287
chicken (♂)	9.0	$^{149}/_{43}$	178-460	262
hagfish	-	$^{9}/_{0}$* $^{5}/_{3}$**	30-40	-
lamprey	8.5	-	-	-
dogfish	6.8	$^{30}/_{24}$* $^{17}/_{16}$**	39-48	22-25
seawater eel	2.9	-	32	-
shortfin eel	-	$^{39}/_{23}$ ***	53.5	7.0
cod	-	$^{29}/_{18}$*	30	9.3
lingcod	-	$^{39}/_{29}$ ***	29.8	10.9
rainbow trout	2.8-3.8	$^{40}/_{32}$* $^{29}/_{25}$**	46	16
Chaenocephalus	9.0	$^{23}/_{15}$* $^{12.2}/_{8.1}$**	16-21	99-153

Note: blood pressure in mammals and birds is systolic/diastolic in the aorta, for fish in the dorsal aorta (*) or ventral aorta (**), or systolic ventral aorta/dorsal aorta (***). Sources of data: Handbook of Physiology, Circulation III; Prosser (1973); Randall (1970); Forster (1981); Farrell and Smith (1981); Hemmingsen et al (1972).

TABLE 5.2. Limitations in the use of sharing factor, $\bar{N}(f,c)$, as descriptor of fish muscle capillary supply.

Slow muscle	$\bar{N}(f,c)^1$	$\bar{N}(f,c)^2$	$N_N(f,c)$	Ref.
Galeus	-	2.91	1.16	1
Etmopterus	-	3.78	2.70	1
Chimaera	-	2.73	8.90	1
Acipenser	-	3.29	1.43	2
Anguilla	3.3	2.18	2.22	3
Conger	3.5	2.70	1.80	3
Intermediate (superficial white)				
Galeus	-	2.29	2.88	1
Etmopterus	-	2.22	5.56	1
Chimaera	-	2.00	9.56	1
Acipenser	-	2.47	2.75	2
Anguilla	3.1	1.93	6.67	3
Conger	-	-	-	3
Fast muscle				
Galeus	-	2.86	7.29	1
Etmopterus	-	2.00	52.25	1
Chimaera	-	3.33	11.10	1
Acipenser	-	6.45	32.73	2
Anguilla	3.2	1.71	14.29	3
Conger	2.9	3.55	10.80	3

Note: $N_N(f,c)$ = fibre to capillary ratio; $\bar{N}(f,c)^1$ = measured sharing factor; $\bar{N}(f,c)^2$ = calculated sharing factor, using:-

$$\bar{N}(f,c) = \frac{\bar{N}(c,f)}{N_N(c,f)}$$ (see Plyley and Groom 1975; Mosse 1978),

using data presented in the references. The very small variance is compared to the large spread of values found using the calulation. The limitation of such an approach lies in the presence of a significant proportion of the muscles which have no capillary contact. This is reflected in the widely differing, often large, values for $N_N(f,c)$. The species represent fish with focally-innervated fast muscle (elasmobranchiomorphs, a chondrostean and two primitive teleosts) that is assumed to be mainly, or wholly, dependent on anaerobic glycolysis for energy metabolism (Bone 1978). References: 1, Totland et al 1981; 2. Kryvi et al 1980; 3. This study (see also Chapter 2).

TABLE 5.3. Comparison of the two numerical (count) estimates of capillary supply in fish muscle, referred to as "caps/fibre" in published literature.

	$N_N(c,f)$	$\bar{N}(c,f)$	Ref.
Slow muscle			
Galeus	0.86	2.5	1
Etmopterus	0.37	1.4	1
Scyliorhinus	1.76	3.75	1
Chimaera	0.11	0.3	1
Acipenser	0.70	2.3	2
Anguilla[2]	0.45	0.98	3
Anguilla	-	1.35	3
Conger	0.56	1.71	3
Clarias	1.07	1.90	4
Engraulis[3]	-	12.9	5
Carassius[3]	-	4.8	6
Carassius[4]	-	2.2	6
Fast muscle			
Galeus	0.14	0.4	1
Etmopterus	0.02	0.04	1
Scyliorhinus	1.92	3.45	1
Chimaera	0.09	0.3	1
Acipenser	0.03	0.2	2
Anguilla[1,2]	0.07	0.12	3
Anguilla	-	1.00	3
Conger	0.09	0.22	3
Clarius	0.24	0.30	4
Carassius[3]	-	2.9	6
Carassius[4]	-	1.4	6

Note: The capillary to fibre ratio is seen to vary widely among species and co-varies with capillary density, representing an average, tissue supply. The average number of capillaries in contact with a fibre represents a higher resolution of the physiological supply, but fails to take account of fibre area or geometry; in this way the slow muscle fibres of the Anchovy, Engraulis, are flattened and enable a much greater capillary contact than found with the more rounded fibres of other species.

References: 1) Totland et al 1981; 2) Kryvi et al 1980; 3) this study; 4) Johnston and Bernard, unpublished data; 5) Johnston 1982a; 6) Johnston 1982b).

Note: 1) whole muscle estimate; 2) vascularised portion of the muscle only; 3) 2°C-acclimated fish; 4) 28°C-acclimated fish.

TABLE 5.4 Morphometric analysis of Conger slow muscle. Mean ± S.E.M. n=46.

Region	$V_V(nuc,f)$	$V_V(mf,f)$	$V_V(mit,f)$	$V_V(lip,f)$	$V_V(sp,f)$	$\bar{a}(f)$ μm^2	$\bar{b}(f)$ μm	$\bar{N}(c,f)$	$\bar{l}(c,f)$
Whole fibre	0.007 ±0.0015	0.472 ±0.0225	0.227 ±0.0106	0.179 ±0.0124	0.115 ±0.0226	981.8 ±105.41	114.2 ±6.71	1.783 ±0.1700	0.134 ±0.0122
Subsarcolemmal zone	-	-	0.139 ±0.0008	0.132 ±0.0126	0.082 ±0.0238	-	-	-	-
Intermyofibrillar zone	-	-	0.090 ±0.0053	0.047 ±0.0038	0.033 ±0.0030	-	-	-	-

Note: the sample site was chosen was similar to that described for the elver. The subsarcolemmal zone is taken to include everything beneath the sarcolemma, but external to the envelope of the peripheral myofibril edges.

TABLE 5.5 Morphometric analysis of Conger fast muscle. Mean ± S.E.M.

Region	$V_V(nug,f)$ nuc	$V_V(mf,f)$	$V_V(mit,f)$	$V_V(lip,f)$	$V_V(sp,f)$	$\bar{a}(f)$ μm^2	$\bar{b}(f)$ μm	$\bar{N}(c,f)$	$\bar{l}(c,f)$
Whole fibre (n=59)	0.004 ±0.0011	0.788 ±0.0295	0.030 ±0.0036	0.002 ±0.0008	0.110 ±0.0079	1764.2 ±293.78	141.4 ±13.35	0.169 ±0.0493	0.012 ±0.0038
Whole fibre [1] (n=68)	0.004 ±0.0010	0.803 ±0.0260	0.027 ±0.0032	0.002 ±0.0007	0.108 ±0.0070	2417.1 ±343.06	-	0.176 ±0.0466	-
Subsarcolemmal zone (n=68)	-	-	0.013 ±0.0021	0.0002 ±0.0001	0.041 ±0.0041	-	-	-	-
Intermyofibrillar zone (n=68)	-	-	0.016 ±0.0016	0.002 ±0.0007	0.066 ±0.0038	-	-	-	-

[1] Analyses from wedge segments of larger fibres included (see Methods).

TABLE 5.6. Comparative data on capillary supply to fish and mammalian aerobic muscles.

SPECIES	MUSCLE	$\bar{a}(f)$ μm^2	$\bar{N}(c,f)$	$N_A(c,f)$ mm^{-2}	$V_V(mit,f)$	REF
Elver	Slow	190.5	0.98	2364	0.214	1
Catfish	Slow	660.0	1.90	1899	0.160	2
Conger	Slow	950.5	1.71	615	0.227	1
Anchovy	Slow	1115	12.90	6000	0.455	3
Icefish	Slow	3772	2.40	625	0.304	4
Rat	Soleus	-	2.05	396	-	5
Man	Quadriceps	4150	1.36	329	-	6
Genet Cat	VM	-	-	731	0.069	7
Dik Dik	VM	1234	-	923	0.036	7
Wildebeest	VM	1248	-	716	0.032	7
Eland	VM	-	-	332	0.035	7

Note: VM = M. vastus medialis. References: 1) This study; 2) Johnston and Bernard, unpublished data; 3) Johnston (1982a); 4) Johnston and Wood, unpublished data; 5) Plyley and Groom (1975); 6) Andersen and Henriksson (1977); 7) Hoppeler et al (1981).

TABLE 5.7. Determination of the degree of anistropy in the capillary bed of Conger slow muscle.

	Angle of sectioning	
	$\theta = 0$	$\theta = \pi/2$
$\sum \hat{Q}_A$	1727	235
No. of grids counted (area = 0.017mm^2)	170	233
$Q_A \pm$ S.D.	597.6 $\pm$ 80.82	59.3 $\pm$ 20.58
n (sections)	12	10
$\frac{Q_A(0)}{Q_A(\pi/2)}$	10.027	
K	16.80	
C(K,0) (see Fig. 6.19)	1.016	

$$\therefore J_V(c,f) = 597.6 \times 1.016 = 607.2\text{mm}^{-2}$$

Note: Q_A = individual capillary count estimates; n = number of samples, ≡ quadrats in Mathieu et al (1982). The original estimate of $N_A(c,f) = 615\text{mm}^{-2}$ was derived from a larger sample size and is assumed to be a better estimate of the true population mean. The small discrepancy between the two estimates is taken to be due to the intra-sample variance, which is quite high.

TABLE 5.8. The mitochondrial content and capillary supply of skeletal muscle in Anguilliform teleosts

	Anguilla anguilla (young)			Conger conger (adult)	
	Slow	Superficial Fast	Fast	Slow	Fast
$\bar{a}(f)$; μm^2	204.4	332.7	775.0	950.5	4339
$V_V(mit,f)$	0.214	0.076	0.012	0.227	0.027
$N_A(c,f)$; mm^{-2}	2364	529	229	615	21.3
$J_V(c,f)$; $cm^{-2} \times 10^4$	24.0	5.37	2.33	6.25	0.22
$\bar{a}(c)$; μm^2	13.5	12.4	10.9	25.7	30.5
$\bar{b}(c)$; μm	14.3	13.9	12.8	21.6	21.4
$V_V(c,f)$	0.032	0.007	0.003	0.016	0.0007
$S_V(c,f)$; cm^{-1}	343.2	74.6	29.8	135.0	4.7

Note: The length density, $J_V(c,f)$, is calculated from the capillary density, $N_A(c,f)$, using a multiplication factor of 1.016 (see Table 5.7). Although the mitochondrial content within homologous muscles from the two species are quite similar, the larger size of Conger fibres is reflected in the lower capillary density estimates. The larger size of capillaries does little to offset this difference, leaving both capillary volume and surface densities to be much lower than found in other species (see Table 5.9).

TABLE 5.9. Quantitative analysis of the capillary bed in five teleost species, illustrating the variability of homologous muscles.

SPECIES	$\bar{a}(c)$ μm^2	$\bar{b}(c)$ μm	$V_V(mit,f)$	$N_A(c,f)$ mm^{-2}	$V_V(c,f)$	$S_V(c,f)$ cm^{-1}	Ref.
Slow muscle:							
Anguilla anguilla	13.5	14.3	0.214	2364	0.032	343	1
Clarias mossambicus	20.3	18.7	0.160	1633	0.034	310	2
Tinca tinca	21.8	19.4	0.230	2672	0.059	527	2
Conger conger	25.7	21.6	0.227	615	0.016	135	1
Chaenocephalus aceratus	53.3	37.2	0.304	625	0.034	236	3
Fast muscle:							
Anguilla anguilla	10.9	12.8	0.012	229	0.0027	29.8	1
Clarias mossambicus	20.3	18.7	0.025	189	0.0039	35.9	2
Tinca tinca	16.3	14.5	0.025	679	0.0112	100.0	2
Conger conger	30.5	21.4	0.027	21.3	0.0007	4.7	1

References: 1) this study; 2) Johnston and Bernard, unpublished data; 3) Johnston and Wood, unpublished data.

Fig. 5.1. Semi-thin sections of conger slow and fast muscle. Toluidine blue stain, scale bar = 200μm.

a) Slow muscle, showing the relatively homogeneous distribution of fibre size and capillary supply. The adipocytes are seen to form a continuous layer on either side of the muscle.

b) The capillary supply to adipocytes varies between different regions, and can be quite dense. If these capillaries lie close to the slow muscle, as in this case, they will provide an additional oxygen source not accounted for by the quantification of muscle capillary density.

c) A portion of the adipocyte layer between fast and slow muscle. Such an extensive population must provide an effective barrier for metabolite diffusion between the two muscle types. Note also the large size of the lipid deposits, relative to the muscle fibres.

d) Interface between slow fibres of the lateral line triangle (bottom) and the superficial fast muscle. Note in particular the reduction of the adipocyte layer to isolated lipid droplets, and the larger spread of fibre size in the slow muscle.

e) Deep fast muscle, showing the range in cross-sectional area, between adjacent fibres. A capillary is seen, bottom right.

f) Deep fast muscle, from the same section as e), showing the heterogeneity of fibre size distribution within a sample. The extracellular lipid deposit, top right, is a rare occurrence. Note the number of fibres without any capillary contact.

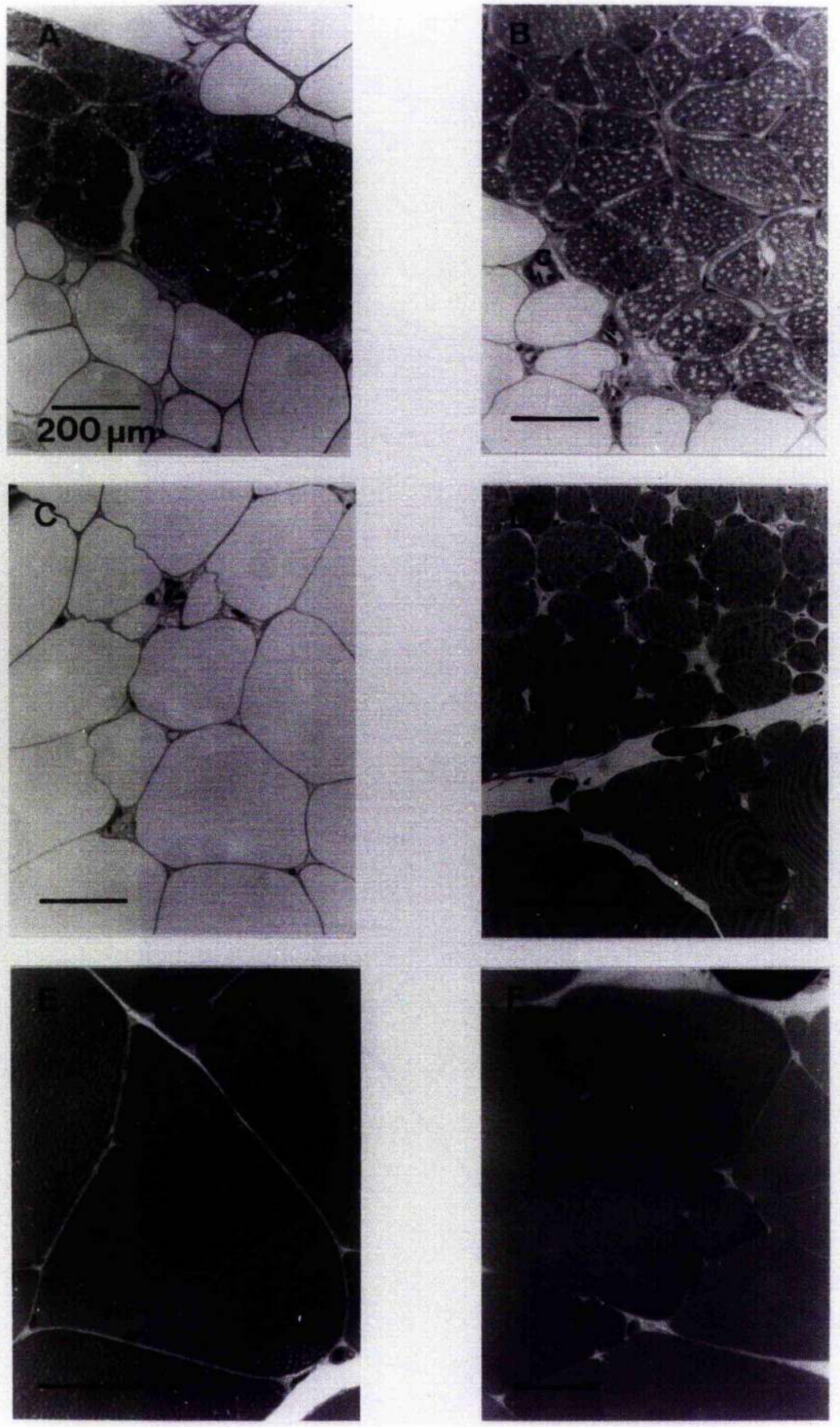
A
200 µm
B
C
E
F

Fig. 5.2 Semi-thin section of conger slow muscle, showing the variability of capillary supply within the tissue. The dark areas are lipid deposits. Note the variation in capillary (c) size and the presence of a larger, non-capillary, blood vessel (V).

Fig. 5.3 Histograms of fibre size distribution. The slow muscle (A) shows a heavily skewed distribution, with most fibres $<2000\mu m^2$. Fast muscle (B) shows an extended distribution over a much larger range of fibre sizes, with a significant portion of the muscle consisting of very large fibres, $>9000\mu m^2$. The presence of a large population of small fibres, $<500\mu m^2$, is similar to the distribution pattern noted for elver fast muscle (Fig. 2.18). Inserts show an expanded view of the distribution over the first $1000\mu m^2$ interval.

Fig. 5.4 Capillary supply to conger muscle. a) slow muscle, showing an average of 3.5 fibres surrounding each capillary, and a range of values for capillary contact. Note that a significant portion of the fibres have no capillary contact at all.
b) fast muscle, showing the distribution of measured values for the sharing factor, $\bar{N}(f,c)$, from two different samples. Although the spread of values is slightly different, the model category is the same.

Fig. 5.5 Semi-thin section of conger fast muscle, illustrating the full range of fibre size. The problems of correlating the oxygen supply with fibre size is complicated by the low density of capillaries (c) and the presence of a number of larger blood vessels (V), presumably venules.

2

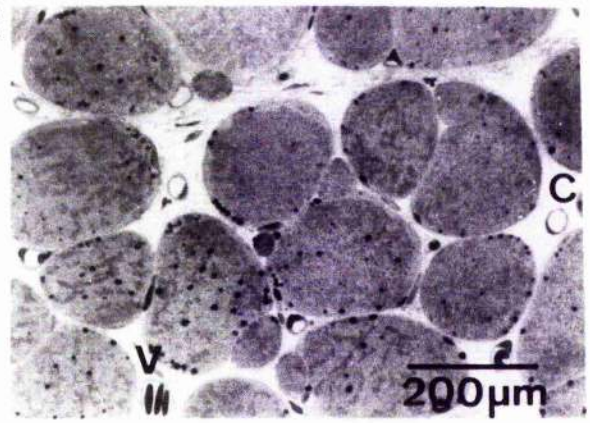
C
V
200µm

3

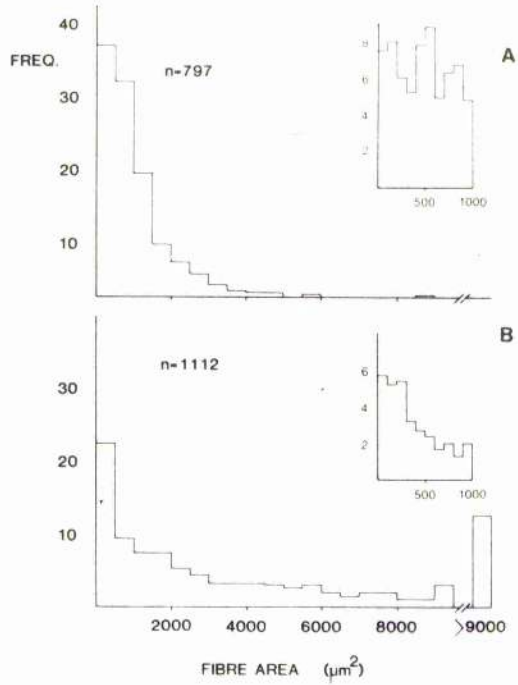
FREQ.
40
30
20
10
n=797
A
500
1000
n=1112
B
2000
4000
6000
8000
>9000
FIBRE AREA (µm²)

4

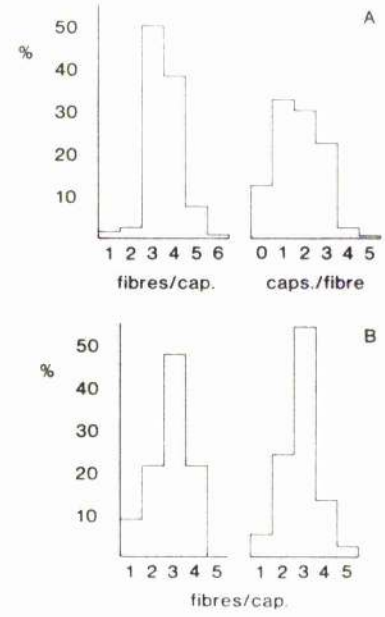
%
50
40
30
20
10
A
1 2 3 4 5 6
fibres/cap.
0 1 2 3 4 5
caps./fibre
B
1 2 3 4 5
1 2 3 4 5
fibres/cap.

5

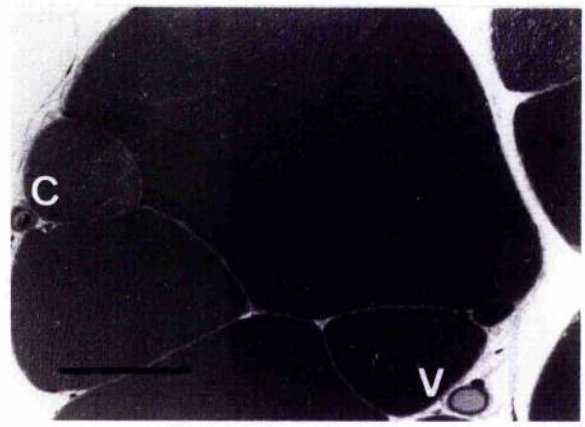
C
V

Fig. 5.6. Electronmicrographs of capillaries from conger skeletal muscle. Scale bar = 2μm.

a) Slow muscle; typical appearance of a capillary, showing endothelial processes invading the lumen, and the presence of cellular functions.

b) Slow muscle; capillary sectioned through the endothelium of the branch, running between two fibres. L = intracellular lipid deposit, $\bar{N}(f,c) = 4$.

c) Slow muscle; a common profile of slow muscle capillaries, displaying a prominent endothelial cell nucleus (N), and distinct intercellular functions; $\bar{N}(f,c) = 3$.

d) Slow muscle; large capillary sectioned through the lumen of an obliquely-running branch. A prominent nucleus and pericyte profile is seen on the right.

e) Fast muscle; showing the most common localisation of a capillary, in the interstitial space at the fibre apices; $\bar{N}(f,c) = 3$.

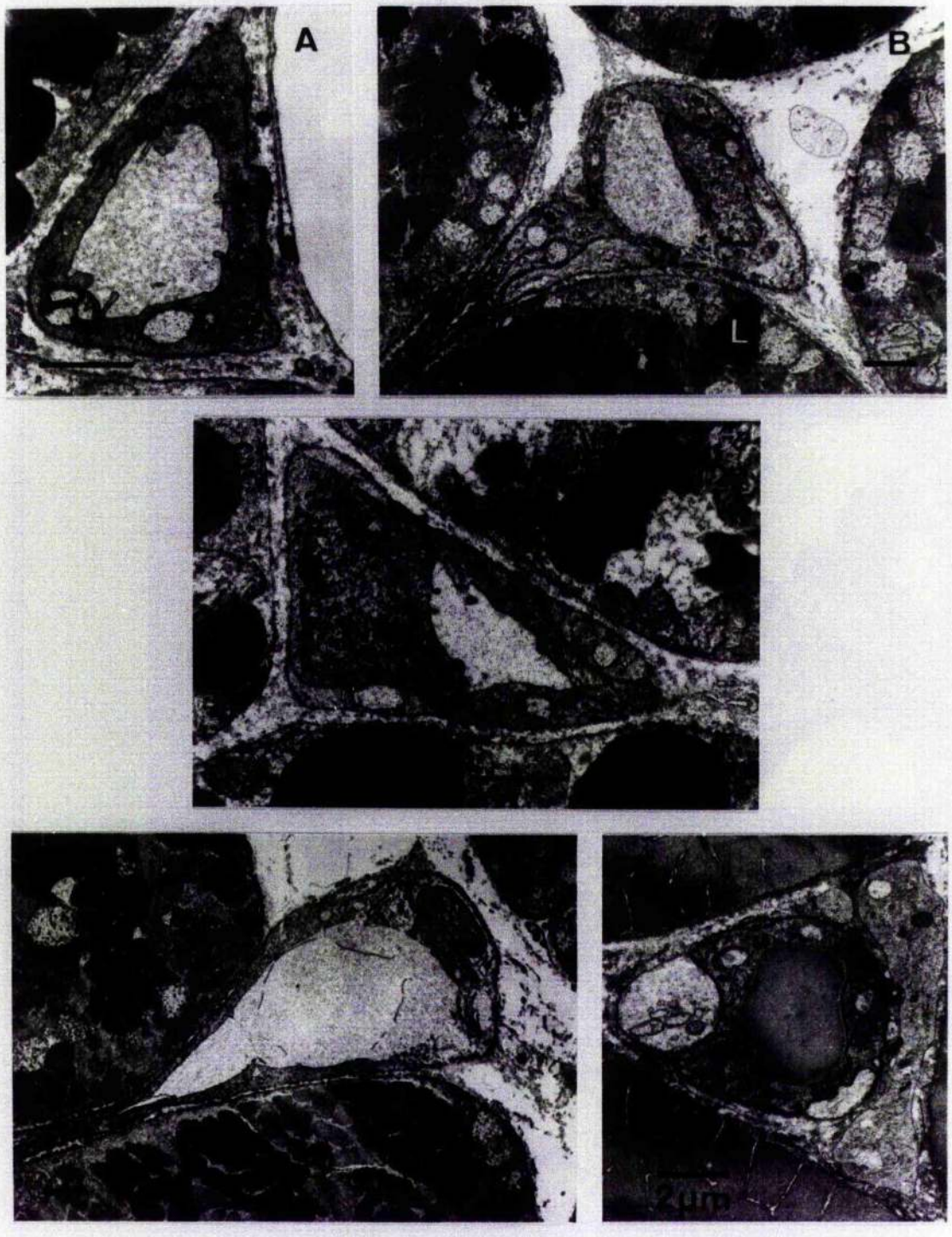
A
B
L
2um

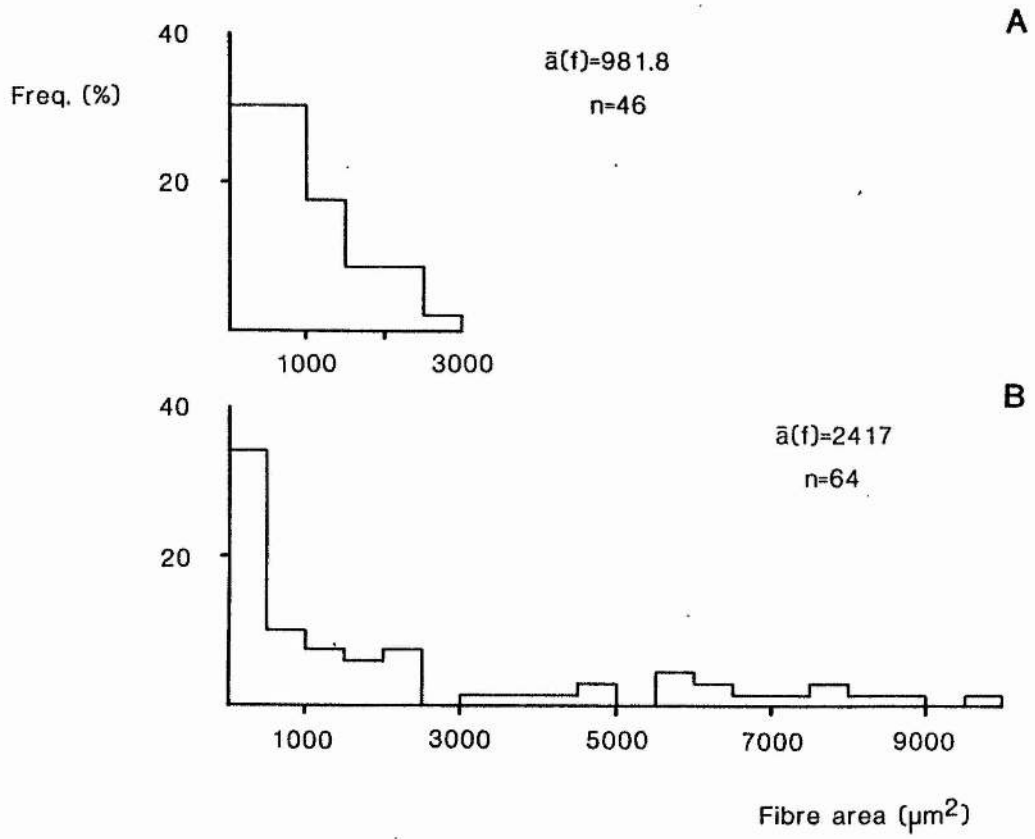

Fig. 5.7 Size distribution of fibres used in the morphometric analysis of conger slow (A) and fast (B) muscle. Note that the distribution of the slow fibres is similar to that determined from a much larger sample size (Fig. 5.3), although slightly truncated at the upper end. The fast muscle, on the other hand, shows a greater proportion of fibres in the lowest size category, $< 500\mu m^2$.

Fig. 5.8. Graph showing the variation in estimate of population mean, relative to the sample size used for the analysis. The capillary density, $N_A(c,f)$, is seen to be dependent on $N(f)$; whereas the fibre area, $\bar{a}(f)$, is relatively independent. This indicates a heterogeneous capillary supply in a muscle of homogeneous fibre size, and suggests a low correlation between $\bar{N}(c,f)$ and $\bar{a}(f)$. The example is taken from tench slow muscle and is an extreme example of the caution required in estimating a variable parameter; there is no a priori reason why the change in population estimate may not form a positive slope. Parameters calculated from Johnston and Bernard (unpublished data).

Fig. 5.9. Distribution of capillary size within tench slow muscle. Note the skew distribution and the presence of large blood vessels, $>70\mu m^2$, which may not represent part of the true capillary supply. Calculated from Johnston and Bernard (unpublished data).

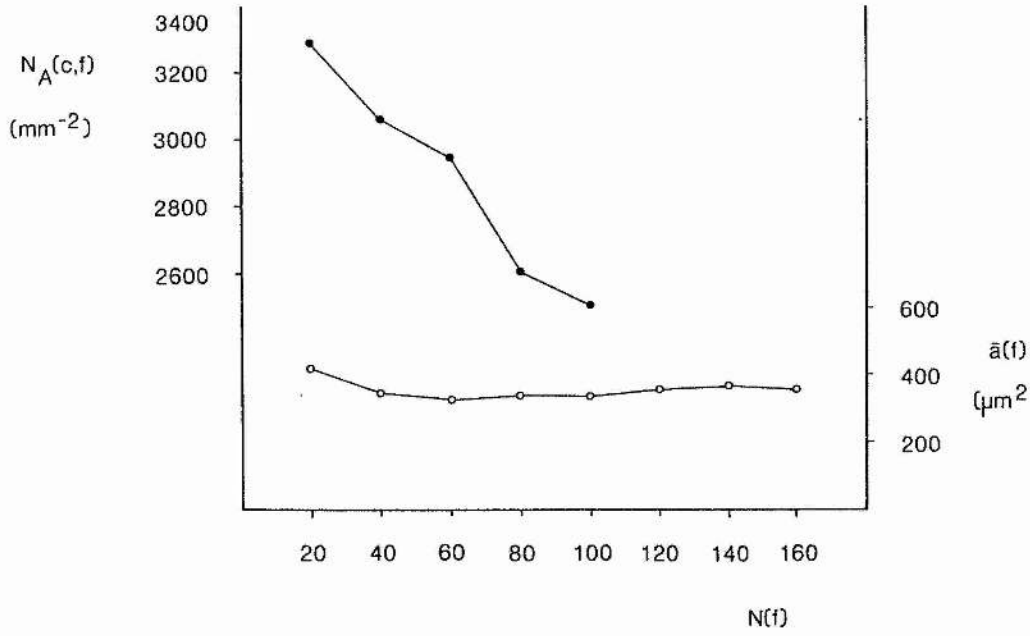
$N_A(c,f)$
(mm^{-2})
3400
3200
3000
2800
2600
600
400
200
$\bar{a}(f)$
(μm^2)
20
40
60
80
100
120
140
160
N(f)

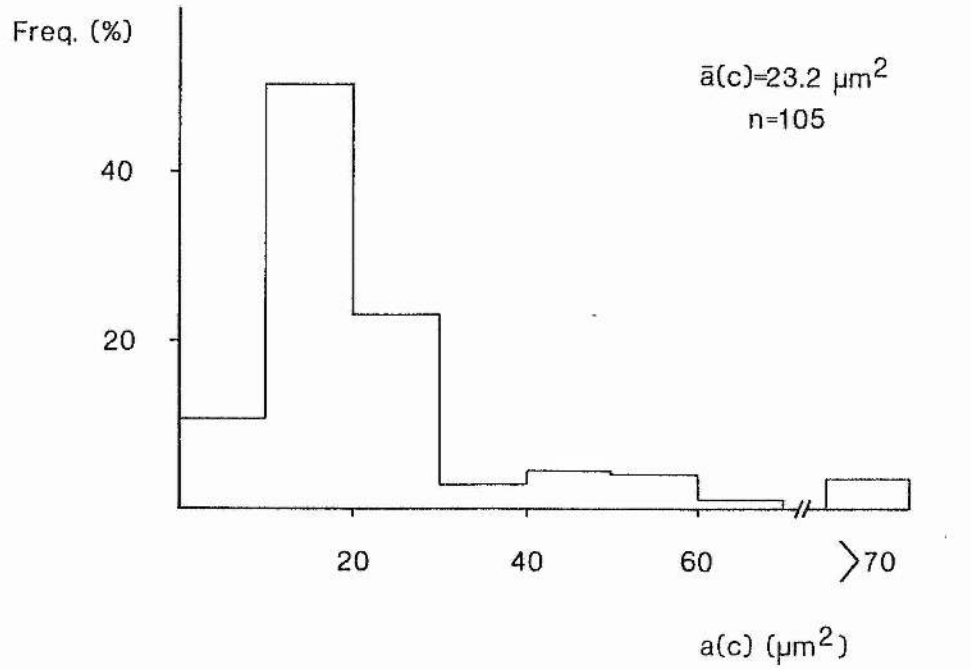
Freq. (%)
40
20
$\bar{a}(c)$=23.2 μm^2
n=105
20
40
60
>70
a(c) (μm^2)

Fig. 5.10. Change in estimate of population mean with sample size, showing the opposite relationship between $N_A(c,f)$ and $N(f)$ to that seen in tench. Data from a similarly-sized species, the Crucian carp (Carassius carassius) of 75g body weight. Sub-sample means (closed circles) show a wide scatter relative to the cumulative mean (open circles). Note a similar insensitivity of the fibre area, $\bar{a}(f)$, to the sample size. Calculated from Johnston and Bernard (unpublished data).

Fig. 5.11. Analysis of data from one specimen sample (section) of conger fast muscle, showing the variation in the estimate of fibre area with increasing sample size. Mean fibre area (upper trace) shows an initial decline, reflecting a more even sampling of smaller fibres, while the median value (bottom trace) indicates that the spread of values does not significantly alter. The regular decline of SEM (closed circles), from n = 20 to n = 180, reflects the similar variance of the data at all sample increments. Plots for other individual fish, and indices, gave similar results.

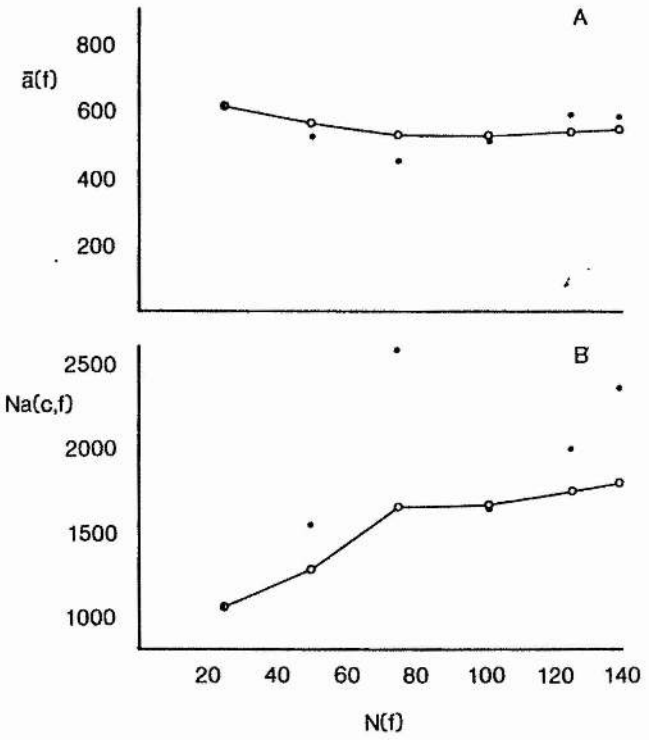
A
800
ā(f)
600
400
200
B
2500
Na(c,f)
2000
1500
1000
20
40
60
80
100
120
140
N(f)

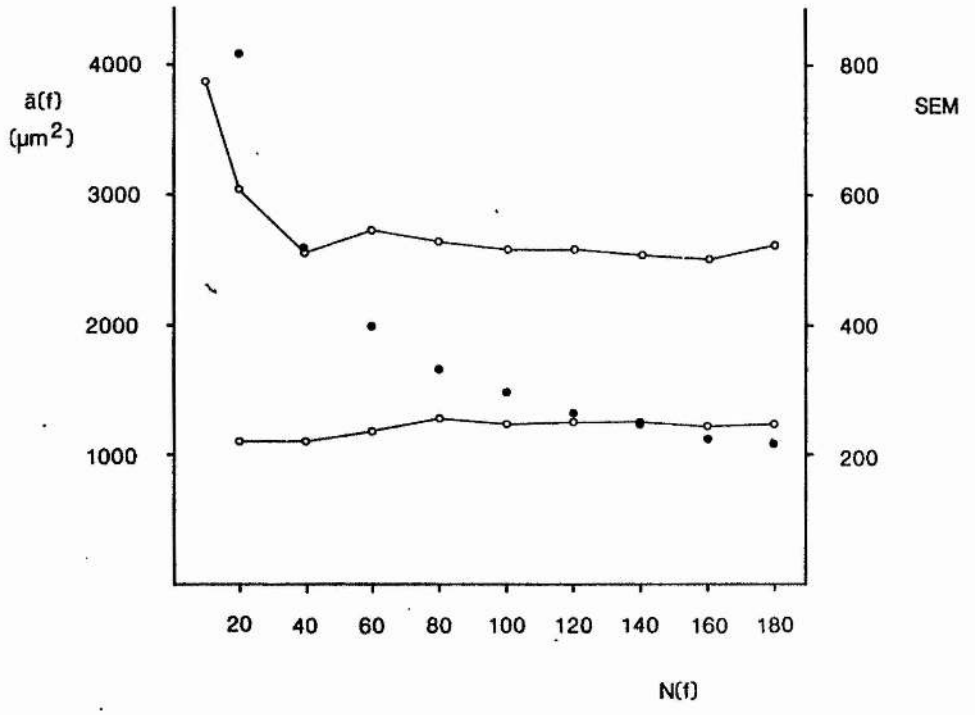
4000
ā(f)
(μm²)
3000
2000
1000
800
SEM
600
400
200
20
40
60
80
100
120
140
160
180
N(f)

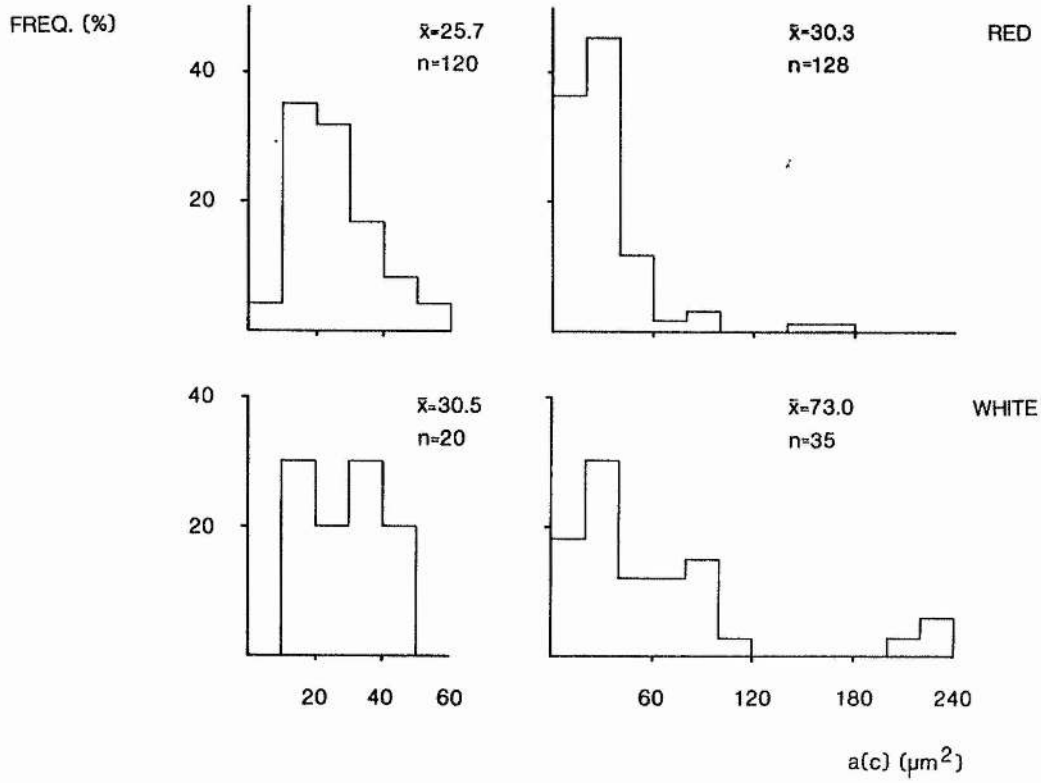

Fig. 5.12 Frequency distribution of the size of blood vessels in conger slow (top) and fast (bottom) muscle. Profiles < 60μm² were clearly identifiable as capillaries, and were included in the analyses. Blood vessels < 100μm² consisted of smooth endothelium only, and were considered to be venules; a significant portion of the fast muscle vascular supply falls into this category. The range of vessels > 60 < 100μm² was unclear; in general, and could not be definitely classified as being capillaries. This is seen to make little difference to extent of the vascular bed in the slow muscle, but would markedly affect the mean values for capillary dimensions when included in any morphometric analysis of the fast muscle. In view of the low capillary density, any small-scale morphometric analysis is likely to result in an erroneous estimate of $\bar{a}(c)$.

Fig. 5.13 The relationship between the mean fibre capillary supply, $\bar{N}(c,f)$, and average fibre area, $\bar{a}(f)$, for skeletal muscle in a selection of fishes. 1) = elver, 2) = conger; the other species remain unmarked, for clarity, although their values are given below:

SPECIES	Slow muscle $\bar{N}(c,f)$	Slow muscle $\bar{a}(f)$	Fast muscle $\bar{N}(c,f)$	Fast muscle $\bar{a}(f)$	REF.
Crucian carp (2°C)					1
" (28°C)					1
" (hypoxic)					2
" (normoxic)	4.8	752	2.9	1528	2
	2.2	705	1.4	1258	
Tench (hypoxic)	1.9	594	0.36	1040	2
" (normoxic)	1.5	564	0.35	1267	
	0.94	370	0.2	846	2
Catfish (hypoxic)	1.73	345	0.8	838	2
" (normoxic)	1.4	581	0.19	809	
	1.9	660	0.3	1265	2
Anchovy	12.9	1115	-	-	3
Elver	.98	191	0.12	290	
Galeus	2.5	1778	0.4	12217	4
	1.4	2617	0.04	6993	5
Etmopterus	0.3	954	0.3	11150	5
Rat fish	2.3	470	0.2	335	6
	0.9	300	0.24	656	7
Sturgeon	1.2	274	0.5	537	
Hatchet fish	3.75	2148	3.45	11295	8
Silver Dollar	2.36	3772	-	-	9
	2.76	1600	0.69	4700	6
Dogfish	4.22	613	-	-	
Chaenocephalus	2.98	455	1.10	2244	10
	3.07	614	0.27	2671	11
	3.93	952	1.60	5387	12
Australian salmon(a)	3.07	894	1.53	7637	
Mackeral	6.62	2044	0.63	6596	12
	1.92	614	-	-	12
Australian salmon(b)	2.95	3154	0.99	6078	
	3.42	471	-	-	12
Pilchard	3.80	907	-	-	
Yellowtail scad	-	-	0.83	6020	12
Flathead	1.78	981	.176	2417	12
Australian salmon(c)					12
Grass whiting					12
Brook trout (control)					13
" (trained)					13
Leather Jacket					12
Conger eel					4

Note: The positive correlation is only present in slow muscle of relatively small fibres, $\bar{a}(f) < 1000\mu m^2$, after which the index would indicate an insufficiency of supply. No correlation is found in fast muscle, where other variables would appear to be limiting. For Australian salmon a), b) and c) refer to the deep, average and lateral slow muscle, respectively, showing a heterogeneity of supply.
References: a) Johnston 1982a; 2) Johnston and Bernard 1982; 3) Johnston 1981b; 4) this study; 5) Kryvi and Totland 1977; 6) Totland et al 1981; 7) Kryvi et al 1980; 8) Salamonski and Johnston 1982; 9) Johnston and Salamonski, unpublished data; 10) Johnston and Wood, unpublished data; 11) Flood 1977; 12) Mosse 1979; 13) Johnston and Moon 1981a.

A) = slow muscle
B) = fast muscle

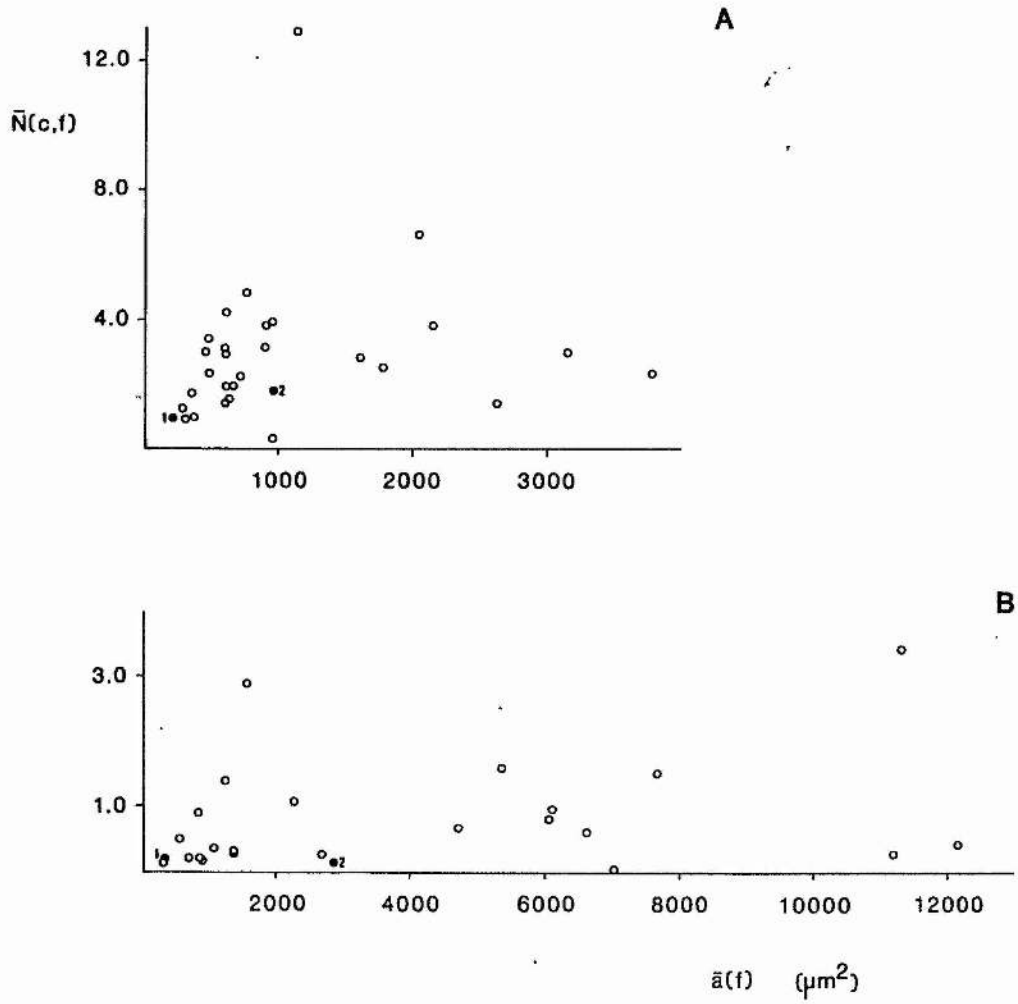
A
12.0
8.0
4.0
$\bar{N}(c,f)$
1000
2000
3000
B
3.0
1.0
2000
4000
6000
8000
10000
12000
$\bar{a}(f)$ (μm^2)

Figs. 5.14. - 5.17. Electronmicrographs of Conger skeletal muscle.

Fig. 5.14. TS slow fibres, showing the distribution and size of capillaries around the large-diameter fibres. Intracellular lipid deposits (black circles) are widespread, particularly in the subsarcolemmal zone. Mitochondria follow a similar distribution pattern. Magnification X1595.

Fig. 5.15. TS of peripheral nerve bundle running just inside the slow muscle region, close to the fast muscle interface. Note the composition of the bundle and compare with the results from Anguilla in Chapter 7. Magnification X3610.

Fig. 5.16. TS of a quite small fast fibre, adjacent to larger neighbour (left). Note the virtual absence of mitochondria. Magnification X1547.

Fig. 5.17. TS of large, deep fast fibre showing the irregular array of central myofibrils. Note the poorly developed mitochondria, situated close to the Z-disc band. SR forms a series of small vesicle-type profile around the myofibril periphery. Magnification X15,400.

14

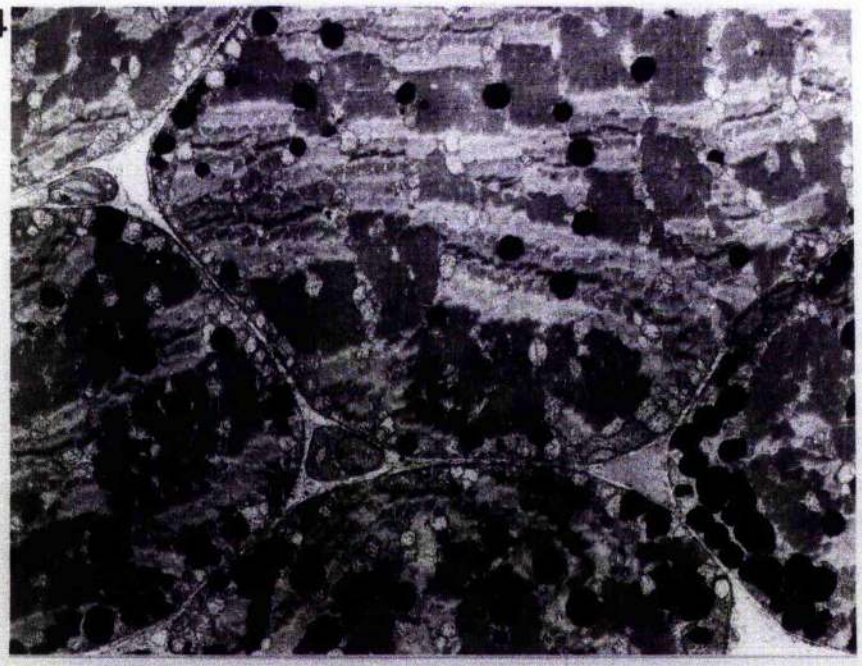

15

16

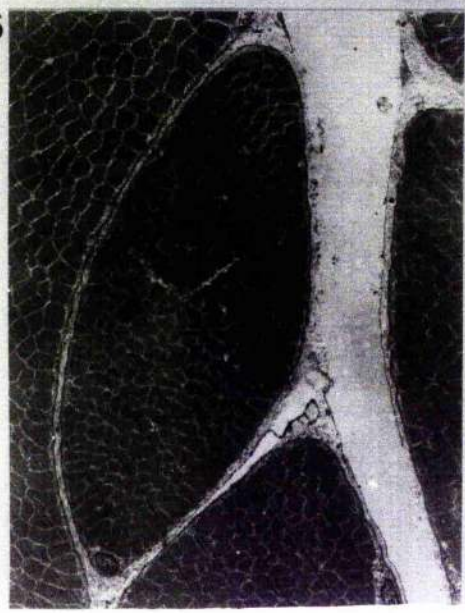

17

Fig. 5.18 Variation in estimate of mean fibre area and capillary density for conger slow (A,C) and fast (B,D) muscle against sample size. Closed circles represent the sub-sample mean and open circles the cumulative mean. Sample increment was 20 fibres from each specimen (block), combined to form a sub-sample. Little variation is seen in the estimates; however, significant error can be introduced if the sampling is not regular, as in the case of slow muscle $\bar{a}(f)$ where only 4 fish were analysed after $N(f) = 400$. Delineation of the sample area will cause an error in any density estimate, such as $N_A(c,f)$, and a larger increment is preferred.

Fig. 5.19 Similar plots to Fig. 5.18., but using a sample increment of 100 fibres. In this way, the sub-sample now represents a mean value from an individual specimen. The large variation of sub-sample means, relative to the cumulative mean, is representative of the intra-specific variation. This sample increment is known to provide a reliable estimate from any individual specimen (Fig. 5.11), and should therefore provide the best estimate of intra-specific variance.

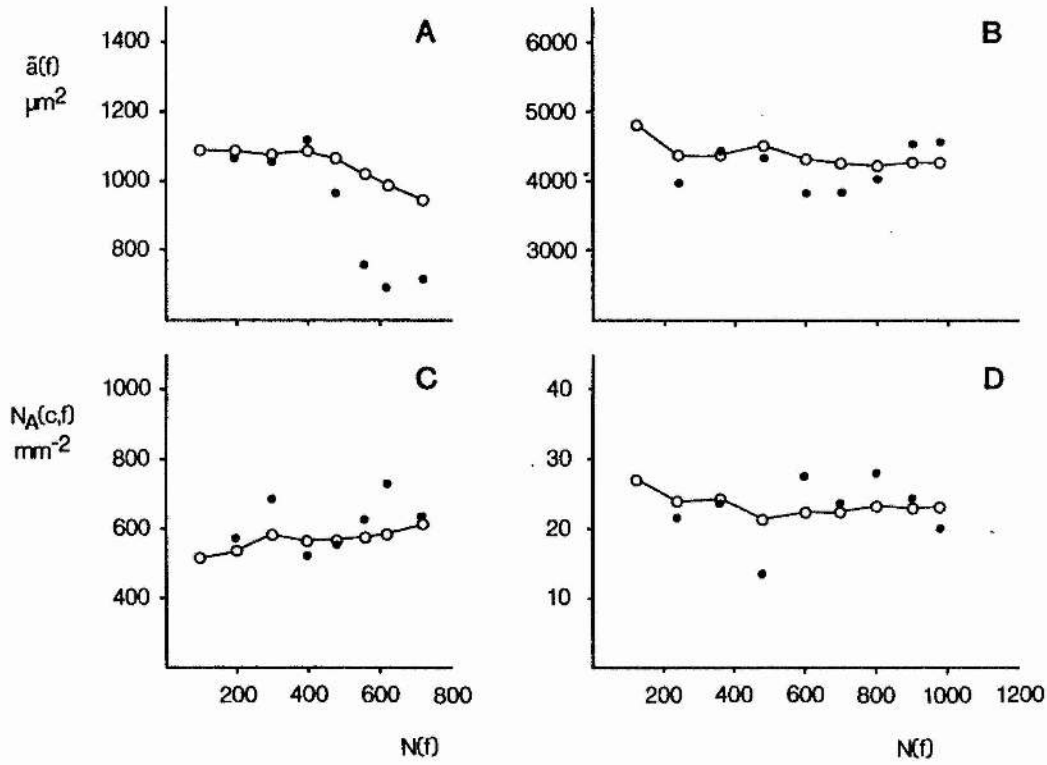
A
B
C
D
ā(f)
μm²
N_A(c,f)
mm⁻²
N(f)
1400
1200
1000
800
6000
5000
4000
3000
1000
800
600
400
40
30
20
10
200
400
600
800
1000
1200

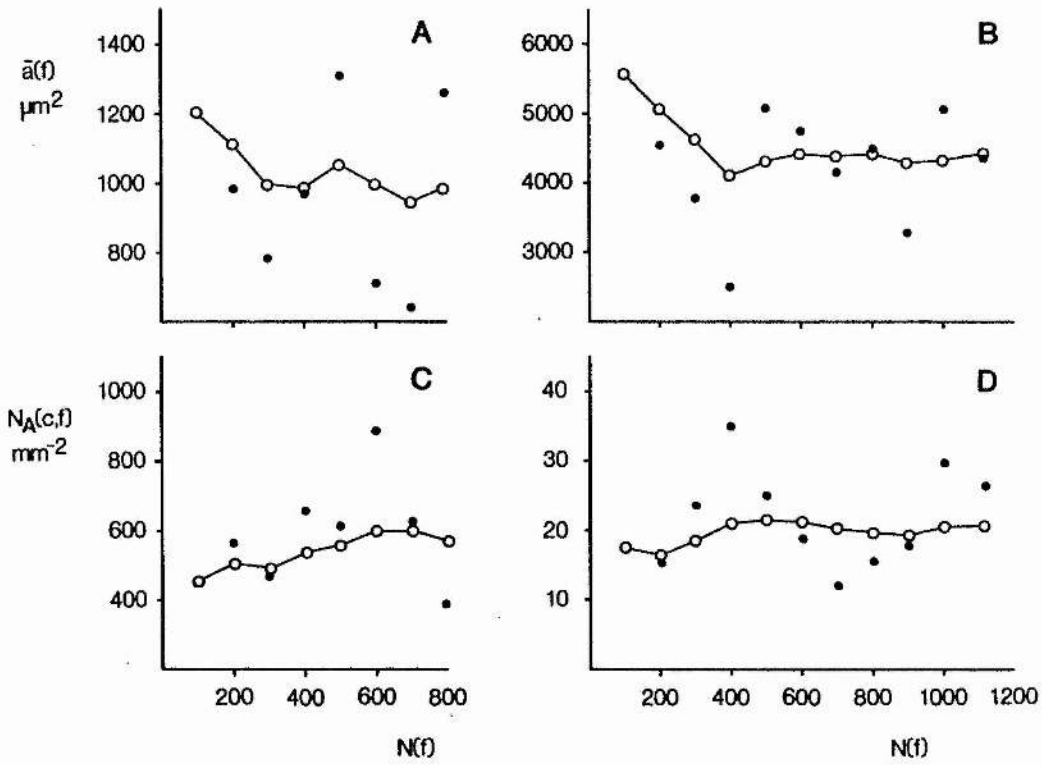
A
B
C
D
ā(f)
μm²
N_A(c,f)
mm⁻²
N(f)
1400
1200
1000
800
6000
5000
4000
3000
1000
800
600
400
40
30
20
10
200
400
600
800
1000
1200

Fig. 5.10 Correlation of skeletal muscle mitochondrial volume density, $V_V(mit,f)$, with capillary density, $N_A(c,f)$, for a range of fish species. 1) = elver, 2) = conger. For clarity, the other species are not labelled, although the values are given below.

Species	Slow muscle		Fast muscle		Ref.
	$V_V(mit,f)$	$N_A(c,f)$	$V_V(mit,f)$	$N_A(c,f)$	
Crucian carp (hypoxic)	0.25	1811	.030	260	1
Crucian carp (normoxic)	0.15	1639	0.018	240	1
Tench (hypoxic)	0.15	1371	0.018	250	1
Tench (normoxic)	0.23	2672	0.045	676	1
Catfish (hypoxic)	0.19	1657	0.024	136	1
Catfish (normoxic)	0.16	1633	0.025	189	1
Anchovy	0.46	6000	-	-	2
Elver	0.214	2364	0.012	229	3
Galeus	0.341	484	0.009	11	4
Etmopterus	0.304	141	0.005	3	4
Rat-fish	0.052	118	0.003	8	4
Sturgeon	0.300	1488	0.007	91	5
Hatchet fish	0.443	3002	0.084	366	6
Silver Dollar	0.277	4386	0.031	932	7
Dogfish	0.216	805	0.011	201	4
Chaenocephalus	0.304	625	-	-	8
Conger eel	0.227	615	0.027	21.3	3

Note: teleosts (closed circles) show a positive correlation which deviates somewhat from the values for elasmobranch (open circles) in slow muscle (A). This separation is less distinct in fast muscle (B). In both cases, the scatter of data suggests that the inter-relation of the two parameters is complex, being affected by other variables.

References: 1) Johnston and Bernard 1982; 2) Johnston 1981b; 3) this study; 4) Totland et al 1981; 5) Kryvi et al 1980; 6) Salamonski and Johnston 1982; 7) Johnston and Salamonski, unpublished data; 8) Johnston and Wood, unpublished data.

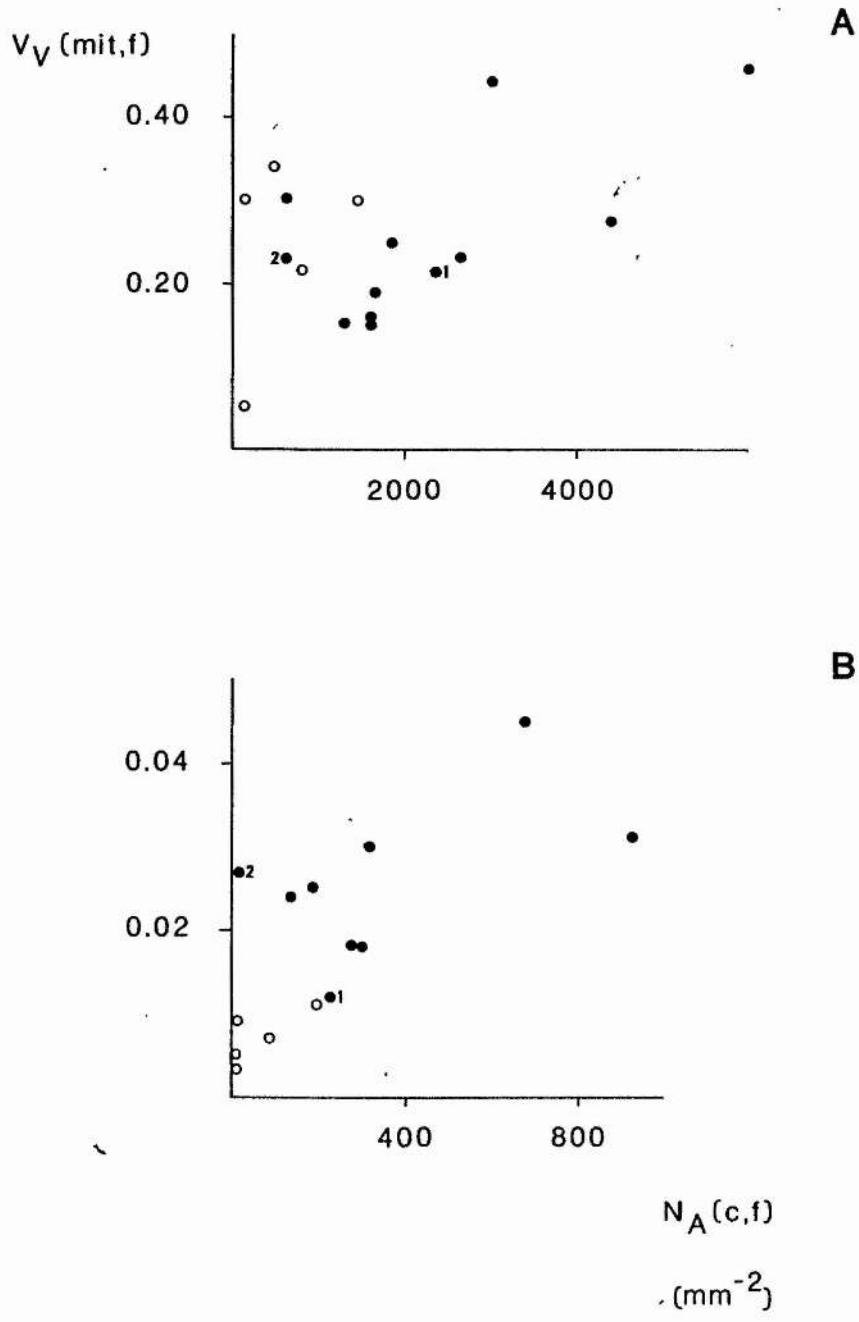
A
V_V (mit,f)
0.40
0.20
2000
4000
B
0.04
0.02
400
800
N_A (c,f)
(mm^{-2})

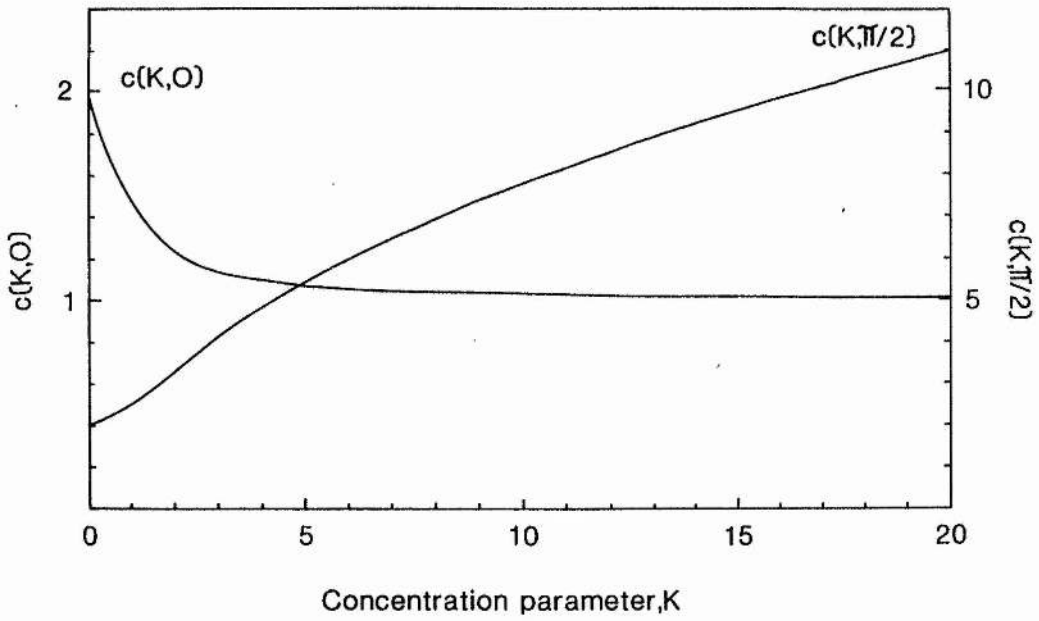

Fig. 5.21 Theoretical relationship between the concentration parameter, K, and the proportionality constants required to calculate the length density, $J_V(c,f)$, from the capillary density, $N_A(c,f)$. Once K has been experimentally determined for a muscle, subsequent analysis may rely on a capillary density estimate from either TS or LS sections. Note that K may show considerable differences between homologous muscles in different species, and between different muscles within a species. For example, the complex orientation of muscle fibres in fast muscle (Chapter 4) will result in a preferential orientation of capillaries that is not parallel to the longitudinal axis of the fish. The extremely low capillary density for conger fast muscle would require an extremely large number of samples to be analysed, in order to obtain an accurate estimate of K. The error involved in applying the value of c(K,0) derived from slow muscle is unknown, but thought to be relatively small; this was adopted as being the closest available estimate.
After Mathieu et al (1982).

CHAPTER 6

INTRODUCTION

A number of factors are known to have a profound influence on muscle phenotype (Prosser 1973; Vrbová 1980; Jolesz and Sreter 1981); although the mechanism of action is not always known, many are clearly mediated by the nervous system (Close 1972; Lomo 1976). For ectotherms experiencing a large diurnal or seasonal perturbation in climate, temperature is one of the most important extrinsic factors, either through its effect on the nervous system, or by direct action at the cellular level (Somero 1975b).

During its anadromous (upstream) migration the juvenile eel (elver) is subjected to a change in salinity and temperature, and an increased variability of available oxygen and various physical obstructions to locomotion, within river inlets and streams. Such factors are all known to be, directly or indirectly, modulators of muscle plasticity (Chapter 1). The post-metamorphic nature of the elver is reflected in the differential expression of haemoglobin isozymes (Rizzotti et al 1977), development of pigmentation and scales (Strubberg 1913; Pankhurst 1982), increase in swimbladder function (McCleave and Kleckner 1982), and reversal of the progressive decline in size following the start of feeding (Tesch 1977; Deelder 1970). It is not known whether a wide physiological tolerance to changing conditions is required, in addition to these adaptations.

Although the apparent aerobic capacity of elver muscle is low, compared to other migratory species (Chapters 2 and 3), there is little information available concerning the oxygen consumption ($\dot{V}o_2$) of the animal. Few studies have been made of the developmental biology, making it difficult to assign any physiological correlates to either behavioural or morphological characteristics. However, the variation in the start of upstream migration with physical condition of the elvers (Boëtius and Boëtius 1967), and the progressive change in behaviour (Boëtius 1976; Deelder 1970), would suggest that the primary

survival strategy is behavioural and that the animal is only capable of a limited physiological adaptation. In general, little attention is paid to the prior history of fish before temperature acclimation, although the stage of development is likely to affect the nature of the response; this may go some way to explaining the variability of published results. An attempt has been made to improve on the use of morphological criteria for identification, by describing more fully the physiology of elvers used in this study. Samples were taken throughout the migration and evidence sought for the end of the metamorphic influence.

The time-course and final response to different temperatures, with respect to Q_{10} and structural reorganisation of the muscle, were used to indicate the thermal plasticity of the tissue. In addition, the development of hypoxic tolerance was used to delineate the stages at which anaerobic metabolism is of most importance. These results suggest that a tolerance, rather than adaptive strategy is present in the migratory elver.

MATERIALS AND METHODS

Fish

Elvers were netted, and maintained, as described previously (Chapter 2) and kept under a constant 12L:12D photoperiod for 4-7 days prior to any initial sampling. After 2 or 3 days the majority of weak or damaged fish had died; this "settling in" period prevented inclusion of any unhealthy fish in experiments. Mortality was between 1 and 2% of initial stock. Where practical, weight and standard length (snout to caudal peduncle) were determined from MS222-anaesthetised fish, for greatest accuracy. Experimental protocol was developed during preliminary experiments, using elvers from the 1979-1980 migration. Fish were maintained at ambient (river) temperature of 15°C on arrival until feeding began, approximately 2 weeks later. Initial size was 0.210 $\pm$ 0.054g and 7.27 $\pm$ 0.31cm (n=13), becoming 0.239 $\pm$ 0.055g and 7.06 $\pm$ 0.49cm (n=31; $\bar{x} \pm$ S.D.) after all elvers had begun feeding, 3 weeks after capture. Subsequently, a 7 week acclimation to 8° and 30°C was performed (Table 6.2).

The main experiments used elvers from the 1980-1981 migration, caught at the same geographical location. Samples were taken between the earliest moderate-size migratory wave (Group 1) and the end of the main migration (Group 4), at approximately 3 week intervals. Morphologically, they represented early to late Stage VIA, as described by Strubberg (1913). The slightly higher reference temperature (22°) than used previously, was adopted as the temperature preferendum for eels, using a number of criteria, is thought to lie between 20 and 24°C (Nyman 1972; Tesch 1977; Deelder 1970). As soon as all elvers were feeding (100% feeding rate) two groups (~50 elvers in each) were gradually (5°C/day, maximum) introduced to the acclimation temperatures of 10 $\pm$ 0.5°C and 29 $\pm$ 1.0°C. A range of temperatures was attempted, with elvers surviving up to 32°C and down to 2°C; acclimation proved difficult at

>30°C or <5°C due to a progressive mortality. As this temperature range is within that reported for eels in the wild (Tesch 1977), this may represent either an ontogenetic difference in temperature tolerance, or a laboratory stress reaction. The large reduction in body weight in the preliminary (1980) experiments indicate non-optimal conditions. Subsequently, an attempt was made to maintain similar body weights during acclimation; lyophilised tubifex was fed 2 or 3 times per week to cold- and hot-acclimated elvers, respectively. The 8°C elvers showed little interest in the food, however, and appeared semi-torpid.

Yellow eels were a gift from Dr. M.G. Poxton, Department of Biological and Brewing Sciences, Heriot-Watt University. Acclimation followed a similar regime to that for elvers. Silver eels were trapped (fyke-net) on their seaward (downstream) migration from Lake , southern Finland; the annual temperature fluctuation in this habitat is remarkably low, maintaining 6 ± 1°C. Oxygen consumption measurements were carried out at the Department of Zoophysiology, University of Helsinki after 6-8 weeks acclimation in continuously cycled, filtered tapwater maintained at 5 ± 1°C and 25 ± 0.5°C. Photoperiod was approximately 12h:12D.

Oxygen consumption

Water oxygen content ($C.O_2$) was determined by a modification of the 1888 Winkler titrimetric assay, adapted from various sources (van Dam 1935; Fox and Wingfield 1938):

(i) Combine 0.5ml 50% $MnCl_2 . 4H_2O$

0.5ml a solution containing 50% NaOH and 30% KI

prepared hot, with constant stirring, and gradual addition of chemicals.

100ml water sample in a glass-stoppered bottle (volume 100ml)

(ii) Allow precipitate to settle. Add 2.0ml 85% H_3PO_4

(iii) Allow precipitate to dissolve. Titrate against freshly-prepared 0.01N Na_2SO_3 using 1% starch as an end point indicator.

The method has a reported accuracy of 0.01ml O_2 l^{-1} (van Dam 1935); in this study the repitition error was <2%. The major advantages are a high accuracy, and relative independance of temperature and pressure; these factors are a source of error in the more usual respiratory analyses, using polarographic oxygen electrodes. However, analysis is very time-consuming, limiting the number of samples taken per day, particularly when care is taken to avoid diurnal rhythms in $\dot{V}o_2$. This involved limiting the experiments to two periods of 4 to 5 hours (beginning 0900 and 1500 hrs), including 3 fish from both acclimation groups in each batch. No statistical difference could be seen between the results from the two periods.

Basal metabolism is extremely difficult to measure in fish (Brett 1972, 1979), requiring continuous monitoring of the difference in oxygen tension (ΔPo_2) or content ($\Delta C.O_2$) between inlet and outlet of a continuous throughput (open) respirometer. For large eels, stoppered (dark) tubes with a baffled inflow were used, calculating:

$$\text{(Eq. 6.1)} \qquad \dot{V}o_2\ (mg.g.hr^{-1}) = \frac{\Delta C.O_2\ (mg/l) \times \text{flow rate (ml/min)} \times 60}{\text{weight (g)} \times 100}$$

This was not possible with elvers, since the rate of flow necessary for a measurable $\Delta C.O_2$ was too low for accurate measurement from anything other than a very small, stressful respirometer. Hence, a closed respirometer system was adopted, using a point-determination of $C.O_2$ at different times:

$$\text{(Eq. 6.2)} \qquad \dot{V}o_2\ (mg.g.hr^{-1}) = \frac{\Delta C.O_2\ (mg/l) \times \text{volume of water(ml)} \times \text{t(hrs)}}{\text{weight (g)} \times 100}$$

for the determination of individual respiration rates. In the initial series of experiments (1980) each value recorded was an average of three separate determinations per animal. Variation was small (c.5%) and this was abandoned for the second migration (1981) experiments. These figures represent "standard" or "routine" (i.e. >basal < active) metabolism, and are probably more meaningful than attempts at measuring basal metabolism, even though the variance will be greater (Brett 1972; 1979).

The extrapolation from time t=o to t assumes a linear decrement of oxygen content, i.e. a constant $\dot{V}o_2$. In the absence of a continuous monitor this is difficult to test, although repeated sampling tended to show a linear decline over the period used for the assays after an initial, small, stress reaction (Fig. 6.3).

A further complication is the number of elvers used in an assay, possibly due to measurement error. Single elvers were used in order to obtain information concerning any weight-specific differences in $\dot{V}o_2$. A scaled-up experiment, using 20 elvers in 20X volume respirameter resulted in a 10% reduction in $\dot{V}o_2$ estimate. Similarly, on a much larger scale respiration rate of a 5 tonne sample of elvers ($\sim 5 \times 10^6$) approximates $0.12 mg.g.hr^{-1}$ at $12^{\circ}C$ (Wheeler, pers. comm.) compared to individual estimates of $0.21 mg.g.hr^{-1}$ at $8^{\circ}C$ from a laboratory sample of the same migration.

Residual oxygen

Elvers were treated in an identical manner to those used for $\dot{V}o_2$ experiments, but allowed to deplete the oxygen to lethal levels. Some fish are known to become hypoxia comatose at low Po_2, such that recovery is possible on restoration of normoxic conditions. In this study it was found that if an elver was unresponsive to mechanical disturbance (inversion of the sealed container) no recovery was possible, and death (cessation of heart beat) followed rapidly.

Morphometric analysis

Electronmicrographs of slow muscle fibres from 10°C and 29°C-acclimated elvers were analysed, as described previously (Chapter 3). A similar sample site was used, restricted to the first epaxial myotome to the lateral line triangle(Fig. 1.1) changes in mean component values, for both individual fish and acclimation groups, with increasing sample size (see Chapter 5) indicate that within- animal and between-animal variance are similar. Fibres adjacent to myosepta were not included in the analysis.

Capillary supply

Planimetry of semi-thin sections enabled the capillary density, $N_A(c,f)$, to be determined from a large sample size (60-80 fibres/fish, 6 fish/group). Numerical density counts (magnification X 650) were used to calculate the capillary:fibre ratio, $N_N(c,f)$ and mean number of capillaries per fibre, $\bar{N}(c,f)$. The derivision of other calculated indices is given in the text (Table 6.5) and described in detail elsewhere (Chapter 5).

RESULTS

Comparison of 1980 and 1981 migrations reveals only a small variation in time of ascent, and physical condition of the elvers. The decrease in weight prior to feeding is small, although a distinct reduction in length is observed (Group 2, Table 6.1; see Figs. 6.1 and 6.2). At this point both the $\dot{V}o_2$ and residual oxygen ($C.O_2$) are lowest. The reduction in size seems to stabilise between Group 3 and Group 4, although the $\dot{V}o_2$ and $C.O_2$) both rise (Table 6.1). The spread of data within each group is quite large (Fig. 6.1), reflecting the heterogeneous population that is sampled during any migratory wave; other workers have resorted to samples of many thousand elvers in order to differentiate the composition (Boëtius and Boëtius 1967; Tesch 1977; Ezzat and El-Serafy 1977).

The time course of thermal acclimation in elvers is plotted (Fig. 6.4) and tabulated (Table 6.4), with data from the reference (22°C) stock. A partial (Precht Type 3, Prosser 1973) compensation is seen in whole-animal $\dot{V}o_2$; the upper (29°C) group reaches an asymptote after about 4 weeks and the lower (10°C) group between 5 and 6 weeks, following an initial decline. The slight elevation in $\dot{V}o_2$ towards the end of the experiment is paralleled by a similar increase in the reference stock, and may be due to further developmental changes. At week 9, when samples were taken for morphometric analyses, the differences in weight were quite small; 0.247 ± 0.089g (29°C, n=19) and 0.218 ± 0.063g (10°C, n=20; $\bar{x} \pm$ S.D., see Fig. 6.4). An estimate of the compensation is given by the temperature coefficient, $Q_{10(10-29°C)} = 1.43$, which is very similar to the value obtained with elvers from the previous (1980) year's migration ($Q_{10(8-30°C)} = 1.33$; Table 6.3). This partial compensation is also revealed by the response of elver $\dot{V}o_2$ to assay at 19.5°C (mid-way between the two acclimation temperatures), which were 0.237 ± 0.063 mg.g.hr^{-1} (29°C elvers, n=6) and 0.319 ± 0.062 mg.g.hr^{-1} (10°C elvers, n=6; $\bar{x} \pm$ S.D.).

Interestingly, assay at the reciprocal temperatures showed no further depression of $\dot{V}o_2$ in the 29°C-acclimated elvers (0.256 $\pm$ 0.059 mg.g.hr^{-1} at 10°C, n=9) whereas 10°C-acclimated elvers were unable to withstand the upper temperature. These elvers died after 4 to 5hrs. and at an oxygen concentration of 6.30 $\pm$ 0.41mg l^{-1} ($\bar{x} \pm$ S.D., n=9), being 79.6% of the initial $C.O_2$ at 29°C and around 55% of the average $C.O_2$ at 10°C, indicating that this was due purely to thermal shock and not to any reduction in oxygen availability. In both reciprocal assays elvers were allowed to slowly reach the assay temperature, over a period of 2 to 3 hours, before the experiment was begun.

The allometric relationship of $\dot{V}o_2$ was investigated using elver, yellow and silver stages of the eel, acclimated to similar temperature regimes (Fig. 6.6; Table 6.3). In general, the effect of small differences in both body size and assay temperature increased with size, and may explain the larger spread of values found in silver eels (Fig. 6.6). The small effects of body weight on elver $\dot{V}o_2$ suggests that, despite the variation in size of elvers used, the experimental results reflect the heterogeneous physiological composition of the migration and are a good estimate of the population means. The low Q_{10} value, relative to older stages, suggest that elvers are better able to adapt to a 20°C temperature differential. The similar Q_{10} values for yellow and silver eel, over the similar range of temperature, is in contrast to their absolute $\dot{V}o_2$ and the supposed elevation of aerobic capacity found during the migratory (silver) stage (Fontaine 1975; Table 6.3).

No discernible difference could be seen in the histochemical profile of the skeletal muscle in the trunk of elvers acclimated to 10°C or 29°C, relative to the original study of 20°C-acclimated elvers (Chapter 2). In this way, the proportion of slow muscle remained at 10 to 12% of the muscle mass, and the lateral myotomes at a depth of 2 to 3 fibres. The PAS, SDH and m.ATPase reactivity were identical in slow, superficial fast and deep fast muscle to that

previously described (Chapter 2). The superficial fast muscle (intermediate SDH staining zone) remained at a depth of 2 or 3 fibres. These results suggest that no proliferation of the slow muscle occurred on cold-acclimation, as reported for other species, nor was there any visible reorganisation of metabolic fibre types. Consequently, no further quantitative analysis of frozen sections was attempted.

Morphometric analysis revealed little difference for most muscle components, although there was an increase in fibre mitochondrial content on cold-acclimation. Proliferation of mitochondria was found in both sub-sarcolemmal and intermyofibrillar regions of the fibre, and the extra volume accounted for by a reduction in sarcoplasm (Table 6.4). No difference in cristae density, or average size of mitochondria was visible. Fibre area and myofibrillar content were very similar in both groups. Interestingly, there is an appreciable difference in section quality between muscle samples taken from the two acclimation groups, with 10°C-acclimated fibres giving much clearer electronmicrographs (Figs. 6.9 and 6.10). It would appear, therefore, that difficulty in obtaining good section contrast in the original study (Chapter 3) was compounded by the high (20°C) maintenance temperature. No quantitative analysis of fibres from the fast muscle was attempted.

The large sample size used for the analysis of capillary supply revealed a trend towards increased fibre area in the 10°C-acclimated elvers, that was not evident from electronmicrographs (Table 6.4 and 6.5). There was only a small increase in the average number of capillaries around a fibre, the capillary: fibre ratio, and the capillary density in the slow muscle of 10°-acclimated elvers (Table 6.5). The similar dimensions of the capillaries suggests that the instantaneous blood volume may be little altered on exposure to a 20°C difference to temperature, although the significance of this is uncertain (see later).

DISCUSSION

Developmental physiology

The initial reduction in size of elvers during the upstream migration (Fig. 6.2) is well documented (Schmidt 1922; Boëtius 1976; Tesch 1977) and appears to reach a minimum at Group 3 (Table 6.1). In a similar study carried out in two Danish localities, this minimum was observed at Stage VIA_{II-III} (Boëtius 1976). The discontinuous growth pattern of the late-arriving elvers (Groups 3 and 4 in this study) is thought to be the result of starvation rather than any effect of prolonged metamorphosis, as the earliest arrivals show a much less pronounced weight minimum at similar developmental stages (Boëtius 1976). Some geographical variability is to be expected, and in experiments based on Lake Tunis a gradual reduction in weight was noted from the earliest arrivals, Stage VIA 0.23g, to a slightly later minimum of Stage VIA_{III2-3} 0.18g, followed by an exponential growth pattern (Fig. 6.2). A parallel reduction in length was noted by Schmidt (1909) from the pre-metamorphic leptocephalus Stage I (75mm) to glass eels of Stage VA (70mm) and a minimum in young elvers of Stage VIA (65mm).

From the present data it would appear that the annual migrations have a similar composition, but with considerable overlap between each migratory wave. The development of an individual will therefore depend on time of arrival at a collection point, and not necessarily follow the same temporal pattern as the main migration, proceeding upstream. This explains the reported increase in mean length towards the end of the season (Ezzat and El-Serafy 1977). As the histochemical character of trunk muscle shows little variation between migration groups (Chapter 2), and an extensive fine structure investigation would be too time-consuming, the gross metabolic rate ($\dot{V}o_2$) was chosen as an appropriate physiological index to follow development, in addition to purely morphological criteria (Strubberg 1913). As muscle constitutes 70-75% of the body weight, it is likely that its metabolic

activity will be reflected in the $\dot{V}o_2$. The reduction of $\dot{V}o_2$ at Group 2 identifies this as the developmental inflection point sought by earlier workers, using weight and length measurements, levelling of these parameters in Groups 3 and 4 reflects the extended migration and late arrival of these elvers. The size minimum has been experimentally confirmed to coincide with the start of feeding, with feeding of all individuals only present from Stage VIA_{II-III} (Tesch 1977). The subsequent rapid rise in body weight (Fig. 6.2), assumed to be due to an accelerated growth phase, results in a 5 to 10-fold increase in muscle mass by a month or so after the end of the migration (pers. obs.). Resorption of body tissue during the reduction in size of the early migratory stages is reflected in the decreased $\dot{V}o_2$ (group 2). A change in the aerobic capacity during metabolic reorganisation from catabolism to anabolism, and the subsequent growth, contribute to an increased $\dot{V}o_2$ in Groups 3 and 4. The relative contribution of each process is unclear, although growth is likely to only account for a small (10-20%) portion of basal metabolism. Elvers from Group 3, therefore, represent animals that have slightly delayed the onset of accelerated growth and entered the early stages of starvation. At this point, the physiological adjustments required for freshwater life are presumably complete, and the elver is in a true post-metamorphic state, although some development may continue for a short while after. The earlier assumption (Chapters 2 and 3), that this stage represents juvenile (late elver) eels, is therefore justified. In addition, the haemoglobin electrophoretograms represent the final elver pattern before expression of the adult phenotype (pers. obs; see also Rizzotti et al 1977). The difference in muscle structure between early and late elvers is not known.

The low aerobic capacity of elver muscle (Chapters 2 and 3) is reflected in the low $\dot{V}o_2$, relative to other species (Brett 1972; Doudoroff and Shumway 1968). However, the wide variation in methodology used by various

workers makes comparisons difficult; although a study of young (juvenile) fish in the Mediterranean (red and grey mullet, eel, and sandsmelt) has shown the basal and active metabolism ($\dot{V}o_2$) of elvers to be significantly lower than other species (Alekseyeva 1973). The usual trend of a decrease in $\dot{V}o_2$ with an increase in body size (Mb) is shown in comparing values for elver, yellow eel and silver eel (Table 6.3). The low metabolic rate is emphasised by the range found in elvers ($\dot{V}o_2$ = 0.2 to 0.4mg.g.hr^{-1} at 22°C) being similar to that for an adult salmonid, Onchorhynchus nerka (at 15°C, Brett and Zala 1975); this represents a 1000-fold difference in body weight.

A reduction in $\dot{V}o_2$ is known to occur with progressive starvation (Love 1980); in the migrating elver this seems to be correlated with development, since the decline in $\dot{V}o_2$ is reversed in the later arrivals (Groups 3 and 4) when starvation has already begun (Boëtius 1976).

A further test of the metabolic state of the animal, is the residual oxygen bioassay. Initially this was used as an indicator of pollution (Gordon and McLeay 1977), where gill oedema reduces oxygen extraction efficiency, and causes death by asphyxiation. It is, essentially, a test of hypoxic resistance. This is of interest in the present study, since the low aerobic capacity of the muscle is assumed to impose limitations on the migratory capabilities of the muscle, probably requiring the use of anaerobic metabolism (Chapter 2). As the development of hypoxic tolerance is mirrored by the induction of anaerobic metabolism in some fish (Prosser et al 1957; Thillart et al 1978), this assay may be expected to delineate the stages at which anaerobic metabolism is of most importance. The lowest critical C_{O2} (Group 2) is indicative of an increased oxygen utilization which, coupled with the lowest $\dot{V}o_2$, will provide a degree of hypoxic resistance. Interestingly, the main elver migration has been shown to coincide with the lowest water oxygen content (Ezzat and El-Serafy 1977); a reduction in both $\dot{V}o_2$

and critical Co_2 would be necessary to maintain migratory efficiency, under such unfavourable conditions.

An extension of lipid reserves is often undertaken before migration (Fontaine 1975) and is one of the first reserves to be utilised during starvation (Love 1970). The presence of fast fibres in varying stages of disassembly in most Group 3 and 4 elvers (see also Beardall and Johnston 1982) suggests that protein is being utilised as an energy reserve, and seems incongruous with the very large amount of lipid stores (Chapter 2). Although lipid reserves in adult eels are thought to be a possible pre-adaptation for winter torpor (Tesch 1977), this seems unlikely to be the sole reason for their presence in a juvenile fish. It is possible that it acts as an additional buoyancy mechanism (prior to full swimbladder function), which, in addition to behavioural adaptations (Chapter 2), will reduce the metabolic cost of swimming. The possibility remains, however, that overland migrations (Tesch 1977) may be sustained by anaerobic metabolism, if undertaken by the older juveniles or "bolters".

Temperature acclimation

Habitat salinity may affect the acclimatory response: in stenohaline species such as freshwater stickleback, the temperature preferendum is higher is isomotic (brackish) water than at any other salinity (Garside et al 1977). Likewise, euryhaline mummichog and banded killifish have a preferred temperature 3-6° and 5-8° higher in normal (habitat) salinity, respectively (Garside and Morrison 1977). However, the response to an extra osmoregulatory load may be complex; Tilapia has a higher temperature preferendum on either side of isomolarity (Beamish 1970). Adaptation to seawater by freshwater eels involves an increase in the active transport of sodium across gill epithelia, under hormonal control (Epstein et al 1971); the reverse process is likely to involve adjustment of the same mechanism. The break (transition

temperature) in the Arrhenius plot of gill Na^+K^+ ATPase, or "sodium pump", increases on warm acclimation when the membrane composition is similar between both freshwater (FW) and seawater (SW) eels (Thomson et al 1977).

Salinity affects membrane composition since FW eel gills are rich in (n-6) unsaturated fatty acids, and are only able to decrease the transition temperature (on cold acclimation) by incorporating essential (n-3) unsaturated fatty acids into the membrane.
In addition, the pattern of ^{32}P-incorporation into gill lipis appears to have a salinity-specific pattern (Hansen and Abraham 1979). Euryhaline species usually show a quick adaptation to different salinities (Fontaine 1975), and it is likely that Group 3 elvers are fully FW-adapted. Ionic and osmotic homeostasis places a large demand on the energy budget of fish, the earliest (SW-adapted) elvers may actually incur a smaller metabolic cost for thermal compensation.

If the adaptive response to changing temperature is mainly behavioural (cf locomotory adaptation to aerobic scope), then only a limited compensation would be expected in $\dot{V}o_2$. On the basis of Q_{10}, the elver shows a better compensation than either sub-adult (yellow) or adult (silver) stages (Table 6.3). Jankowsky (1966) found that yellow eels acclimated to 14°C for 10 days showed a 1.5-fold increase in $\dot{V}o_2$, relative to those acclimated to 25°C when assayed at 18°C; no information is given concerning $\dot{V}o_2$ at the acclimation temperatures. Similar evidence for acclimation is found in the Japanese eel (Anguilla japonica) where acute temperature changes between 13° and 30°C, over a few hours, give a $Q_{10} = 3.19$. After acclimation to these temperatures for 1 week or more, $Q_{10} = 1.39$ (Chan and Woo 1978); European eels become torpid at water temperatures of 10 to 12°C (Sinha and Jones 1975; Tesch 1977) and burrow in the mud at 8°C or below (Nyman 1972). Similarly, American eels apparently cease feeding and become less active around 8°C (Renaud and Moon 1980);

A. rostrata show a rate compensation in $\dot{V}o_2$ on acclimation between 10° and 20°C (Q_{10} = 1.12 to 1.65), but fail to show compensation at 5°C (Q_{10} (5-10°C) = 4.10; Moon, pers. comm.). In this study the higher Q_{10} of silver eel (5°C-acclimated) may reflect a direct temperature effect on metabolic rate, whereas elvers and yellow eel would appear to differ in their response (Table 6.3). Elvers arrive at river estuaries during winter (December to February) when water temperatures are <5°C; as melt water can keep the rivers below 10°C for many months, a similar lack of compensation to that shown by yellow eels would severely restrict the start of the upstream migration. The response of elver $\dot{V}o_2$, at intermediate and reciprocal temperatures, suggests that there is only a partial compensation, sufficient to give the elver a wide thermal tolerance, as shown by the similar $\dot{V}o_2$ of 29°C-acclimated elvers at both 19.5° and 10°C (see Results). A decreased metabolism during the winter months, as shown by the absence of a compensatory rise in $\dot{V}o_2$ at low temperature in A. rostrata, would reduce the consumption of metabolic reserves during the annual starvation period (Tesch 1977). In young elvers at least, an excessive metabolic deactivation in response to low temperatures would be a disadvantage with respect to the post-metamorphic reorganisation of tissues, freshwater-adaptation, and the metabolic demands of migration. It would be interesting to see if earlier-arriving elvers (Group 1) have a lower Q_{10} than the Group 3 elvers used in this study, thereby emphasising the scale of physiological adjustment taking place.

The lack of any visible fibre-type conversion, at the histochemical level is similar to that found in rainbow trout, which shows no change in proportion or morphology of the different fibre types on acclimation, although an adjustment of metabolic pathway utilization and an increased metabolism may occur (Dean 1969). In contrast, the slow muscle increases in cold-acclimated goldfish (Johnston and Lucking 1978; Sidell 1980),

crucian carp (Johnston and Maitland 1980) and sub-adult eels (Wodtke 1974b). Whether this represents hyperplasia or true fibre-type conversion is not known. Muscle aerobic capacity has often been found to increase on cold-acclimation (Hazel 1972; Smit et al 1974; Thillart and Moddeskolk 1978; Johnston and Maitland 1980), sometimes more so in slow, relative to fast muscle (Malessa 1969; Jones and Sidell 1982). Although there is no quantitative change in elver slow muscle, a qualitative change (structural reorganisation) may be sufficient to maintain locomotory efficiency. The increased V_V(mit,f) will increase the rate of ATP production, but not the contractile activity, whereas the minor change in V_V(mf,f) suggests maximum tension development will be similar in the two groups. The small increase in IMF mitochondria may limit the maximum power output, although burst swimming speed may be almost temperature-independent (Beamish 1978), suggesting that glycolytic ATP production is not a rate-limiting factor. It is perhaps significant that the only enzyme to show qualitatively different properties after acclimation is myofibrillar Mg^{2+} Ca^{2+} -ATPase (m.ATPase) (Johnston et al 1975b; Johnston 1979; Sidell 1980; Johnston et al 1982). However, the kinetic properties of brook trout m.ATPase is not affected by acclimation to 4° and $24^{\circ}C$, this may represent a seasonal compromise, with behavioural adaptations regulating body temperature (Walesby and Johnston 1981). In addition, goldfish m.ATPase may only compensate within limits that allows tolerance of a wide temperature range (Penney and Goldspink 1979).
The limited compensation in elver muscle may be the result of metabolic compromise, rather than extensive adaptation, explaining the delayed upstream migration until rivers reach $6^{\circ}C$ (Milne, pers. comm; Tesch 1977).

In fish muscle, mitochondrial enzymes usually show a marked compensation to temperature (Sidell 1982); the elevated metabolic rate on cold-acclimation seems to be mirrored by the fine structure correlates of oxygen supply and

demand, increased capillary (Johnston 1982b) and mitochondrial content (Johnston and Maitland 1980), respectively. On acclimation to 2° and 28°C for 8 weeks, crucian carp (Carassius carassius) slow muscle V_V(mit,f) was 0.25 and 0.14, and fast muscle 0.04 and 0.01, respectively (Johnston and Maitland 1980). This is similar to the change in elver slow fibre V_V(mit,f), over a slightly narrower temperature range (0.26 and 0.19, Table 6.4). Interestingly, the majority of the change occurred within the subsarcolemmal (SS) population of mitochondria (Table 6.5). This region is assumed to be responsible for the active transport of metabolites (glucose, amino acids etc.) across the sarcolemma, with intermyofibrillar (IMF) mitochondria producing ATP for muscle contraction (Kubista et al 1971; Müller 1976). Two biochemically and functionally distinct types of mitochondria may therefore exist, with the SS population limiting endurance performance in mammalian oxidative fibres (Müller 1976). Proliferation of mitochondria may, in addition to an increase in aerobic enzyme concentration, be required to reduce metabolite diffusion distances in a kinetically unfavourable thermal environment (Sidell 1982). In contrast to elver, carp slow muscle has a reduced SS:IMF ration on cold-acclimation; this may reflect the diffusion distances imposed by fibre size: carp $\bar{a}(f) = 752\mu m^2$ at 2°C and elver $\bar{a}(f) = 127\mu m^2$ at 10°C. V_V(mit,f), however, only gives a coarse description of the quantitative nature of O_2-flux from the point of supply (capillaries) to consumption (mitochondria); this requires more information about the density and specific activity of respiratory chain units. Goldfish acclimated to 5° and 25°C show an increase in concentration and activity of muscle cytochrome oxidase (COX) by 66% and 45%, respectively, at the lower temperature (Wilson 1977). The increase in cytochrome c in green sunfish (Lepomis cyanellus) on cold acclimation (5°C vs 25°C) is due to a differential reduction in protein synthesis (40%) and degredation (60%, Sidell 1977), thereby giving an

adaptive increase in enzyme concentration with a minimum anabolic energy demand. Interestingly, although yellow eel has a behavioural response to low temperatures (torpor), it also shows a partial compensation in slow muscle COX and SDH activities (Malessa 1969), as well as an increase in both the relative amount and $\dot{V}o_2$ of mitochondria (Wodtke 1974b). The lack of a compensatory increase in slow muscle shown by elvers suggests that the proliferation of mitochondria, and perhaps specific mitochondrial $\dot{V}o_2$, may have a greater functional importance.

The elevated $V_V(mit,f)$ of cold-acclimated elvers presumably requires an improved oxygen delivery. During muscular contraction there may be an increase in capillary recruitment (% patent capillaries) of around 50% (Hudlická et al 1982), although the proliferation of capillaries in response to a higher $V_V(mit,f)$ in fish slow muscle (Johnston 1982) is indicative of a smaller reserve (% non-perfused capillaries). However, an increased blood delivery may be effected by an increased blood flow velocity (Hudlická et al 1982). The similar $V_V(c,f)$ values for both elver groups may therefore only limit the maximum blood supply, not that during routine metabolism; this may be adjusted by other factors. A reduced temperature decreases plasma volume in brook trout, thereby regulating blood oxygen carrying capacity (Houston and De Wilde 1969), although a variety of responses have been reported (De Wilde and Houston 1967; Cameron 1970; Houston and Smeda 1979). In general, the O_2-affinity of fish blood increases invèrsely with temperature (Grigg 1974; Randall 1970). Adjustment to these parameters may produce a 30% increase in blood O_2-content, from 10° to 2°C-acclimated rainbow trout, giving an elevated oxygen transfer to the tissues (Nikinmaa et al 1980), which may be counteracted by a temperature-induced decrease in heart minute volume (Heath and Hughes 1973). In general, ventilatory frequency increases in response to a temperature rise;

this may become self-limiting due to the high metabolic cost, reaching 70% of total metabolism at maximal ventilation rates in tench (Tinca, tinca, Burton 1979). In contrast to rainbow trout, yellow eel dorsal aorta Po_2 is lowered on cold-acclimation, and rises in line with increasing temperature due to an elevated breathing rate (Jankowsky and Prosser 1965). However, the changes in muscle respiration are not sufficient to account for the differences in whole-animal $\dot{V}o_2$ on acclimation (Janowsky 1966; Malessa 1969; Wodtke 1974a). As the respiration rate is under neuronal control, the discrepancy may be the result of a poor adaptive response in the nervous system (Prosser et al 1965); e.g. the inverse compensation found in nervous tissue, in particular the neuromuscular acetylcholinesterase (Prosser 1973).

Conclusion

The muscle capillary supply would appear to have a sufficient functional reserve to accommodate a 19°C difference in temperature; this may be the result of adjustments in cardio-vascular haemodynamics (e.g. perfusion pressure) and modification of the oxygen-haemoglobin association curve. The limited metabolic compensation available suggests a marked difference in the scope for activity between the two groups, and would explain the semi-torpor at low temperatures and the delay of migration. This behavioural strategy would support the notion of the elver as a "eurytolerant" animal, a situation considered to be a general migration strategy among ectotherms (Fontaine 1975).
More recent work suggests that the basic mechanisms underlying the acclimation may be revealed by analysis of the response at even lower temperatures. Interestingly, the American elver (Anquilla rostrata) may adopt a different strategy, since the upstream migration is known to begin at 1°C (McCleave and Kleckner 1982). This could be the result of either a more extensive metabolic compensation, or modified tolerance limits, compared to A. anquilla.

TABLE 6.1. Oxygen consumption and critical oxygen concentrations for elvers during the upstream migration; 1981 migration. Mean ± S.D. (n).

Group	Date	Weight (g)	Length (cm)	$\dot{V}o_2$ (mg/g/hr)	Co_2 (mg/l)
1	5.4.81	0.268 ±0.0520 (33)	7.36 ±0.352 (34)	0.218 ±0.0806 (12)	1.414 ±0.7344 (11)
2	25.4.81	0.247 ±0.0447 (52)	7.07 ±0.385 (51)	0.159 ±0.0245 (21)	1.040 ±0.2939 (19)
3	13.5.81	0.238 ±0.0510 (55)	7.02 ±0.362 (53)	0.223 ±0.0600 (22)	1.615 ±0.3774 (22)
4	4.6.81	0.232 ±0.0346 (57)	7.10 ±0.333 (56)	0.282 ±0.0490 (27)	1.570 ±0.6024 (17)

Note: assay temperature = 22°C

Weight and length were determined under MS222 anaesthesia. $\dot{V}o_2$ = standard (routine) oxygen consumption; $C.O_2$ = residual oxygen concentration (at death).

TABLE 6.2. Elver Oxygen consumption; time-course of temperature acclimation in Group 3 elvers. Mean ± S.D. (n).

Week	Date	Assay T°C	$\dot{V}o_2$ (mg/g/hr)	Wt. (g)	Assay T°C	$\dot{V}o_2$ (mg/g/hr)	Wt (g)
1	15.5.81	22	0.223 ±0.0600 (22)	0.229 ±0.0436 (35)	-	-	-
2	2.6.81	29	0.297 ±0.0648 (6)	0.198 ±0.0557 (6)	10	0.310 ±0.0954 (6)	0.239 ±0.0424 (6)
3	9.6.81	29	0.360 ±0.108 (6)	0.189 ±0.0245 (6)	10	0.166 ±0.0316 (6)	0.255 ±0.0469 (6)
4	16.6.81	29	0.318 ±0.0374 (6)	0.148 ±0.033 (6)	10	0.143 ±0.0224 (6)	0.247 ±0.0458 (6)
5	23.6.81	29	0.428 ±0.0686 (6)	0.202 ±0.0510 (6)	10	0.177 ±0.0332 (6)	0.232 ±0.0825 (6)
6	30.6.81	29	0.376 ±0.0510 (6)	0.215 ±0.0447 (6)	10	0.187 ±0.0480 (6)	0.249 ±0.0520 (6)
7	14.7.81	29	0.396 ±0.0539 (6)	0.221 ±0.0500 (6)	10	0.214 ±0.0663 (6)	0.219 ±0.0316 (6)
8	21.7.81	29	0.422 ±0.0869 (6)	0.218 ±0.0638 (6)	10	0.215 ±0.0533 (6)	0.225 ±0.0397 (6)
9	28.7.81	22	0.276 ±0.0749 (9)	0.189 ±0.0333 (8)	-	-	-

Note: 22°C elvers act as the reference group.

TABLE 6.3. Comparison of oxygen consumption values for three stages of eel, acclimated to two different temperatures. Mean ± S.D. (n).

Animal	Temp (°C)	$\dot{V}o_2$ (mg/g/hr)	Wt (g)	Temp (°C)	$\dot{V}o_2$ (mg/g/hr)	Wt (g)	Q_{10}
Elver	8	0.212 ±0.0519 (10)	0.1911 ±0.0513 (10)	30	0.395 ±0.0632 (10)	0.1602 ±0.0759 (10)	1.33
Elver	10	0.215 ±0.0533 (6)	0.225 ±0.0397 (6)	29	0.422 ±0.0869 (6)	0.218 ±0.0638 (6)	1.43
Yellow	8	0.032 ±0.0083 (13)	99.0 ±35.32 (13)	28	0.197 ±0.0488 (8)	83.9 ±33.50 (8)	2.48
Silver	5	0.007 ±0.0004 (15)	588.1 ±179.86 (15)	25	0.045 ±0.0045 (20)	663.1 ±339.26 (20)	2.54

Note: data for elvers from closed respirometry systems, and that for yellow and silver eels from an open system. Calculation based on the relationship:

$$Q_{10} = \left(\frac{K_1}{K_2}\right)^{\frac{10}{t_1 - t_2}} \quad \text{i.e. } \log Q_{10} = \left(\frac{10}{t_1 - t_2}\right) \cdot \log (K_1/K_2)$$

where K_1 and K_2 are the $\dot{V}o_2$ at temperatures t_1 and t_2, respectively.

Elvers acclimated to 8° and 30°C were from the 1979-1980 migration; elvers acclimated to 10° and 29°C were taken from the following year's migration, sampled at the same geographical locality and time of season.

TABLE 6.4. Morphometric analysis of the thermal acclimatory response in slow muscle fibres, from elvers maintained at a difference of 19°C, for 8 to 9 weeks. $\bar{x} \pm$ S.D. (n).

TEMPERATURE	V_V(nuc,f)	V_V(mit,f)	V_V(lip,f)	V_V(mf, f)	V_V(sp,f)	$\bar{a}$(f) μm^2
10 ± 0.5°C (37)	0.018 ±0.020	0.264 ±0.055	0.001 ±0.003	0.650 ±0.050	0.067 ±0.033	126.7 ±47.7
29 ± 1.0°C (39)	0.017 ±0.018	0.188 ±0.052	0.001 ±0.002	0.683 ±0.056	0.112 ±0.033	128.1 ±86.8

For explanation of symbols, see Chapter 3

TABLE 6.5. Temperature acclimation response of elvers, with respect to whole-animal and muscle aerobic capacities, and the capillary supply. $\bar{x} \pm$ S.D.

PARAMETER	ACCLIMATION TEMPERATURE 10°C	29°C
Standard Vo_2, $mg.g.hr^{-1}$ (whole-animal)	0.215 ± 0.053	0.422 ± 0.087
$V_V(mit,f)$ (subsarcolemmal)	0.177 ± 0.047	0.122 ± 0.051
$V_V(mit,f)$ (intermyofibrillar)	0.087 ± 0.034	0.066 ± 0.030
$\bar{a}(f)$, μm^2	152.1 ± 63.5	126.1 ± 54.5
$\bar{a}(c)$, μm^2	10.7 ± 5.89	11.6 ± 4.73
$\bar{b}(c)$, μm	12.5 ± 4.23	13.0 ± 2.54
N(f)	383	469
N(c)	120	141
$\bar{N}(c,f)$	1.04 ± 0.76	0.90 ± 0.76
$*N_N(c,f)$	0.312 ± 0.049	0.300 ± 0.048
$N_A(c,f)$, mm^{-2}	2473	2347
$V_V(c,f)$	0.027	0.028
$S_V(c,f)$, cm^{-1}	314.1	310.0

* = average of 6 fish $group^{-1}$.

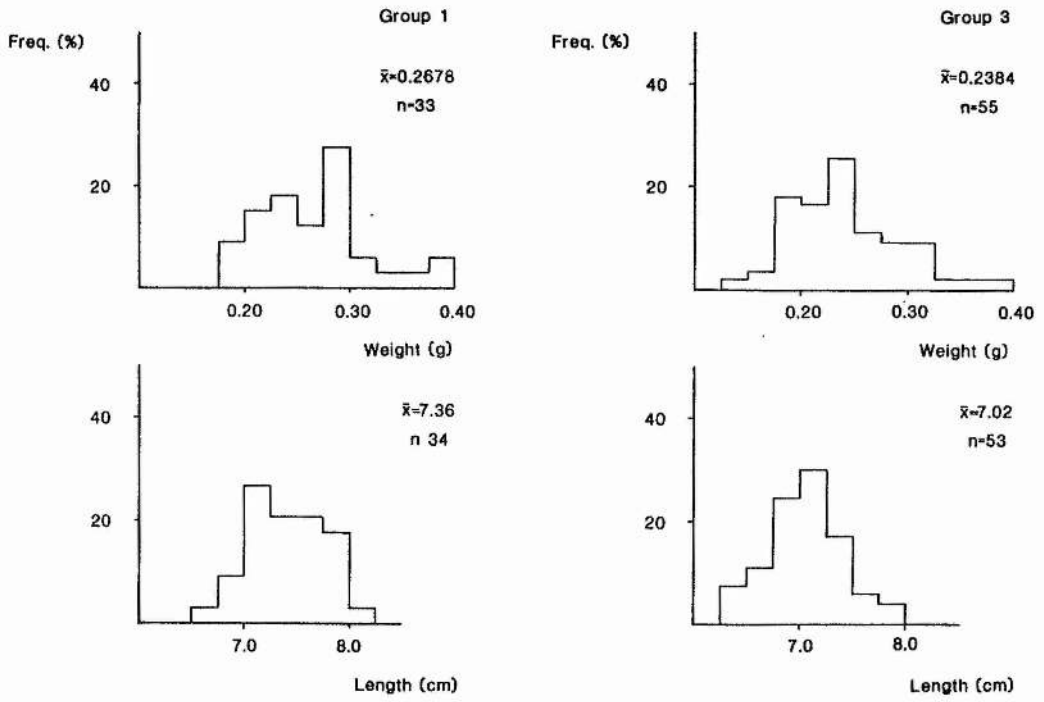

Fig. 6.1. Change in the size composition of the elver migration for the early (Group 1, left) and late stages (Group 3, right). The heterogeneity of the samples is evident by the spread of values, although the trend of size reduction is clear. 1980-1981 migration, see Table 4.3.

Fig. 6.2. The change in size of elvers, correlated with the morphological development during upstream migration. Data from Tesch (1977). The pigmentation stages refer to the classification of Strubberg (1913) and the key to the axis number is as follows:

pigmentation stage No.	1	≡ Strubberg's stage	VA
	2		VB
	3		VI AI
	4		VI AII_1
	5		VI AII_2
	6		VI AII_3
	7		VI AII_4
	8		VI $AIII_1$
	9		VI $AIII_2$
	10		VI $AIII_3$
	11		VI AIV_1
	12		VI AIV_2
	13		VI AIV_3
	14		VI AIV_4
	15		VI B

Stage V elvers are those which usually accumulate in river estuaries before commencing the upstream migration, and Stage VI B elvers are only present towards the tail end of the migration, being morphologically similar to young eels.

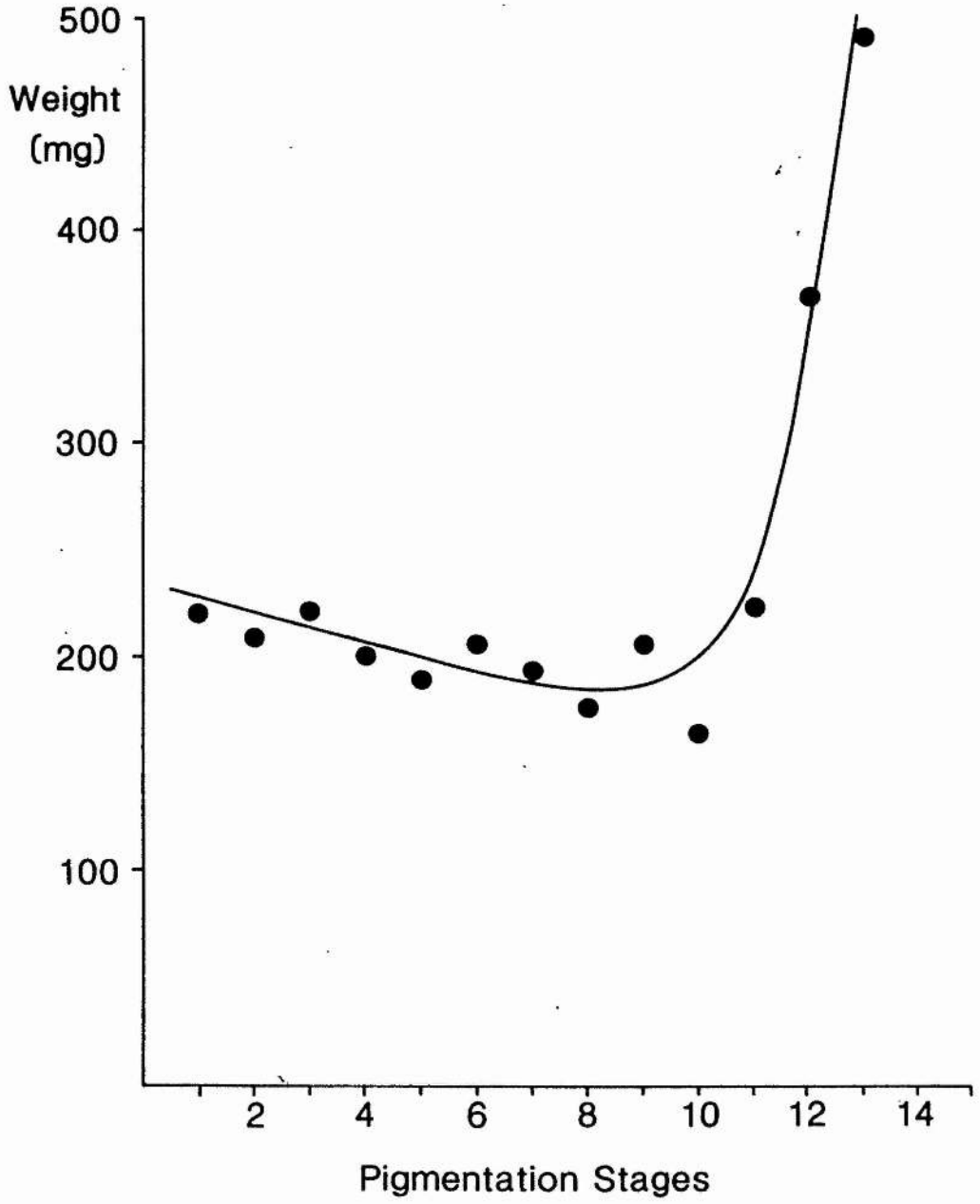
500
Weight
(mg)
400
300
200
100
2
4
6
8
10
12
14
Pigmentation Stages

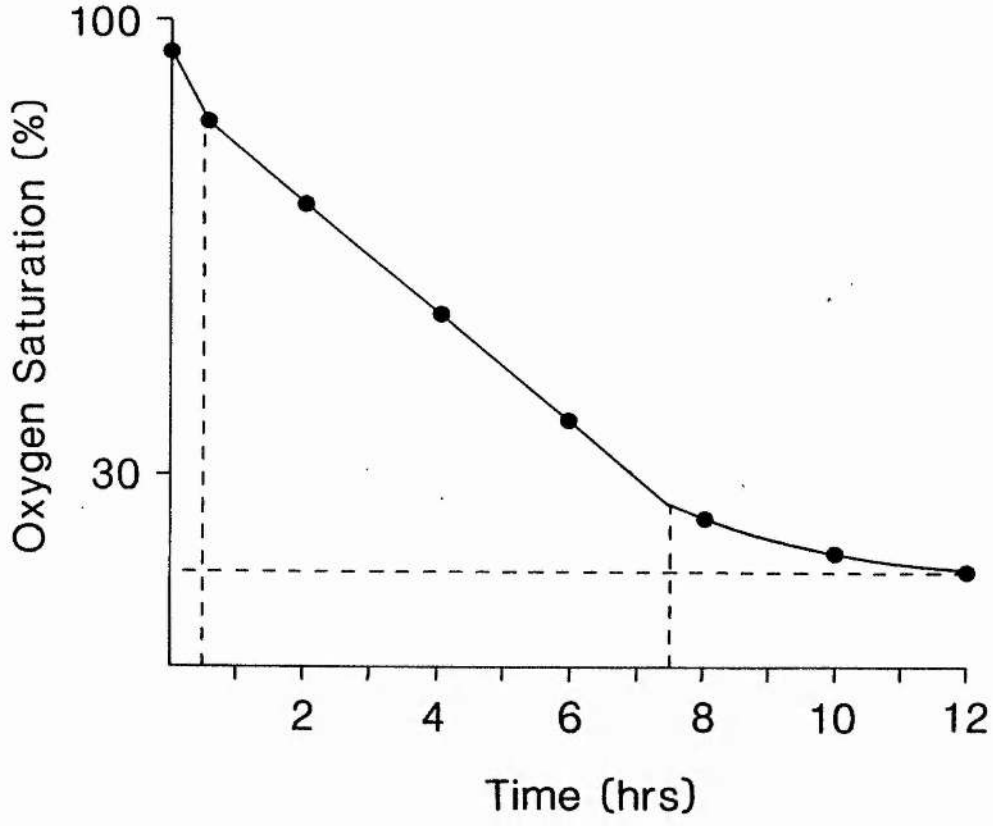

Fig. 6.3. Normalised control curve used to determine the optimal duration of the closed respirometry, for estimation of elver $\dot{V}o_2$. Results are combined from 10 animals, plotted at 2 hour intervals. Initial oxygen content of the water was usually around 95% saturation at the assay temperature, and fell steadily for 7 to 8 hours (22°C) or until saturation approached 30%. This value corresponds to a similar point (3mg/l) which is regarded as the limit of Po_2 - independent respiration in a range of fish species (Douderoff and Shumway 1968). After this point the animals responded to the hypoxia by a reduction in $\dot{V}o_2$, following an exponential decline until death occurred between 10 and 20% saturation. The initial stress reaction, giving rise to an elevated $\dot{V}o_2$, usually only lasted ~ 15 mins. Experiments were therefore conducted using a 4-5 hour interval, resulting in the oxygen saturation at the end always being > 60%. The initial high $\dot{V}o_2$ could only be seen to be significant in yellow eels assayed in a similar manner, as determined from a series of 4 X 2hr experimental cycles.

Fig. 6.4. Time-course of the thermal acclimatory response of elvers from Group 3 of the 1980-1981 migration.

a) Oxygen consumption. The 'hot' elvers showed a progressive increase in $\dot{V}o_2$ over the first month, giving fairly steady values thereafter in line with the small increase in $\dot{V}o_2$ found within the control (22°C) elvers. This is taken to be part of the normal development of the animals, see Table 4.3. The 'cold' elvers showed a transient elevation of $\dot{V}o_2$, which is assumed to be a stress reaction, before exhibiting the decline in respiration rate expected for most ectotherms. The metabolic compensation is seen to begin quite early, before week 4, and plateau well before the end of the experiment. In common with most fish, the scatter of data from the cold-acclimated elvers is much less than that from the hot elvers.

b) Body weight. Attempts to regulate the food intake to maintain a steady condition were successful. The slight decline in the hot elver weight at week 3 is correlated with a decline in $\dot{V}o_2$. Control elver weights remained remarkably constant.

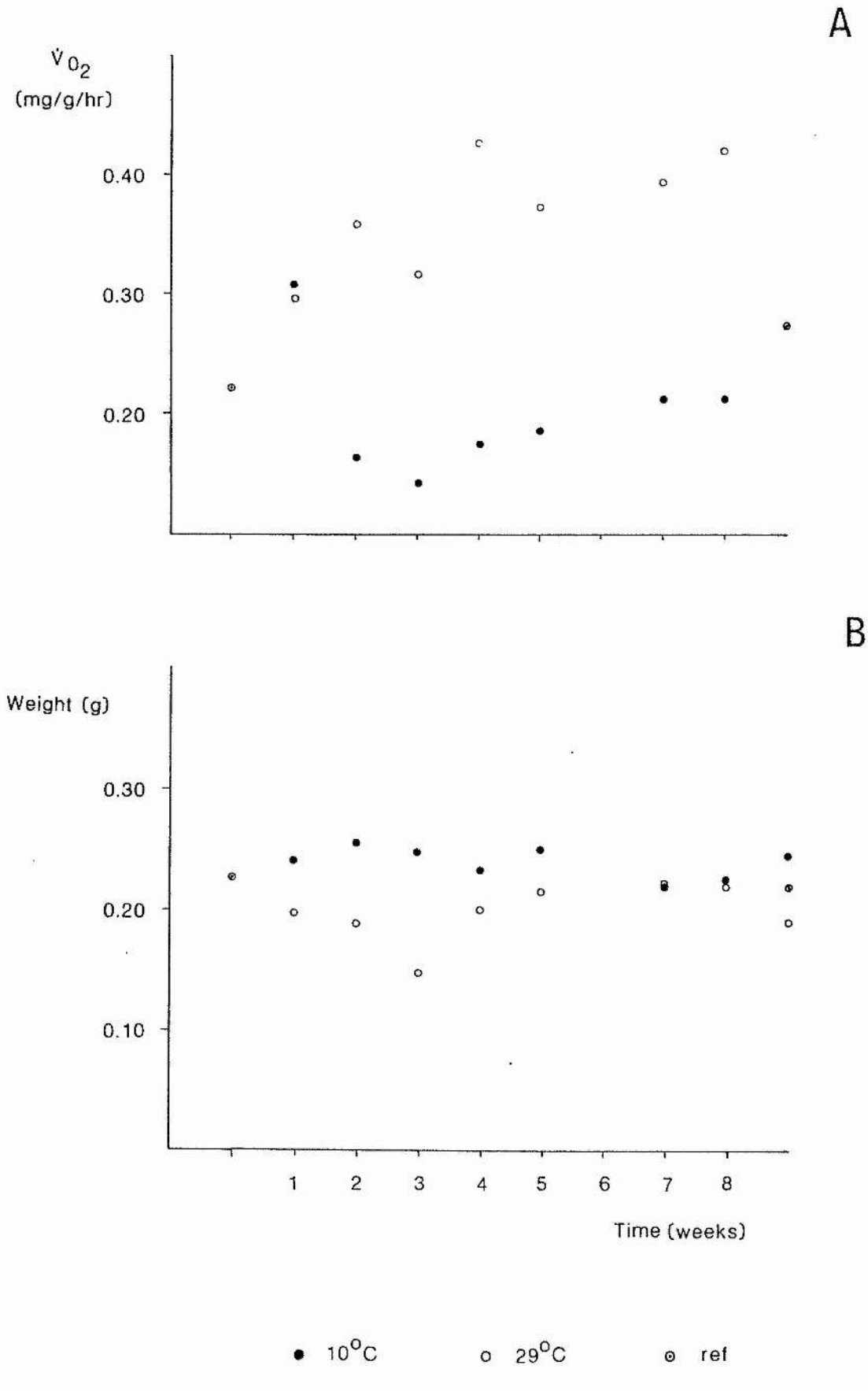
A
$\dot{V}O_2$
(mg/g/hr)
0.40
0.30
0.20
B
Weight (g)
0.30
0.20
0.10
1
2
3
4
5
6
7
8
Time (weeks)
10°C
29°C
ref

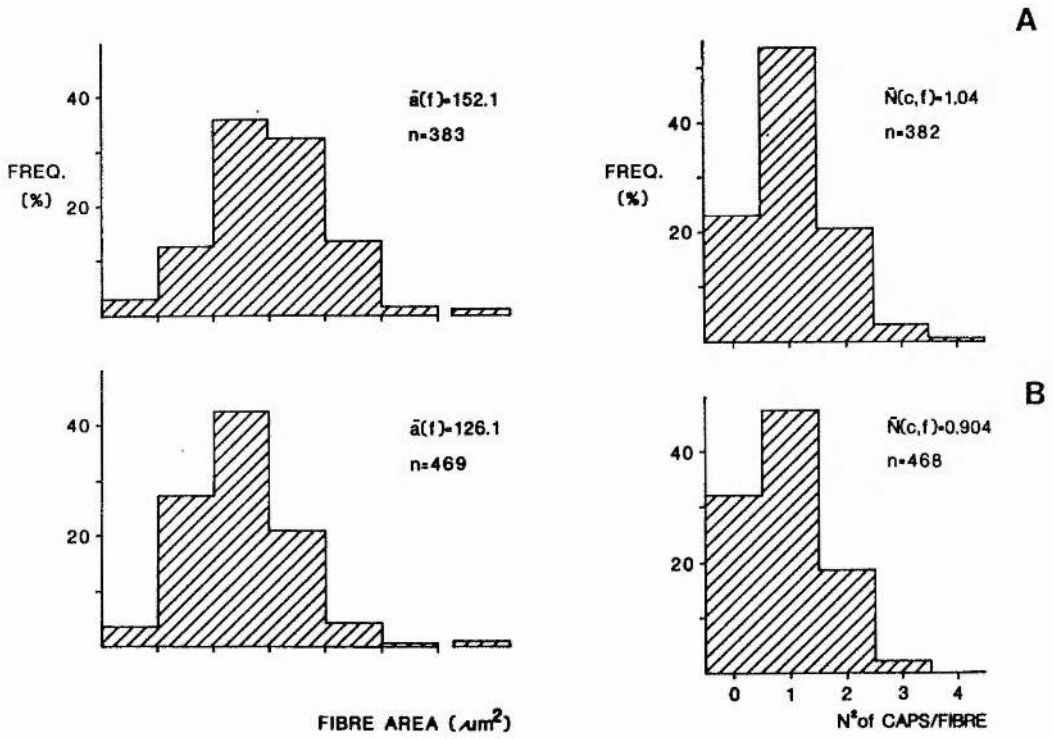

Fig. 6.5. Histograms of slow fibre area, and number of capillaries per fibre distributions for 10°C (A) and 29°C-acclimated elvers (B). Note the trend towards a large fibre size in the cold fish, and a slight elevation in the number of peripheral capillaries.

Fig. 6.6. Histograms illustrating the variability in $\dot{V}o_2$ measurements from three stages of eel.

Elvers (top) show a normal distribution of values when assayed at 22°C (Table 6.1), although the separation of the distributions at the acclimation temperatures is quite distinct (Table 6.2). Yellow eels (bottom, left) show a similar separation of values at 8°C and 28°C (hatched bars). Silver eels (bottom, right) show a large degree of overlap between the two acclimatory groups (5° and 25°C, Table 6.3), due mainly to the extensive spread of data within the higher temperature group.

Note the difference in absolute values between the three groups of animals.

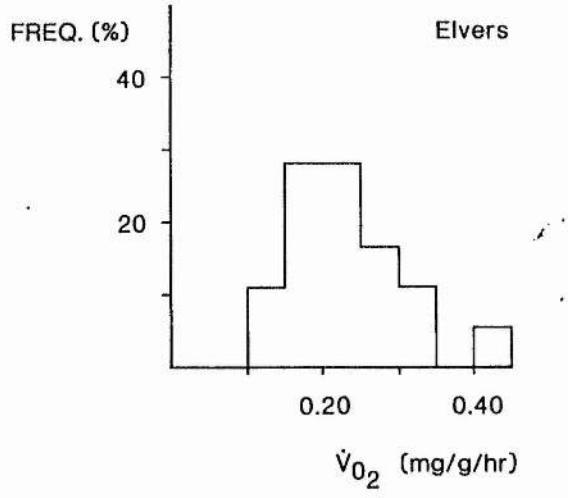
FREQ. (%)
Elvers
40
20
0.20
0.40
$\dot{V}_{O_2}$ (mg/g/hr)

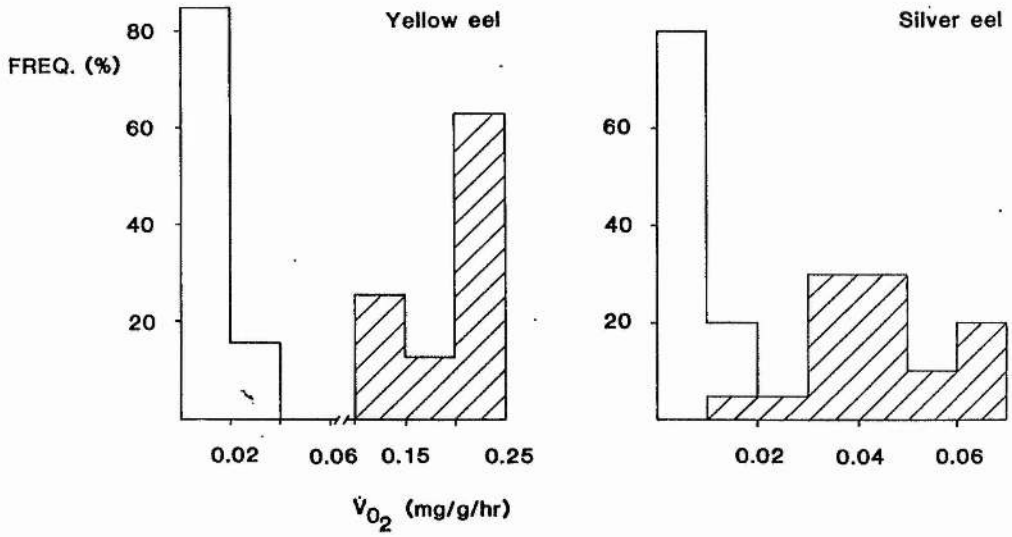
FREQ. (%)
80
60
40
20
Yellow eel
0.02
0.06
0.15
0.25
$\dot{V}_{O_2}$ (mg/g/hr)
Silver eel
60
40
20
0.02
0.04
0.06

Figs. 6.7. - 6.10. Electronmicrographs of slow fibres from temperature-acclimated elvers

Fig. 6.7. TS large fibre, showing the extensive inter-myofibrillar mitochondrial population, with regular cristae packing. Note the virtual absence of IMF lipid. Skin is at bottom, right. 10°C elver. Magnification X4760.

Fig. 6.8. TS small fibre, showing the absence of lipid and mitochondria in the inter-myofibrillar zone. The morphology is similar to that found in young fast fibres, of similar size (see Chapter 4). 10°C elver. Magnification X12,740.

Fig. 6.9. TS slow muscle capillary, supplying two fibres. Note the accommodation of the capillary by the fibre boundaries. The reported accumulation of sub-sarcolemmal mitochondria adjacent to capillaries, in mammalian muscle, is absent. Nucleus is at the bottom. Note also the improved section clarity with respect to both 22°C (Chapter 3) and 29°C elvers (Fig. 6.10). 10°C elver. Magnification X9555.

Fig. 6.10. TS fibres from 29°C elver. Note the similar morphology to that of 10°C elvers, but with a reduced mitochondrial content. Magnification X4655.

7

8

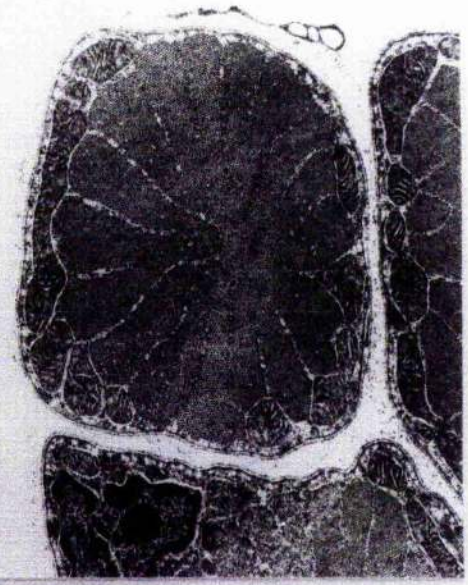

9

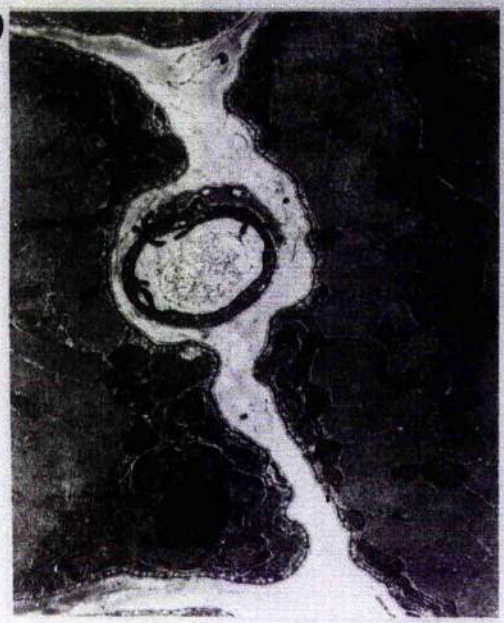

10

CHAPTER 7

INTRODUCTION

Studies on the innervation of body musculature in fish are mainly restricted to the pattern of sensory or motor endings (Bone 1964; Roberts 1969). Both fast and slow motoneurons are assumed to be present in spinal nerves, although the amount of sensory afferents (within the mixed spinal nerve or as a separate ramus) is variable, and not well documented. The importance of peripheral (sensory) innervation has not been established for teleosts (Roberts 1981).

Polyneuronal innervation of higher teleost fast skeletal muscle has been correlated with a graded recruitment of fibres, and an extended range of sustainable swimming speeds (Chapters 1 and 3). However, experimental evidence for the control of locomotion is restricted to spinal cord-spinal nerve interactions (Grillner 1975; Roberts 1981); little is known about the extent and distribution of the nerve net within trunk muscle. It is not known to what extent the complex innervation pattern, revealed by intracellular recordings, is representative of higher teleosts, No similar study is available for the focally-innervated, primitive teleosts.

The innervation pattern of fast skeletal muscle in fish has also been used as a physiological classification index (Bone 1964; Johnston 1981a). However, there is little comparative data concerning the structure of the neuromuscular junction, and the extent of pre-terminal branching is ambiguous when described by histological or histochemical means. This study investigates a number of ways in which a clearer picture may be assembled with respect to the extent of nerve branching both within, and between segments. In order to further reduce the possible ambiguity of earlier studies, using a phylogenetically diverse range of species, fast muscle from two representative teleosts were compared, showing focal (eel) and multiple (cod) innervation patterns.

MATERIAL AND METHODS

Fish

Cod were obtained from local (North Sea) fishermen and used within one week of capture. Yellow eels were caught by rod-and-line in the River Eden, Fife; little damage was done by this method and all were used within two months of capture, being maintained in filtered tapwater at 20 $\pm$ 2°C.

Tissue preparation

Two preparations were used, trunk and abdominal wall:

1) The trunk preparation was located approximately $^{2}/_{3}$ along the body, myotome number 30 to 38 in cod and 65 to 85 in eel. Dissection involves removing a fillet of muscle from the left side of the fish, approximately half the depth of the lateral muscle, before commencing fine dissection to isolate the major spinal nerves. These are referred to as the dorsal and ventral rami (DR and VR), according to their anatomical location.

2) The abdominal wall preparation was similar to that used previously for neurophysiological experiments (Roberts 1969; Hudson 1969). It consists of an excised segment (right hand side) of the fish with dissection proceeding from the medial (visceral cavity) wall; myotome number 9 to 17 in cod and 22 to 35 in eel. In this way the same aspect was preserved between the two preparations; the abdomen being more accessible for intracellular recordings and localisation of the fine nerve branches. Cod spinal nerves are relatively large, the VR being 0.5 to 0.6mm in diameter at the proximal end, allowing an easy dissection (under saline) with the aid of a binocular microscope and fibre-optic light guides. Eel nerves are more difficult to isolate, partly on account of size (VR = 0.3 to 0.4mm diameter).

This is not due to allometric differences as nerves in eel are usually $^{2}/_{3}$ the size of homologous nerves in cod of similar weight.

Dissection of small nerves in eel is hampered by extensive lipid deposits. It proved impossible to stain any but the most superficial running nerves, especially around the vertebral column, since ruptured adipocytes

deposit an impenetrable layer of lipid. A complete anatomical description was only possible during the fixation of nerves for electronmicroscopy. For optimal fixation the preparation was immersed in 2.5% gluteraldehyde during dissection; frequent rinsing was required, but the increased contrast allows complete tracts of spinal nerves to be isolated, although this required extensive dissection (4 to 5 hours). Samples were taken at regular intervals along the length, for all four preparations, and processed for electronmicroscopy (Chapter 3); semi-thin (0.5μm) sections were taken to elucidate the composition of the nerve bundle.

Electronmicroscopy

Longitudinal sections of cod fast muscle were taken from anterior (epaxial) myotomes where small-diameter, parallel-running fibres could be dissected out with ease. Samples from eel fast muscle were taken from a similar site, but the LS muscle sections concentrated on the myoseptal region, taking an oblique section of the connective tissue sheath. The myoseptum proved very fragile under the electron beam, necessitating quite thick sections (90-100nm) to maintain structural integrity. Improved quality of the image was possible using TS sections of the neuromuscular junction in elver fast muscle, sampled near the myosepta; in most cases the section plane was oblique to both muscle fibre, and myoseptum, longitudinal axes. Dimensions of neuromuscular junctions and synaptic vesicles were determined by planimetry of projected electronmicrographs, final magnification X45,000 to X63,000.

Mapping the nerve routes

The major nerve bundles, branches and individual axons were supra-vitally stained, in situ, with neutral red (0.01 - 0.02mg/ml; Stuart et al 1974) or Methylene blue (0.2 - 0.5mg/ml; Wales et al 1970), in teleost ringer. Both dyes appeared not to impair the viability of nerves, over the short incubation time (2-4 hours, 4°C), which remained responsive to

mild stimulation. Resolution of Methylene blue was superior to neutral red; staining and stabilisation protocol broadly followed that of other workers (Whiting 1948; Hudson 1969; Wales et al 1970). There are limitations, however, in that only part of the nerve mass may be visualised at any one time, since staining occurs in a progressive manner through the nerve bundle, and overstaining causes bleaching (Plotnikova 1980). Hence, the superficial and deep portions of the myotomal nerve net cannot be investigated simultaneously; nerve routes can therefore only be followed in subsequent preparations if the pattern is constant. In addition to any reduction in structural integrity of the network, due to dissection difficulties (see later), the limited penetration of stain into the muscle mass (accentuated, in the case of the eel, by lipid deposits) clearly demands an alternative method for visualising the axonal tree.

The introduction of cobalt as an intracellular marker, through the cut ends of an axon bundle (Pitman et al 1972) has proved a powerful tool for the analysis of the neural circuitry in insects and crustacea (Florey and Cahill 1982). The applicability of axonal filling to the identification of the innervation pattern in teleost trunk muscle, was therefore tested. Cut nerve ends were immersed in 6.0% $CoCl_2$, surrounded by a vaseline igloo, for 24-36 hours (under saline, 4°C) and visualised with 0.2% NH_4S. Penetration was limited to just over 1cm down the nerve. Longer incubation only marginally increased this. Filtering (0.22mμ pore size "Millipore" filter) increased the distance to 1.5 - 2.0cm, allowing the distribution pattern of the VR to be mapped by repeated fills at different levels of the nerve (Fig. 7.17). The method proved especially useful in distinguishing between parallel-running nerves, and their origins at the vertebral column. Preparations are susceptible to fading, even when stored in the dark, and small or weakly-filled axons are very difficult to see. A silver-intensification

step was therefore incorporated into the schedule (Bacon and Altman 1977; Pitman 1979). Alcohol-fixed material was generally superior to that fixed in Bouins or Formalin, supporting the contention that aldehyde-fixatives may produce a non-specific silver nitrate reduction (Bacon and Altman 1977). Intensification prevented fading of the preparations, but was prone to the same diffusion limitations as block-staining. Clearing in Canada balsam or xylene was adequate, but cedar wood oil allowed further dissection and methyl salicylate gave a superior clarity of background tissue. The method was essentially that of Pitman (1979), with incubation times doubled to allow for the greater tissue bulk.

Histochemistry

Frozen sections were used to confirm the nature of the muscle used for intracellular recordings and anatomical description. Cod fast muscle has a homogeneously anaerobic character, consisting of large diameter fibres showing a high alkaline-stable m.ATPase activity, with little or no reaction for SDH or PAS. In contrast, the eel fast muscle is composed of a mixture of small, PAS +ve fibres and large, PAS -ve fibres and, in this respect, resembles elver trunk muscle (Chapter 2). In both species no difference in histochemical staining pattern could be seen between muscle taken from the abdomen or trunk preparations.

Acetylcholinesterase activity was demonstrated by the Naik modification of Koelle's method (Chapter 2). However, this can give variable results, especially in eels where background staining is usually quite high. A number of other methods were assessed for use with fish muscle: Gomori's modification (Pearse 1972) proved to be more problematical; the "direct-colouring" copper-ferricyanide method of Karnovsky and Roots gave poor contrast, although slight modifications gave a superior differentiation of endplates, due to a reduced background stain, and could be easily applied to

frozen sections. Both micro-dissected fibre bundles and frozen sections were stained, cod and eel samples treated in parallel; a positive control was also included, using a strip preparation of Auerbach's plexus from guinea pig jejunum. In view of the difficulty of reagent penetration in eel muscle, particular emphasis was placed on the application of the method to longitudinal cryostat sections. For Koelle's method, optimal conditions were found to be:

(i) fix muscle bundle for 5 hrs at 4°C in 10% Ca^{2+}-formol, pH 6.5

(ii) wash overnight (~12 hrs) at 4°C, using 0.1N phosphate buffer, pH 6.5. This is most important, as aldehyde fixatives interfere with the reaction.

(iii) frozen tissue blocks are prepared (Chapter 2) and thick, 18µm sections collected on subbed coverslips, prepared by dipping very clean coverslips into a warm (60°C) solution of 1% gelatin + 0.1% chrome alum in 30% alcohol for a few seconds, and draining in a warm place.

(iv) Incubation commences immediately in freshly-prepared medium, at room temperature: dissolve 100mg acetylthiocholine iodide in 4ml d.H_2O; add 7ml 0.1M Cu $SO_4.5H_2O$ dropwise, with stirring; centrifuge at 600g for 15 mins. to remove the precipitate; add 62.5mg glycine $10ml^{-1}$ of supernatant; adjust pH to 6.0 with 1.0M sodium acetate, just before use; adjust to final volume with d.H_2O, 35ml being sufficient for 2 or 3 small coplin jars.

(v) Rinse thoroughly in buffer, followed by d.H_2O; clear in glycerol and mount individual fibre bundles in glycerol-gelatin directly. Preparations should be examined, and pictures taken, the same day as section quality deteriorates noticeably within 24hrs.

For the direct-colouring method, the protocol is the same up to stage IV, thereafter:

(iv) Freshly-prepared incubation medium includes 10mg acetylthiocholine iodide in 13.0ml 0.1M phosphate buffer, pH 6.0; add, in order, 1.0ml 0.1M sodium citrate, 2.0ml 30mM $CuSO_4$, 1.0ml distilled water or 1M eserine sulphate (inhibitor), and 1.0ml 5mM potassium ferricyanide.

(v) Prepare slides as per stage (v) of the modified Koelle's method.

Intracellular recordings

Standard neurophysiological apparatus was used to record spontaneous VR activity, using small diameter hook electrodes placed under a proximal region of the nerve, 0.5 to 1.0mm separation, after careful dissection of connectives. Electrodes could also be used in a stimulus mode; the preparation was immersed in refrigerated (10 to 12°C) teleost ringer of composition:

142mM NaCl
2.7mM KCl
0.45mM $MgCl_2$
10mM $NaHCO_3$
3mM NaH_2PO_4
2.6mM $CaCl_2$

pH 7.4, aerated with 95% O_2, 5% CO_2.

Glass micropipettes (average resistance 25MΩ in 3M potassium acetate were used) to record intracellular potentials. Potassium acetate was used to obviate any Cl^--dependant hyperpolarisation artefacts. Signals from micropipettes and electrodes were displayed simultaneously on an oscilloscope and recorded either by direct printing on Kodak positive roll-film, or photographing individual frames on Ilford FP4. Recordings were restricted to fibres located at the point of forward inflexion of the myotome, from fibres less than 3 or 4 in depth. Endplate potentials were also recorded from both intact and de-afferent (transected VR) myotomes, from either whole-body segments or a finely dissected sequence of hypoxial myotomes. Experiments lasted 4 to 6 hours after initial dissection.

RESULTS

Gross Morphology

The distribution of ventral and dorsal spinal nerves, and major branches, to fast skeletal muscle is illustrated for both the abdomen and trunk (Figs. 7.1 - 4). Diagrams are composed of camera-lucida tracings, using results obtained from 6 cod and 7 eels, 2-4 preparations per fish. Weight and length were 592.7 $\pm$ 186.7g, 35.9 $\pm$ 4.0cm and 239.7 $\pm$ 162.2g and 51.3 $\pm$ 10.9cm ($\bar{x} \pm$ S.D.), for cod and eel respectively. Major trunk nerves run deep, to a varying extent, and close to the vertical septa; the more superficial abdomen VR were used to record the more common patterns of nerve branching (Figs. 7.5,6). The path of a spinal nerve branch is much more tortuous than suggested by a 2-D tracing. In cod this makes following a particular branch difficult as it often disappears into the myotome and divides, one part then re-appearing at a superficial level. In eel, the branches either proceed directly to the myosepta, or ramify to deeper regions of the muscle.

In the eel trunk there is little evidence of cross-innervation between myotomes, except at the most proximal (vertebrae) and distal (fin) ends where branches from adjacent rami are interconnected (Fig. 7.1). The dorsal spinal nerve (DR) is composed of a major bundle and 2 smaller, parallel running nerves supplying the myotomal caudal to their origin. The VR is restricted to the segment of origin. In cod trunk intersegmental passage of nerve bundles is common, although the extent is masked by the dissection procedure. Both DR and VR supply the myotome caudal to their origin, with smaller branches running along the rostral edge of the original segment (Fig. 7.2). Extensive connection between adjacent rami occurs at both proximal and distal ends, forming a more complex network of small branches than found in eel.

Eel abdominal spinal nerves appear to follow a pattern similar to that of the trunk, although the restricted distribution of the VR branches is more evident (Fig. 7.3). Both preparations show a correlation between the path of major nerve branches, and the largest (pigmented) blood vessels. Around 75% of all VR branching is orientated rostral with relatively large branches traversing the myotome, invading muscle close to the more caudal myoseptum (Fig. 7.3); only one small branch was found within an adjacent myotome (Fig. 7.5). Cross-innervation between myotomes is widespread in cod CR, and is clearly illustrated in the abdomen (Fig. 7.6). Only one branch was seen to invade a sub-adjacent myotome; whether this is an accurate reflection of the lateral extent of the nerve net, or merely due to the limited penetration of cobalt, remains to be clarified. The VR innervates the segment of origin (similar to eel) and traces an oblique path across the myotome. An extensive network of small and large branches is present, with a higher density appearing on the rostral side of the myotome (Fig. 7.4); the larger branches supplying deep muscle appear to sprout mainly to the caudal part of the myotome (Fig. 7.6).

Quantification of myotomal branching pattern is only possible with unequivocal localization of axons; the cobalt preparations identify superficial-running axons of the nerve net (Fig. 7.16), although the limited migration restricts its use to shorter, atypical branches. This may be improved by filling small branches and/or applying extracellular current pulses. However, the tortuosity of axon routes makes an absolute count of branch points extremely difficult, if not impossible. The results intra-cellular marking is similar to the pattern of vital dye staining (Methylene blue) (Fig. 7.15); both are applicable only to the more superficial muscle layers. Here, cod fast muscle is innervated by an extensive network of multi-branched nerves and axons (Figs. 7.15 and 7.16). However, removal of the tough, triple-layered abdominal wall connective tissue is difficult without damage to the underlying

nerve net, as can be seen by staining the discarded material. It is unlikely, therefore, that this approach can be used to quantify the amount of axonal division within a myotome (cf Hudson 1969). Eel muscle is rarely stained other than at the myoseptal ends. Although intra-specific differences in the gross organisation of the nerve net are small (within each preparation), a complete map of the "axon tree" can only be derived from an individual preparation.

Light microscopy

Elver spinal cord represents the typical teleost pattern with prominent grey and white zones, the development of ventral horns and a distinct pia mater/dura mater covering (Fig. 7.11 ; see Kappers et al 1967). The dorsal root emerges slightly caudal to the ventral root (Fig. 7.11); this displacement is only minor, since both roots may be sectioned simultaneously (Fig. 7.12). The roots join via segmental ganglia (Fig. 7.11) to form mixed spinal nerves. Semi-thin sections show a single spinal nerve going to each quadrant of the body, with a series of smaller nerve bundles appearing at the fin bases and adjacent to myosepta. The lateral line nerve (cranial nerve 10) has no connection with any of the "myotomal" nerves.

Branching of spinal nerves was examined in muscle LS semi-thin sections (100 x 0.5µm). In eel, most branches contain 7-9 axons, and only infrequently split into smaller units. No evidence of axon division could be seen. In cod, there are two broad categories of branches within the muscle, one containing 10 to 20 axons (mean = 15), the other 3 to 6 axons (mean = 5). A progressive reduction in the number of axons/bundle is seen with increasing distance from the spinal nerve. Axon division is seen in smaller bundles, e.g. a bundle of 3 axons may divide into 2 bundles, each containing 3 axons

Although division is not usually so regular, it may occur twice along a bundle, thereby removing any possible artefact of cutting direction.

In contrast to eel, where most nerve profiles run parallel or oblique to the muscle longitudinal axis, the nerves in cod have many orientations, with a large proportion running across the fibre axis.

Cod spinal nerves run in close proximity to the myosepta (in trunk, and distal regions of abdomen) but remain quite separate (Fig. 7.24); large nerves usually have their own blood supply, distinctly visible in vivo. The composition varies between VR branches, differences originating at the vertebral column. Mean axon diameters are around 2 and 12μm (Fig. 7.26); only minor differences are found between the two preparations, e.g. trunk motor axons have 2 modes at 5-6μm and 10-12μm diameter (Fig. 7.25). In electron micrographs, the small diameter, densely-staining axons of semi-thin sections have a much thinner axon wall (myelin sheath) and are bounded by cell bodies. These tend to be grouped within the main, and subsidiary branches (Fig. 7.24A,F); they run as a homogeneous nerve only in a few myotomal branches (Fig. 7.24G,H). The smaller members of the thick-walled population are probably slow motor efferents (see Barets 1961; Roberts 1969). In contrast, the organisation of eel nerves is much simpler, an even division of the nerve bundle giving rise to 2 VR (Fig. 7.8), resembling the rostral branch of cod VR. There are fewer densely staining, small axons; motor axons have a unimodal distribution and a smaller mean diameter $\sim$ 8μm (Fig. 7.25). The small size of eel nerves and the length of time required for dissection, reduces the clarity of sections when compared to cod. The composition of major nerves varies little, both with respect to the position within the myotome, and origin (Figs. 7.9, 10), whereas in cod there is significant regional variation (Fig. 7.24). Both species show a slight reduction in total axon number between abdomen and trunk, with cod having a smaller number of motor axons, but many more sensory axons in the VR, relative to eel (Fig. 7.25, 26).

Histochemistry

Staining for acetylcholinesterase (AChe) activity on frozen sections is illustrated (Figs. 7.13, 14 ; see also Figs. 2.25 and 2.26). Published methods often use low pH 5.2 which is known to inhibit esterase activity (Pearse 1972; Bancroft and Stevens 1977); a superior resolution is obtained with fish muscle using a shorter incubation at pH 6.0. Cod fast fibres have a large number of endplates/fibre, as seen in both whole muscle preparations and frozen sections (Fig. 7.13), confirming an earlier study (Altringham and Johnston 1981; Table 7.2). Masking of the reaction site by lipid in eel muscle (see above) is reduced by the use of frozen sections, but background staining of the myoseptum makes differentiation difficult; this is compounded by the numerous melanophores and axons that run within, or adjacent to, the myoseptum. In elvers most fibres stain only at one end, the largest percentage being at the rostral edge of the myotome. In both yellow eels and conger eels an alternating pattern of stained and non-stained fibres appear along the myosepta. Resolution of more than 1 pre-terminal axon was not possible, in any preparation.

Electron microscopy

Similar endplate morphology is found in eel and cod (Fig. 7.22 ,23). Usually, endplates appear as a single profile beneath the basal lamina; 2 or 3 profiles may be seen within a short (1μm) distance of each other (eel), or as a cluster (cod). Average depth and width of endplates in elver and cod are similar: 0.85, 1.47μm and 0.64, 2.60μm, respectively; those in yellow eel are larger: 1.39, 3.9μm. The lateral extent is usually ~ 2 or 3 sarcomeres, occasionally longer in eel. Poorly developed subjunctional folding is present in cod, but absent in elvers and eels where endplates are closely associated with the myoseptal invaginations (Fig. 7.22, 23). Most synaptic vesicles are of the electron-translucent type; occasional dense-cored vesicles (DCV) can be seen, with a greater frequency of slow, relative to

fast muscle endplates. A single population of vesicle size is present in both species, with mean diameter around 22 to 25nm (Fig. 7.28). There is no evidence of dual innervation, either by the presence of more than one axon/endplate (Best and Bone 1973), or by the presence of a double-endplate with distinct vesicle sizes (Bone 1972).

Intracellular recordings

Spontaneous discharges are recorded from VR whilst still attached to the spinal cord, for up to 1 hour post mortem. Occasionally these action potentials can be correlated with muscle fibre junction potentials, although spontaneous contractions (especially in eel) makes statistical analysis difficult. The nerve remains responsive to stimuli for many hours after endogenous activity has become quiescent. Miniature endplate potentials (MEPPs) and endplate potentials (EPPs) can be recorded from most fibres (Fig. 7.21), although this activity is reduced on isolation of the preparation from the vertebral column, and shows a reduction in amplitude with age of the preparation. Cod shows a qualitatively similar picture to Myoxocephalus fast muscle (see Hudson 1969), with junction potentials (JP) being recorded, at varying stimulus strengths, from fibres up to 2 myotomes distant from the stimulated VR. The threshold for fibre action and junction potentials are very close, making JP summation difficult to analyse. In most fibres (n=15) 2-3 classes of JP were visible (3-15mV), with 5 classes found in 2 other fibres. Common JP were recorded in adjacent fibres and from fibres in separate myotomes. No attempt was made to further quantify the extent of polyneuronal innervation. No JP summation could be found in eel muscle (n=12), nor any common stimulus response (n=8). MEPPs and EPPs could be recorded (Fig. 7.21), the size of which appears to vary along the fibre length. The presence of maximal and minimal EPP sizes at the fibre ends suggests a single, focal innervation point. Resting membrane potentials were similar in the two

species, -57.0 and -54.0 mV for cod and eel, respectively (Fig. 7.27). Interestingly, both muscles show a bi-modal distribution of values, with a minimum between -50 and -55 mV; it is probable that the lower values represent damaged fibres or poor impalements, and recalculation of mean values from fibres with RP > -50 mV gives values of -62.2 and -58.3 mV (Table 7.27).

DISCUSSION

It is known that a single axon in polyneuronally innvervated mammalian muscles may branch up to 50 times to different fibres (Young, 1969); a similar magnitude may be expected for fish muscle. The majority of fine branching occurs lateral to the VR in cod, with subsequent reflexing of axons to the mid-myotome regions. Muscle is therefore not innervated by axons sprouting individually from the VR but by subdivision of intramuscular bindles, distributing axons over a large area of muscle. It should therefore be possible to delineate the motor unit, using fine-dissection cobalt-fills for detailed maps, for electrophysiological characterisation. The branching pattern is good (anatomical) supportive evidence for the polyneuronal, multiterminal innervation proposed for cod fast muscle on the basis of histochemistry (Altringham and Johnston 1981; this study). In the similarly innervated sculpin the VR is thought to pass within the myoseptum for most of its length, especially within trunk myotomes (Hudson 1967), as assumed for other species (Barets 1961; Bone 1963; Best and Bone 1973; Bone 1978); also, no evidence could be found for branching. Cobalt-filled Myoxocephalus VR clearly show a myotomal, branched pathway (pers. obs.), underlining the need for accurate anatomical description prior to physiological investigation. The central position of cod VR will produce an overlap between rostral and caudal branches of adjacent spinal nerves; the similar intracellular data to that found in Myoxocephalus suggests that excitation will initiate contraction, to varying extents, in 3 to 5 myotomes. In contrast, eel VR branching patterns suggest a more well-defined motor unit, and the ability to contract individual myotomes.

The low frequency of sensory axons in eel VR is in agreement with the limited amount of sensory afferents found in teleosts (Kappers et al 1967; Roberts 1981), although cod VR has a large, distinct sensory population.

This contrasts with the findings of Roberts (1969) who described the sensory bundles as a separate ramus of cod VR; it is clear that classification as a separated or mixed spinal nerve depends on sample location. It had been thought (Roberts 1965) that the presence of separate motor and sensory bundles is correlated with the absence of proprioceptive endings within fish muscle, giving no a priori reason why the VR should be mixed (as it is in mammals). The exception, Raja, does have sensory endings in the musculature (Roberts 1969). However a related species, Torpedo, has a similar (sensory) innervation (Bone 1964) and has 2 (mixed) rami (Roberts 1969) with a composition similar to that found in catfish and tench (focally- and multiply-innervated teleosts, respectively, see plates in Barets 1961 and Roberts 1969). The similar results of this study suggest this pattern is more widespread than previously realised.

In both cod and eel VR there is a progressive reduction in axon number, proximal to distal (Figs. 7.24); in Myoxocephalus the abdomen VR declines from 781 to 153 axons, with a similar distribution over the 1 to 18μm diameter range (Hudson 1967). The number of motor axons in a VR is related to the extent of axonal branching, and size of the motor unit. For example, the density of endplates in multiply-innervated muscle (Chapter 1) means that a similar motor unit size to that found in focally-innervated muscle will require around a 20-fold increase in branching, if there is 1 axon/end plate (Hudson 1969), although less if pre-terminal branching occurs (Altringham and Johnston 1981, Fig. 7.14). The motor unit, calculated as N° of fibres/ No. of axons, is thought to be very large in Myoxocephalus (~12 per abdominal myotome, Hudson 1969) although smaller in dogfish (50-100 fibres, Bone 1978); the corresponding number of axons/VR is 306 vs 360. Data from cod (~100 axons/ VR) and eel (~130 axons/VR) also suggests that polyneuronal, multiterminal innervation results in larger motor units, and a considerable degree of

branching and may explain the larger size of axon found in cod (Table 7.3).

The small, electron-translucent nmj vesicles are similar to those containing acetylcholine found in mammals (Heuser and Reese 1977), frog (Elmqvist and Quaster 1965), and crustacean (Florey and Cahill 1982) skeletal muscle; the apparently random quantal events recorded near synapses (Fig. 7.21) are known to be due to the release of transmitter from single vesicles (Elmqvist and Quaster 1965; see Heuser and Reese 1977). The modal category for cod and eel is at the lower end of the range in vertebrate nmj's: 20-60nm (Birks et al 1960), 30-50nm (Conteaux 1972), 40-50nm (Best and Bone 1973), and 25-50nm (Ono and Poss 1982). The two (separate) populations in dogfish nmj's, 50 and 100nm diameter, are similar to those of lamprey slow muscle (Terävåinen 1971). The larger, electron-dense cored, vesicles may contain noradrenaline (Anderson et al 1963; Heuser and Reese 1977); DCV's are rare in teleosts (Best and Bone 1973; Bone 1978) and Myxine (Jansen et al 1963), and their precise function is unclear (Bone 1972). Some "false transmitters" are oxidised by EM aldehyde fixatives, giving a mixed clear and DCV population e.g. rat vas deferens (Heuser and Reese 1977), which may explain their distribution in fish muscle. Little structural difference is visible between cod and eel endplates, apart from the poorly developed SJF; these are not present at all in most teleosts (Nishihara 1967; Best and Bone 1973), with the exception of swimbladder muscles (Ono and Poss 1982).

In the work on swimming pattern generation (Grillner 1975; Roberts 1981) there is nothing to suggest the redundancy of peripheral inhibition. Indeed, the habituation of lamprey fin muscle motoneurons is mediated by inhibitory interneurons, and display depolarising EPP's (IPSP's) on stimulation of ipsilateral skin (Birnberger and Rovainen 1971). In some fibres a small (0.5mV) hyperpolarising membrane potential is recruited before the first (depolarising) function potential; this is phase-locked to the stimulus

(5-10msec latency) and can be recorded from adjacent fibres within the same myotome, but not from fibres in different myotomes (pers. obs.). However, the mechanism of inhibition is not clear for skeletal muscle, since recurrent inhibition cannot be demonstrated in the VR (lamprey) Teräväinen and Rovainen 1971). Likewise, the presence of dual innervation (dogfish, Bone 1972; conger eel, Best and Bone 1973) is inexplicable on the basis of present knowledge. A possible mechanism may be if one endplate is able to inhibit vesicle release in the adjacent endplate, then no muscle hyperpolarisation need be recorded. As function is not synonymous with morphology, the cluster of (similar) endplates in cod may have a parallel function to those in eel.

The distribution and variety of innervation patterns has only recently been subjected to an extensive systematic survey: multiple (en grappe) innervation may have arisen independtly on several occasions during the radiation of fishes (Bone and Ono 1982). A taxonomic transition group (Stomiiformes) has a unique mixture of terminal and distributed innervation, and some teleost orders have examples of focal or multiple innervation in the fast muscle of different species. It has been assumed that the innervation pattern of primitive teleosts resembles that of urodela amphibia, where each fast fibre receives two axons, forming a single motor endplate at either fibre end (Fatt and Katz 1951; Barets 1961; Bone 1964; Bone and Ono 1982). In contrast, focal innervation at one myoseptal end has been proposed for hagfish (Jansen et al 1963), dogfish (Bone 1972) and conger eel fast muscle (Best and Bone 1973; see Table 7.2). The low resolution of AChe staining at eel (this study) and catfish myosepta (see Barets 1961) may give equivocal results, although alternating stain deposits suggests innervation occurs at only one fibre end in Anguilla (this study) and Conger (Best and Bone 1973).

Multi-terminal innervation may be present as an adaptation for rapid tail-beat frequencies (Chapter 3). This requires many closely-spaced endplates in order to excite a fibre faster than a single endplate, producing an action

potential, due to junction potential decrement. This is also reflected in the large space constant (~3.1mm), almost a third of the fibre length (Hudson 1967). The non-overshoot depolarisation (Chapter 1) may provide economies in sarcolemmal ion transfer, as contraction is not solely dependant on propagated action potentials (Hudson 1969). However, there would appear to be little difference in total ion flux, as shown by the similar RP of eel and cod fast muscle (-58.3 and -62.2mV, respectively). These are much lower (closer to zero potential) than found for dogfish (-85.2mV, Stanfield 1972) or Myoxocephalus (-75.3mV, Hudson 1969), but similar to that for snakefish (-65.7mV, Takeuchi 1959) and conger eel (-54 to -65mV, Hudson 1967). The extra myofibrillar mass accommodated in focally-innervated fibres has likewise been considered an adaptation for rapid swimming, fulfilling the large power requirement (Best and Bone 1973). This would appear to outweigh the disadvantage of an increased time for action potential propagation. The limiting factor in speed of contraction would therefore appear to lie within the fibre (membrane conductance), and not in nervous transmission. Eel VR contain mostly large diameter axons similar to those responsible for initiation of action potentials in both frog and fish fast fibres, smaller axons producing the slow muscle function potentials (Barets 1961; Bone 1978). Frog fast muscle is innervated by axons 10-12μm in diameter, conducting at 20-35m/sec and slow muscle by axons 5-8μm diameter, with a conduction velocity of 2-8m/sec (Prosser 1973). This is slightly quicker than the fast motor axons in Myoxocephalus (10-14μm diameter; 17-24m/sec at 10-12°C, Hudson 1967) and tench (13μm diameter; 15-24m/sec at 22°C, Barets 1961). Mammalian axons of comparable diameters conduct around 3 times this velocity (Bullock and Horridge 1965).

Development of the advanced innervation pattern may have been for efficient low-speed swimming, rather than the infrequent burst-swimming. Junction potentials may cause partial activation of the fast muscle, in

order to overcome the passive resistance against which slow muscle has to act during sustained swimming. Indeed, the consideration of contraction velocity as a limiting step in muscle physiology may be superfluous, in view of the near-isometric nature of contraction in fish muscle (Johnston 1982c) and the low conduction velocity of the nerves (see above). Also, V_{max} of dogfish skeletal muscle fibres is twice that of cod, although the latter may swim much faster (Altringham and Johnston 1982).

There are, then, many similarities between cod and eel; the type of innervation pattern being determined by both the body form and nature of the generated swimming pattern. The direct (cod) and indirect (Myoxocephalus) evidence for cross-innervation suggests that this may be widespread among the higher teleosts, although the functional consequences are only now becoming clear. It has been pointed out that in Myxine, where axons from one VR innervate adjacent myotomes, it would be difficult to contract myotomes individually (Bone 1963); a situation greatly exaggerated in cod. The restricted influence of eel VR would facillitate the sequential contraction of myotomes. This will result in a more coarse control over the form of the locomotory wave passing down the body in cod, relative to eel. It would appear, therefore, that cod has sacrificed the fine control over body contraction for economies in both the initiation of fibre contraction, and the recruitment of motor units, such that energy expenditure is minimal at intermediate swimming speeds. Species that use predominantly tail-propulsion (cod, salmon) represent an intermediate form between the extreme eel- and tuna-like locomotion; propulsive force is delivered from a stiff (though not rigid) body to the caudal fin. A complete cross-section of the cod trunk will only shorten if 4 to 5 adjacent myotomes are simultaneously contracted (Wardle and Videler 1980). Any TS section adjacent to this will only be partially contracted. This smooth transition from a relaxed to contracted state would require a very complex

arrangement of nerve-muscle control if the myotomes were not of a staggered form (Willemse 1966). Anguilliform locomotion requires the fine control over body curvature presumably given by 1:1 innervation of the myotome. The relatively small number of sensory axons in eel spinal nerves suggests that monitoring skin deformation plays a minor role in locomotry co-ordination, reflecting the limited amount of sensory feedback required for the generation of a swimming pattern in anguilliform fish (Gray 1936; Grillner 1975; Roberts 1981). In contrast, cod may rely heavily on afferent (cutaneous) stimuli for modification of the central pattern generator (Wardle and Videler 1980; Videler 1981) in addition to the facilitation required from the brainstem (Grillner 1975). Monosynaptic endings of sensory afferents on motoneurons has only been shown to occur in rays, but not in teleosts (see Roberts 1981). However, the recent demonstration of proprioceptive endings beneath the stratum compactum of chain pickerel (Esox niger (Ono 1982) suggests that these findings should be reviewed. This worker was unable to demonstrate continuity with spinal nerve afferents, although it should be possible with a cobalt-fill preparation; many other assumptions inherent in earlier work may also now be tested.

TABLE 7.1. Composition of the ventral ramus of fish spinal nerves; division into 1 or 2 separate rami

CLASS	GENUS	1	2	REFERENCE
AGNATHA	Myxine	+	-	Peters 1963
	Petromyzon	-	+	Goodrich 1930
	Lampetra	-	+	Whiting 1948
CHONDRICHTHYES	Scyliorhinus	-	+	Roberts 1965
	Mustelus	-	+	Roberts 1969
	Squatina	-	+	-"-
	Squalus	-	+	-"-
	Galeorhinus	-	+	-"-
	Torpedo	-	+	-"-
	Raja	+	-	-"-
OSTEICHTHYES	*Latimeria	-	+	Millot and Anthony 1966
	Acipenser	-	+	Troitzky 1929
	Anguilla	+	-	This study
	*Ameiurus	+	-	Barets 1961
	*Tinca	+	-	-"-
	Callionymus	-	+	Roberts 1969
	Lophius	-	+	-"-
	Trigla	-	+	-"-
	Myxocephalus	+	-	Hudson 1967
	Gadus	-	+	Roberts 1969
	Gadus	+	-	This study

Note: * = deduced from plates presented in the study, not stated.

TABLE 7.2. A comparison of the various schemes proposed for the innervation pattern of fast muscle in a range of fishes.

SPECIES	INNERVATION PATTERN				REFERENCE
	Polyneuronal	Distributed	Focal(1)	Focal(2)	
Agnathans					
Hagfish	-	-	+	-	1
Lamprey	+	-	-	+	2
Elasmobranchs					
Dogfish	-	-	-	+	3
Primitive teleosts					
elver, yellow eel	-	-	+	-	4
conger eel	-	-	+	-	4
"	-	-	-	+	5
herring	-	-	+	-	5
catfish	-	-	+	-	5
"	+	-	-	+	6
Higher teleosts					
snakefish	+	?	-	-	7,8
tench	+	+	-	-	6
sculpin	+	+	-	-	9
cod	+	+	-	-	4,10

Note: Polyneuronal innervation refers to individual muscle fibres receiving terminations from more than one axon, of different origin; distributed innervation refers to the termination of more than one fibre, by an individual axon; focal innervation (1) refers to the presence of a single axon, at one fibre end making a motor termination; focal innervation (2) refers to the presence of 2 axons at the fibre end (dogfish), or innervation at both ends by a single axon (catfish, lamprey). For comparison, frog sartorius muscle has this latter form of innervation (Fatt and Katz 1951).

Although the results are taken from direct observations, there is some discrepancy among workers (e.g. catfish). It should be noted that different experimental techniques have been used: intracellular recordings, histology, histochemistry, electronmicroscopy and supravital staining. The technical difficulty of such studies is emphasised by the differing schemes proposed by an author at different times (contrast Bone 1964; Best and Bone 1973; Bone and Ono 1982).

References: 1. Jansen et al 1963; 2. Teräväinen and Rovainen 1971; 3. Bone 1972; 4. this study; 5. Best and Bone 1973; 6. Barets 1961; 7. Takeuchi 1959; 8. Nakajima 1969; 9. Hudson 1967; 10. Altringham and Johnston 1981.

TABLE 7.3. Number and size of axons in teleost VR.

SPECIES	PREPARATION	MOTOR AXONS		SENSORY AXONS	
		Number	diameter (μm)	Number	diameter (μm)
Anguilla anguilla	abdomen	134	8	90	1.6
	trunk	104	8	55	1.2
Gadus morhua	abdomen	94	13	1181	3.5
	trunk	99	12	998	1.9

Note: The function of the axon categories is assigned using anatomical criteria (see Barets 1961; Prosser 1973), no electrophysiological data being available. They are, therefore, strictly "presumptive motor" and "presumptive sensory" axons. For distribution and confidence limits, see Figs. 7.25 and 7.26 .

Fig. 7.1. Eel trunk, composite of camera lucida tracings of cobalt-fills. Each spinal nerve is seen to originate in a mid-myotome position, but quickly follows the myosepta (MS) whilst at all times remaining separate from the connective tissue sheath. Blood vessels (BV, stippled) traverse a number of myotomes, giving off branches in a regular pattern; distal sprouting of the DR and VR is most closely associated with BV as they innervate the fin musculature (F). A fine nerve branch (N) runs dorsal to the vertebrae, interconnecting the segmental nerves. The DR is seen to be composed of two major branches, which innervate the my tome caudal to their origin. Again, distal sprouting is associated with the innervation of the fin, forming an interconnecting network. A rostral branch of the VR is destroyed during preparative dissection, and it is unclear whether this runs laterally (innervating both fast and slow muscle as suggested by Barets, 1961, for catfish) or along a similar course to the major VR branch, at a more superficial position.

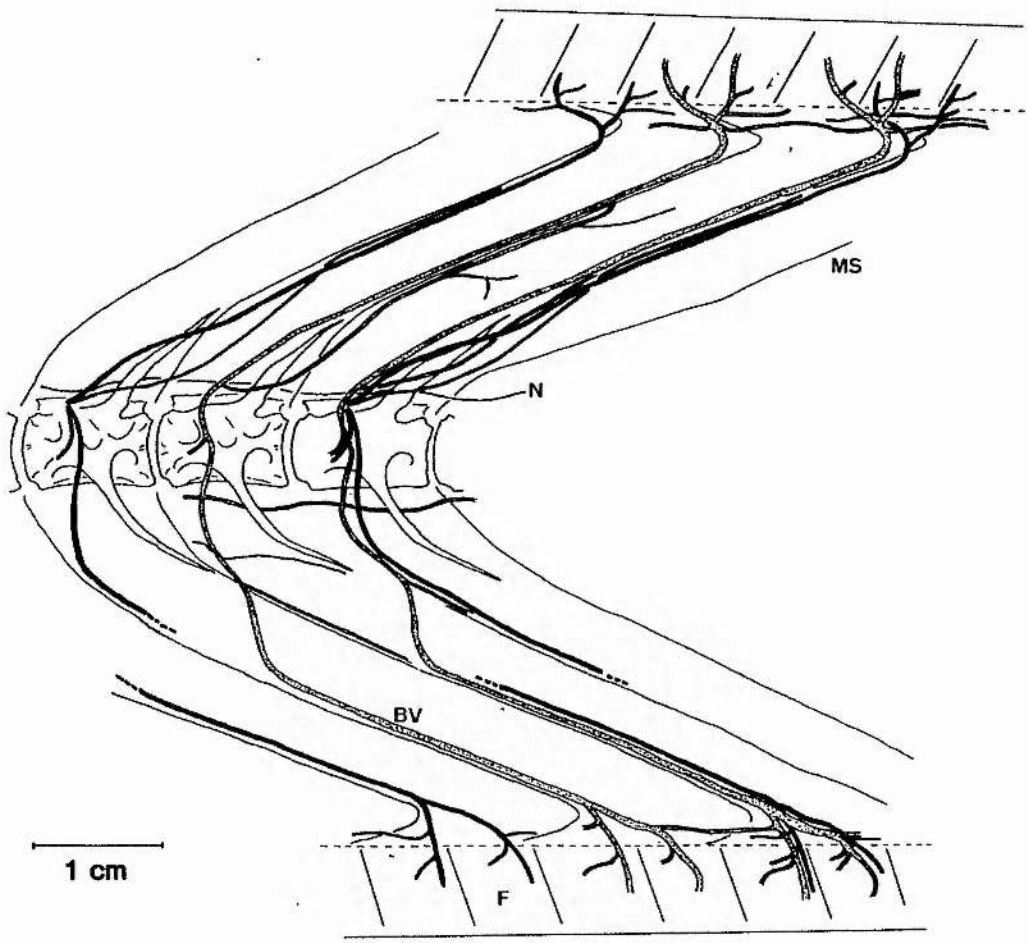
MS
N
BV
1 cm
F

Fig. 7.2. Cod trunk, cobalt fills. The pattern of both VR and DR nerves is much more complicated than in eel. The VR sends two branches to the rostral edge of the myotome of origin, with the major branch traversing the segment to run along the rostral edge of the adjacent (caudal) myotome. Minor branches are seen to invade the mid-myotome region, and to connect adjacent VR at the level of the vertebrae. Distal branching is again responsible for fin (F) innervation, and the construction of an intersegmental network. The DR follows a similar pattern to that in eel, but with the addition of a major (rostral) branch to the myotome of origin, and a large number of fine connectives. Both DR and VR contain at least 3 separate nerve bundles.

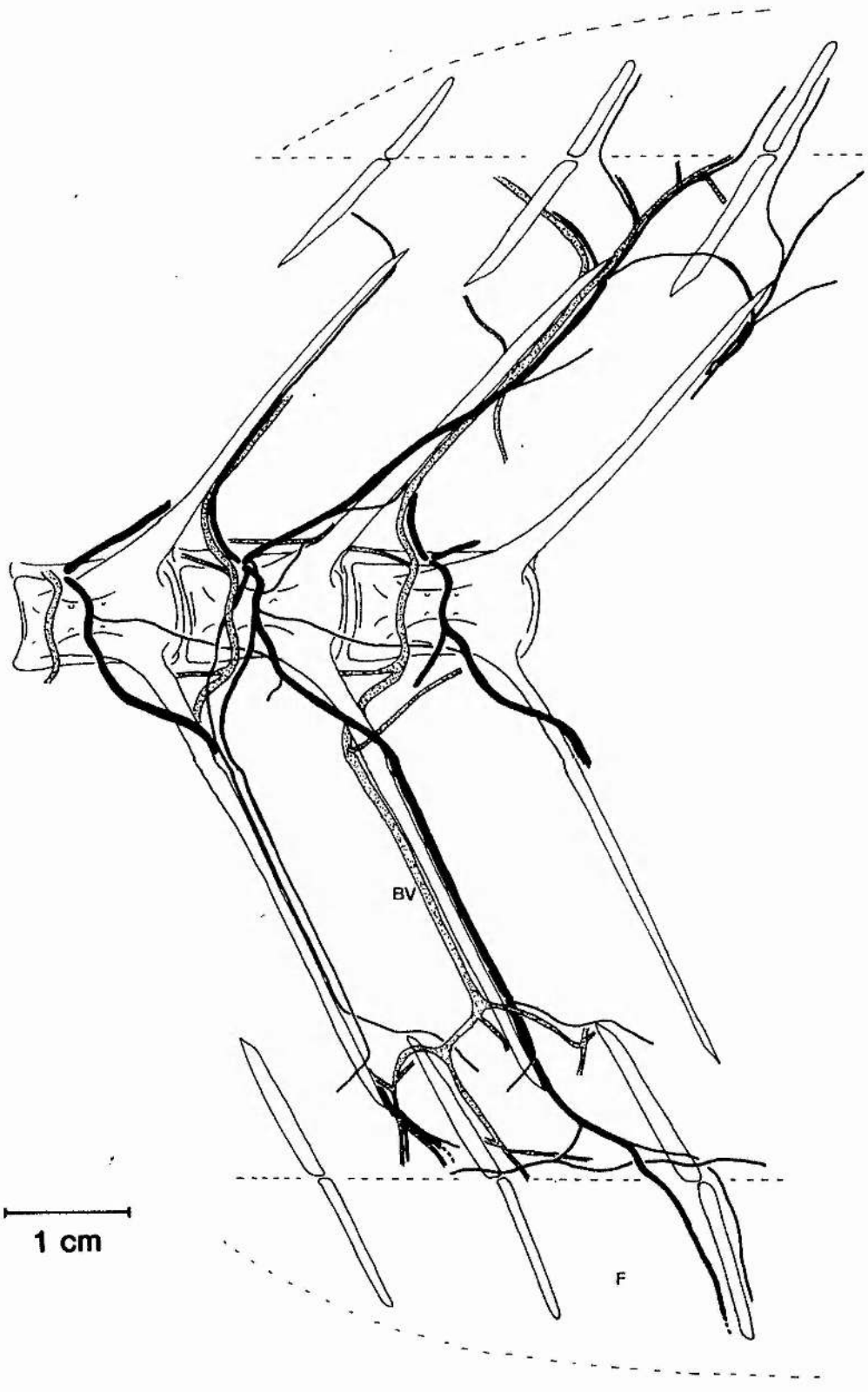
BV
F
1 cm

Fig. 7.3. Eel abdomen, cobalt-fills of VR. The origin of the spinal nerve is seen to be similar to that in the trunk, but follows the myoseptum at a greater distance away from the myotomal edge. Many of the branches follow the regular pattern of BV, although this relationship is lost in the distal regions where BV branching becomes less predictable. Note that all visible branching is confined to one myotome; the majority appear rostrally and can be seen to reflex in order to innervate the deeper regions of the myotome. Occasional large VR branches traverse the myotome and run down the caudal myoseptum.

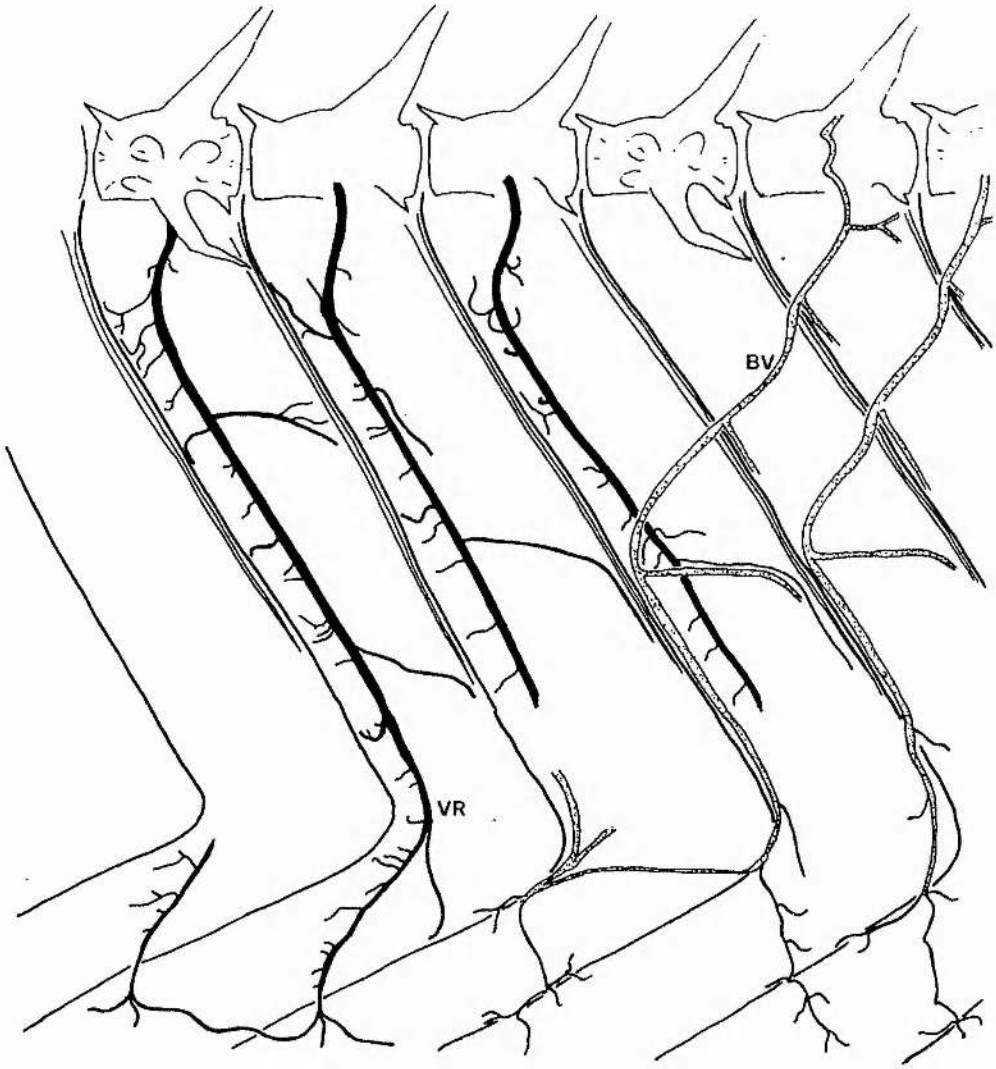
BV
VR
1 cm

Fig. 7.4. Cod abdomen, cobalt fills. The origin of the VR is again mid-myotome, but in this case only gradually traverses the myotome before following the myoseptum (ms) after the rostral inflexion of the myotomes. Again, the major branches follow blood vessels (BV). However, a much more even frequency of branching is found rostral and caudal to the VR, many of which invade adjacent myotomes, although the main VR is confined to the myotome of origin.


VR
BV
MS
1 cm

Fig. 7.5. Outline of the major nerve routes in eel trunk (left) and abdomen (centre) preparations, as revealed by cobalt-fills. The letters refer to the position of sampling for semi-thin sections; abbreviations on the orientation grid are a = anterior, p = posterior, d = dorsal, v = ventral. The camera lucida tracings on the right are two examples (different fish) of the variation in VR branch pattern within abdominal myotomes; whole-mount preparations, cedar wood oil cleared. Myosepta are denoted by the parallel lines (to scale) and the numbers refer to counts made of the numbers of muscle fibres visible at the surface of the myotome. The bottom tracing is of the only example of a VR branch found to appear in an adjacent myotome, in any preparation of eel nerves.

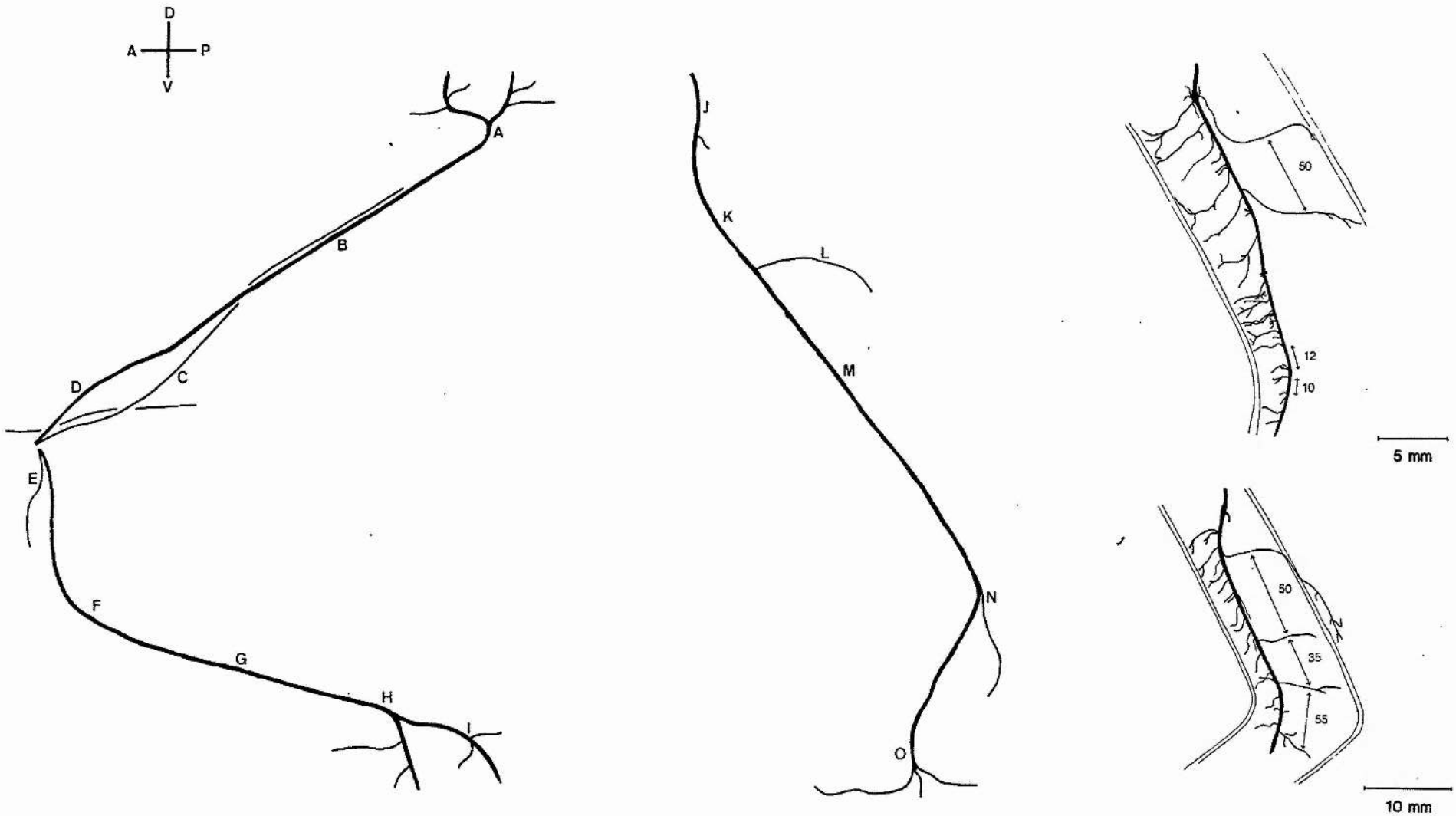
D
A
P
V
A
B
C
D
E
F
G
H
I
J
K
L
M
N
O
50
12
10
5 mm
50
35
55
10 mm

Fig. 7.6. Similar presentation to Fig. 7.5, for cod trunk (left) and abdomen (centre) preparations. Tracings 1. and 2. refer to the variability of the first major branch (N) in the VR, which invades the deepest portion of the fast muscle. The degree of bifurcation varies between myotomes and individual specimens, with some smaller branches reflexing from the caudal sprouting position to innervate the muscle at a rostral position (2.). Tracing 3. (with fibre outlines superimposed) details the amount of branching, at a position between N and O, which is seen to result in a preferred orientation parallel to the muscle fibres. Tracings 4. and 5. detail the second major caudal branch (P), illustrating the lateral extent of subsidiaries; some may invade adjacent myotomes (4.) or innervate the proximal regions of the myotome that is also well served by the first major caudal branch (5.). Tracing 7. illustrates the branch pattern of the more distal rami (T and U). Tracing 6 shows the detail that the cobalt-fills reveals, more especailly at the distal ends of the VR where density of stain is somewhat less; overloading of cobalt at the proximal ends obscures detail, but distally individual axons can be followed in the VR and traced out along the nerve branches. Note especially that, in basic outline, the similarity between DR and VR patterns of the two species is only masked by the large amount of cross-innervation and extensive branching of cod nerves.


D
A
A
B
C
D
E
F
G
H
I
J
K
L
4
5
6
7
1 mm
M
N
O
P
Q
R
S
T
U
V
W
1
2
3
1 mm

Fig. 7.7. Semi-thin section of eel spinal nerve (sample site E) showing the composition to be predominantly of large diameter axons. Note the extensive surrounding layer of lipid. Magnification X33

Fig. 7.8. Similar to 7.7, but more distal, where the spinal nerve has bifurcated into two similar nerves. Magnification X21

Fig. 7.9. Eel abdomen VR, sampled at site J; the nerve is completely surrounded by adipocytes and has a thick sheath. Magnification X45

Fig. 7.10. Eel trunk VR, sampled at site F; the composition is broadly similar to the homologous nerve in the abdomen (Fig. 7.9). Magnification X48

Fig. 7.11. Elver spinal cord, TS, showing the emergence of the dorsal roots caudal to the ventral root. Spinal ganglia are also present (bottom, left). Magnification X42

Fig. 7.12. Similar to 7.11, but a rostral aspect showing the transection of both dorsal and ventral roots. Magnification X41

Fig. 7.13. Acetylcholinesterase stain (direct-colouring method) of cod fast muscle, cryostat sections (18μm). Note the extensive branching of the termination at bottom, right. Magnification X27

Fig. 7.14. Similar to 7.13, showing pre-terminal division of the axon. Magnification X27

Fig. 7.15. Methylene blue staining of cod abdomen superficial fast muscle. The VR runs across the top. Note the extensive ramification of the smaller nerve bundles, their refleXing onto the original route. Dorsal is at the right. Magnification X2

Fig. 7.16. Similar preparation to 7.15, using cobalt-filled nerves. A fine branch of the VR can be seen (bottom, left) and sprouting a single, followed by a double axon branch running predominantly along the longitudinal axis of the muscle fibres. Magnification X15

7

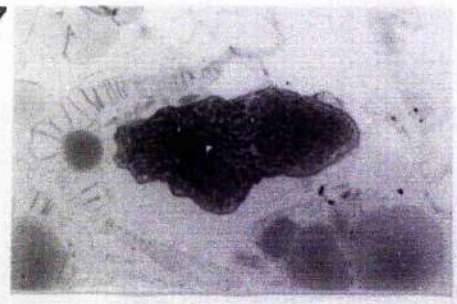

8

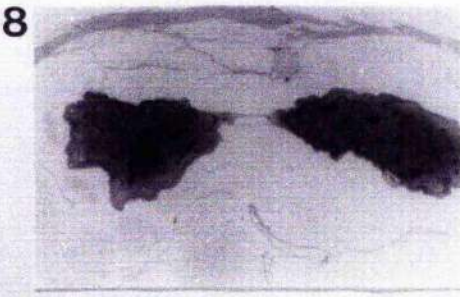

9

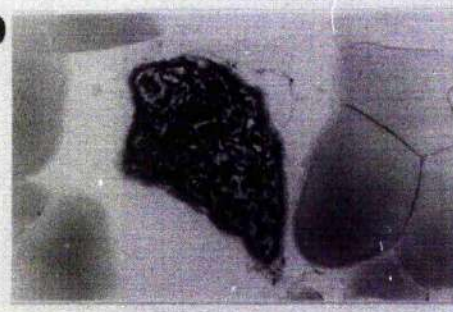

10

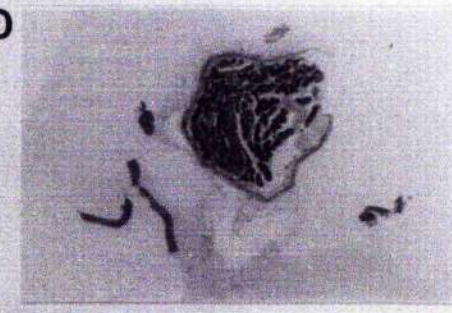

11

12

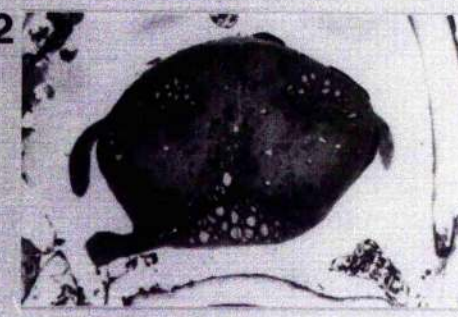

13

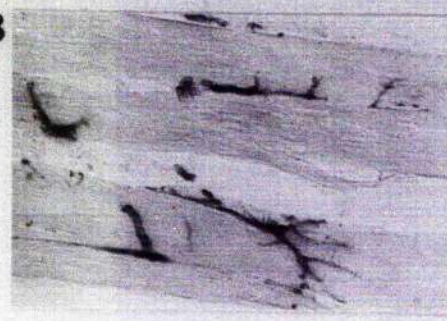

14

15

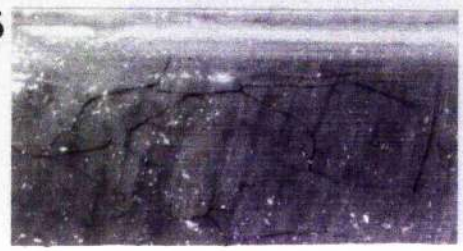

16

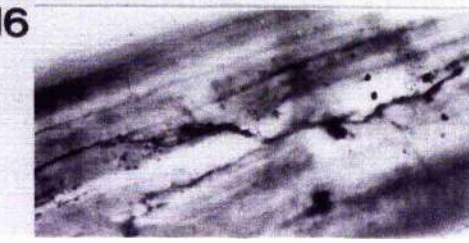

Fig. 7.17. Cobalt-fill preparation of eel VR (abdomen). Proximal end showing the higher frequency of rostral, relative to caudal branches. The mid-myotome position is clear, and the relative dimensions given by the pigmented blood vessel and myosepta, running left to right. Magnification X1.9.

Fig. 7.18. Similar to 7.17, distal end. Note the regular spacing of the rostral branches and subsequent progression into the deeper muscle adjacent to the myoseptum. Magnification X2.05.

Fig. 7.19. Cod, abdomen VR. Proximal end showing the simultaneous appearance of rostral (left) and caudal (right) main branches, and numerous fine branches. Magnification X2.06.

Fig. 7.20. Eel, abdomen VR. Similar aspect to 7.19, showing the similar (though more rare) pattern of branching, with fewer accessory branches. Magnification X2.0.

Fig. 7.21. Miniature endplate potentials (MEPPs) recorded from fast muscle fibre in eel abdomen. Vertical scale = 1mV, horizontal scale = 0.5sec.

Fig. 7.22. Cod fast muscle endplate, showing a composite structure of similar morphology and vesicle content. Magnification X28,500.

Fig. 7.23. Elver fast muscle endplate, showing a simpler organisation and reduced mitochondrial content to that of cod. Magnification X25,650.

17

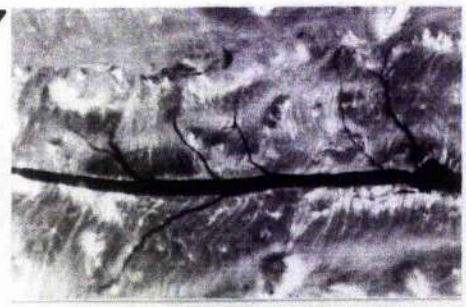

18

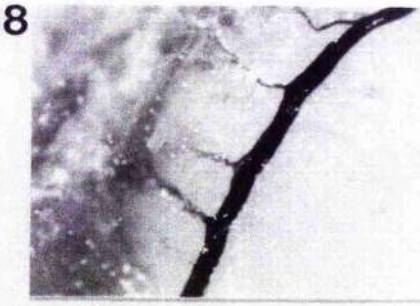

19

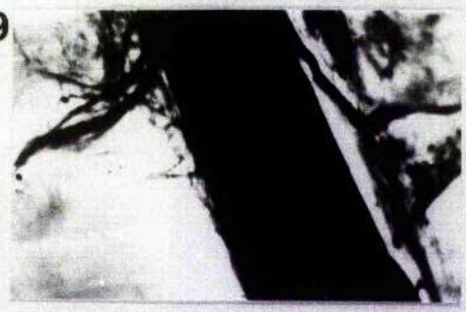

20

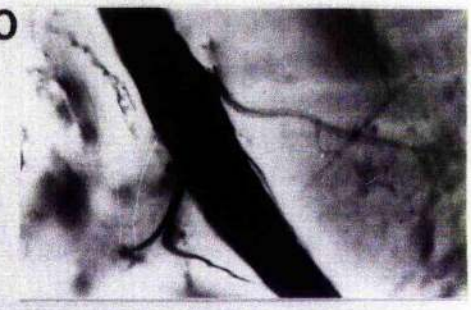

21

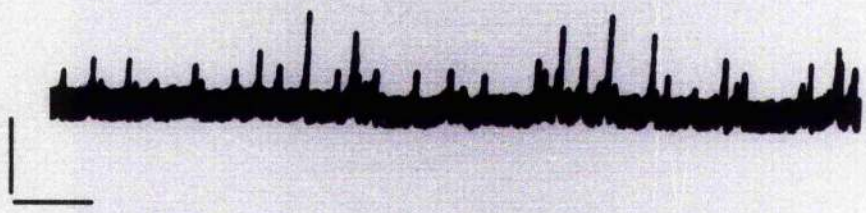

22

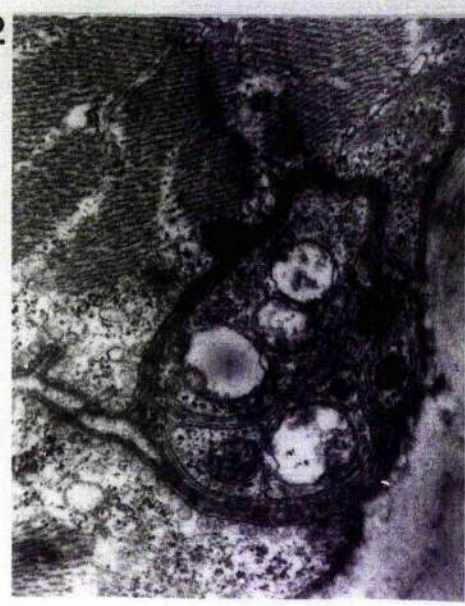

23

Fig. 7.24. Composite of cod spinal nerves.

A) Rostral branch of DR, showing a predominantly small diameter axon content. Side E.

B) Caudal branch of DR, with thick sheath, S. A mixed composition is evident, derived in part from the addition of a small branch, bottom right. Site B.

C) Similar to B), but sampled more proximal, showing the segregation of large- and small diameter axons. Site D.

D) The major spinal nerve mass, emerging from the vertebral column. The regional divisions may be followed in the path of subsequent branches. Site F.

E) Rostral branch of VR, predominantly of large axons. S small branch, r, is visible. Site G.

F) Caudal branch of VR, mixed composition: sampled at a similar level to E), site H.

G) View of the VR distal to G, showing the reduction in axon number and the close association of predominantly large- and predominantly small-diameter axon bundles.

H) View of the VR distal to F), showing the segregation of the two parallel-running nerves. Site J.

I) Distal VR, viewed before the division into the fin muscle. White muscle (W), myoseptum (SP) and large blood vessel (BV) are visible. The covering sheath (S) may be quite thick. The segregation of the two axon classes within the nerve is very clear. Site K.

J) Distal VR, section of the nerve as it enters the fin musculature. The mixed composition is still present, though axon number is reduced.

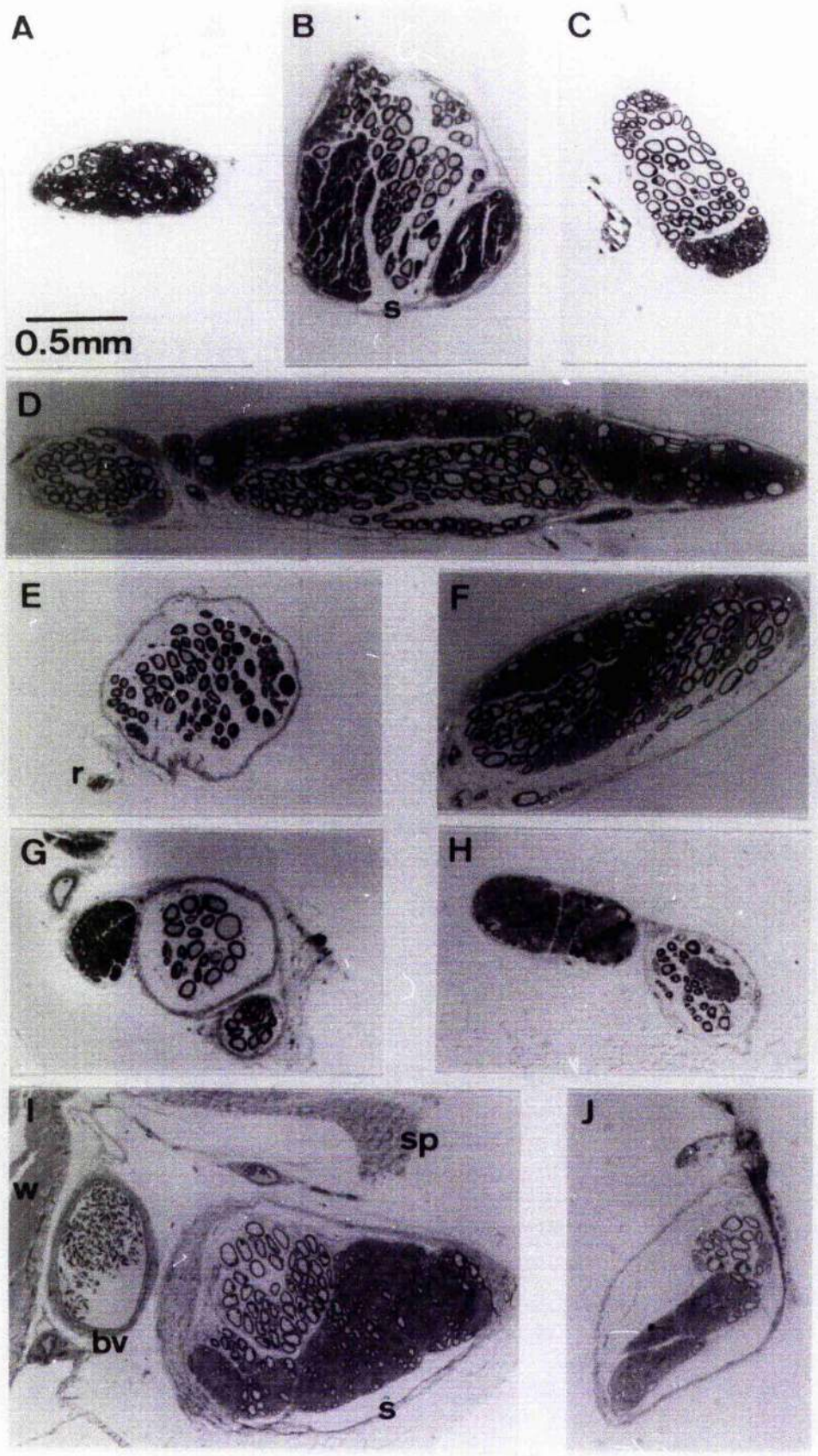
A
B
C
0.5mm
s
D
E
r
F
G
H
I
sp
w
bv
s
J

Fig. 7.25. Frequency-distribution histograms of the large diameter, presumptive motor, axon populations of eel and cod ventral rami. Mean diameter (d) is shown, with number of axons (n) in each case. Mean axon areas are given in appropriate legends ($\bar{x} \pm$ D.S.).
(A) Eel, abdomen. The unimodal distribution peaks at around 6μm diameter, but contains a sufficient number of large axons to raise the mean value to 8μm $\bar{x} = 52.5 \pm 41.10\mu m^2$.

(B) Eel, trunk. A similar distribution to that found in the abdomen, although a larger proportion of both very small and very large axons are present. Note that the number of axons in the VR is less than found in (A). $\bar{x} = 49.6 \pm 58.62\mu m^2$.

(C) Cod, abdomen. A continuum of axon diameters is present with a significant proportion of quite large axons, around 8% 200μm^2. The average diameter is clearly much larger than found in the homologous preparation in the eel, although the number of axons is less. $\bar{x} = 132.9 \pm 155.21\mu m^2$.

(D) Cod, trunk. A more discontinuous composition is found in this VR, with modal diameters of around 5-6, 10-12 and 13-14μm. The average size of axons is only slightly less than found within the abdomen VR, mean diameter = around 12μm, and contains a similar number of axons. $\bar{x} = 106.6 \pm 71.10\mu m^2$.

Fig. 7.26. Frequency-distribution of the small diameter, thin-walled (sensory) axons found within the mixed spinal nerves. Mean diameter and number of axons are shown; mean areas are given ($\bar{x} \pm$ S.D.).

(A) Eel, abdomen. The skewed distribution shows a preponderance of quite small axons, with diameters around 1μm; the porportion of larger axons present in this sample (4% 5.0μm^2) may well belong to the motor categories described in Fig. 7.13 $\bar{x} = 1.56 \pm 1.59\mu m^2$.

(B) Eel, trunk. A similar distribution to that found in the abdomen is found, but with a smaller mean diameter of 1.2μm. Note the reduction in axon number. $\bar{x} = 1.19 \pm 0.64\mu m^2$.

(C) Cod, abdomen. A more even distribution of axon diameters is found, compared to that in the homologous eel preparation, although both the number and average size of axons is very much larger. Note that the scale is half that of the other diagrams, i.e. each bar represents a 1.0μm^2 category. $\bar{x} = 3.54 \pm 2.08\mu m^2$.

(D) Cod, trunk. The distribution of axon size is much reduced, with respect to the abdomen preparation, and more closely resembles the situation found in eel with mean diameter being around 1.5μm. The number of axons is less than found in the abdomen VR but still significantly greater than that found in eels. $\bar{x} = 1.93 \pm 1.99\mu m^2$.

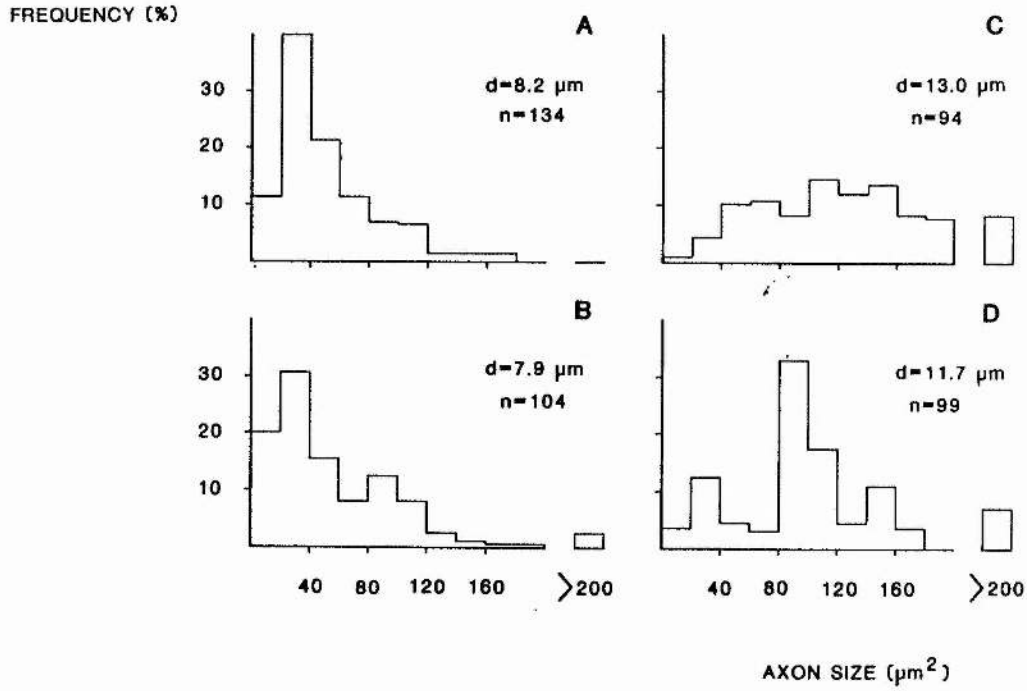
FREQUENCY (%)
A
d=8.2 µm
n=134
C
d=13.0 µm
n=94
B
d=7.9 µm
n=104
D
d=11.7 µm
n=99
30
20
10
40
80
120
160
>200
AXON SIZE (µm²)

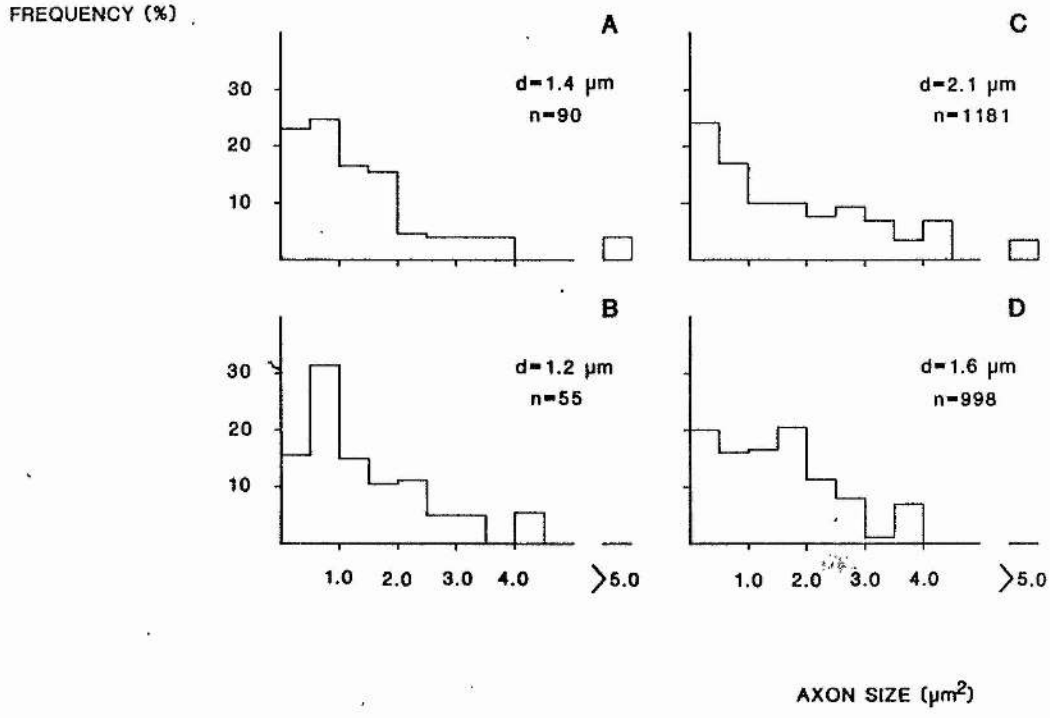
FREQUENCY (%)
A
d=1.4 µm
n=90
C
d=2.1 µm
n=1181
B
d=1.2 µm
n=55
D
d=1.6 µm
n=998
30
20
10
1.0
2.0
3.0
4.0
>5.0
AXON SIZE (µm²)

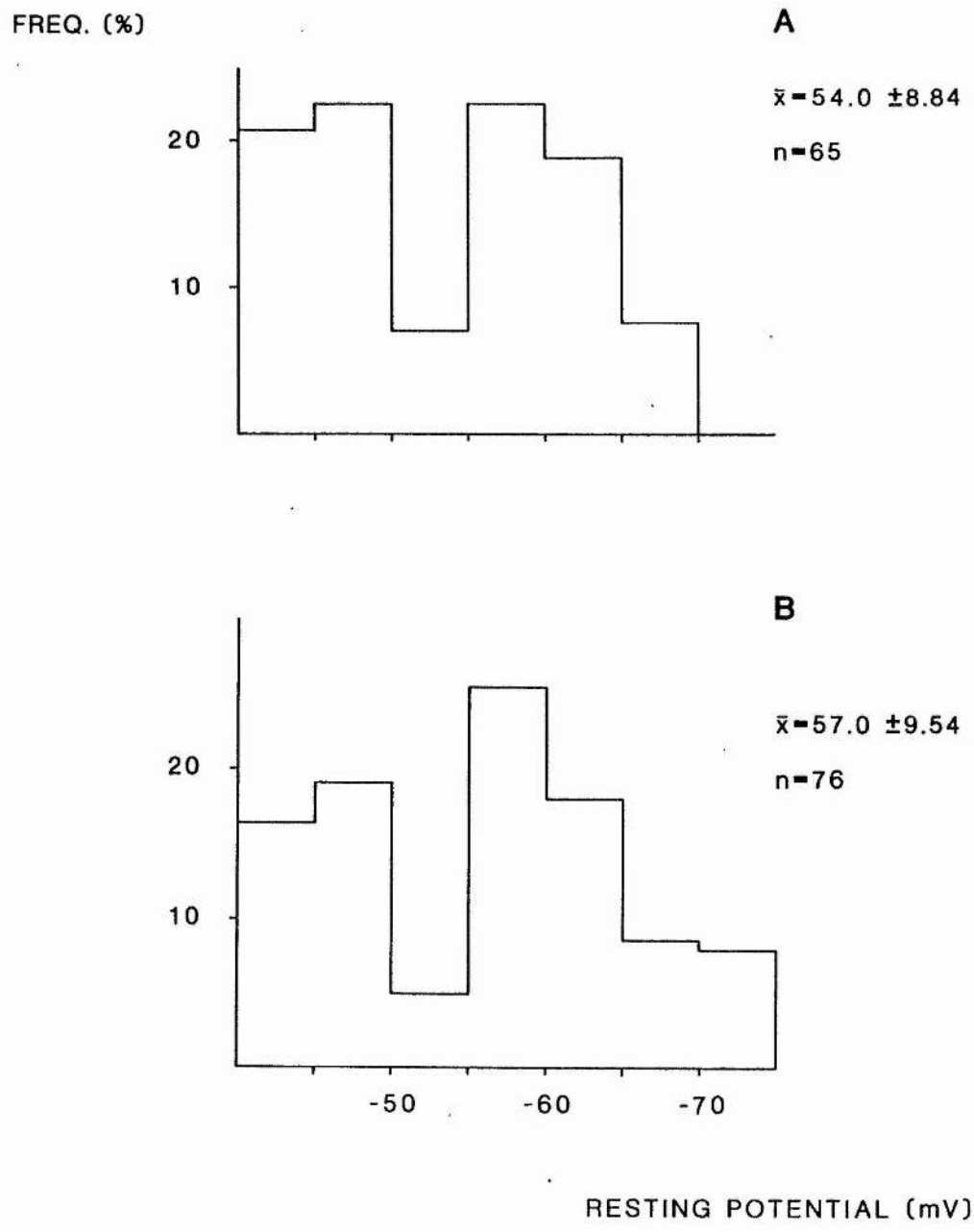

Fig. 7.27. Resting membrane potentials for eel (A) and cod (B) fast muscle fibres. The bimodal distribution suggests the lower (closer to zero) potentials may be artefactual (see Results).

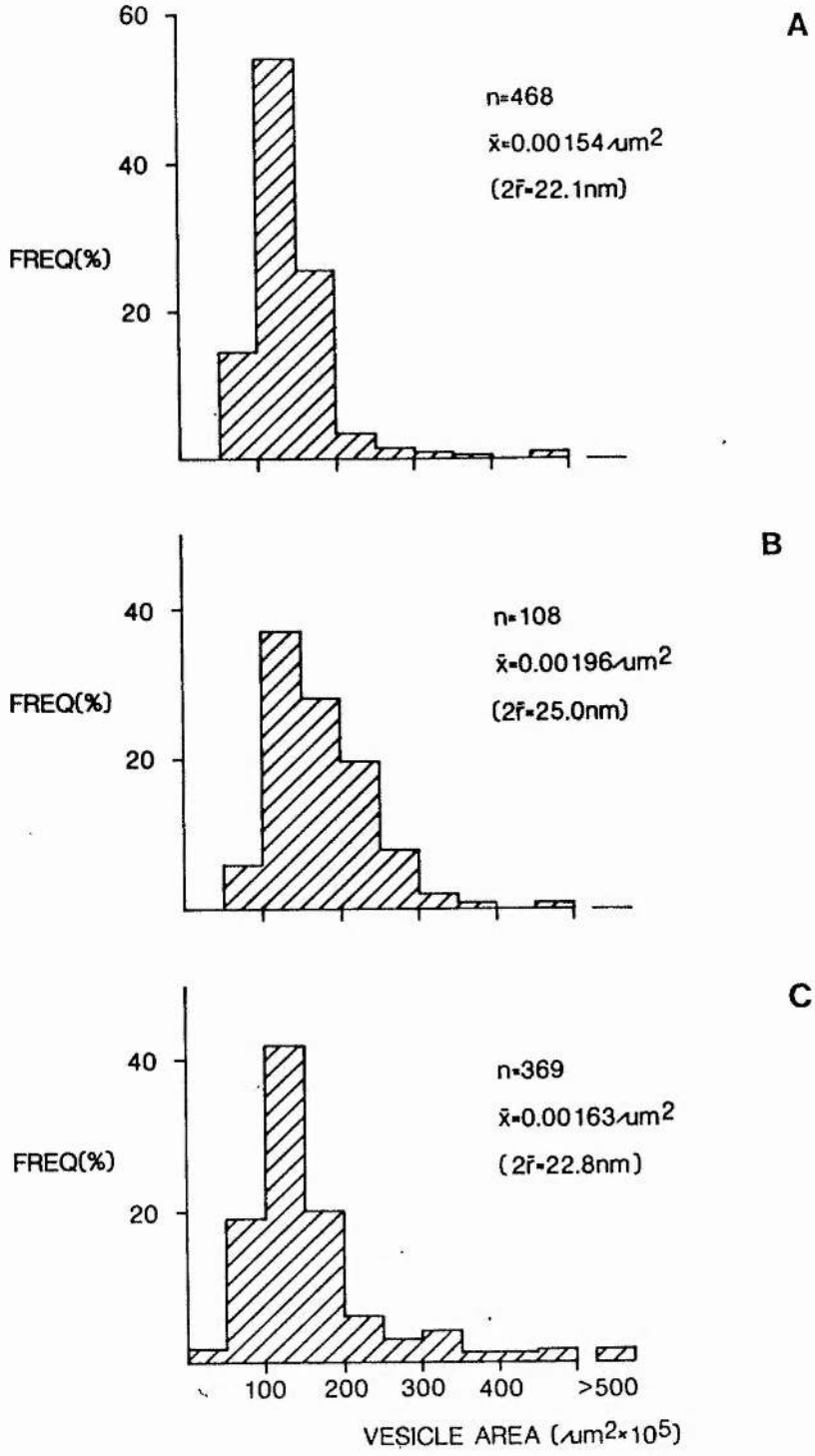

Fig. 7.28. Synaptic vesicle dimensions for elver (A), eel (B), and cod (C) fast muscle endplates. Note the similarity of both average diameters, and the areal distribution.

GENERAL DISCUSSION

Primitive teleosts occupy a central position between the lower taxonomic orders, agnathans and elasmobranchs, and the "advanced" or higher teleosts which comprise some 20,000 of the 25,000 or so extant fish species, and have been most studied. Eels form a rather isolated teleost group, Order Apodes, first appearing in the Cretaceous (~100M years ago) and diverging early from the main stem. Such types retain many "primitive" features and do not attract much physiological research, although having exploited a particular niche for so long they must be superbly well adapted. Caution should (though sadly often is not) exercised in extrapolating data from a few species to the whole range of fishes. The amazing diversity is reflected in their presence in most aquatic habitats from the ocean and rapid flowing rivers, to high altitude or soda lakes. Inhabited temperatures range from -2°C (antarctic "supercooled" species) to ~ +45°C (ocean trenches); adaptation is largely due to modifications in protein structure, rather than behaviour or physiology. Several species tolerate dry land, either by excursion (mud-skipper, Periopthalmus) or aestivation (lungfish, Protopterus). Functional specialisation in a common structure is often seen, e.g. the use of pectoral fins as simple ailerons in dogfish Scyliorhinus, for underwater "flying" in eagle ray Myliobatis and "walking" in gurnard Trigla. Flying fish Exocoetus use enlarged fins for gliding up to 400m; consecutive flights are possible without re-entry, propelled by rapid (~ 70Hz) tail beats. The correlation between life-style and muscle form is apparent for salmon that can leap 8 or 9 feet out of water; such fish need powerful, rapid contracting muscles. Uusually it is less clear. The development of skeletal muscle in these other species is largely a matter of speculation, although their study would more clearly outline muscle

adaptability to different work-loads and function. The need to correlate environment and physiology is illustrated by temperature acclimation, where both developmental stage and size may directly affect the nature of the response, in line with normal ecological constraints. Prior history of experimental animals is often ignored, or not controlled for, which exaggerates the large amount of interspecific variability. Although often used in temperature-acclimation experiments, goldfish may be unusual in the extent of their response.

Ectotherms do not necessarily need to achieve perfect compensation (or adaptation) for optimal (ecological) function (Brett 1979). Although this premise focusses primarily on temperature, it is equally applicable to other aspects of fish physiology.

Development of the teleost swimbladder removes buoyancy problems and is reflected in the great variety of body forms: from the slender sea-horse Hippocampus to the spherical globe-fish Chilomycterus. Trunkfish Ostracion use a rigid bony shell for predator-protection, only using the caudal fin for fast swimming; this involves almost simultaneous contraction of ipsilateral myotomes. Habitat-selection has produced typical sprinters (pike, perch), sneakers (eel), crawlers with "staying power" for escape (rudd, bream), and stayers for migration (salmon) or feeding (carp) (Boddeke et al 1959). The undulatory swimming of eel is the simplest use of force from contracting muscles, passing it directly to water, by including most of the body in the waveform (Gray 1933). It is also the most hydrodynamically inefficient mode, producing large vortices and cross-flows; the considerable drag limits performance to relatively low speeds. In contrast, tunas have a laminar body (reducing surface turbulance) and are fast, efficient swimmers maximising thrust which is provided almost entirely by the high aspect ratio, lunate

caudal fin (Fierstiene and Walters 1968). Most species fall between these extremes. Maximum efficiency in cod requires "kick-and-glide" locomotion, as the drag on a steady swimming fish is 3.3 fold greater than on a gliding fish (Videler 1981). This may allow partial recovery of the muscle, or rotation of motor units; an alternate strategy is to swim at twice the basal metabolic rate, resulting in a doubling of efficiency. Although some data is available for eel, it would be premature to assign similar locomotry energetics to other species showing the metastable, anguilliform locomotion e.g. lamprey and butterfish. The correlation of intersegmental innervation and importance of sensory afferents, with the mode of swimming is now easily testable; both pelagic and demersal species, of different innervation types, should be compared to assess the contribution of the body in propulsion. An important corollary of this would be the screening of suitable species for electrophysiological analysis of the spinal cord generator, and its afferent modification (see Grillner 1975).

All locomotory adaptations impose different mechanical and energetic constraints on the musculature. The efficiency, work out/(work out + heat out), of fish skeletal muscle is not known. Heat liberated during shortening is greater than during static tension development and is proportional to the distance, not the rate, of contraction. Most fish slow fibres shorten by around 10%, whereas fast fibres may be similar (7-9% in dogfish) or much less (2-3% in cod; Alexander 1969). This is important in determining whether adaptation has been for isotonic or isometric contraction, involving the simultaneous measurement of both thermal and mechanical properties. An alternate approach measures biochemical efficiency: chicken slow muscle is 15-18X more efficient (cost of a contraction/μmol ATP/unit time) than fast (twitch) muscle during isometric contraction, although very inefficient during isotonic contraction (Goldspink 1977). Locomotory efficiency forms only part of the selective pressure: voluntary day-to-day movements use ~20% of maximum aerobic capacity, which is probably utilised <10% of a fish's life.

Many species undergo a period or periods of natural starvation due to fluctuations in food supply and/or during the spawning migration; fast muscle appears to have a central role in supplying precursors for intermediary metabolism. Regional variation in both structure and metabolic profile may define areas of selective fibre degredation.

With the varied functional requirements it is not surprising that there is a great diversity of muscle types. Assumptions about the homogeneity of muscle samples can lead to erroneous results, particularly biochemical assays (e.g. Boström and Johanson 1972), and the reliance on single criteria to discrepancies in the literature. Recent work on the differentiation of sarcoplasmic proteins supports the conclusion that broad categories - "fast", "intermediate", "slow" - are not sufficient to describe different fish muscle phenotypes; e.g. there is evidence for a fast-twitch red muscle with a high parvalbumin content, and for a population of fast-twitch white fibres with a low parvalbumin content (Hamoir et al 1981). Knowledge of the extent of nerve-muscle interaction, with respect to phenotype modification, is restricted to circumstantial evidence for fish skeletal muscle. In mammalian muscles, where the form of innervation can dramatically alter histochemical and contractile properties (Vrbova 1980), it has been shown that sequential appearance of adult myosin heavy chain, following the neonatal form, is not affected by nerve lesion (Butler-Brown et al 1982). In addition, plasticity of the neuronal input itself requires consideration; in insects, the same motorneuron can innervate both types of muscle (tonic and phasic) at different developmental stages (Rhenden and Kammer 1980). The existence of a similar myogenic sequence, in fully differential muscle and embryonic myogenesis, may make it easier to experimentally determine the proximate factors in cellular differentiation. It may also be possible to follow the developmental switch

from regional growth nodes to myotomal hyperplasia, following a particular cell line e.g. by immunohistochemical localisation of isozymes, and the labelling of mitotic nuclei.

Analytical

The development of stereological models for analysis of structure removes much of the speculative nature of comparative physiology. Unfortunately, many articles appear to ignore the theoretical basis on which these methods are based, and misuse the optimisation process inherent in any analytical protocol. A thorough examination of the tissue is required before adopting a particular strategy. Oblique sections are used for stereological analysis of mammalian muscle, since there is a periodicity of structure in LS; this does not apply to elver muscle, and therefore TS sections are available for quantification of both volume densities and boundary lengths. The derivision of parameters more closely describing the functional capacity of the capillary bed should replace the erroneous indices in the literature, although more information is required concerning the response to physiological adaptation. Further insight into the limiting role in oxygen supply may be afforded by the quantification of branching along a longitudinal transect of the myotome. The presence of capillary recruitment during muscular activity has not been demonstrated, although this should be possible by means of intravital microscopy and measurement of peripheral vascular resistance. The most promising new development is likely to be the measurement of $\dot{V}o_2$ and metabolite release from discrete muscle regions, with the construction of energy budgets. This should be possible using the isolated tail preparation (Davie 1981), and will allow the construction of more realistic models of the systemic circulation (see Loats et al 1978).

In conclusion, the present study has provided the first quantitative data concerning structure and organisation of myotomal muscles in primitive teleosts. Evidence is provided that the prior history of experimental animals, and the magnitude of the sample size, will greatly affect parameter accuracy. Methods have been described whereby functional correlates of the capillary network and innervation pattern may be studied in more detail than previously possible. The hetergeneity of muscle is such that the continuum of form and function can only be adequately studied by a diversity of approach.

REFERENCES

AKMAL, K BRULEY, D.F BANCHERO, N ARTIGUER, R MALONEY, W (1978) Multi-capillary model for oxygen transport to skeletal muscle. Adv Expl Med Biol 94 139-147

AKSTER, H.A OSSE, J W M (1978) Muscle fibre types in head muscles of the perch Perca fluviatilis (L), Teleostei. Neth J Zool 28 94-110

ALEKSEYEVA, K D (1973) The metabolic rate in the young of certain Mediterranean fishes. Hydrobiol J 9 24-29

ALEXANDER, R. McN (1969) The orientation of muscle fibres in the myomeres of fishes. J mar biol Ass U K 49 263-290

ALTRINGHAM, J D JOHNSTON, I A (1981) Quantitative histochemical studies on the peripheral innervation of cod (Gadus morhua) fast myotomal muscle fibres. J Comp Physiol 143 123-127

ALTRINGHAM, J D JOHNSTON, I A (1982) The pCa-tension and force-velocity characteristics of skinned fibres isolated from fish fast and slow muscles. J Physiol (Lond) (in press)

ANASTASI, G SALLEO, A FALZEA, G DENARD, M G SPADA, G MACAUDDA, L (1979) Scanning electron microscopy of satellite cells in the plantaris muscle of rat during post-natal growth. J Submier Cytol 11 463-472

ANDERSEN, P JANSEN, J K S LØYNING, Y (1963) Slow and fast muscle fibres in the Atlantic Hagfish (Myxine glutinosa). Acta Physiol Scand 57 167-179

ANDERSEN, P HENRIKSSON, J (1977) Capillary supply of the quadriceps femoris muscle of man: adaptive response to exercise. J Physiol (Lond) 270 677-690

APPELL, H-J HAMMERSEN, F (1978) Capillary density and patterns in skeletal muscle II. the effect of the capillary patterns on capillary counts. Pflügers Arch 373 R60

ATWOOD, H L (1972) Crustacean muscle in: Bourne, GH "the structure and function of muscle". Academic Press London

BACON, J P ALTMAN, J S (1977) A silver intensification method for cobalt-filled neurones in wholemount preparations. Brain Res 138 359-363

BAGUST, J LEWIS, D M WESTERMAN, R A (1981) Motor units in cross-reinnervated fast and slow twitch muscle of the cat. J Physiol (Lond) 313 223-235

BAINBRIDGE, R (1962) Training, speed and stamina in trout. J exp Biol 35 109-133

BALDWIN, J & HOCHACHKA, P W (1970) Functional significance of isozymes in thermal acclimation-acetylcholinesterase from trout brain. Biochem J 116 883-887

BANCROFT, J D STEVENS, A (1977) eds: "Theory and practice of histological techniques". Churchill Edinburgh

BÁRÁNY, M (1967) ATPase activity of myosin correlated with speed of muscle shortening. J gen Physiol 51 197-216

BARETS, A (1961) Contribution à l'étude des systemes moteur lent et rapide du muscle lateral des teleostéens. Arch Anat Morph exp 50: (Suppl.): 91-187

BASS, A BRDICZKA, D EYER, P HOFER, S PETTE, D (1969) Metabolic differentiation of distinct muscle types at the level of enzymatic organisation. Eur J Biochem 10 198-206

BEAMISH, F W H (1970) Influence of temperature and salinity on temperature preferenda of the euryhaline fish Tilapia nilotica. J Fish Res Bd Can 27 1209-1214

BEARDALL, C H JOHNSTON, I A (1982) Muscle atrophy during starvation in a marine teleost. Eur J Cell Biol (in press)

BENNETT, A F (1978) Activity metabolism of the lower vertebrates. An Rev Physiol 40 447-469

BERG, G STEEN, J B (1965) Physiological mechanisms for aerial respiration in the eel. Comp Biochem Physiol 15 469-484
BERTIN, L (1956) "Eels. A biological study". Clever-Hulme Press London
BEST, A C G & BONE, Q (1973) The terminal neuromuscular junctions of lower chordates. Z Zellforsch mikrosk Anat 143 495-504
BILINSKI, E (1974) Biochemical aspects of fish swimming. In Biochemical and biophysical perspectives in marine biology 1 239-288 Maline, D C & Sargent, J R (Eds) London & New York: Academic Press
BIRKS, R HUXLEY, H E KATZ, B (1960) The fine structure of the neuromuscular junction of the frog. J Physiol (Lond) 150 134-144
BIRNBERGER, K L ROVÄINEN, C M (1971) Behavioural and intracellular studies of a habituating fin reflex in the sea lamprey. J Neurophysiol 34 983-989
BODDEKE, R SLIJPER, E J VAN DER STELT, A (1959) Histological characteristics of the body musculature of fishes in connection with their mode of life. K Ned Ak Wetensch Pro Ser C 62 576-588
BOËTIUS, I and BOËTIUS, J (1967) Studies on the European eel (Anguilla anguilla L.) Medd fra Dan Fisk og Havunders 4 339-405
BOËTIUS, J (1976) Elvers, Anguilla anguilla and Anguilla rostrata from two Danish localities. Medd fra Dan Fisk og Havunders N S 7 199-220
BONE, Q (1963) Some observations upon the peripheral nervous system of the hagfish Myxine glutinusa. J Mar Biol Assoc U K 43 31-47
BONE, Q (1964) Patterns of muscular innervation in the lower chordates. Int Rev Neurobiol 6 99-147
BONE, Q (1966) On the function of the two types of myotomal muscle fibres in elasmobranch fish. J mar biol Ass U K 46 321-349
BONE, Q (1972) The dogfish neuromuscular junction: Dual innervation of vertebrate striated muscle fibres? J Cell Sci 10 657-665
BONE, Q (1978a) Locomotor muscle. In Fish physiology 7 361-424. Hoar, W S & Randall, D J (Eds). New York & London: Academic Press
BONE, Q (1978b) Myotomal muscle fibre types in Scomber and Katsuwonus. In The physiological ecology of tunas 183-205 Sharp G D & Dizon A E (Eds) New York & London:Academic Press
BONE, Q & CHUBB, A D (1978) The histochemical demonstration of myofibrillar ATPase in elasmobranch muscle. Histochem J 10 489-494
BONE, Q KICZNUIK, J & JONES, D. R (1978) On the role of the different fibre types in fish myotomes at intermediate swimming speeds. Fish Bull U S 76 691-699
BONE, Q ONO, R. D (1982) Systematic implications of innervation patterns in teleost myotomes. Breviora No. 470 1-23
BOSTRÖM, S L JOHANSSON R G (1972) Enzyme activity patterns in white and red muscles of the eel (Anguilla anguilla) at different developmental stages. Comp Biochem Physiol 42 533-542
BOSSEN, E J SOMMER, J R & WAUGH, R A (1978) Comparative steriology of the mouse and finch left ventricle. Tissue & Cell 10 773-784
BRETT, J R (1972) The metabolic demand for oxygen in fish, particularly salmonids, and a comparison with other vertebrates. Resp Physiol 14 151-70
BRETT, J R (1979) Environmental factors and growth in: Hoar, W S Randall, D J Brett, J R (eds) "Fish Physiology" 8 Academic Press
BRETT, J R ZALA (1975) quoted in Love 1980
BRILL, R W & DIZON, A E (1979) Red and white muscle fibre activity in swimming skipjack tuna. Katsuwonus pelamis (L.) J Fish Biol 15 679-685
BRIDGE, D T ALLBROOK, D (1970) Growth of striated muscle in an Australian marsupial (Setonix brachyurus). J Anat 106 285-295
BROWN, M D COTTER, M A HUDLICKA, O VRBOVA, G (1976) The effects of different patterns of muscle activity on capillary density, mechanical properties and structure of slow and fast rabbit muscles. Pflügers Arch 36 241-250

BUCHANAN, J T COHEN, A H (1982) Activities of identified, motoneurons, and muscle fibres during fictive swimming in the lamprey. J Neurophys 47

BULLER, A J ECCLES, J C ECCLES, R M (1960) Interaction between motoneurones and muscles in respect of the characteristic speeds of their responses. J Physiol (Lond) 150 417-439

BULLOCK, T M HORRIDGE, G A (1965) "Structure and function in the nervous system of invertebrates". W H Freeman London

BURKE, R E LEVINE, D M TSAIRIS, P ZAJAC, C E (1973) Physiological types of histochemical profiles in motor units of the cat gastrocnemius. J Physiol (Lond) 234 723-748

BURTON, D T (1979) Ventilatory frequency compensation responses of three eurythermal estuarine fish exposed to moderate temperature increases. J Fish Biol 15 589-600

BUTLER-BROWN, G S BUGAISKY, L B CUÉNOUD, S SCHWARTZ, K WHALEN, R G (1982) Denervation of newborn rat muscles does not block the appearance of adult fast myosin heavy chain. Nature (Lond) 299 830-833

BYCZKOWSKY-SMYK, W (1958) The respiratory surface of the gills in Teleosts. Acta Biol Cracoviensia Sr Zool 1 83-97

CAMERON, J N (1970) The influence of environmental variables on the hematology of pinfish (Lagodon rhomboides) and striped mullet (Mugil cephalus). Comp Biochem Physiol 32 175-192

CAREY, F G TEAL, J M (1966) Heat conservation in tuna fish muscle. Proc Natl Acad Sci U S A 56 1464-1469

CASLEY-SMITH, J R GREEN, H S HARRIS, J L WADEY, P J (1975) The quantitative morphology of skeletal muscle capillaries in relation to permeability. Microvasc Res 10 43-64

CHAN, D K O WOO, W Y S (1978) The respiratory metabolism of the Japanese eel, Anguilla japonica. Gen Comp Endocr 35 160-168

CLOSE, R I (1972) Dynamic properties of mammalian skeletal muscles. Phys Rev 52 129-197

COLQUHOUIN, W R RIEDER, C L (1980) Contrast enhancement based on rapid dehydration in the presence of phosphate buffer. J Ultrastruct Res 73 1-8

COSSINS, A R (1977) Adaptations of biological membranes to temperature. The effect of temperature acclimation of goldfish upon the viscosity of synaptosomal membranes. Biochim Biophys Acta 470 395-411

COTTER, M HUDLICKÁ, O PETTE, D STAUDTE, H VRBOVA, G (1973) Changes of capillary density and enzyme pattern in fast rabbit muscles during long-term stimulation. J Physiol (Lond) 230 34-35

COUTEAUX, R (1973) Motor end-plate structure in: Bourne, G H (ed) "The structure and function of muscle" Vol. 2 Academic Press London

CRABTREE, B & NEWSHOLME, E A (1972) The activities of phosphorylase, hexokinase, phosphofructokinase, lactate dehydrogenase in muscles from vertebrates and invertebrates. Biochem 126 49-58

CREUTZBERG, F (1958) Use of tidal streams by migrating elvers (Anguilla vulgaris Turf) . Nature Lond 181 857

CRUZ, L M (1976) Quantifying pattern. A stereological approach. Jl Microsc 107 1-18

CRUZ-ORIVE, L M (1982) Modelling structural anisotropy. Proceedings of ISS-"Stereology 82" Acta Stereologica (in press)

DAHL, H A NICOLAYSEN, K (1971) Actomyosin ATPase activity in Atlantic hagfish muscles. Histochemie 28 205-210

VAN DAM, L (1935) A method for determining the amount of dissolved oxygen in 1cc of water. J exp Biol 12 80-85

DAVIE, P S (1981) Vascular resistance responses of an eel tail preparation alpha constriction and beta dilation. J exp Biol 90 65-84

DAXBOECK, C RANDALL, D J JONES, D R (1982) Cardiac output redistribution during swimming exercise in a teleost fish, Salmo gairdneri. J exp Biol (in press)

DEAN, J M (1969) The metabolism of tissues of thermally acclimated trout (Salmo gairdneri). Comp Biochem Physiol 29 185-196
DEELDER, C L (1970) Synopsis of Biological Data of the Eel. FAO fish Synop No 80 82pp Rome
De WILDE, M A HOUSTON, A H (1967) Haematological aspects of the thermo-acclimatory process in the rainbow trout Salmo gairdneri. J Fish Res Board Can 24 2267-2281
DRIEDZIC, W R & HOCHACHKA, P W (1978) Metabolism of fish during exercise In Fish Physiology (Edited by Hoar, W S & Randall, D J) pp 503-543 Academic Press New York San Francisco London
DUBOWITZ, V (1970) Differentiation of fibre types in skeletal muscle in Briskey, E J Cassebs, R G Marsh, B B (eds) "The physiology and biochemistry of muscle as a food" Wisconsin Press Madison
DOUDOROFF, P SHUMWAY, D L (1968) Dissolved oxygen requirements of freshwater fishes. Fisheries Synopsis FIRI/T86 FAO Rome
EISENBERG, B R & KUDA, A M (1975) Steriological analysis of mammalian skeletal muscle II. White vastus muscle of the adult guinea pig. J Ultrastruct Res 51 176-187
ELMQUIST, D QUASTER, D M J (1965) A quantitative study of end-plate potentials in isolated human muscle. J Physiol (Lond) 178 505-529
EPSTEIN, F H CYNAMON, M McKAY, W (1971) Endocrine control of Na-K-ATPase and seawater adaptation in Anguilla rostrata. Gen Comp Endocr 16 323-328
EVANS, R M PURDIE, F C & HICKMAN, C P (1962) The effect of temperature and photoperiod on the respiratory metabolism of rainbow trout. Can J Zool 40 107-118
EZZAT, A EL-SERAFY, S (1977) The migration of elvers of Anguilla anguilla L in the Mex canal, Alexandria, Egypt. J Fish Biol 11 249-256
FARRELL, A P SMITH, D G (1981) Microvascular pressures in gill filaments of Lingcod (Ophiodon elongatus). J exp Zool 216 341-344
FATT, P KATZ, B (1951) An analysis of the end-plate potential recorded with an intracellular electrode. J. Physiol (Lond) 115 320-370
FIERSTIENE, H L WALTERS, V (1968) Studies in locomotion and anatomy of scombroid fishes. Mem S Calif Acad Sci 6 1-31
FISCHMAN, D A (1972) Development of striated muscle in: Bourne, G H "The structure and function of muscle" Vol 1 2nd Edn. Academic Press London
FLITNEY, F W (1966) The time course of the fixation of albumin by formaldehyde, gluteraldehyde, acrolein and other higher aldehydes. J Roy Microsc Sco 85 353-364
FLITNEY, F W (1971) The volume of the T-system and its association with the sarcoplasmic reticulum in slow muscle fibres of the frog. J Physiol (Lond) 217 243-257
FLITNEY, F W & JOHNSTON, I A (1979) Mechanical properties of isolated fish red and white muscle fibres. J Physiol 295 49-50P
FLOOD, P R (1979) The vascular supply of the three fibre types in the parietal trunk muscle of the Atlantic hagfish (Myxine glutinosa, L) Microvasc Res 17 55-70
FLOREY, E CAHILL, M A (1982) The innervation pattern of crustacean skeletal muscle. Cell Tiss Res 527-541
FONTAINE, M (1975) Physiological mechanisms in the migration of marine and amphihaline fish. Adv Mar Biol 13 241-355
FORSTER, M E (1981) Oxygen consumption and apnoea in the shortfin eel, Anguilla australis schmidtii. N Z Jnl Mar F W Res 15 85-90
FOX, M H WINGFIELD, C A (1938) A portable apparatus for the determination of oxygen dissolved in a small volume of water. J exp Biol 15 437-445

FREADMAN, M A (1979) Role of partitioning of swimming musculature of striped Bass. Morone saxatilis Walbaum and Bluefish, Pomatomus saltatrix L. J Fish Biol 15 417-423
FREED, J M (1971) Properties of muscle phosphofructokinase of cold- and warm-acclimated Carassius auratus. Comp Biochem Physiol 39B 747-764
GARSIDE, E T MORRISON, G C (1977) Thermal preferences of mummichog, Fundulus heteroclitus L., and banded killfish, F. diaphanus (Le Sueur), (Cyprinodontidae) in relation to thermal acclimation and salinity. Can J Zool 55 1190-1194
GOLDRING, J M KUNO, M NÚNEZ, R WEAKLEY, J N (1981) Do identical activity patterns in fast and slow motor axons exert the same influence on the twitch time of cat skeletal muscle? J. Physiol (Lond) 321 211-223
GOLDSPINK, G (1961) Fixation of muscle. Nature (Lond) 192 1305-1306
GOLDSPINK, G (1972) Post embryonic growth and differentiation of striated muscle. In; Bourne, G H (ed) "The Structure and Function of Muscle". 1 Academic Press New York
GOLDSPINK, G (1977) Muscle energetics and animal locomotion in: Alexander, R M Goldspink, G (eds) "Mechanics and energetics of animal locomotion" Chapman and Hall London
GOODRICH, E S (1930); quoted in Roberts 1969
GORDON, M R McLEAY, D J (1977) Sealed-jar bioassays for pulpmill effluent toxicity: effects of fish species and temperature. J Fish Res Bd Can 34 1389-1396
GOVIND, C K KENT, K S (1982) Transformation of fast fibres to slow prevented by lack of activity in developing lobster muscle. Nature (Lond) 298 755-757
GRAY, J (1933) Studies in animal locomotion. J exp Biol 10 88-104
GRAY, J (1936) Studies in animal locomotion: IV. The neuromuscular mechanism of swimming in the eel. J exp Biol 13 170-180
GRAY, S D RENKIN, E M (1978) Microvascular supply in relation to fibre metabolic type in mixed skeletal muscles of rabbits. Microvasc Res 16 406-425
GREENE, C W (1913) An undescribed longitudinal differentiation of the great lateral muscle of the King salmon. Anat Rec 7 99-101
GREER-WALKER, M G (1970) Growth and development of the skeletal muscle fibres of the cod (Gadus morhua L.). J Cons perm int Explor Mer 33 228-244
GREER-WALKER, M & PULL, G A (1975) A survey of red and white muscle in marine fish. J Fish Biol 7 295-300
GRIFFITHS, J S & ALDERDICE, D F (1972) Effects of acclimation and acute temperature experience on the swimming speed of juvenile coho salmon. J Fish Res Bd Can 29 251-264
GRIGG, G C (1974) Respiratory function of blood in fishes in: Florkin, M Scheer, B T (eds) Chemical Zoology Vol 8 Academic Press New York
GRILLNER, S (1975) Locomotion in vertebrates-central mechanisms and reflex interaction. Physiol Rev 55 247-304
GRILLNER, S KASHIN, S (1976) On the generation and performance of swimming in fish. Adv Behavioral Biol 18 181-201
GRILLNER, S WALLEN, P (1977) Is there a peripheral control of the central pattern generators for swimming in dog fish? Brain Res 127 291-295
GRILLNER, S WALLEN, P (1980) Does the central pattern generation for locomotion in lamprey depend on glycine inhibition? Acta Physiol Scand 110 103-105
GUNDERSEN, H J G (1977) Notes on the estimation of the numerical density of arbitrary profiles: the edge effect. J Microsc 111 219
GUNDERSEN, H J G ØSTERBY, R (1981) Optimising sampling efficiency of stereological studies in biology: or "do more less well!" J Microsc 121 65-73

HOUSTON, A H WILDE, M A De (1969) Environmental temperature and the body fluid system of the freshwater teleost. Comp Biochem Physiol 28 877-885

HOUSTON, A H SMEDA, J S (1979) Thermoacclimatory changes in the ionic microenvironment of haemoglobin in the stenothermal rainbow trout (Salmo gairdneri) and eurythermal carp (Cyprinus carpio) J Exp Biol 80 317-340

HOWELL, B J BAUMGARDNER, F W BONDI, K RAHN, H (1970) Acid-base balance in cold-blooded vertebrates as a function of body temperature. Am J Physiol 218 600-606

HUDLICKÁ, O SCHRODER, W (1978) Factors involved in capillary growth in a normal adult skeletal muscle. Fed Proc 37 314

HUDLICKÁ, O ZWEIFACH, B W TYLER, K R (1982) Capillary recruitment and flow velocity in skeletal muscle after contraction. Microvasc Res 23 201-213

HUDSON, R C L (1967) "Histological and electrophysiological investigations of the fast muscle of the teleost Cottus bubalis". PhD Thesis St. Andrews

HUDSON, R C L (1969) Polyneuronal innervation of the fast muscles of the marine teleost Cottus scorpius L. J exp Biol 50 47-67

HUDSON, R C L (1973) On the function of the white muscles in teleosts at intermediate swimming speeds. J exp Biol 58 509-522

HULBERT, W C MOON, T W (1978) A histochemical, light and electron microscopic examination of eel, Anguilla rostrata, red or white muscle. J Fish Biol 13 (5) 527-533

HULBERT, W C & MOON, T W (1978) The potential for lactate utilization by red and white muscle of the eel Anguilla rostrata L. Can J Zool 56 128-135

INGJER, F (1979) Effects of endurance training on muscle fibre ATP-ase activity, capillary supply and mitochondrial content in man. J Physiol (Lond) 294 419-432

JAMES, N T (1976) Compensatory muscular hypertrophy in the extensor digitorum longus of the mouse. J Anat 122 121-131

JAMES, N T (1977) Stereology in: Meel, G A Elder, H Y (eds) "Analytical and quantitative methods in microscopy" SEB Sem Srs 3 9-28

JAMES, N T (1981) A stereological analysis of capillaries in normal and hypertrophic muscle. J Morphology 168 43-

JANKOWSKY, H-D (1966) The effect of adaptation temperature on the metabolic level of the eel Anguilla vulgaris L. Helgolander wiss Meeresunters 13 402-407

JANKOWSKY, H D & KORN, H (1965) The influence of acclimation temperature on mitochondrial content of fish muscle. Naturwissenchaften 52 642

JANSEN, J ANDERSEN, P JANSEN, J K S (1963) On the structure and innervation of the parietal muscle of the hagfish (Myxine glutinosa). Acta Morph Neer Scand 5 329-338

JOHNSTON, M S (1977) Association of allozymes and temperature in the crested blenny, Anoplarchus purpurescens. Mar Biol 41 147-153

JOHNSON, P V & ROOTS, B J (1964) Brain lipid fatty acids and temperature acclimation. Comp Biochem Physiol 11 303-309

JOHNSTON, I A (1979) Calcium regulatory proteins and temperature acclimation on actomyosin from a eurythermal teleost (Carassius auratus L.) Comp Physiol 129 163-7

JOHNSTON, I A (1980a) Specialization of fish muscle In 'Development and Specializations of Muscle' Goldspink, D F (ed) SEB Sem Srs 7 123-148

JOHNSTON, I A (1980b) Contractile properties of fish fast muscle fibres. Marine Biol Lett 1 323-328

JOHNSTON, I A (1981a) Structure and function of muscles in: Day, M H (ed) "Vertebrate Locomotion". Zool Soc Symp 45 71-113
JOHNSTON, I A (1981b) Quantitative analyses of ultrastructure and vascularisation of the slow muscle fibres of the European Anchovy (Engraulis encrasicolus). Tiss Cell (in press)
JOHNSTON, I A (1982a) Physiology of muscle in hatchery raised fish in 'Physiology of Salmonid Cultivation' Cowey C (ed) Comp Biochem Physiol Suppl In Press
JOHNSTON, I A (1982b) Biochemistry of myosins and contractile properties of fish skeletal muscle. Molecular Physiol 2 15-29
JOHNSTON, I A (1982c) Capillarisation, oxygen diffusion distances and mitochondrial content of carp muscles following acclimation to summer and winter temperatures. Cell Tiss Res 222 325-337
JOHNSTON, I A FREARSON, N GOLDSPINK, G (1972) Myofibrillar ATPase activities of red and white muscles of marine fish. Experentia 28 713-714
JOHNSTON, I A & GOLDSPINK, G (1973a) A study of the swimming performance of the crucian carp Carassius carassius (L.) in relation to the effects of exercise and recovery on biochemical changes in the myotomal muscles and liver. J Fish Biol 5 249-260
JOHNSTON, I A & GOLDSPINK, G (1973b) A study of glycogen and lactate in the myotomal muscles and liver of the coalfish (Gadus virens L.) during sustained swimming. J mar biol Ass U K 53 17-26
JOHNSTON, I A PATTERSON, S WARD, P GOLDSPINK, G (1974) The histochemical demonstration of myofibrillar adenosine triphosphatase activity in fish muscle. Can J Zool 52 (7) 871-877
JOHNSTON, I A & TOTA, B (1974) Myofibrillar ATPase in the various red and white trunk muscles of the tunny (Thunnus thynnus L.) and the Tub Gurnard (Trigla lucerna L.) J comp Biochem Physiol 49 367-373
JOHNSTON, I A DAVISON W & GOLDSPINK, G (1975b) Adaptations in Mg^{2+} activated myofibrillar ATPase activity induced by temperature acclimation. FEBS Lett 50 293-295
JOHNSTON, I A WARD, P S GOLDSPINK, G (1975) Studies on the swimming musculature of the rainbow trout. 1. Fibre types. J Fish Biol 7 451-458
JOHNSTON, I.A DAVISON, W GOLDSPINK, G (1977a) Energy metabolism of carp swimming muscles. J comp Physiol 114 203-216
JOHNSTON, I A WALESBY, N J DAVISON, W & GOLDSPINK G (1977b) Further studies on the adaptation of fish myofibrillar ATPase to different cell temperatures. Pflügers Arch ges Physiol 371 257-262
JOHNSTON, I A LUCKING, M (1978) Temperature induced variation in the distribution of different types of muscle fibre in the goldfish (Carassius auratus). J Comp Physiol 124 111-116
JOHNSTON, I A & MOON, T W (1979) Glycolytic and gluconeogenic enzyme activities in the skeletal muscles and liver of a teleost fish (Pleuronectes platessa). Trans Biochem Soc 7 661-663
JOHNSTON, I A MAITLAND, B (1980) Temperature acclimation in Crucian carp: a morphometric analysis of muscle fibre ultrastructure. J Fish Biol 17 113-125
JOHNSTON, I A MOON, T W (1980a) Exercise training in skeletal muscle of brook trout (Salvelinus fontinalis). J exp Biol 87 177-194
JOHNSTON, I A MOON, T W (1980b) Endurance exercise training in the fast and slow muscles of a teleost fish (Pollachius virens). J Comp Physiol 135B 147-156
JOHNSTON, I A MOON, T W (1981) Fine structure and metabolism of multiply innervated fast muscle fibres in teleost fish. Cell Tissue Res In press
JOHNSTON, I A BERNARD, L M (1982) Routine oxygen consumption and characteristics of the myotomal muscle in tench: Effects of long-term acclimation to hypoxia. Cell Tiss Res 227 161-177

JOHNSTON, I A SIDELL, B D MOERLAND, T S GOLDSPINK, G (1982) Molecular plasticity in the myofibrillar protein complex of the mummichog (Fundulus heteroclitus). J Muscle Res Cell Mot (in press)

JOHNSTON, J B (1908) Additional notes on the cranial nerves of Petromyzontia J comp Neurol 18 569-608

JOLESZ, E SRETER, F A (1981) Development innervation and activity pattern induced changes in skeletal muscle. Ann Rev Physiol 43 531-52

JONES, D R & RANDALL, D J (1978) The respiratory and circulatory systems during exercise. In Fish physiology 7 425-492. Hoar, W S & Randall, D J (Eds). Academic Press London

JONES, P L SIDELL, B D (1982) Metabolic responses of striped bass (Morone saxatilis) to temperature acclimation II. J Exp Zool (In press)

KANUNGO, M S PROSSER, C L (1959) Physiological and biochemical adaptation of goldfish to cold and warm temperatures-II. J Cell Comp Physiol 54 265-274

KAPPERS, C U A HUBER, G C CROSBY, E C (1967) "The comparative anatomy of the nervous system of vertebrates, including man" Vol. 1 Hafner Publishing New York

KARNOVOSK, M J (1965) A formaldehyde-gluteraldehyde fixative of high osmolarity for use in electronmicroscopy. J Cell Biol 27 137A

KEMP, P SMITH, M W (1971) Effect of temperature acclimatization on the fatty acid composition of goldfish intestinal lipids. Biochem J 117 9-15

KHAN, M A (1977) The histoenzymology of striated muscle fibres: an overview. Cell Mol Biol 22 383-393

KIELBÓWNA, L KOSCIELSKI, B (1979) Myotomal myogenesis in Bombina variegata L. Roux's Arch 185 295-303

KILARSKI, W KOZLOWSKA, M (1979) Myofibrillogenesis of the lateral musculature in the trout (Salmo trutta L.). Develop Growth and Differ 21 (4) 349-360

KNIPPRATH, W G & MEADS, J F (1968) The effect of environmental temperature on fatty acid composition and on the in-vivo incorporation of (1-^{14}C) acetate in goldfish (Carassius auratus). Lipids 3 121-8

KORDYLEWSKI, L (1979) Morphology of motor endplate and its size relation to the muscle fibre size in the amphibian submandibular muscle. Z mikrosk-anat Forsch 6 1038-1050

KORNELIUSSEN, H (1972) Identification of muscle fibre types in "semithin" sections stained with p-phenylene diamine. Histochemie 32 95-98

KORNELIUSSEN, H (1973) Dense-core vesicles in motor nerve terminals. Monoaminergic innervation of slow non-twitch muscle fibres in the Atlantic hagfish (Myxine glutinosa L.) Z Zellforsch Mikrosk Anat 140 425-432

KORNELIUSSEN, H DAHL, H A & PAULSEN, J E (1978) Histochemical definition of muscle fibre types in the trunk musculature of a teleost fish (cod, Gadus morhua L.). Histochemistry 55 1-16

KROGH, A (1919) The number and distribution of capillaries in muscles with calculations of the oxygen pressure head necessary for supplying the tissue. J Physiol (Lond) 52 409-415

KRYVI, H (1975) The structure of the myosatellite cells in axial muscles of the shark Galeus melastomus. Anat Embryol 147 35-44

KRYVI, H (1977) Ultrastructure of the different fibre types in axial muscles of the sharks Etmopterus spinax and Galeus melastomus. Cell Tiss Res 184 287-300

KRYVI, H (1978) Ultrastructure of the different fibre types in axial muscles of the sharks Etomopterus spinax and Galeus melastomus. Cell Tiss Res 184 287-300

KRYVI, H & EIDE, A (1977) Morphometric and autoradiographic studies on the growth of red and white axial muscle fibres in the shark Etmopterus spinax. Anat Embryol 151 17-28

KRYVI, H TOTLAND, G K (1977) Histochemical studies with microphotometric determinations of the lateral muscles in the sharks Etmopterus spinax and Galeus melastomus. J mar biol Assoc U K 57 261-271

KRYVI, H FLOOD, P R GULYAEV, D (1980) The ultrastructure and vascular supply of the different fibre types in the axial muscle of the Sturgeon Acipenser stellatus, Pallas. Cell Tiss Res 212 117-126

KUBISTA, V KUBISTOVA, J PETTE, D (1971) Thyroid hormone induced changes in the enzyme activity pattern of energy-supplying metabolism of fast (white), slow (red) and heart muscle of the rat. Eur J Biochem 18 553-560

LÄNNERGREN, J (1978) The force-velocity relation of isolated twitch and slow muscle fibres of Xenopus laevis. J Physiol (Lond) 183 504-521

Le PEUCH, C J DEMAILLE, J & PECHÈRE, J F (1978) Radioelectrophoresis: a specific microassay for parvalbumins, application to muscle biopsies from man and other vertebrates. Biochem Biophys Acta 537 153-159

LEWANDER, K DAVE, G JOHANSSON, M-L LARSSON, A LINDMAN, V (1974) Metabolic and haematological studies on the yellow and silver phases of the European eel, Anguilla anguilla, L. Comp Biochem Physiol 47B 571-581

LEWIS, D M KEAN, C J C McGARRICK, J D (1974) Dyanamic properties of slow and fast muscle and their trophic regulation. Ann N Y Acad Sci 228 105-120

LINDSEY, C C (1978) Form, function, and locomotory habits in fish. in: Hoar, W S Randall, D J (eds.). Fish Physiology 7 Academic Press New York

LOATS, J T SILLAU, A H BANCHERO, N (1978) How to quantify skeletal muscle capillarity. Adv Expl Med Biol 94 41-48

LONGERICH, L L FELTHAM, L A W (1978) Changes in muscle PFK in temperature acclimated winter flounder (Pseudopleuronectes americanus). J Therm Biol 3 61-67

LØMO, T (1976) The role of activity in the control of membrane and contractile properties of skeletal muscle. In 'Motor-innervation of Skeletal Muscle', (Thesleff, S) (ed) pp 289-321 Academic Press London

LONGMUIR, I S (1981) Channels of oxygen transport from blood to mitochondria. Adv Physiol Sci 25 19-22

LOVE, R M (1970) The chemical biology of fishes. Academic Press London

LOVE, R M (1980) The Chemical Biology of Fishes Vol 2 Academic Press London

MALESSA, P (1969) Contributions to the temperature adaptation of the eel (Anguilla vulgaris). Mar Biol 3 143-158

MARUENDA, E C de ARMSTRONG, C F (1978) Satellite and invasive cells in frog sartorius muscle. Tiss Cell 10 749-772

MATHIEU, O CRUZ-ORIVE, L M HOPPELER, H WEIBEL, E R (1981) Measuring error and sampling variation in stereology: comparison of various methods for planar image analysis. J Microscopy 121 75-88

MATHIEU, O CRUZ-ORIVE, L M HOPPELER, H WEIBEL, E R (1982) Estimating length density and quantifying anisotropy in skeletal muscle capillaries. J Mircoscopy (in press)

MAURO, A (1961) Satellite cells of skeletal muscle fibres. J Biophys Biochem Cytol 9 493-495

MAXWELL, L C WHITE, T P FAULKNER, J A (1980) Oxidative capacity, blood flow, and capillarity of skeletal muscles. J Appl Physiol 49 627-633

McCLEAVE, J D KLECKNER, R C (1982) Selective tidal stream transport in the estuarine migration of glass eels of the American eel (Anguilla rostrata) J Cons int Explor Mer (in press)

McARDLE, H J JOHNSTON, I A (1981) Ca^{2+}-uptake by tissue sections and biochemical characteristics of sarcoplasmic reticulum isolated from fish fast and slow muscles. Eur J Cell Biol 25 103-107

METCALFE, J C (1975) Organisation and disorder in membranes. Nature (Lond) 255 576-578
MELLGREN, S I MATHISEN, J S (1966) Oxidative enzymes, glycogen and lipid in striated muscle. Z Zellforsch 71 169-188
MILLOT, J ANTHONY, J (1966) quoted in Roberts 1969
MOERLAND, T S SIDELL, B D (1981) Characterisation of metabolic carbon flow in hepatocytes isolated from thermally acclimated killifish Fundulus heteroclitus. Physiol Zool 54 379-389
MOSS, F P LEBLOND, C P (1971) Satellite cells as the source of nuclei in muscles of growing rats. Anat Rec 170 421-436
MOSSE, P R L (1978) The distribution of capillaries in the somatic musculature of two vertebrate types with particular reference to teleost fish. Cell Tissue Res 187 281-303
MOSSE, P R L (1979) Capillary distribution and metabolic histochemistry of the lateral propulsive musculature of pelagic teleost fish. Cell Tiss Res 203 141-160
MOSSE, P R L HUDSON, R C L (1977) The functional roles of different muscle fibre types indentified in the myotomes of marine teleosts: a behavioural, anatomical and histochemical study. J Fish Biol 11, 417-430
MULLER, W (1976) Subsarcolemmal mitochondria and capillarisation of soleus muscle fibres in young rats subjected to an endurance training. Cell Tissue Res 174 367-389
MYRHAGE, R HUDLICKA, O (1978) Capillary growth in chronically stimulated adult skeletal muscle as studied by intravital microscopy and histological methods in rabbits and rats. Microvasc Res 16 73-90
NACHLAS, M M TSOU, K-C SOUZA, E de CHENG, C-S SELIGMAN, M (1957) Cytochemical demonstration of succinic dehydrogenase by the use of a new p-nitrophenyl substituted ditetrazole. J Histochem Cytochem 5 420-429
NAG, A C (1972) Ultrastructure and adenosine triphosphatase activity of red and white muscle fibres of the caudal region of a fish, Salmo gairdneri. J Cell Biol 55 42-57
NAG, A C NURSALL, J R (1972) Histogenesis of white and red muscle fibres of trunk muscles of a fish Salmo gairdneri. Cytobios 6 227-246
NAIK, N T (1963) Technical variations in Koelle's histochemical method for demonstrating cholinesterase activity. Q J Microsc Sci 104 89-100
NEMETH, P HOFER, H W PETTE, D (1979) Metabolic heterogeneity of muscle fibres classified by myosin ATPase. Histochemistry 63 191-201
NEMETH, P PETTE, D (1981) Succinate dehydrogenase activity in fibres classified by myosin ATPase in three hind limb muscles of rat. J Physiol (Lond) 320 73-80
NEWSHOLME, E A ZAMMIT, V A & CRABTREE, B. (1978) The role of glucose and glycogen as fuels for muscle. Trans Biochem Soc 6 512-520
NICOLAYSEN, K (1976) Spread of the junction potential in the T-system in hagfish slow muscle fibres. Acta Physiol Scand 96 50-57
NIKINMAA, M TUURALA, H SOIVIO, A (1980) Thermoacclimatory changes in blood oxygen binding properties and gill secondary lamellar structure of Salmo gairdneri. J comp Physiol 140 255-260
NISHIHARA, H (1967) Studies on the fine structure of red and white fin muscles of the fish (Carassius auratus). Arch histol jap 28 425-447
NURSALL, J R (1956) The lateral musculature and the swimming of fish. Proc Zool Soc London 126 127-143
NYMAN, L (1972) Some effects of temperature on eel (Anguilla) behavior. Inst Freshwater Res (Drottningholm, Sweden) 52 90-102
OBINATA, T HAREGAWA, T MASAKI, T HAYASHI, T (1976) The subunit structure in myosin from skeletal muscle of the early chick embryo. J Biochem 79 521-531

ONO, R D (1982) Proprioceptive endings in the myotomes of the pickerel (Teleostei Esocidae) J Fish Biol 21 525-535
ONO, R D POSS, S G (1982) Structure and innervation of the swimbladder musculature in the weakfish, Cynoscion regalis (Teleostei: Sciaenidae) Can J Zool 60 1955-1967
PANKHURST, N W (1982) Changes in body musculature with sexual maturation in the European eel, Anguilla anguilla (L.). J Fish Biol 21 417-428
PATTERSON, S GOLDSPINK, G (1976) Mechanism of myofibril growth and proliferation in fish muscle. J Cell Sci 22 607-616
PATTERSON, S JOHNSTON, I A GOLDSPINK, G (1975) Histochemical study of the lateral muscles of five teleost species. J Fish Biol 7 159-166
PEARSE, A G E (1972) "Histochemistry, Theoretical and Applied". Vol 2 3rd Edn Churchill London
PECHÈRE, J-F DERANCOURT, J & HAIECH, J (1977) The participation of parvalbumins in the activation-relaxation cycle of vertebrate fast skeletal muscle. FEBS Lett 75 111-114
PENNEY, R K GOLDSPINK, G (1979) Compensation limits of fish muscle myofibrillar ATPase enzyme to environmental temperature. J Therm Biol 4 269-272
PERRY, S V (1979) The regulation of contractile activity in muscle. Trans Biochem Soc 7 593-617
PETERS, A (1963) The peripheral nervous system in: "The Biology of Myxine" Universitets-for laget Oslo
PETTE, D WIMMER, M NEMETH, P (1980) Do enzyme activities vary along muscle fibres? Histochemistry 67 225-231
PITMAN, R M (1979) Block intensification of neurones stained with cobalt sulphide. J exp Biol 78 295-297
PITMAN, R M TWEEDLE, C D COHEN, M J (1972) Branching of central neurones: intracellular cobalt injection for light and electronmicroscopy. Science NY 176 412-414
PLACE, A R & POWERS, D A (1979) Genetic variation and relative catalytic efficiencies: Lactate dehydrogenase B allozymes of Fundulus heteroclitus. Proc Natn Acad Sci USA 76 2354-2358
PLOTNIKOVA, S I NEVMYVAKA, G A (1980) The Methylene blue technique in: Strausfeld, N J Miller, T A. "Neuroanatomical Techniques" Spring-Verlag New York
PLYLEY, M J GROOM, A C (1975) Geometrical distribution of capillaries in mammalian striated muscle. Am J Physiol 228 1376-1383
PROCTOR, C MOSSE, P R L & HUDSON, R C L (1980) A histochemical and ultrastructural study of the development of the propulsive musculature of the brown trout, Salmo trutta L in relation to its swimming behaviour. J Fish Biol 16 303-321
PROSSER, C L BARR, L M PINC, R A LAUER, C Y (1957) Acclimation of goldfish to low concentrations of oxygen. Physiol Zool 30 137-141
PROSSER, C L (1973) "Comparative Animal Physiology" W.B. Saunders Philadelphia
RAAMSDONK, W van POOL, C W MIJZEN, P MOS, W van der STELT, A (1977) On the relation between movements and the shape of somites in early embryos of the teleost Brachydanio rerio. Bijdragen tot de Dierkunde 46 264-274
RAAMSDONK, W van POOL, C W te KRONNIE, G (1978) Differentiation of muscle fibre types in the teleost Brachydanio rerio. Anat Embryol 153 137-155
RAAMSDONK, W van te KRONNIE, G POOL, C W van de LAARSE, W (1980) An immune histochemical and enzymatic characterization of the muscle fibres in myotomal muscle of the teleost Brachydanio rerio, Hamilton-Buchanan. Acta Histochem 67 200-216
RAKUSAN, K MORAVEC, J HATT, P-Y (1980) Regional capillary supply in the normal and hypertrophied rat heart. Microvasc Res 20 319-326

RANDALL, D J (1970) The circulatory system in: Hoar, W S Randall, D J (eds) "Fish Physiology" Vol 4 Academic Press London
RASMUSSEN, S W BULOW, A BACHHOLM, P (1975) An improved method of making formvar film for electron microscopy. Science Tools 22 (3) 40
RENAUD, J M & MOON, T W (1980) Characterisation of the isolated American eel (Anguilla rostrata Le Sueur) hepatocyte. J comp Physiol 135 115-127
REVEL, J P (1962) The sarcoplasmic reticulum of the bat cricothyroid muscle. J Cell Biol 12 571-588
REYNOLDS, E S (1963) The use of lead citrate at high pH as an electron-opaque stain in electron microscopy. J Biophys Biochem Cytol 10 308-312
RHEUBEN, M B KAMMER, A E (1980) Comparison of slow larval and fast adult muscle innervated by the same motor neurone. J exp Biol 84 103-118
RIDDERSTRALE, Y (1979) Observations on the localization of carbonic anhydrase in muscle. Acta Physiol Scand 106 239-240
RIZZOTTI, M COMPARINI, A RODINÒ, E (1977) The hemoglobins of Anguilla anguilla (L. Ontongenetic variations. Comp Biochem Physiol 58A 173-176
ROBERTS, B L (1965) The spinal nerves of the dogfish. J Physiol (Lond) 179 23-24
ROBERTS, B L (1969) The spinal nerves of the dogfish (Scyliorhinus). J Mar Biol Ass UK 49 51-74
ROBERTS, B L (1981) The organisation of the nervous system of fishes in relation to locomotion. Symp Zool Soc Lond 48 115-136
ROBINSON, G (1977) in: Bancroft, J D Stevens, A (eds) "Theory and practice of histological techniques". Churchill Edinburgh
ROMANUL, F C A (1965) Capillary supply and metabolism of muscle fibres. Arch Neurol 12 497-509
SALAMONSKI, J H JOHNSTON, I A (1982) Capillary supply and mitochondrial volume density in the axial muscles of the mesopelagic teleost Argyropelecus hemigymnus. Mar Biol 69 1-5
SALMONS, S VRBOVÁ, G (1969) The influence of activity on some contractile characteristics of mammalian fast and slow muscles. J Physiol (Lond) 201 535-549
SCHMALBRUCH, H HELLHAMMER, U (1977) The number of nuclei in adult rat muscles with special reference to satellite cells. Anat Rec 189 169-176
SCHMIDT, J (1922) The breeding place of the eel. Phil Trans Roy Soc Lond Ser B 211 179-208
SCHMIDT-NIELSEN, K PENNYCUIK, P (1961) Capillary density in mammals in relation to body size and oxygen consumption. Am J Physiol 200 746-750
SCHMID-SCHÖNBEIN, H (1981) Adv Physiol Sci 25 279-289
SCHULTZ, E (1978) Changes in the satellite cells of growing muscle following denervation. Anat Rec 190 299-312
SELIGMAN, A M KARNOVSKY, M J WASSERKRUG, H L HANKER, J S (1968) Nondroplet ultrastructural demonstration of cytochrome oxidase activity with a polymerizing osmophilic reagent, diaminobenzidine (DAB). J Cell Biol 38 1-14
SHAFIQ, S A GORYCKI, M A MILHORAT, A T (1967) An electron microscopic study of regeneration and satellite cells in human muscle. Neurology 17 567-574
SHAKLEE, J B CHRISTIANSEN, J A SIDELL, B D PROSSER, C L WHITT, G S (1977) Molecular aspects of temperature acclimation in fish: contributions of changes in enzymic activities and isoenxyme patterns to metabolic reorganisation in the green sunfish. J Exp Zool 201 1-20
SIDELL, B (1977) Turnover of cytochrome c in skeletal muscle of green sunfish (Lepomis cyanellus R.) during thermal acclimation. J Exp Zool 199 233-250
SIDELL, B D (1980) Responses of goldfish (Carassius auratus L.) muscle to acclimation temperature: alterations in biochemistry and proportions of different fibre types. Physiol Zool 53 98-107

SIDELL, B D (1982) Cellular acclimatisation to environmental change by quantitative alterations in enzymes and organelles in: "Cellular Acclimatisation". SEB Sem Srs (in press)
SIMENSKY, M (1974) Homeoviscous adapation - a homeostatic process that regulates the viscosity of membrane lipids in Escherichia coli. Proc Natl Acad Sci 71 522-525
SINHA, V R P JONES, J W (1975) "The European freshwater eel". Liverpool University Press
SMIT, H KOUTSTALL, J M A VHERBERG, J von VAUPEL-KLEIN, J C (1971) Oxygen consumption and efficiency of swimming goldfish. Comp Biochem Physiol 39A 1-28
SMIT, H Van den BERG, R J KIJN-den HARTOG, I (1974) Some experiments on thermal acclimation in the goldfish (Carassius auratus L.). Neth J Zool 24 32-49
SNOW, M H (1978) An autoradiographic study of satellite cell differentiation into regenerating myotubes following transplantation of muscles in young rats. Cell Tiss Res 186 535-540
SOMERO, G N (1975) The role of isozymes in adaptation to varying temperatures. In Isozymes II. Physiological-Function (Edited by Markert, C L) pp 221-234 Academic Press New York
SOMERO, G N (1975) Temperature as a selective factor in protein evolution: the adaptational strategy of 'compromise'. Journal of Experimental Zoology 194 175-88
SOMERO, G N (1978) Temperature adaptations of enzymes: Biological optimization through structure-function compromises. An Rev Ecol Syst 9 1-29
SRÉTER, F HOLTZER, S GERGELY, J HOLTZER, H (1972) Some properties of embryonic myosin. J Cell Biol 55 586-594
STANFIELD, P R (1972) Electrical properties of white and red muscle fibres of the elasmobranch fish Scyliorhinus canicula. J Physiol 222 161-186
STEVENS, E D (1968) The effects of exercise on the distribution of blood to various organs in rainbow trout. Comp Biochem Physiol 25 615-625
STRUBBERG, A (1913) The metamorphosis of elvers as influenced by outward conditions. Some experiments. Meddr Komm for Havunders Ser Fiskeri 4 (3) 1-11
STUART, A E HUDSPERTH, A J HALL, Z W (1974) Vital staining of specific monoamine-containing cells in the leech nervous system. Cell Tiss Res 153 55-61
SYROVÝ, I GUTMAN, E (1971) ATPase activity of two rabbit laryngeal muscles. Experientia 27 248
TAKEUCHI, A (1959) Neuromuscular transmission of fish skeletal muscles investigated with intracellular microelectrodes. J Cell Comp Physiol 54 211-20
TARGETT, T E (1978) Respiratory metabolism of temperature acclimated Fundulus heteroclitus (L): Zones of compensation and dependance. J Exp Mar Biol Ecol 32 197-206
TERÄVÄINEN, H (1971) Anatomical and physiological studies on muscles of lamprey. J Neurophysiol 34 954-973
TERÄVÄINEN, H & ROVAINEN, C M (1971) Fast and slow motoneurones to body muscle of the sea lamprey. J Neurophysiol 34 990-998
TESCH, F-W (1977) The Eel. Chapman and Hall London
THILLART, G van den MODDERKOLK, J (1978) The effects of acclimation temperature on the activation energies of state III respiration and on the unsaturation of membrane lipids of goldfish mitochondria. Biochim Biophys Acta 510 38-51

THOMSON, A J SARGENT, J R OWEN, J M (1977) Influence of acclimatization temperature and salinity on (Na K)-dependent adenosine triphosphatase and fatty acid composition in the gills of the eel (Anguilla anguilla) Comp Biochem Physiol 56B 223-228

TOTLAND, G K (1976) Three muscle fibre types in the axial muscles of Axolotl (Ambystoma americanum, Shaw). A quantitative light and electron microscopic study. Cell Tiss Res 168 65-78

TOTLAND, G K KRYVI, H BONE, Q FLOOD, P R (1981) Vascularization of the lateral muscle of some elasmobranchiomorph fishes. J Fish Biol 18 223-234

TROITZKY, Y (1929) quoted in Roberts 1969

UNDERWOOD, E E 1970 "Quantitative stereology" Addison-Wesley Massachusetts

VIDELER, J J (1981) Swimming movements, body structure and propulsion in cod Gadus morhua in: Day, M H (ed) Symp Zool Soc Lond 48 1-27

VRBOVÁ, G (1980) Innervation and differentiation of muscle fibres. In 'Development and Specialization of Muscle' (Goldspink DF) (ed) Soc Exp Biol Seminar series Symp 7

WALES, W CLARKE, F DANDO, M R LAVERACK, M S (1970) Innervation of the receptors present at the various joints of the pereiopods and the third maxilliped of Homarus gammarus (L.). Z vergl Physiol 68 345-384

WALESBY, N J JOHNSTON, I A (1980) Fibre types in the locomotory muscles of an Antarctic teleost, Notothenia rossii: A histochemical, ultrastructural and biochemical study. Cell Tissue Res 208 143-164

WARDLE, C S (1975) Limit of fish swimming speed. Nature (Lond.) 255 725-727

WARDLE, C S VIDELER, J J (1980) Fish swimming in: Elder, H T Trueman, E R (eds) "Aspects of animal movement". SEB Sem Srs 5 125-150

WATANABE, K SASAKI, F KHAN, M A (1978) Light and electron microscopic study of adenosine triphosphatase activity of anuran tadpole musculature. Histochemistry 55 293-305

WATERMAN, R E (1969) Development of the lateral musculature in the teleost Brachydanio rerio: a fine structural study. Am J Anat 125 457-494

WEATHERLEY, A H GILL, H S ROGERS, S C (1979) Growth dynamics of muscle fibres: dry weight and condition in relation to somatic growth rate in yearling trout (Salmo gairdneri). Can J Zool 57 2385-2392

WEBB, P W (1978) Hydrodynamics: nonscombroid fish. in: Hoar, W S Randall, D J (eds) Fish Physiology 7 189-237 Academic Press New York

WEIBEL, E R (1973) Stereological techniques for electron microscopic morphometry. Chapter 6 in: Hayat, M A (ed.). Principles and techniques of electron microscopy. Vol 3 237-296 Van Nostrand-Reinholt, Amsterdam

WEIBEL, E R (1979) "Stereological Methods" Vol 1 Practical methods. Academic Press London

WEIBEL 1980 "Sterological Methods" Vol 2 Theoretical foundations. Academic Press London

WEIBEL, E R TAYLOR, C R GEHR, P HOPPELER, H MATHIEU, O MALOIY, G M O (1981) Design of the mammalian respiratory system. IX Functional and Structural limits for oxygen flow. Resp Physiol 44 151-164

WILLEMSE, J J (1966) Functional anatomy of the myosepta in fishes. Proc k ned Akad wet 69 58-63

WILLEMSE, J J (1975) Some remarks on the structure and function of musculus lateralis in the European eel, Anguilla anguilla (L) (Pisces;Teleostei). Z Morphol Tiere 81 195-208

WILLEMSE, J J (1976) Characteristics of myotomal muscle fibres and their possible relation to growth rate in eels Anguilla anguilla. Aquaculture 8 251-258

WILLEMSE, J J van den BERG, P G (1978) Growth of striated muscle fibres in the M. lateralis of the European eel Anguilla anguilla (L.) (Pisces, Teleostei). J Anat 125 (3) 447-460

WILLEMSE, J J De RUITER, A (1979) A quantitative identification of four types of fibres in the lateral musculature of immature European eel, Anguilla anguilla, L. Aquaculture 17 105-111

WILSON, T L (1977) Inter-relations between pH and temperature for the catalytic rate of the M_4 Isozyme of lactate dehydrogenase (EC1,1,1,27) from goldfish (Carassius auratus L). Arch Biochem Biophys 179 378-390

WHITING, H P (1940) Nervous structure of the spinal cord of the young larval brook-lamprey. Q Jl Microsc Sci 82 359-385

WITTENBERGER, C COPREAN, D & MORAR, L (1975) Studies of the carbohydrate metabolism of the lateral muscles in carp(influence of phlorizin, insulin and adrenaline). J comp Physiol 101 161-172

WODTKE, E (1974) Properties of isolated mitochondria of the eel and their dependancy on acclimation temperature with special regard to oxidative phosphorylation. J Comp Physiol 91 277-307

WODTKE, E (1976) Discontinuities in the Arrhenius plots of mitochondrial membrane-bound enzyme systems from a poikilotherm. Comp Physiol 110 145-157

WOKOMA, A JOHNSTON, I A (1981) Lactate production at high sustainable cruising speeds in rainbow trout (Salmo gairdneri Richardson) J Exp Biol 190 361-364

WOLFF, J R GOERZ, Ch BÄR, Th GÜLDNER, F H (1975) Common morphogenetic aspects of various organotypic microvascular patterns. Microvasc Res 10 373-395

YAMAMOTO, T (1972) Electrical and mechanical properties of the red and white muscles in the silver carp. J exp Biol 57 551-567

YOUNG, J Z (1933) The autonomic nervous system of Selachians. Q Jl Microsc Sci 75 571-624

YOUNG, J Z (1969) "The life of vertebrates" 2nd ed. OUP

ZAMMIT, V A & NEWSHOLME, E.A (1979) Activities of enzymes of fat and ketone-body metabolism and effects of starvation on blood concentrations of glucose and fat fuels in teleost and elasmobranch fish. Biochem J 184 313-322

ZUMSTEIN, A MATHIEU, O HOWALD, H HOPPELER, H (1982) Morphometric analysis of the capillary supply in muscles of trained and untrained subjects; its limitations in muscle biopsies. Pflügers Arch (in press)

HANSEN, H J M ABRAHAM, S (1979) The influence of environmental salinity, temperature, ionizing radiation and yellow and silver stage on lipid metabolism in the gills of the European eel (Anguilla anguilla). Comp Biochem Physiol 63B 483-490